Investigating the oncolytic properties of a group B adenovirus on cancer cells and its effects on the local immune response



Hugo Calderon

Linacre College

A thesis submitted for the degree of Doctor of Philosophy

to the Department of Oncology, University of Oxford

Trinity Term 2017

Supervisors: Professor Leonard Seymour and Doctor Kerry Fisher

Abstract

Oncolytic viruses are characterised by their ability to selectively infect and kill tumour cells. Recently it has emerged that they can exert an additional anticancer mechanism stimulating adaptive immune-mediated cancer cell killing. Enadenotucirev (EnAd, formerly known as ColoAd1), is a chimeric Ad11p/Ad3 virus group B oncolytic adenovirus that binds CD46 and is under development for the systemic treatment of metastatic carcinomas. The central aim of this thesis was to to assess whether EnAd provides an adjuvant effect on tumour-associated antigen presenting cells (APCs) that could drive T_H1 polarisation for an effective anti-tumour immune response.

This thesis describes the potent oncolytic properties, fast replication and high numbers of virus progeny production by EnAd in cancer cells. Recombinant EnAd variants were engineered to investigate the roles of the mutant regions in the genome of EnAd, and how these influence the modified phenotype. A chemical drug panel was used to identify pathways and cellular factors involved in cellular production of EnAd, finding that several mTOR inhibitors and microtubule inhibitors could improve virus replication.

An *in vitro* system using partially matured human monocyte-derived dendritic cells (DCs), which displayed a similar phenotype to tumour-infiltrating DCs, was used to explore the effect of EnAd on APC responses. EnAd induced a strong adjuvant effect on these cells by up-regulating surface markers and secretion of pro-inflammatory factors. Further mechanistic experiments, alongside a CAR-binding group C adenovirus 5, indicated these adjuvant effects were virus particle-mediated and dependent on CD46 binding. To understand the functional implications downstream of these interactions, T cell activation and phenotype was assessed using a mixed lymphocyte reaction approach. The data indicated EnAd was a good candidate compared to other adenoviruses, that may steer the response of activated T-cells towards a T_H1 phenotype, for an effective immune response.

In conclusion, the potent oncolytic properties of EnAd virus may provide an adjuvant effect on tumour-associated APCs, helping to harness an adaptive immune response.

Declaration of authentication

All the work presented in this thesis is my own, and any pertinent contributions made by others have been acknowledged. The content submitted here in no way forms part of any other thesis in this or any other university. This work was performed under the supervision of Professor Leonard Seymour, Department of Oncology, Medical Sciences Division, University of Oxford, and Doctor Kerry Fisher and Doctor Alice C.N. Brown, PsiOxus Therapeutics, Abingdon.

Acknowledgements

First of all, I would like to thank my academic supervisors Professor Len Seymour and Doctor Kerry Fisher, as well as my industry supervisor, Doctor Alice C.N. Brown, for giving me the opportunity to undertake part in this project, providing scientific insight and indulging in discussion and guidance throughout the work presented in this thesis. I am equally gratified to Doctor Brian Champion, for his complementary supervision within the industry.

Co-workers of PsiOxus Therapeutics have been crucial in my scientific development. I am grateful to Prithvi Kodialbail, Doctor Daniel Cochrane, Sam Illingworth, Magda Kieltyka, Doctor Darren Plumb and Nalini Marino for their support over the course of my studies and ensuring sessions in the afternoons (also known as *siesta* time where I come from) were more amenable. I am also thankful to Doctor Mathieu Besneux and Doctor Gianfranco Di Genova for their in depth knowledge of immunology. I most certainly would not have been able to progress though this thesis without the valuable time dedicated by Doctor Simon Alvis to educate me in use of statistics and at times, the English language. This being a limited space to try to mention everyone within the ever-growing structure of PsiOxus Therapeutics, I have to specially mention MD MBA John Beadle, CEO of PsiOxus, for empowering everyone working within the organisation. Outside of work environment, I would like to thank my group of Oxford friends for ensuring these past few years were epic and full of music.

My family has always been a source of inspiration and support. I want to acknowledge and thank, that my personal and professional development was only possible due to the dedication of my parents, and my sister's insistence that I study abroad. Furthermore, over the course of my education numerous teachers/mentors have greatly influenced on me, however, the creativity of Doctor Ramon Alemany, has been crucial for my dedication to cancer virotherapy. I am also grateful to the European Union for funding Marie Skłodowska-Curie Action and 7th Framework Programme, for giving me the privileged position to network with scientific leaders along with a generous scholarship to undertake this work.

Lastly, and most importantly, I would like to thank my life companion and partner, Ariadna, for her love and support. I can only hope this science will build-on and contribute to better treatments for people like your mum, that suffer from cancer.

Table of Contents

Abstract 2
Declaration of authentication 3
Acknowledgements 4
List of abbreviations 12
1 Introduction 16
1.1 Cancer therapies 18
1.2 Cancer immunology 20
1.2.1 Early association of immune system and cancer 20
1.2.2 Immunosurveillance 20
1.2.3 Immunoediting and immunoescape 21
1.2.3.1 Immune evasion via reduction of antigenicity and immunogenicity 21
1.2.3.2 Immune evasion mediated by suppressive tumour microenvironment 22
1.2.4 Cancer immunotherapy 22
1.2.5 Dendritic cells in cancer immunotherapy 24
1.3 Human adenovirus 27
1.3.1 The structure of human adenovirus 27
1.3.2 The cellular life cycle of human adenovirus 30
1.3.2.1 Cell attachment 30
1.3.2.2 Cell entry and endosome escape 31
1.3.2.3 Nuclear import, early genome transcription and genome replication 32
1.3.2.4 Late virus gene expression and virus particle release 33
1.3.2.5 Immune response to adenovirus infection 35
1.4 Viruses and cancer 36
1.4.1 Oncolytic virotherapy 37
1.4.1.1 Wildtype viruses with intrinsic oncotropism 38
1.4.1.2 Genetically modified viruses to improve the selectivity for cancer cells 39
1.4.1.3 Genetically modified viruses to express therapeutic payloads to improve the anti-tumour efficacy 42
1.4.1.4 Bioselection of oncolytic viruses using cancer cell lines 43
1.4.1.5 Oncolytic viruses and clinical trials 44
1.4.1.6 The limitations of oncolytic viruses 47
1.5 The oncolytic adenovirus Enadenotucirev 50

1.5.1 The genomic structure of EnAd virus 50
1.5.2 The properties of EnAd virus 53
1.6 Hypothesis 54
2 Materials and Methods 56
2.1 Methods used in cell line culturing 56
2.1.1 Adherent cell culture 56
2.1.2 Non-adherent cell culture 57
2.1.3 Manual cell counting 57
2.1.4 Automatic cell counting 57
2.1.5 Cell plating 58
2.1.6 Adherent cell line cryopreservation 58
2.1.7 Non-adherent cell line cryopreservation 58
2.1.8 Cell line revival 59
2.2 Molecular biology methods 59
2.2.1 Restriction endonuclease digestion of DNA 59
2.2.2 Agarose gel electrophoresis of DNA 60
2.2.3 Phenol/chloroform extraction of DNA 60
2.2.4 Ethanol precipitation of DNA 61
2.2.5 Transformation of competent bacteria with adenovirus plasmids 61
2.2.6 Large scale preparation and purification of adenovirus plasmid 61
2.2.7 DNA extraction using Minipreps 62
2.2.8 DNA extraction in 96 well-plate, vacuum format 62
2.2.9 DNA extraction in 96 well-plate, centrifuge format 63
2.2.10 Standard curve preparation for qPCR 63
2.2.11 DNA quantification using Taqman qPCR 64
2.2.11.1 Primer and probes design 64
2.2.11.2 DNA quantification using Taqman qPCR 65
2.2.12 RNA extraction using Miniprep 67
2.2.13 RNA quantification by retro transcriptase qPCR 67
2.2.14 Western Blot 68
2.2.14.1 Cell lysis and immunoprecipitation 68
2.2.14.2 Sample preparation and gel loading 69
2.2.14.3 Transfer to PVDF membrane 69

2.2.14.4 Immunoblot, development and reprobing 70
2.3 Virology-related methods 71
2.3.1 Adenovirus production 72
2.3.1.1 Adenovirus genome vector design and amplification 72
2.3.1.2 Transfection of mammalian cells with adenovirus genome 72
2.3.1.3 Adenovirus amplification from transfection 73
2.3.1.4 Adenovirus amplification from purified virus stock 73
2.3.1.5 Adenovirus purification from Hyperflasks 74
2.3.1.6 Inactivation of EnAd genome by psoralen and UV light method 75
2.3.2 Adenovirus characterisation assays 76
2.3.2.1 HPLC titration and evaluation of virus capsid integrity 76
2.3.2.2 Evaluating the endotoxin levels in purified virus stock 76
2.3.2.3 Oncolytic potency assay 77
2.3.2.4 Infectivity assay by hexon staining 78
2.3.3 Cell infection with virus 79
2.3.4 Drug and virus treatment studies 79
2.4 Procedures for immunology studies 80
2.4.1 Peripheral blood mononuclear cells extraction 80
2.4.2 Enrichment of immune cells by magnetic-activated cell sorting 81
2.4.3 Mixed leukocyte reaction assay 82
2.4.3.1 Generation of d3iDC cells 82
2.4.3.2 MLR assay 82
2.4.3.3 Extended MLR assay 83
2.4.3.4 MLR polyclonal re-stimulation 83
2.4.4 Antibody coating of culture plates 83
2.4.5 Immuno-based assay to determine soluble factors 84
2.4.6 Assessment of the soluble T_H cytokines from supernatant by flow cytometry 85
2.4.7 Enzyme-linked immunosorbent assay 86
2.4.8 Immunofluorescence staining and flow cytometry 87
2.4.8.1 Antibody titration 88
2.4.8.2 Cell surface staining and vital staining 89
2.4.8.3 Intracellular marker staining 90
2.4.8.4 Intranuclear marker staining 91

2.4.8.5 Flow cytometry 92
2.5 Statistics 92
3 Studying the life cycle of EnAd virus in cancer cells 94
3.1 Introduction 94
3.2 Chapter aims 95
3.3 Results 95
3.3.1 EnAd and Ad11p molecular differences in cancer cells 95
3.3.1.1 Comparison of EnAd and Ad11p oncolytic potency on HT29 cells 95
3.3.1.2 Comparison of EnAd and Ad11p genome replication in HT29 cells 97
3.3.1.3 Supernatant assessment to compare EnAd and Ad11p virus production in HT29 cells 98
3.3.1.4 Comparison of the number of viral mRNA transcripts produced by EnAd and Ad11p in HT29 cells 100
3.3.2 Investigating the role of EnAd-associated mutations in its improved oncolytic phenotype 101
3.3.2.1 Production of EnAd variants containing wtE2B, wtE3 and wtE4 101
3.3.2.2 Evaluation of oncolytic potency and virus production of EnAd-wtE2B and EnAd-wtE3 virus in HT29 cells 104
3.3.2.3 Troubleshooting the difficulties of producing EnAd-wtE4 virus 106
3.3.3 Evaluation of cellular factors involved in EnAd virus replication in cancer cells using drugs 113
3.3.3.1 Optimising the virus replication assay for drug screening 113
3.3.3.2 Virus replication screening 114
3.3.3.3 Families of drugs enhancing EnAd replication 117
3.3.3.4 Optimising the drug concentration for priority agents identified in the screen 118
3.3.3.5 Evaluation of virus replication of priority drugs in A549 cells 123
3.4 Chapter summary 125
3.5 Chapter discussion 126
3.5.1 Discussion of results 126
3.5.2 Limitations and future work 130
4 Comparing the adjuvant nature of EnAd and Ad5 virus on an in vitro human TIDC-like model 132

4.1 Introduction 132
4.2 Chapter aim 133
4.3 Results 133
4.3.1 Evaluating the adjuvant effect of EnAd virus particles on d3iDC cells by immunophenotyping DC maturation markers 133
4.3.2 Assessment of soluble factors produced by d3iDC cells stimulated with EnAd virus particles 136
4.3.3 Assessment of the EnAd particles effect on d3iDC model compared to the archetype adenovirus 5 139
4.3.3.1 Assessing EnAd and Ad5 virus particle adjuvant effect on the d3iDC by immunophenotyping DC maturation markers 139
4.3.3.2 Comparison of soluble factors produced by d3iDC treated with same dose of EnAd and Ad5 virus particles 142
4.3.3.3 Transcriptome analysis of immune-related genes in d3iDC cells treated with EnAd and Ad5 virus particle 144
4.3.3.4 Assessing the adjuvant effect of EnAd and Ad5 virus particle at different doses on d3iDC model 147
4.3.4 Evaluating the consequences of tumour cell virolysis on the effects of EnAd virus on d3iDC cells 150
4.4 Chapter summary 157
4.5 Chapter discussion 158
4.5.1 Discussion of results 158
4.5.2 Limitations and future work 161
5 Understanding the adjuvant effect of EnAd virus particles on the TIDC-like model 163
5.1 Introduction 163
5.2 Chapter aim 164
5.3 Results 164
5.3.1 Investigating the mechanism by which EnAd particles induce superior stimulation on d3iDC model 164
5.3.1.1 Investigating whether the greater adjuvant effect of EnAd on d3iDC cells is virus gene-mediated 164
5.3.1.2 Investigating whether the superior adjuvant effect of EnAd virus on d3iDC is virus particle-mediated 174

5.3.2 Evaluating the role of NF-kB for the expression of EnAd E3 mRNA in d3iDC cells 183
5.4 Chapter summary 187
5.5 Chapter discussion 188
5.5.1 Discussion of results 188
5.5.2 Limitations and future work 192
6 Evaluating the potential of EnAd-treated TIDC-like cells to functionally harness an anti-cancer adaptive immune response 194
6.1 Introduction 194
6.2 Chapter aims 196
6.3 Results 196
6.3.1 Mixed leukocyte reaction model development 196
6.3.2 Comparing EnAd and Ad5 virus particles in an MLR for their ability to activate CD4 T cells via d3iDC 200
6.3.3 Evaluating whether PD-L1 blockade can further enhance the T cell activation mediated by EnAd-treated d3iDC in an MLR assay 205
6.3.4 Evaluating the potential of EnAd to activate T cells within the tumour context 207
6.3.5 Assessing the ability of EnAd virus to activate CD4 T cells via d3iDC when pre-infected in A549 cell 207
6.3.6 Investigating the role of EnAd virus particles on CD4 T cell stimulation 211
6.3.7 Evaluating whether EnAd and Ad5 virus particles can potentially prime anti-cancer adaptive immune responses using a 9 days MLR assay 213
6.3.7.1 Assessing EnAd- and Ad5-treated d3iDC for their ability to induce differentiation of naïve CD4 T cells ‘primed’ in a 9 days MLR assay 214
6.3.7.2 Evaluating the proliferation of naïve CD4 T cells exposed to EnAd- and Ad5-treated d3iDC cells over the course of 9 days of MLR assay 217
6.3.7.3 Studying EnAd- and Ad5-treated d3iDC for their effect on the polarisation of naïve CD4 T ‘primed’ in a 10 days MLR assay 219
6.4 Chapter summary 227
6.5 Chapter discussion 228
6.5.1 Discussion of results 228
6.5.2 Limitations and future work 232

7 Discussion....234
7.1 Summary and discussion of results....234
7.1.1 Assessing the virus and cellular factors involved in the oncolytic activity of EnAd 234
7.1.2 The adjuvant effect of EnAd virus on TIDC-like cells....235
7.1.3 The mechanism underlying the adjuvant effect of EnAd virus particles....237
7.1.4 Evaluating whether EnAd can sway T_H1 adaptive immune response....238
7.2 Final discussion and future directions....240
7.2.1 Future directions....240
7.2.2 Final conclusions....242
8 Bibliography....244
9 Appendix....260
9.1 Part A....260
9.2 Part B....262
9.2.1 PBMC isolation and monocyte selection method....262
9.2.2 Immunophenotyping human monocytes during their differentiation into DCs by flow cytometry....265
9.2.3 Assessment of soluble factors produced by d3iDC cells stimulated with LPS268

List of abbreviations

/ Per

3’ or 5’ Three or five prime end of a DNA/RNA molecule

µ Micro

Ab Antibody

Ad Adenovirus

AdPol Adenovirus polymerase

AMPK AMP-activated protein kinase

ANOVA Analysis of variance

APC Antigen presenting cell

BSA Bovine serum albumin

CAR Coxsackie and adenovirus receptor

CMV Cytomegalovirus

CPE Cytopathic effect

CpG-N Neutralising CpG

CpG-S Stimulatory CpG

C_T Threshold cycle number

CTL Cytotoxic T cell

CTLA-4 Cytotoxic T lymphocyte associated protein 4

CVL Crude virus lysate

d3iDC Day 3 immature dendritic cell

Da Daltons

DAB Diaminobenzidine

DAMP Damage-associated molecular pattern

DC Dendritic cell

DMEM Dulbecco’s modified eagle’s media

DMSO Dimethyl Sulphoxide

DNA Deoxyribonucleic acid

DSG Desmoglein

E Early adenovirus gene

EDTA Ethylenediamine tetra-acetic acid

eIF Eukaryotic initiation factor

ELISA Enzyme-Linked Immunosorbent Assay

FBS Fetal bovine serum

FITC Fluorescein isothiocyanate

g Grams

g Gravitational force

GFP Green fluorescent protein

GM-CSF Granulocyte-macrophage colony-stimulating factor

HEPES 4-(2-hydroxyethyl)-1-piperazineethanesulfonic acid

HEK293 Human embryonic kidney cells

HLA Human leukocyte antigen

HSV-1 Human herpes simplex virus type 1

HPLC High-performance liquid chromatography

HRP Horseradish peroxidase

ICAM Intracellular adhesion molecule

iDC Immature dendritic cell

IFN Interferon

IL Interleukin

IgG Immunoglobulin isotype G

IP Immunoprecipitation

ITR Inverted terminal repeat

IV intravenous

k Kilo

kb Kilobase

L Late adenovirus gene

l Litre

LPS Lipopolysaccharide

M Molar

MFI Median fluorescence intensity

MHC Major histocompatibility complex

MIF Migration inhibition factor

MLP Major late promoter

MLR Mixed leukocyte reaction

MTLR Mixed tumour leukocyte reaction

mRNA Messenger RNA

MT Microtubule

mTOR Mammalian target of rapamycin

Edm-MV Edmonston strain measles virus

n Number

N/A Not applicable

ng Nanograms

NF-κB Nuclear factor kappa-light-chain-enhancer of activated B cells

OD Optical density

ORF Open reading frame

OV Oncolytic virus

PBMC Peripheral blood mononuclear cells

PBS Phosphate buffered saline

PCR Polymerase chain reaction

PD-1 Programmed death-1

PD-L1 Programmed death-1 ligand

PE Phycoerythrin

PAMP Pathogen-associated molecular pattern

PD Pixel density

PP2A Protein phosphatase 2A

ppc Particles per cell

pRB Retinoblastoma protein

PRR Pathogen recognition receptor

pTP Pre-terminal protein

PVDF Polyvinylidene fluoride

RNA Ribonucleic acid

RPMI Roswell Park Memorial Institute media

SD Standard deviation

SN Supernatant

TCR T cell receptor

T_H T Helper cell

T_H1 Helper T cell type 1

T_H2 Helper T cell type 2

TIDC Tumour-infiltrating dendritic cell

TLR9 Toll-like receptor 9

TME Tumour microenvironment

TNF Tumour necrosis factor

TP Terminal Protein

Tregs Regulatory T cells

T-VEC Talimogene laherparepvec

vp Virus particle

wt Wild-type

x Multiplied by

VSV Vesicular stomatitis virus

WB Western blot

1 Introduction

Cancer survival has doubled in the last 40 years thanks to advances in diagnosis, early intervention and targeted therapies. However, the disease remains the most common cause of death in the UK and is still associated with considerable morbidity (Cancer research UK). Early diagnosed and localised, accessible tumours can be cured by surgery. But for metastatic malignancies, standard treatments do not cure and only lengthen the patient survival for a limited time, sometimes at the expense of quality of life. Nevertheless, improvements in immunotherapy have recently raised the possibility of improved remission for some patients. Originally, only very small numbers of patients with specific indications responded to immunotherapies such as interleukins[1]. Nowadays, biologic therapeutics that inhibit immune checkpoints and engineered T cells, have raised once more the concept of immunotherapy to the spotlight of cancer treatments. As increasing numbers of cancer patients respond to these treatments, the first agents have received commercial licenses[2]. Yet life-changing, immunotherapy efficacy is restricted to few types of malignancies, with many cancer patients currently unresponsive to the treatments[3].

Oncolytic viruses (OVs) have attracted interest as a new type of cancer therapy, partly because of their dual mechanisms of action to kill tumour cells. Initially, OVs were engineered to replicate selectively within tumour cells and lyse the infected cell. These agents were shown to potently kill a wide range of tumour cells, including cancers resilient to conventional treatments or even with cancer stem cell-like phenotype[4,5]. Recent evidence suggests that OVs have a second mechanism which can also kill nearby non-infected cancer cells. As a consequence of their oncolytic activity, tumour antigens and endogenous danger signals are released from dying infected cells, and along with the progeny virus particles, may act to rebalance the local

immune environment and ultimately harness an anti-tumour immune response. This provides a basis for the development of 'immunovirotherapy' field.

This thesis focuses on the study of one oncolytic adenovirus, Enadenotucirev (EnAd, formerly known as ColoAd1)[6], which is currently in phase I/II clinical trials[7]. However, relatively little is known about the underlying mechanisms of its direct oncolytic activity, nor its adjuvant potential to stimulate cancer-associated APCs to harness anti-cancer immune responses. The oncolytic phenotype of EnAd, underpinning its direct cytotoxicity, will be studied in chapter 3. Subsequent chapters will explore the adjuvant effect of the virus on immature DCs (developed to model the immature phenotype of many tumour-infiltrating DCs) and the potential to stimulate a T_H1 adaptive immune response, using a range of reductionist *in vitro* human model systems. In accomplishing such studies, new information about EnAd virus and its mechanisms of action will be gathered, along with potential combination therapy strategies and some insights about the design of next generation 'armed' viruses. To provide a framework for the different chapters, this Introduction describes the background of cancer biology and immunology, before moving to the rationale for using OVs, including a detailed discussion of adenovirus and the properties known for EnAd.

1.1 Cancer therapies

In developed countries, cancer is a leading cause of death. In fact, in England and Wales 28.5% of deaths were caused by cancer during 2016 (Office for National Statistics, 2016). For primary, localised tumours, surgery remains the most effective treatment option and is frequently followed by loco-regional radiotherapy and/or systemic chemotherapy. However, once tumours have metastasised, effective treatment options become more limited and the patient's prognosis deteriorates. Although screening programmes have been implemented to enable the early detection of tumours ideally leading to curative treatment before metastasis, alternative effective therapies for metastatic disease are still required. Current therapy for metastatic disease includes radiation therapy. However, radiotherapy does not always eradicate the entire tumour mass so it is often combined with surgery, and/or chemotherapy. Cytotoxic chemotherapeutic agents have different mechanisms of action that can be broadly grouped into five different groups: alkylating agents (direct DNA damage), anthracyclines (inhibitor of enzymes necessary for DNA replication), antimetabolites (inhibit DNA synthesis), topoisomerase inhibitors (prevent DNA unwinding) and plant alkaloids (disruptor of cytoskeleton). Most of these chemotherapeutics are non-specific and cytotoxic to all active or proliferating cells, including non-cancerous rapidly proliferating tissues (such as blood, digestive epitheliums and hair follicles). The cytotoxicity on healthy cells leads to a broad list of severe side effects that impairs the patient's quality of live. The side effects range from general fatigue and pain, to digestive disorders like nausea, vomiting and diarrhoea, as well as blood disorders. For this reason, treatment regimens are often designed to administer cytotoxic chemotherapeutics at the maximum tolerated dose with treatment-free periods that allow normal cells to recover. However, this method along with the tumour heterogeneity is thought to contribute to drug resistance, as malignant cells that are resistant to treatment survive and

thrive during treatment free periods[8]. Additionally, chemotherapeutic agents are sometimes thought to induce the epithelial-mesenchymal transition (EMT), by which cancer cells lose cell polarity and cell-cell adhesion, and transition to multi-drug resistant mesenchymal stem cells is promoted[9]. As a result of all these challenges, combined with the fact that several traditional chemotherapeutic agents are carcinogenic themselves, there has been an urgent need to develop new therapeutic agents that exhibit increased selective toxicity in cancer cells. Such 'targeted' drugs have been developed as a detailed understanding of the molecular differences between cancer cells and normal cells is gained[10,11]. Currently, some kinase inhibitors and biologic therapeutics are extremely effective for some types of cancer[11,12]. An example of such development would be the use of Imatinib, a specific inhibitor of Abelson proto-oncogene (ABL), for Philadelphia chromosome – a type of chronic myelogenous leukaemia. In Philadelphia chromosome, myeloid cells have a specific chromosome translocation between ABL and breakpoint cluster region (BCR), resulting in a fusion protein that constantly activates cell division. Imatinib is now first-line treatment for this condition improving the five-year survival rate from 31% to 59%[13]. However, most patients do not currently have mutations that can be drugged in this way, but the whole basis for 'personalised medicine' in cancer showing promising results.

1.2 Cancer immunology

1.2.1 Early association of immune system and cancer

William Coley in late 1800s made the observation that sarcoma patients went into spontaneous remission following a post-surgical bacterial infection[14]. This inspired Coley to try and recreate the effects in cancer patients using what came to be known as "Coley's toxin," a cocktail of heat-killed bacteria[15]. Despite a few significant responses, the overall response of Coley's toxin was limited[16]. Nevertheless, his discovery set ground to further understand the interplay between the immune system and cancer. At the same time the principle of cancer immunotherapy was established, indicating that given the correct stimulus the immune system can eliminate cancer cells.

1.2.2 Immunosurveillance

Burnet initially proposed in 1957 that the immune system actively surveyed the body to eliminate malignant transformation[17], also known as immunosurveillance. However, this was challenged for decades because of a lack of direct experimental evidences. Over time, studies in which tumour formation was assessed in mouse models with specific immune deficiencies gradually accumulated, showing a trend between immune deficiency and susceptibility to both chemically induced and spontaneous cancers[18]. The spread of the human immunodeficiency virus contributed to epidemiological evidences that individuals with acquired immunodeficiency syndrome were more prone to cancer, especially Kaposi sarcoma and non-Hodgkin lymphoma[19]. By 2003, the concept of tumour immune surveillance was widely accepted[20]. However, even though the immune system was capable of both identifying and killing nascent tumour cells, tumours still grew in immunocompetent individuals.

1.2.3 Immunoediting and immunoescape

Cancerous cells express different antigens to normal cells. This was first demonstrated in studies that found mice immunised with chemically induced tumours were protected against subsequent re-challenge with the same tumour[21]. The tumour antigens can be derived from foreign agents – such as oncogenic viruses – or tumour antigens raised from 'self' – as the result of acquired genetic mutations, overexpression of proteins or the aberrant expression of proteins restricted to specific developmental stages. Building on previous work, Thomas and Burnet proposed that the constant pressure of the immune surveillance promoted a Darwinian selection on cancer cells that expressed the tumour antigens, this was termed immune editing[22,23]. As a consequence of immune editing, cells which are resistant to immune deletion survive creating an heterogenic population of cancer cells with multiple immune evasive strategies that allow the immune escape and the progression of the disease[24].

1.2.3.1 Immune evasion via reduction of antigenicity and immunogenicity

In advanced stages of the disease, tumour cells have decreased antigenicity (expressing few antigens) translated into a reduced visibility to the effector immune response. The downregulation of antigen expression generally originates from mutations in genes responsible for antigen presentation. For example, transporter associated with antigen processing-1 (TAP-1) is responsible for transport of endogenous antigens across the endoplasmic reticulum for loading onto major histocompatibility complex (MHC) class I molecules[25]. Tumour-associated mutations in TAP-1 have been shown to impair this function, leading to a significant reduction in surface MHC class I[26].

Alternatively, other cancer cells can still be antigenic but they are selected for their ability to suppress immunogenicity, by expressing molecules that directly inhibit the effector T cell

immune responses. An example of this mechanism is the up-regulation of the programed-cell death-1 ligand (PD-L1) on cancer cells[27].

1.2.3.2 Immune evasion mediated by suppressive tumour microenvironment

More recently, the abnormal differentiation of the myeloid compartment has been identified as another immunological hallmark of cancer[28]. Although the biology leading to this process is not yet fully understood, evidence from tumour-bearing mice and cancer patients show an accumulation of regulatory polymorphonuclear neutrophils, tumour-associated macrophages (TAM), tumour-infiltrating DCs (TIDCs), as well as pathologically activated immature myeloid cells with a potent ability to suppress immune responses. These cells are termed myeloid-derived suppressor cells (MDSC)[29]. Although these cells were observed in tumour-bearing hosts since the 1970s, their true biological role only recently became apparent[30]. Altogether, this amalgam of cells secrete soluble factors generating an immune-suppressive tumour microenvironment (TME), that added to cell-cell interaction tolerise the effector antigen-specific immune response, preventing immune destruction[31,32]. This heterogenic population also contributes greatly to other aspects of carcinogenesis hallmarks. In recent years, they have been directly implicated in the promotion of tumour metastasis and angiogenesis[29,33].

1.2.4 Cancer immunotherapy

As reviewed in the previous section, the immune system plays a critical role in tumour biology with the capacity to support or inhibit tumour development, growth and invasion. Since 'Coley's toxin', many have tried to harness the immune system against the tumour without much success. Nevertheless, this contributed towards a better understanding of the cancer immunobiology, leading to the design of new promising therapeutic approaches[34]. These

agents are often based on the concept that it is more effective to intervene at the level where the tumour inhibits the immune system, rather than directly at the level of the cancer cell – and thereby allows the immune system to recover its normal activity. In other words, many of these agents aim to reverse immune suppression rather than treat the cancer directly. For example, therapeutic monoclonal antibodies designed to interrupt the T cell checkpoint inhibitory signals, received by the cytotoxic T-lymphocyte-associated antigen 4 (CTLA-4) and programmed cell death-1 (PD-1) molecules, are demonstrating long-term survival benefits for some conditions[3,35]. In addition, synthetic biology has allowed to overcome the limitations of cancer vaccines by engineering *ex vivo* the patient's T cells before reinfusing them. This strategy provides T cells with a chimeric antigen receptor against specific tumour antigens, resulting in impressive remissions in patients with specific advanced malignancies[36,37].

However, a large proportion of tumours remain unresponsive to these single targeted strategies, often referred to an immunologically 'cold' tumours. This emphasises the heterogeneity of cancer and suggests the existence of multiple immunoregulatory pathways, for example the loss of antigenicity by MHC class I down-regulation or lack of stimulatory DC able to harness the anti-cancer immune response. In addition, in some cancer types (most notably colorectal cancer) tumour-associated lymphocytes often appear to be physically marginalised to stromal areas and are not able to enter the tumour parenchyma, presumably interfering with any anti-cancer activities they might otherwise demonstrate[38]. Understanding these resistance mechanisms and finding strategies to tackle them at once, may be cancer immunotherapy's major challenge[32].

1.2.5 Dendritic cells in cancer immunotherapy

DCs are considered the most prominent antigen presenting cells for their potent ability to harness immune responses against specific antigens. During the early stage of cancer disease DCs are considered to promote tumour-specific adaptive immune response, which mediate the cancer cell killing[39]. Initially, DCs prime peptide-specific CD4 T cell in the lymph node by providing 3 different signals. The main signal – signal 1 – comes from the T cell receptor (TCR) recognising the specific antigen presented by the MHC (also known as human leukocyte antigen (HLA) in humans) of the DC. The second signal is derived from the interaction of costimulatory molecules and the third signal is provided by soluble factors, notably cytokines. The latter two signals play a key role to polarise CD4 mediator T cells into one of the several helper T (T_H) subset[40]. Helper T cell type 1 (T_H1) secretes tumour necrosis factor alpha (TNF-a), interferon gamma (IFN-g) and interleukin 2 (IL-2), cytokines known to directly inhibit the growth of cancer cells and contribute to the activation of effector cytotoxic CD8 T cells (CTL), which can kill cancer cells by specific recognition of HLA-presented tumour antigens[41]. Probably for this reason T_H1 polarisation is considered the most potent mediator of anti-cancer immune responses. Accordingly, multiple sophisticated and targeted DC vaccines have been developed by pulsing all sorts of tumour antigens on autologous DCs. Briefly, DCs are initially obtained from the same patient before the tumour antigens are pulsed *ex vivo* in combination with adjuvants and cytokines that will favour T_H1 polarisation. Later DCs are re-infused to the patient to prime anti-tumour immune responses. However, these trials have demonstrated only limited efficacy in human patients despite eliciting readily detectable CD4+ and CD8+ T cell responses[42]. It is possible that these mediators cannot act effectively on the tumour due to loco-regional suppressive factors, indicating that *ex vivo* stimulation of DC might be very challenging.

In fact, during tumour progression tumour-infiltrating DC hardly express the HLA and costimulatory molecules, and express suppressive cytokines. At later stages, TIDC can deplete tumour-infiltrating effector T cells or induce T cell anergy or even regulatory T cells (Tregs)[40,43-45]. Tregs in turn will secrete more suppressive factors and aggravate the suppressive TME in benefit of the immune evasion and tumour progression[46-52]. Although the process of TIDC transformation is not yet fully characterised, it appears to be mediated by cell-cell interactions and soluble factor, as represented in Figure 1.1 and comprehensively reviewed by others[46].

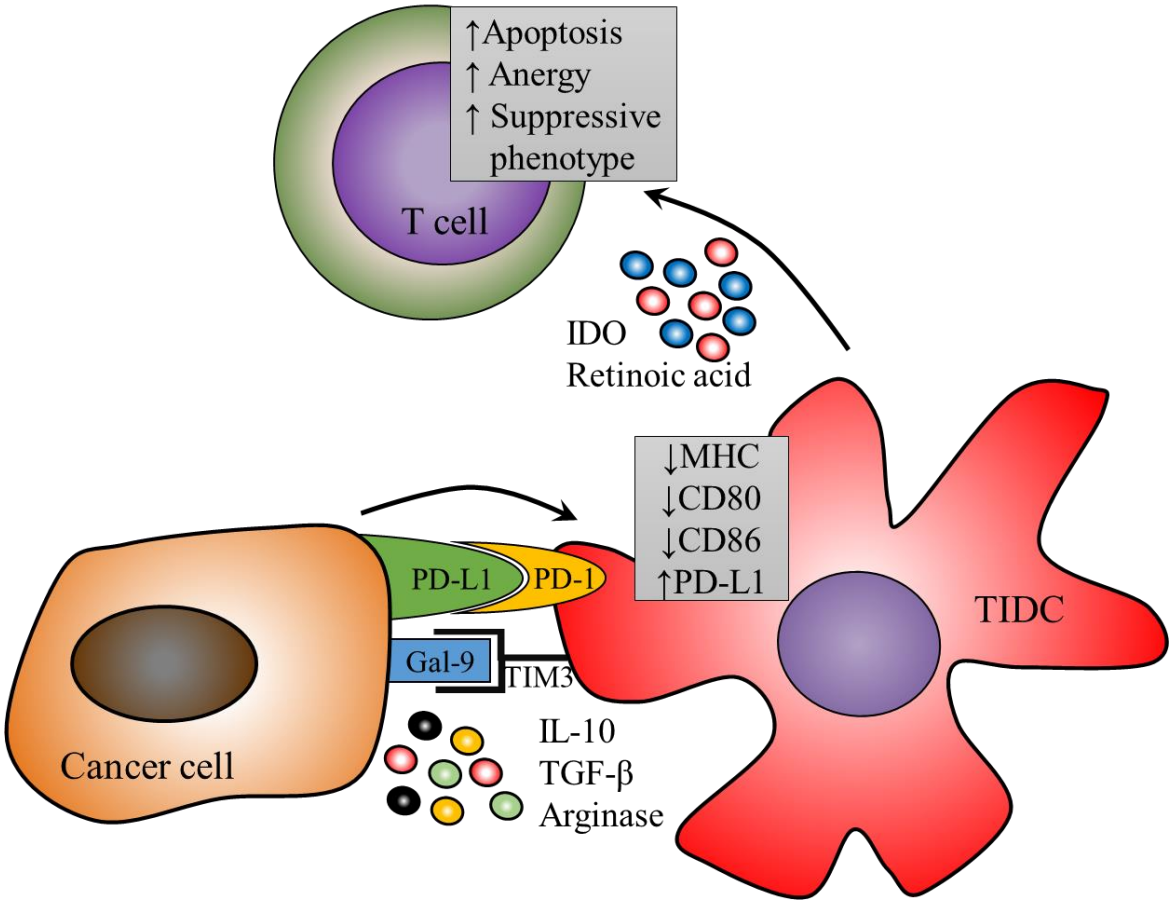


Figure 1.1 Dendritic cells are induced by the TME to up-regulate PD-1 and TIM3 by soluble factors such IL-10, TGF-beta and arginase. In the TME the PD-1/PDL-1 interaction blocks the DC response to danger signals and downregulates the antigen presentation and costimulation molecules. In addition to the lack of appropriate activating signals, T cell responses are blocked by engagement of PD-1/PD-L1 axis on the TIDC surface, resulting in T cell apoptosis, anery and regulatory phenotypes.

TIDC, like many other innate immune cells, are considered to have a degree of phenotype plasticity[49,53]. Following William Coley's principal, some have previously shown that the suppressive phenotype of TIDC can be reversed, to harness adaptive immune response[53,54]. Therefore, stimulating the local APC with the right adjuvant to harness a T_H1 anti-cancer immune response might prove more successful than *ex vivo* DC vaccines. However, a local stimulation of APC should also effectively re-balance the immunity in the tumour to prevent the suppressive TME pitfall of *ex vivo* DC vaccines. Since cytopathic viruses are generally known to promote a strong pro-inflammatory response followed by a T_H1 immune responses[55], it is appealing to consider that oncolytic viruses fulfil this profile, at the same time as they provide tumour antigens from their lytic activity. Evermore, they can locally express immune transgene products if needed, and secrete them from infected tumour cells into the tumour microenvironment.

1.3 Human adenovirus

Human adenoviruses (HAds) were first discovered from adenoids tissue in 1953 by Rowe[56]. Since then 57 subtypes of HAds are arguably accepted and classified into 7 subgroups (A-G) according to their properties[57-59]. The early identification of adenoviruses, was followed by years of thorough investigation to understand their biology. The gathering of knowledge on adenovirus biology along with the availability of of-the-shelf cloning vectors, contributed to engineer these agents for multiple applications, ranging from vaccination to oncolytic virus[60]. Historically, group C human adenoviruses have been the most investigated of all groups, especially subtype Ad2 and Ad5. Therefore, most of the available literature describes the structure and function for these two adenovirus types. Despite the pitfalls, both are used as archetype to describe the adenovirus biology, as it will be the case throughout this thesis.

1.3.1 The structure of human adenovirus

Adenoviruses are non-enveloped double stranded DNA viruses with an organised structural capsid, which core size ranges between 90 to 100nm in diameter. The main structure of the human adenovirus capsid constitutes an icosahedron, formed by 240 homotrimeric hexon (hexon) proteins that form the characteristic 20 faces and 30 edges. On the 12 vertices of the icosahedron, covalently linked complex of homopentameric penton base (penton) are found, from which a homotrimeric fibre proteins (fibre) are projected (Figure 1.2). More virus proteins of smaller size (minor proteins) also interact with the capsid, like for instance proteins: IIIa, VI, VIII and IX[61]. These minor proteins function as the cement between the larger multimeric proteins to rigid the capsid structure. Minor proteins are not only limited to structural roles, some are also involved in virus infection processes. For instance, protein VI promotes the endosome escape after the uptake and protein IX modifies the cellular nuclear structure for the

virus to replicate. The structure and function of the minor adenovirus proteins has been largely reviewed by others[62]. Finally, in the capsid lumen six core proteins are found which maintain double stranded viral DNA associated to the capsid proteins, with the exception of the virus protease.

The most relevant in number of capsid protein in adenovirus is hence the hexon, which might explain why hexon mediate a strong host adaptive immune response[63]. The hexon amino acid identity is widely conserved across serotypes, however, the exposed loops to the external surface of the particle are hypervariable regions (HVR) between subtypes. It has been proposed that the HVR variability between adenovirus subtypes is a strategy to prevent cross-reactivity from host's neutralising antibody of previously exposed subtypes[64]. However, hexon is not the only exposed protein that generates neutralising antibodies.

Fibre is an important functional protein exposed on the external surface of adenovirus. Each fibre protein can be divided into: tail, shaft and knob region. The tail of each fibre contains an N-terminal region that is highly conserved between serotypes and mediates non-covalent binding to a hydrophobic pocket formed between penton base monomers[65]. The shaft of the fibre consists of a variable number of repeating sequences that form anti-parallel strands connected by a β-turn. Importantly, the number of repeats determines fibre length, which can vary between serotype. For example, electron microscopy has determined that Ad3 has very short fibres with only 5.5 pseudo repeats, whereas Ad12 has long fibres with 22.5 pseudo repeats[66]. Insertion of amino acids at specific positions in the β-turns can disrupt the fibre shaft rigidity and create hinge regions that allow flexibility for receptor binding, especially in the KKTK region[67]. At the C-terminal end of the fibre shaft is the globular knob region, which is formed by eight β-barrels that form 3 subunits with a number of variable loops that determine receptor binding[68].

In total, there are around 2,700 polypeptides per adenovirus particle, amounting to a molecular weight of about 1.5 x 10^8 Da[62,69]. This emphasises the complexity of the adenovirus capsid, however, reduced by the highly-organised structure (Figure 1.2), which makes it and efficient infectious agent.

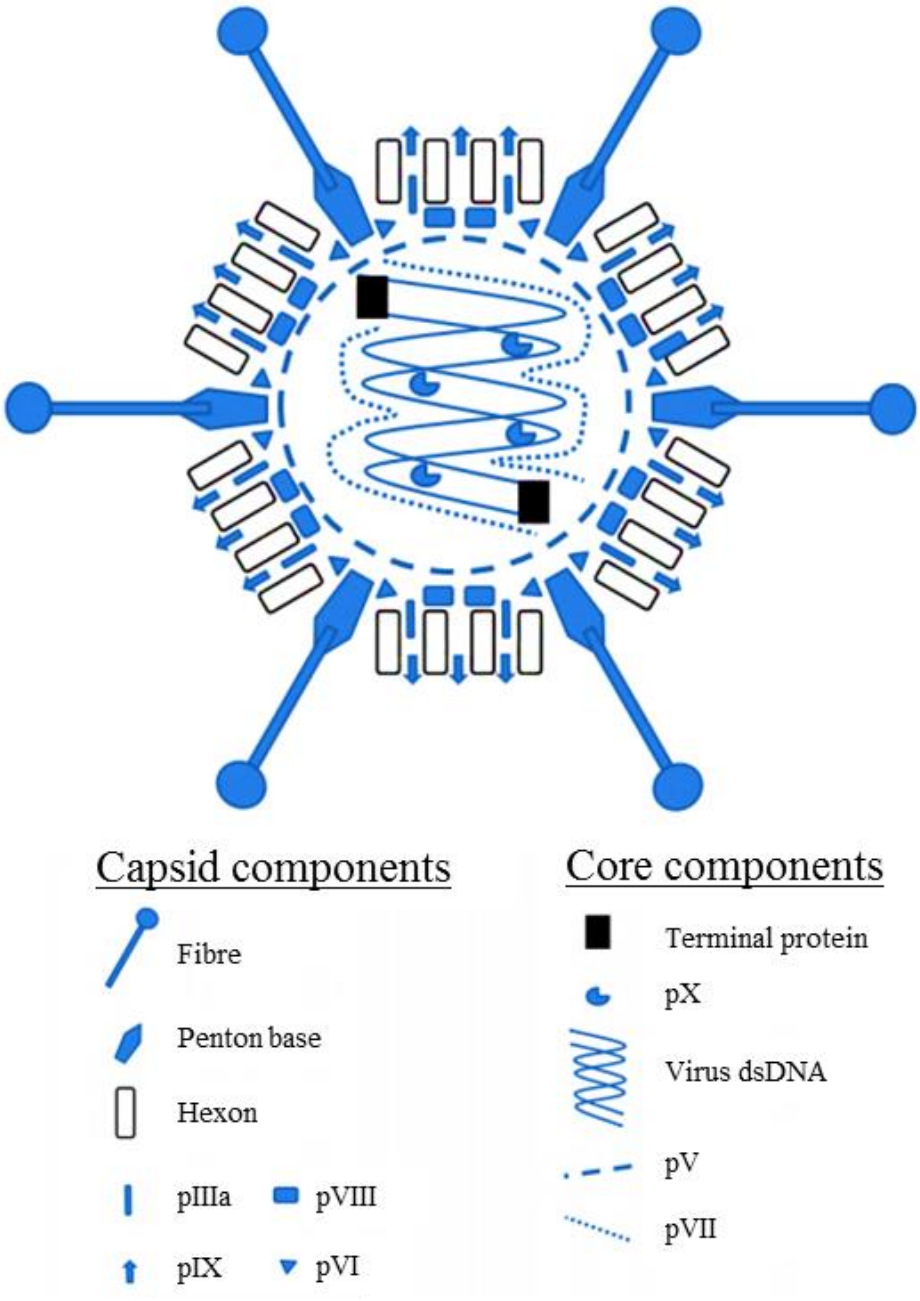


Figure 1.2 Human adenovirus particle structure. Shown are the structural proteins that constitute an imaginary cross-section of the capsid and core (not to scale). Figure adapted from [65] and [69].

1.3.2 The cellular life cycle of human adenovirus

The human adenovirus life cycle is often described in different stages; attachment, internalisation, endosomal escape, nuclear trafficking, replication, packaging and release (Figure 1.3). Although studying the life cycle of tiny particles like adenoviruses is difficult and often controversy is raised, a large amount of literature is particularly available for subtypes Ad2 and Ad5.

1.3.2.1 Cell attachment

Initially, adenovirus binds to the cellular surface receptors thought the fibre knob. Most HAds, groups A, C-F, bind the Coxsackie and adenovirus receptor (CAR)[70,71] via a highly-conserved domain found on the fibre knob. However, different subtypes have been shown in *in vitro* studies to have different affinities for CAR receptor[72]. By contrast, the binding to the cellular receptor is more complex *in vivo* than on *in vitro* monolayers. For instance, CAR appears to be overexpressed during the embryonic stage but the expression fades after birth. Although CAR mRNA can be found at high levels in some tissues in adults[70] CAR is normally located within tight junctions on the basolateral surface of polarised cells, which theatrically should restrict CAR-binding adenoviruses from infecting though apical surface[73,74]. This suggests that CAR detection in tissue might not always predict the adenovirus infection efficiency *in vivo*. In addition, CAR expression actually decreases in some carcinomas such as bladder cancer[75]. Alternatively, group B adenoviruses use CD46 as the primary and main cellular receptor for infection[76], as well as desmoglein-2 (DSG-2)[77]. Since, CD46 expression is found to be overexpressed in many carcinomas[78], it is appealing to think that group B adenoviruses are naturally more tumour selective than CAR-binding HAd.

1.3.2.2 Cell entry and endosome escape

After cell surface attachment, an RGD motif from the penton interacts with αVβ3 and αVβ5 integrins[79], triggering virus internalisation. This integrin binding is thought to shorten the distance between cell and virus, forcing the bending and consequent detachment of the fibre from the virus, which is considered the first step of capsid disassembling. Electron microscopy showed the first evidences that adenovirus internalisation was mediated by clathrin-coated vesicles[80]. Accordingly, cell lines that expressed mutant dynamin, which is required for clathrin-mediated endocytosis, showed infructuous internalisation of adenovirus[81]. Alternatively, group B adenovirus type 35 have been also reported to be internalised by macropinacytosis[82]. After the virus-containing endosome separates from the plasma membrane, the endosomal H+ATPase introduces protons lowering the pH to 6.0. This mildly acid pH further disassembles the capsid exposing the minor protein VI and core protein protease that, along with the penton, disrupt the endosome membrane[83]. After the endosome escape, the dismantled capsid complex with HSP70 and dynein, before traveling towards the minus end of microtubules and the microtubule origin centre (MTOC), usually located next to the cellular nucleus[84].

However, some differences have been highlighted between group C adenoviruses – which rapidly escape the endosome and traffic towards the nucleus shortly after cellular binding – and group B adenoviruses. Although group B adenovirus entry and trafficking are less well characterised. The overall process appears to be slower with particles accumulating in lysosomes located around the cellular nucleus before endosome escape[85] and before then, group B adenoviruses are thought to be capable to be re-exposed to the cell surface[86,87].

It is reasonable to think that the late endosome escape seen with group B adenoviruses is related with their lower pH requirements to lyse endosome membrane compared to group C[88]. It wouldn't be surprising that this difference results from the use of different cellular receptor

attachment and corresponding intracellular trafficking route[86]. In fact, the evidence seem to suggest that group B adenovirus can follow two CD46 internalisation and trafficking pathway depending on multiple factors like cell type and multiplicity of infection[82]. CD46 is constitutively recycled via clathrin-coated pits to peri-nuclear multi-vesicular bodies, which can later be re-exposed to the cell surface. Alternatively, CD46 can be internalised via a macropinocytosis-like process upon severe cross-linking. The clathrin-independent pathway leads to receptor degradation in late endosomes resulting in CD46 downregulation[89].

1.3.2.3 Nuclear import, early genome transcription and genome replication

The virions travelling towards MTOC, come to close distance with the cellular nucleus. At this point, NUp214 on the cytoplasmic side of the nuclear pore complex (NPC) docks to the hexon. It is thought that the forces derived from the motor proteins carrying the virus along the tubules and the docking to the NPC that finally disassemble the partially disrupted capsids, liberating the viral genome along with the viral core proteins in the NPC vicinity. The viral core proteins, especially protein VII, along with cellular factors and nuclear transport receptor will mediate the nuclear import[90]. Once the virus genome has entered the nucleus, E1A genes will be transcribed under their constitutively active promoter as single pre-mRNA, which is alternatively spliced in to two products that are translated into protein 12S and 13S. Both proteins display highly conserved regions across adenovirus serotypes. These proteins bind to the tumour suppressor protein pRb, releasing the E2F factor which drives the expression of E2F-dependent cellular and early virus genes (E2, E3 and E4)[91]. Adenovirus E1A genes have multiple functions fundamental to the virus for taking control of cellular processes, these have been comprehensively reviewed[92].

The E2 pre-terminal protein (pTP) and adenovirus polymerase (AdPol) are subsequently expressed. Initially, pTP and AdPol complex together before recognising the 5’ inverted

terminal repeat (ITR), and along with other cellular transcription factors, the protein-primed DNA synthesis begins [93]. The pTP will stay covalently bound to the 5′ end of the newly synthesised viral genomes where it will remain throughout the viral cycle, whilst AdPol elongates the replication (reviewed by Hoeben[93]). But also, pTP will ensures viral genomes are located in the nuclear punctuated patterns[94], where the viral replication machinery is found[95]. In subsequent stages of viral life cycle pTP is cleaved into intermediates and finally to mature PT version[96]. Several roles have been suggested to intermediates and PT, in example virus infectivity, nuclear genome re-localisation and in some extension packaging of *de novo* virus[96-98]. Overall, TP – and its multiple intermediates – appears to organise the viral genome in nuclear sub-localisation for each virus cycle phase.

1.3.2.4 Late virus gene expression and virus particle release

Late adenovirus proteins are transcribed as a long single mRNA under the major late promoter (MLP) and later spliced in multiple products. Most of which are translated into capsid proteins used for the packaging of adenovirus progeny. Late mRNAs are preferentially translated over host cell proteins thanks to the tripartite leader sequence found in the MLP. The role of the tripartite leader is to load the virus mRNA into the ribosome for a cap-independent translation, through a mechanism known as ribosome shunting[99]. The late proteins are then transported back into the nucleus into what appears to be quite an organised process. Within the nucleus, the structural proteins accumulate near the replication machinery in the punctuated pattern creating large and regular structures perceived as crystals in electronic microscopy[100]. It is believed that immature empty capsids are formed from the margins of these structures. Further maturation, involving the adenovirus protease, package the adenoviral DNA into the capsids[100-102]. Fully mature packaged adenovirus particles gather in the cell before the release by a lytic process which involves the adenovirus death protein (ADP)[103]. Although not every human

adenovirus subtype expresses this protein, for example some group B adenoviruses. Hence the release process is relatively poor understood.

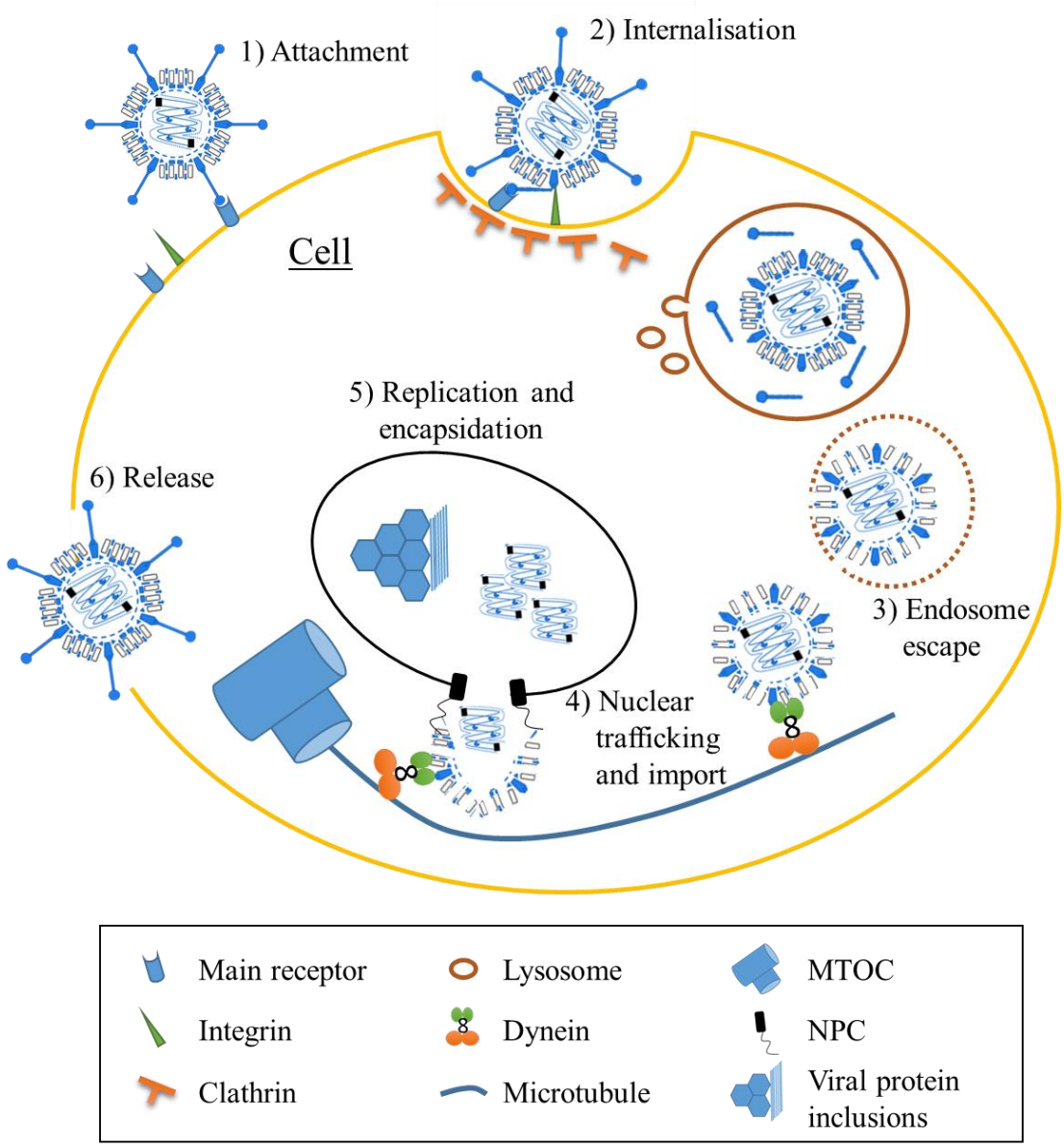


Figure 1.3 Adenovirus 5 lifecycle. Adenovirus infection begins with the attachment to cellular receptors (1), followed by internalisation (2) with subsequent escape from the endosome (3) and trafficking of the partially dismantled capsid along microtubules towards the microtubule organising centre (MTOC) located next to the nucleus (4). By docking to specific proteins of the nuclear pore complex (NPC), the capsid is disrupted and adenoviral DNA is transported into the nucleus where early viral genes are transcribed and after expression of the early viral genes, DNA replication occurs before the late viral proteins are expressed and imported into the nucleus where particles are encapsidated (5) and released (6).

1.3.2.5 Immune response to adenovirus infection

Many innate sensing pathways, like cytosolic STING pathway and endosome TLR9, have been described to recognise different pathogen-associated molecular patterns from adenovirus type 5, as largely reviewed by Hendrickx *et* al.[104]. In addition, Ad5 like adenovirus in general, have a lytic cycle, which means multiple cellular stress signals (also known as danger-associated molecular patterns) are released to the cytosol environment. Both pathogen-associated molecular patterns (PAMPs) and damage-associated molecular patterns (DAMPs) are well known to activate strong pro-inflammatory response on APCs and other innate cells, which intermediates the adaptive immune response against the viruses[105]. This may explain the high prevalence of neutralising antibodies in the population against Ad5[106].

The strong immune response along with its genome versatility, have rendered Ad5 an appealing vaccine vector. Ad5 has been heavily developed as a vaccine platform in human large-scale immunization studies. However, the vectors used for immunization are often E1 and E3 deleted[60]. The deletion of E1 prevents the virus from replicating in the infected cell, preventing the generation of DAMPs. On the other hand, the E3 deletion renders the virus more immunogenic, which are early expressed during the viral infection to counteract host's anti-viral immune responses. Multiple functions have been described for E3 proteins, for instance supressing the transcription factors that mediate the pro-inflammatory response or by preventing infected cells from being recognised and killed by adaptive immunity (largely reviewed by Lichtenstein *et* al.[107]).

1.4 Viruses and cancer

From early on viruses have contributed to the broad knowledge we have gathered on the initiation and progression of malignancies. Initial studies with retroviruses and DNA viruses known to induce tumours in animals, resulted with the discovery of oncogenes and cancer suppressor genes[108]. This triggered the investigation in humans to discover new inherent genes involved in the process of cancer, leading to the identification of several oncogenes and tumour suppressor genes[109]. Studying the cellular consequences of these genetic changes has led to the realisation that cancer cells exhibit quite different biology form normal cells, the so-called 'hallmarks' of cancer. They include the ability of transforming cells to maintain cell proliferation without growth factors while being insensitive to inhibitory signals, to prevent cellular apoptosis, encouraging vasculature growth and tissue invasion[28].

However, most lytic DNA viruses generally do not generate tumours. Due to their intracellular parasite condition, they transiently take control of the host cell to use the cellular resources for their own growth. It is interesting to note that many of virus requirements in normal cells are shared with the phenotype of cancer cells, as reviewed by[110]. Metabolically, both viruses and cancer cells need nucleotides, amino acids and lipids – specially for enveloped viruses – to grow. They also control the replication machinery and nutrient-sensing mTOR pathway to stimulate DNA replication and protein translation. At the same time, they inhibit the apoptosis to prevent cell death induced by stress responses. Similarly, viruses and tumour cells try to delay and evade immune destruction. For example, hiding the antigens by downregulating major histocompatibility molecules from the cell surface[107] or express molecules that supress or attenuate immune responses[111].

Summarising, the hallmarks of cancer and normal virus biology are closely related, it is unsurprising that tumour cells are often extremely suitable milieus for viruses to thrive. For

this reason, the oncotropism of viruses has been exploited therapeutically in cancer patients for many years.

1.4.1 Oncolytic virotherapy

The first written reports describing spontaneous cancer remission after some infectious disease date back to 19th century (1829 Guillaume Dupuytren)[112]. However, the oncolytic virotherapy concept was not coined until early-20th century, were several incidences of spontaneous tumour regression was associated with exposure to viruses, perhaps most notably in shrinkages of Burkitt's lymphoma in individuals who had been vaccinated for measles[113]. This led to the suggestion that wildtype viruses could have oncotropism and directly kill cancer cells. Under this premise, several historically significant clinical investigations were performed using wildtype viruses, such as hepatitis B viruses, West Nile virus, adenoviruses or mumps virus, on different types of cancers, including haematological malignancies and solid tumours. Few regressions were observed[112]. In 1956, Smith *et* al. reported that they had administered wildtype adenovirus to cervical cancer patients, and 65% of inoculations showed tumour necrosis without affecting healthy tissues[114]. At that time, most of the studies administered a single type of wildtype virus to cancer patients. With the gathering of knowledge on virus biology and the implementation of molecular biology techniques, sophisticated viruses were engineered to improve the selectivity for cancer cells, to remove oncogenic genes or enhance the oncolytic potency[115]. More recently, and with immunotherapy on the rise, virotherapy has been suggested to have a second cytotoxic mechanism; promoting immune-mediated cancer killing. More precisely, it is thought that the oncolysis provides tumour antigens and danger-associated molecular patterns, together with the virus natural pro-inflammatory profile, rebalances the immunity in the TME and can promote an anti-tumour vaccination at the same time. Talimogene laherparepvec (T-VEC or commercially known as Imlygic), which encodes an

immunomodulatory transgene, was the first OV to produce convincing human data supporting the idea that direct tumour lysis by a replicating virus locally stimulated anti-tumour immune responses to provide systemic, long lasting, cancer killing immune responses in patients with advanced cancer[116,117]. More recently, data from multiple clinical trials using a wildtype coxsackievirus OV, either as standalone therapy or in combination with checkpoint inhibitors, has shown non-injected metastasis reduction after T cell infiltration and without signs of virus activity[118-120].

1.4.1.1 Wildtype viruses with intrinsic oncotropism

Multiple wildtype viruses that do not grow well in healthy cells have been shown to have oncotropism. Initially, the difference was associated with an up-regulation of the cellular receptors on cancer cells. Different cellular receptors used by viruses were found to be differentially expressed between cancer cells and normal cells. For example, the Edmonston strain of measles virus (Edm-MV) naturally infects via the cell surface receptor CD46[121]. CD46 is commonly overexpressed in many tumours probably as a protective mechanism against complement-mediated cell death[78]. Similar examples exist for poliovirus, which infects via nectin-like molecule 5 (NECL-5), a receptor that is upregulated on glial, colorectal, breast, lung and hepatocellular carcinomas[122]. Coxsackievirus A21 infects via intracellular adhesion molecule 1 (ICAM-1) and/or decay-accelerating factor (DAF), both receptors are upregulated on malignant melanoma and breast cancer cells[123]. The surface cellular expression of virus receptors are crucial for virus entry into the target cell, and a differential expression pattern between malignant and healthy cells is likely to determine some level of tumour cell selectivity. However, the receptor expression alone cannot guarantee successful virus infection and propagation.

Many oncolytic viruses show increased intracellular activity in tumour cells relative to normal cells. In part this is because cancer cells often shutdown the signalling pathways involved in sensing DNA damage, and this can lead on to a loss of ability to detect virus infection. For example, several RNA viruses are able to replicate more successfully within tumour cells without having to spend energy controlling the innate antiviral defence. Vesicular stomatitis virus (VSV), Seneca Valley virus (SVV) and Newcastle disease virus (NDV) have natural selectivity for tumour cells defective in interferon signalling pathway[124-126] (Table 1.1). This might also apply to other RNA viruses shown with oncolytic properties, for instance Enterovirus, Mumps and West Nile virus (WNV), also enjoy from this defect (Table 1.1).

In other settings, up-regulated signalling pathways can also contribute towards productive virus replication in cancer cells. For example, reovirus and herpes simplex virus 1 (HSV-1) are reported to replicate better in tumour cells that have an activated Ras signalling pathway[127,128]. Equally, Myxoma virus shows natural selectivity for cells with up-regulated PI3K-Akt signalling pathway[129], a feature commonly found in human malignancies[130]. These exemplifications highlight the inherent susceptibility and the corresponding mutations of some cancers responsible for the natural selectivity of some wildtype viruses.

1.4.1.2 Genetically modified viruses to improve the selectivity for cancer cells

Better understanding of cancer biology, virology and the advent of virus reverse engineering promoted the design of genetically-modified tumour-selective viruses with attenuated replication in normal cells. Initially this was accomplished by removing genes necessary to the virus for efficient growth in healthy cells. ONYX-015 was originally engineered so it would selectively grow in p53-defective cancer cells. This was envisaged because early after infection adenovirus normally express the E1B-55K protein. E1B-55K associates and inhibits the nuclear factor p53 to prevent a cell-driven apoptosis when virus infection is sensed. It was

hypothesised that deleting the E1B-55K gene, ONYX-015 replication would be restricted to cells with mutant p53 pathways[131], a frequent occurrence in human tumours[132]. By way of validation, ONYX-015 was shown to replicate in multiple cancer cell lines with mutant p53 pathways. In contraposition, no replication was seen in healthy cells with ONYX-015, compared with the wildtype Ad5[133]. Later it was discovered that ONYX-015 replication in cancer cells was largely independent of p53 pathway status[134]. Instead, it was dependent on the enhanced nuclear export of late adenovirus mRNAs in tumour cells[135], which encode the virus capsid proteins necessary to produce infectious particles. Irrespective of the mechanism for ONYX-015 selectivity, this OV advanced to clinical trials (section 1.4.1.5); where selective replication was observed in several tumours with an attenuated activity on normal cells[136]. This observation established the concept that thoughtfully attenuated viruses can show increased therapeutic index in cancer treatment.

Similarly, OncoVex, a herpes simplex virus-1 (HSV-1) with a deletion in the virus *γ34.5* gene that encodes the ICP34.5 protein, is an OV with attenuated replication in normal cells. ICP34.5 inhibits the innate antiviral response of infected cells by binding to protein phosphatase 1 (PP1) and facilitates the dephosphorylation of the eukaryotic initiation factor 2 alpha (eIF2α). Protein kinase R (PKR) has opposing activity and is capable of phosphorylating eIF2α in response to binding intracellular double stranded RNA, however PKR is often defective in tumour cells. Phosphorylation of eIF2α inactivates translation initiation, which inhibits protein synthesis and prevents viral replication. Therefore, in virally infected normal cells, with intact PKR anti-viral signalling pathways, replication is attenuated when HSV-1 lacks the ICP34.5 protein[137]. Additionally, OncoVex has aberrant US12 gene which encodes for ICP47. ICP47, like protein 19K coded in adenovirus 5 E3 region[107], specifically binds to transporters associated with antigen processing (TAP), preventing viral antigens from being loaded on the MHC-I[138]. The

deletion of these genes in HSV-1 and adenoviruses have been used so OVs are rapidly cleared by cytotoxic CD8 T cells when infecting cells in a healthy immune microenvironment.

For nuclear-living DNA viruses, an alternative approach to ensure OV selectively grow in cancer cells, is the usage of tissue or tumour specific promoters replacing key virus promoter/s vital for activating the virus replication, thereby taking advantage of cellular transcription factors to regulate virus activity. This strategy has been used most successfully in adenovirus[139]. For instance, CG7060 is an oncolytic adenovirus whose replication was designed to be controlled by the prostate-specific antigen (PSA) specific promoter-enhancer element. This was intended to permit virus activity in prostate tissue where PSA is particularly highly expressed[140,141]. Furthermore, the replication of the OV CG7870 was controlled by both tissue specific elements; the prostate specific rat probasin promoter and the PSA promoter-enhancer, replacing the adenovirus E1A and E1B gene promoters respectively[142]. Another OV to use tumour specific promoters is CG0070, a replication competent adenovirus that contains the human telomerase reverse transcriptase (hTERT) promoter element in control of viral E1 expression[143]. hTERT gene is commonly up-regulated in many cancer cells, in contrast to healthy differentiated cells[144].

Oncolytic viruses with attenuated activity in healthy cells and selective replication in tumour cells, have greatly contributed to demonstrating the excellent safety profile that genetically modified viruses can achieve in the clinics (section 1.4.1.5). However, the poor anti-tumour efficacy shown by most of these OV displayed in clinical trials, highlighted the need for further improvements in potency. To this end, OVs have been genetically modified to encode transgenes that express their genetic payloads selectively inside the tumour. The payloads can either be directly cytotoxic or mediate cytotoxicity by conversion of a given prodrug. Other encoded transgenes simply express genes that promote immune-killing.

1.4.1.3 Genetically modified viruses to express therapeutic payloads to improve the anti-tumour efficacy

Oncolytic viruses expressing enzyme payloads that make cancer cells sensitive to prodrugs – otherwise known as virus-directed enzyme-prodrug therapy (VDEPT) or suicide therapy – might be closer to gene therapy than oncolytic virotherapy, reviewed in[145]. Two suicide gene strategies have been largely used in combination with OVs to improve anti-tumour efficacy; 1) the HSV thymidine kinase (TK), rendering cells that express the payload sensitive to Ganciclovir and 2) the cytosine deaminase (CD), rendering cells that express the payload sensitive to 5- fluorocytosine (5-FC).

The goal of suicide oncolytic therapy is to improve the OV's anti-tumour efficacy by inducing a direct cell killing on the infected tumour cells. An alternative approach and probably more appealing, is to encode OVs with payloads that can promote the immune system to destroy cancer cells, including tumour cells that are not virally infected. Accordingly, multiple transgenes encoding immunomodulatory agents have been inserted into OVs, as reviewed by [146]. Thus far, granulocyte-macrophage colony-stimulating factor (GM-CSF) has been the most fruitful immune-mediator agent encoded into an OV. T-VEC (formerly OncoVex^{GM-CSF}) is an oncolytic virus based on the OncoVex backbone (section 1.4.1.2) engineered to express GM-CSF in tumour cells. The expression of the transgene was shown to enhance the anti-tumour properties of T-VEC[147]. Importantly, in phase III clinical trials in melanoma patients, intra-tumour injection of T-VEC showed tumour destruction of distant non-injected metastasis, indicating immune-mediated systemic effects[116]. In October 2015, T-VEC gained marketing authorisation from the American Food and Drug Administration (FDA). Ever since, oncolytic viruses have commanded increased attention from the cancer immunotherapy field for local expression of immunomodulatory agents or in co-administration with standard therapeutics. Following this trend, a variety of 'next generation' oncolytic viruses, armed to express various

transgenes, are currently being tested in clinical trials to enhance the therapeutic effect of the checkpoint inhibitors antibodies, reviewed by Russell *et* al.[148]. Some of the most interesting and relevant agents are displayed in Table 1.1.

1.4.1.4 Bioselection of oncolytic viruses using cancer cell lines

The rationally designed oncolytic viruses described in previous sections usually have an increased therapeutic index, largely as a result of their marked attenuation on healthy cells. However, the attenuation often slightly reduces the virus activity in cancer cells, limiting the oncolytic potency of the rationally designed OV. Alternatively, in a process of bioselection (also known as directed evolution) viruses are cultured in cancer cells under a selection pressure, at the same time random mutations are encouraged. This strategy allows viruses to adapt to their environment (cancer cells), as they naturally do in the ecosystem. However, the mutations are artificially directed and selected for an increase of oncolytic potency. The resulting pool of potent OVs, are then selected for their attenuated replication in normal cells. In general, different methods from chemically-induced[149] to altered virus DNA polymerase[149], have been used to promote genetic mutation, but the concept of selection based on the desired phenotype remains the same.

Enadenotucirev (EnAd, formerly ColoAd1) is an example of an oncolytic virus generated by bioselection. Interestingly, the mutations to generate EnAd, were promoted by super-infecting the colon cancer cell line HT29 with an array of adenoviruses from different serotypes. This produced a highly diverse library of recombinant viruses, in which redundant genomic information for survival in this cancer cell line was probably not selected for. The recombinant virus library was then placed under stringent directed selection for fast replication and early release from cells by repeated passage on HT29 cells, using early supernatants to infect the next flask of cells. From a handful of potent oncolytic viruses, EnAd was finally selected for

its oncolytic potency on a range of cancer cells coupled with its low activity on non-transformed cells[6].

1.4.1.5 Oncolytic viruses and clinical trials

Some of the OV presented in the sections above have now advanced through clinical trials, with varying degrees of success. Table 1.1 displays the most relevant OVs assayed in clinical trials, together with their corresponding oncotropism strategy. A comprehensive review of ongoing clinical trials using OVs has been written by[150].

The first studies regarded as real clinical trials were conducted by Onyx in the 1990s, exploring the activity of genetically engineered ONYX-015 (described earlier in section 1.4.1.2). ONYX-015 was initially given as a standalone treatment to humans with head and neck cancer. The virus showed good tolerability, as no maximally tolerated dose was reached by intratumour administration, and virus replication was localised to tumour tissue[151]. However, the anti-tumour activity of ONYX-015 as monotherapy was somewhat disappointing[152,153]. Subsequently, ONYX-015 showed better results in combination with chemotherapy for patients with head and neck cancer, achieving tumour regression (>50%) in approximately 63 percent of treated patients, whereas complete responses were observed in 27% of patients[154]. Despite the encouraging results in combination treatment, safety concerns were raised over adenovirus-based therapeutics after the death of a relatively healthy teenager treated for gene therapy for ornithine transcarbamylase (OTC) deficiency with an adenovirus vector[155], and development of ONYX-015 was terminated after no prospects emerged to find a partner company. Sunway Biotech, a Chinese company rebranded ONYX-015 to H101 and deleted the E3 region to increase its safety profile. In phase III clinical trial, H101 showed significant tumour regression for OV in combination with cisplatin and 5-fluorouracil compared to the

control arm[156]. H101 gained approval from Chinese authorities for use of late stage head and neck malignancies, becoming the first OV to receive a licensing approval for human use.

As mentioned in the previous section, in 2015 Amgen was granted FDA marketing authorisation for commercial sale of T-VEC, after phase III clinical trial successfully achieved significantly better clinical primary end point (durable response rate) and increased secondary end points (overall survival and overall response rate) than the GM-CSF arm for the treatment of malignant melanoma[157]. This proved as an important launch pad for the oncolytic virotherapy field and follows from the success of the H101.

Onco-tropism	Virus type	Mechanism for selective replication	OV (mechanism for selective replication)	Transgene	Treatment combination
Naturally occurring	Enterovirus	Probably exploiting the innate antiviral defects.	RIGVIR	N/A	N/A
	NDV		wt	N/A	N/A
	Mumps		wt	N/A	N/A
	WNV		wt	N/A	N/A
	VSV	Defective IFN pathway	wt	N/A	N/A
	SVV	PKR/IFN pathway	NTX-010	N/A	N/A
	Reovirus	Ras-activated	Reolysin	N/A	Chemotherapy Immunotherapy
	Measles Virus	A) CD46 overexpression. B) Defects innate antiviral defence.	MV-Edm (A+B)	NIS CEA	Chemotherapy Immunotherapy
	Coxsackie virus	A) ICAM-1/DAF overexpression. B) Probably exploiting the innate antiviral defects.	Cavatack (A+B)	N/A	Chemotherapy Immunotherapy
Engineered	Adenovirus	A) Defects in p53 or RB pathway and mRNA export B) E3 deletion acts immune-stimulant. C) RGD modification targets integrins. D) E2F-1, hTERT or tissue-specific promoter-enhancer elements control viral replication.	ONYX-015 (Ad5 with A)	CD/TK	Prodrug
			H101 (Ad5 with A+B)	N/A	N/A
			DNX-2401 (Ad5 with A+C)	N/A	Immunotherapy
			SSTR/TK (ad5 with A+B+C)	SSTR/TK	Prodrug
			CG0070 (Ad5 with A+D)	GM-CSF	N/A
			ONCOS-102 (Ad5:Ad3 with A)	GM-CSF	Chemotherapy Immunotherapy
			ICOVIR-17 (Ad5 with A+C+D)	HAase	Chemotherapy
	Poliovirus	A) NECL-5 overexpression B) Pathogenic polio IRES replaced with rhinovirus IRES	PV1(RIPO) (PV:HRV2 A+B)	N/A	Chemotherapy Immunotherapy
	Vaccinia	A) TK deletion compensated by nucleotide abundance. B) VGF deletions compensated by aberrant EGFR receptor activation. C) Large size requires leaky vessels for viral extravasation.	vvDD (A+B+C)	GFP	N/A
			GL-ONC1 (A+C)	Luciferase	Chemoradiation Immunotherapy
			Pexa-Vec (A+C)	GM-CSF	Angiogenesis inhibitor
	HSV-1	A) HSV-TK and RR mutations compensated by activated cell cycle. B) PKR defects allow γ34.5 deleted HSV to replicate. C) ICP47 deletion acts immune-stimulatory.	Dlsptk (A)	N/A	N/A
			SEPREHVIR (B)	N/A	Immunotherapy
			G207 (B+C + NIG-)	CP450	Chemotherapy Immunotherapy Pro-drugs
			T-VEC (B + C)	GM-CSF	Immunotherapy Chemotherapy
Bio-selected	Adenovirus	A) CD46 overexpression. B) E3 deletion acts immune-stimulant.	EnAd (Ad11p:Ad3 with A+B)	Luciferase GFP Anti-VGF	Chemotherapy Immunotherapy

Table 1.1 OVs that have been or are being tested in clinical trials are sorted by their origin of oncotropism and shown with their individual mechanism for selective replication in cancer cells. Table combined from [148] and [158].

1.4.1.6 The limitations of oncolytic viruses

Development of the oncolytic virotherapy field is thought to have been hampered by multiple hurdles. Most notably the difficulty of delivering enough therapeutic agent to disseminated tumours, the intratumoural physical barriers limiting virus percolation and spread and the anti-virus immunity, especially pre-existing humoral immunity, that prevents effective intravenous delivery.

The majority of OVs discussed in previous sections have been administered by direct intratumoral injection. However, the problem with this approach is that non-injected and metastatic lesions will most likely not be reached. To overcome this limitation and target metastasis, some OV have been intravenously (IV) administrated with the aim of delivering virus particles through the disorganised endothelia of tumour vasculature, like for example reovirus and Pexa-Vec (Table 1.1). Although the IV delivery of latter was controversial[159], as reports claim that vaccinia virus are rapidly destroyed by complement opsonisation when in blood stream.

The bioavailability of oncolytic virus when in the blood stream can be diminished before reaching the tumour with undesired off-target effects. Adenovirus, especially Ad5, is well known to be effectively opsonised by plasma factors such as factor X, complement proteins and immunoglobulins (Ig). These molecules are known to bridge the adenovirus to blood cells such as erythrocyte via complement receptor 1 (CR1) and to monocytes via receptors for the Fc portion of IgG (FcγR), or to hepatocytes via heparan sulphate proteoglycans (HSPG). Also, adenovirus can directly bind to Kuppfer cells via scavenger receptors. In Figure 1.4, the interactions of adenoviruses in the blood stream are summarised from comprehensive reviews[160,161].

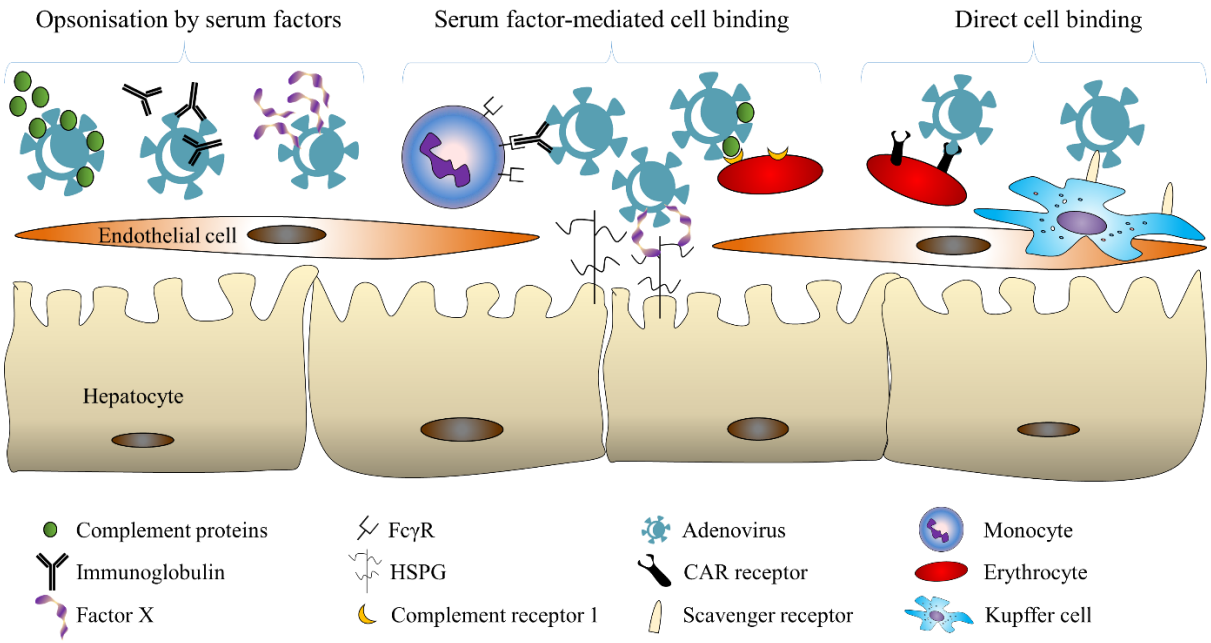


Figure 1.4 Host factors and cells that bind to Ad5 in blood stream, known to limit the virus bioavailability for IV delivery route. FcγR, Fc gamma receptor; HSPG, heparan sulphate proteoglycans.

However, pre-existing neutralising antibodies are probably the most notable element to hamper the number of adenovirus particles circulating in the bloodstream. This has been largely documented for adenovirus 5, against which a large proportion of humans have neutralising antibodies[106]. However, other adenovirus subtypes have lower levels of pre-existing neutralising antibodies, for instance some types from group B[162]. In addition, the expression of CAR receptor on human erythrocytes is known to rapidly limit the amount of group C adenovirus reaching the tumour compared to non-CAR binding adenoviruses, such as serotype B[163]. These renders group B-based oncolytic adenoviruses more appealing for IV delivery. In fact, group B oncolytic adenovirus EnAd (see section 1.4.1.4, Table 1.1), which is under clinical trial assessment for IV delivery, has demonstrated that 20-30% cancer cells stain positive for the virus through this route[7].

Once viruses extravasates into the tumour they encounter stroma and extracellular matrix (ECM) that can prevent the virus from spreading throughout the bulk of the tumour. Some OVs have been encoded with enzymes specially to degrade the ECM. For instance, ICOVIR-17

(Table 1.1) is an adenovirus 5-based oncolytic virus that has been encoded with the human hyaluronidase to degrade ECM. The transgene improves the anti-tumour efficacy in *in vivo* assays relative to the un-armed virus[164]. Alternatively, EnAd has been armed with a human Actin-resistant DNAse I enzyme showing improved intratumour spread and reduced tumour growth in *in vivo* studies[165].

1.5 The oncolytic adenovirus Enadenotucirev

As discussed in previous sections, a large variety of viruses have been used as oncolytic agents. However, the type of virus and delivery route remain important according to the type of cancer. Adenoviruses have been genetically the most versatile OV and probably one of the most largely tested in humans showing great safety profiles. The oncolytic adenovirus EnAd (sections 1.4.1.4 and 1.4.1.6), currently under assessment in multiple clinical trial phase Ia/b for metastatic carcinomas, is probably the first OV to have shown tumour delivery via IV route. The replication of EnAd in cancer cells was followed by a strong tumour infiltration of cytotoxic CD8 T cells[7]. Currently, EnAd might appear as first in class oncolytic adenovirus for treatment of disseminated cancer.

1.5.1 The genomic structure of EnAd virus

EnAd genome contains three large modification relative to Ad11p (Figure 1.5), which is considered the parental virus as they share 98.6% sequence identity[6]. The genetic differences between Ad11p and the commonly studied Ad5 have been reviewed[166,167] and are summarised in Table 1.2 and Table 1.3.

	Ad5	Ad11p	EnAd
Accession number	AC_000008	AY_598970	N/A
Length (bp)	35935	34794	32322
GC content (%)	55.19	48.87	50.00
Fibre type (cellular receptor)	Long (CAR)	Short (CD46 and DSG-2)	Short (CD46 and DSG-2)
Seroprevalence (%)	> 50	< 10	N/A

Table 1.2 Basic differences between commonly used wildtype Ad5, Ad11p and EnAd adapted from [168] and [6].

The first genomic modification of EnAd, starting from the left-hand side of its genome (Figure 1.5), is the frequent substitutions for Ad3 in the E2B region (Table 1.3). E2B region encodes the pre-terminal protein and the adenovirus DNA polymerase, involved in viral replication as

seen in section 1.4.2.3. This mutation has been hypothesised to enhance pTP and viral DNA polymerase activity [6].

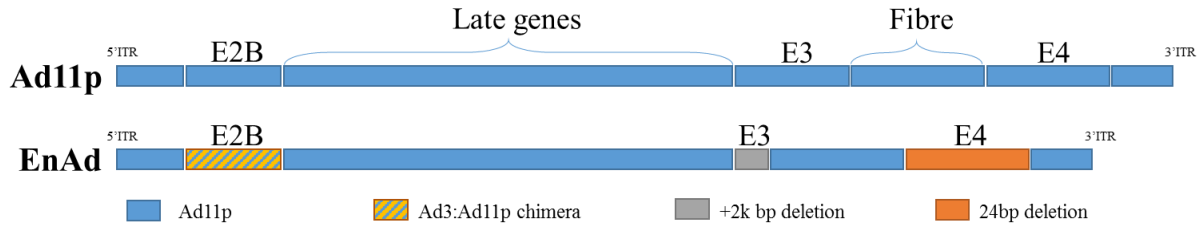


Figure 1.5 Diagram of Ad11p and EnAd virus genome indicating the 3 genetic mutations.

Following the previous order, the second genomic mutation of EnAd is a large deletion in E3 (Figure 1.5). E3 proteins are generally thought to be not essential for growing adenovirus in the laboratory, as this region is commonly lost when adenoviruses are cultured *in vitro* on cell lines without the pressure of the immune system[169]. As seen in sections 1.3.2.5, E3 proteins prevent rapid clearance by host's immune response. Five E3 proteins from Ad5 are found in Ad11p, however the amino acid identity of these proteins lay at the lower end of all shared viral proteins[166]. In addition, E3 20.3kD and 20.6kD proteins with unknown functions, are only found in group B virus[170,171] (Table 1.3), whilst adenovirus death protein (ADP) is missing in this group[168]. TATA box motives control E3 expression in both virus, however, Ad11 E3 regions is transcribed into a single mRNA, whereas Ad5 produces two. In extension, Ad5 E3 has been described to have nuclear factor kappa-light-chain-enhancer of activated B cells (NF-kB) binding sites up-stream E3 to enhance RNA polymerase docking[172]. The +2Kbp deletion in EnAd's E3 region affects several open reading frames, without altering the promoter elements. Only the two first ORF, 12.1K and 16.1K, sequence are unaltered, but have not been described for any previous function. Also, the deletion merged the N-terminal sequence of 18.5K to C-terminal sequence of 15.3K, leaving a chimeric ORF. It is likely that the EnAd E3 deletions affects the ability of the virus to control the host's anti-viral immune response.

Consequently, this might increase the virus selectivity for cancer cells with suppressive TME or potentially benefit the oncolytic immunotherapy.

The third genomic mutation of EnAd is a 24bp small within-reading-frame deletion found on E4-open reading frame (ORF)4 (Figure 1.5). The E4-ORF4 functions have generally been described from Ad5. However, the amino acid (aa) sequence identity between Ad5 and Ad11 E4-ORF4 is only 55.7%, and it is likely that E4-ORF4 have divergent functions between both viruses. Before describing the E4-ORF4 functions, it must be reminded that E4 is a complex region thought to be severely spliced in multiple products depending to the stage of the virus infection[173]. This may reflect the multiple functions attributed to the different ORFs of this region.

E4-ORF4 protein is known to localises inside the cellular nucleus, where it contributes to switch between the transcription of early to late adenoviral genes. Also, E4-ORF4 has been shown to inhibit E1A induced transcription by dephosphorylating transcription factors involved in E1A induced transactivation of early genes, including JunB and c-Fos components of AP-1[174]. The inhibition of E1A transcription is in turn partly responsible for the down regulation of E2 and E4 gene transcription[175]. In addition, E4-ORF4 appeared to help regulate adenovirus genome replication, although point mutation viruses showed is not essential for virus replication[175,176]. In addition, E4-ORF4 induce synthesis-phase in the infected cell needed for virus growth by activating mTOR pathway[177,178]. Finally, E4-ORF4 is known to interact with the regulatory subunit of protein phosphatase 2A (PP2A)[179]. which complex is thought to dephosphorylates SR proteins that are responsible for alternative splicing of late adenoviral mRNAs[180].

However, ORF4 mutation might have extended effects on EnAd biology. Ad5 encodes for an ORF6 downstream from E4-ORF4, that shares 68.6% aa identity with EnAd. A broad range of functions have also been attributed to E4-ORF6 either alone or in association with viral E1B-

55kD protein. For example apoptosis control by disrupting p53[181], viral mRNA metabolism by shuttling mRNA, viral DNA synthesis by relocalizing E1B-55kD around viral replication machinery[182-185] and involved in cell cycle-independent virus growth[186]. However, the expression of ORF-6 appears to be dependent of a prior splicing step in which the first E4 ORFs are removed and interestingly, ORF-6's splicing acceptor resides on E4-ORF4[173]. Consequently, it is probable that EnAd's E4-ORF4 has major effects on the adenovirus life cycle. Overall, the E4-ORF4 mutation has been suggested to render EnAd inefficient at taking cell control, leading to cell swelling and unorganised immunogenic death, known as oncosis[187].

Genes	Ad11p	EnAd	Ad5 (% aa identity with Ad11p)
Early 2			
pTP	+	(Ad3 substitutions)	+ (78.7%)
AdPol	+	(Ad3 substitutions)	+ (57.1%)
BDP	+	+	+ (85.0%)
Early 3			
12.1 kDa	+	+	+ (53.3%)
16.1 kDa	+	+	-
18.5 kDa	+	Partly, fused to E3-15.3 kDa	+ (35.8%)
20.3 kDa	+	-	-
20.6 kDa	+	-	-
10.3 kDa	+	-	+ (50.0%)
15.2 kDa	+	-	+ (31.8%)
15.3 kDa	+	Partly, fused to E3-18.5 kDa	+ (53.1%)
Early 4			
ORF4	+	(in frame 24 bp deletion)	+ (44.3%)

Table 1.3 Genetic differences of the three affected regions between Ad11p to EnAd, and commonly used wildtype Ad5. Details of the aa identity between Ad5 and Ad11p as adapted from [168] and [6].

1.5.2 The properties of EnAd virus

In vitro experiments proved that EnAdenotucirev was significantly more potent oncolytic agent on tumour cell lines than Ad11p. Yet, with a limited activity on healthy human epithelial and

endothelial cells[6]. The physical features of EnAd virus particle were assessed by high-performance liquid chromatography with an anion exclusion column. This proved that the outer capsid was the same as the parental virus[6], which was expected since the mutations were restrained to non-structural proteins (Figure 1.5). The sequence analysis confirmed that Ad11p and EnAd genomes were nearly identical, with a chimeric Ad3:Ad11p E2B region, almost complete deletion of the E3 region and a 24bp deletion on E4 region (Table 1.3). EnAd also showed superior oncolytic potency than both Ad11p and Ad3 *in vitro* on human cancer cell lines. Even further, EnAd killed cells through an immunogenic mechanism, known as oncosis, releasing large amounts of DAMPs from cancer cells resulting in a strong stimulation of APCs. The killing mechanism of EnAd appeared to be different from Ad11p and related to the virus inability to take control of the infected cell[187].

Overall, these suggested that despite EnAd sharing the virus capsid features with Ad11p virus, the genetic alterations lead to an improved oncolytic potency with a pro-inflammatory cell death[6].

1.6 Hypothesis

This thesis addresses the hypothesis that as a consequence of its oncolytic action, EnAd will provide an adjuvant activity on tumour-infiltrating DCs to drive T_H1 polarisation of the adaptive immune response.

Each chapter of this thesis investigates a specific mechanism to address the overall hypothesis (Figure 1.6):

- Chapter 3, characterises the life cycle of EnAd in carcinoma cell HT29 and attempts to identify the role of each genetic mutation of the virus. In addition, a high throughput drug panel is used to identify mechanistic synergies and also to help define cellular factors and pathways that are involved in EnAd growth in cancer cells.

- Chapter 4, the adjuvant effects of EnAd and Ad5 virus on tumour DCs is investigated using an *in vitro* human DC model displaying a tumour-like skewed phenotype (TIDC-like model). In addition, the adjuvant effect of DAMPs and progeny virus particles derived from the virus infection of tumour cells are investigated on the TIDC-like model.
- Chapter 5, the mechanism underlying the adjuvant effect of EnAd virus particles is characterised on the TIDC-like model.
- Chapter 6, introduces the use of T cells to explore whether EnAd-treated TIDC-like cells can drive a polarisation towards an adaptive T_H1 immune response.

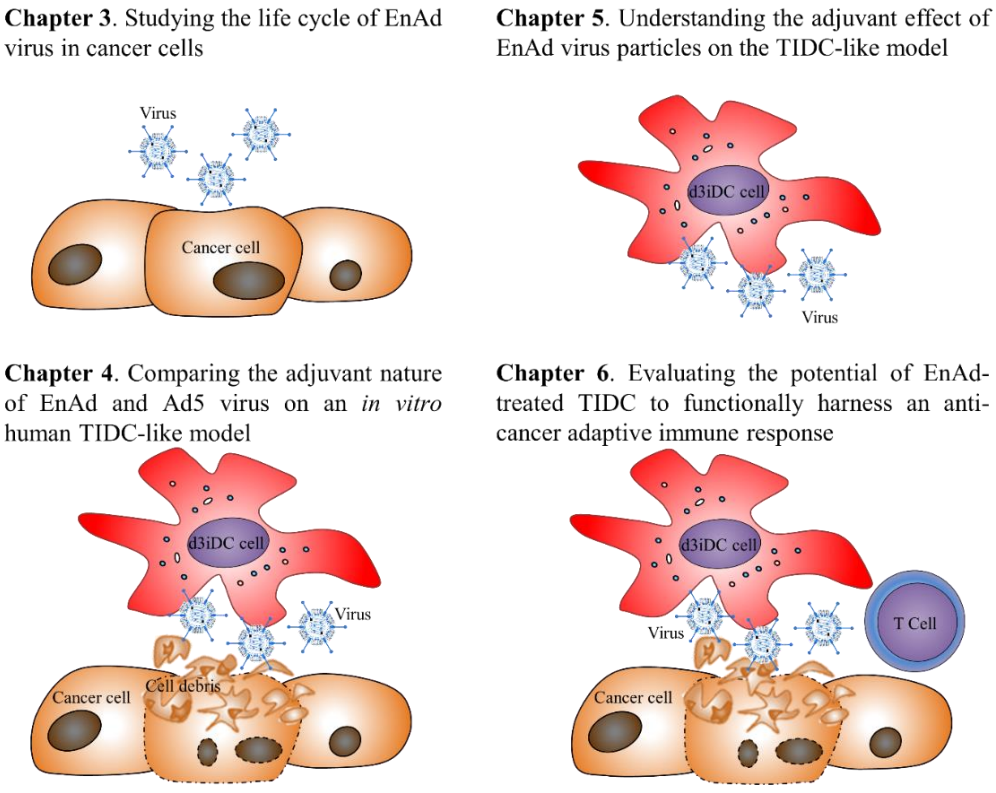


Figure 1.6 Diagram representing the main components used to evaluate the hypothesis of each chapter

2 Materials and Methods

2.1 Methods used in cell line culturing

The cell lines listed in Table 2.1 were cultured using methods from section 2.1.1 to 2.1.8. These cell lines were either cultured up to passage 25 for transformed and carcinoma cell lines or up to passage 12 for the leukemic cell line.

Cell Line	Description	Origin	Growth medium	Supplements
HEK-293	Human embryonic kidney cells transformed by adenovirus E1	ATCC	DMEM	2 or 10% FBS, 4mM L-glutamine, 1% Pen/Strep
AD-293	HEK-293 improved for cell adherence	Agilent	DMEM	2 or 10% FBS, 4mM L-glutamine, 1% Pen/Strep
A549	Human Caucasian lung carcinoma	ATCC	DMEM	2 or 10% FBS, 4mM L-glutamine, 1% Pen/Strep
HT29	Human colon adenocarcinoma	ATCC	DMEM	2 or 10% FBS, 4mM L-glutamine, 1% Pen/Strep
THP1-Lucia	Monocyte cell line with NF-kB-inducible Luc reporter construct	InvivoGen	RPMI	10% FBS, 2mM L-glutamine, 100ug/ml Zeocin

Table 2.1 Details of cell lines used in this thesis.

2.1.1 Adherent cell culture

The HEK-293, AD-293, A549 and HT29 cell lines were grown in a humidity-controlled incubator at 37°C and 5% CO_2. Cells were subcultured once they reached a 70-85% confluency. This was performed using aseptic technique in a class II laminar-flow cabinet sterilised with Trigene (VWR) and 70% isopropanol (IPA, Sigma). First, the spent media was removed from cells, generally cultured in T-175 flasks, and then cells were washed with 10 millilitres (mls) of PBS before incubation with 4 mL trypsin-EDTA until cells had detached from the flask. Cells were resuspended in medium supplemented with 10% heat-inactivated foetal bovine serum (FBS, Gibco), transferred into a falcon tube and spun in a centrifuge (Sorvall) at 300xg for 2 minutes. The supernatant was discarded, the falcon tube was gently

flicked until cells were detached and resuspended in 10mls of fresh supplemented medium. Finally, cells were counted using Countess automated cell counter (section 2.1.4), the cell density adjusted accordingly and corresponding volume of the cell culture was seeded into a new flask/well.

2.1.2 Non-adherent cell culture

THP1-Lucia NF-kB cells are a non-adherent monocyte cell line, designed for monitoring the NF-kB signal transduction pathway by a stable integration of an NF-kB-inducible luciferase reporter construct. THP1-Lucia cells were grown in a T-175 flask containing RPMI-1640 media (ThermoFisher) supplemented with 10% FBS, 10mM HEPES (Gibco), 1 mM sodium pyruvate (Gibco), 2 mM L-glutamine (Gibco) and 100 ug/ml Zeocin (InvivoGen) in a humidity-controlled incubator at 37°C with 5% CO_2. Cells were split every 3-4 days once they reached a density of 2 x 10^6 cells/mL by inoculating 7.5 x 10^5 cells/ml into a new flask containing fresh media.

2.1.3 Manual cell counting

Equal volumes of leukemic cell suspension (section 2.1.2) or primary cell suspension (section 2.4) were mixed with 0.4% Trypan Blue (ThermoFisher), before loading 10 microliters (µl) in a disposable haemocytometer (Cellometer) for a manual cell count under an optical microscope (Labomed). Blue-coloured cells were counted as dead and non-coloured refringent cells were counted as viable. High density samples were pre-diluted 1/10 before mixing with Trypan Blue.

2.1.4 Automatic cell counting

Equal volumes of cell suspension and 0.4% Trypan Blue (ThermoFisher) were gently mixed together before loading a Countess Cell Counting Chamber slide (ThermoFisher) to count the

cells on the Countess Automated Cell Counter (ThermoFisher). Live and dead cells were automatically counted based on pre-established settings for brightness, shape and size set by the user accordingly with the cell type. Total cell count resulted from the addition of dead and live cells, and cell viability was the ratio of live cells to total cells. Samples with high cell density were pre-diluted 1/10 before mixing with trypan blue.

2.1.5 Cell plating

Unless otherwise stated, HT29 cells were routinely seeded overnight either at $1x10^4$ cells/well for a 96 well plate, $3x10^5$ cells/well for a 24 well plate, $1x10^6$ cells/well for a 12 well plate or at $3x10^6$ cells/well in a 6 well plate. Alternatively, A549, HEK-293 and AD-293 cells were seeded at one third of the HT29 cell density as stated above.

2.1.6 Adherent cell line cryopreservation

Carcinoma or transformed cell lines were grown to virtual confluency in T-175 flasks. After discarding the cell media, cells were washed, trypsinised and counted according to section 2.1.1. Cells were spun once more at 300xg for 5min, during which the freezing solution (10% sterile dimethylsulphoxide (DMSO, Sigma) and 90% FBS) was prepared. The pelleted cells were resuspended in this freezing solution and 0.5ml of cell suspension was dispensed into 1 mL cryovial aliquots. Cryovials were transferred into a room-temperature Mr. Frosty container (Nalgene), before overnight storage at 80°C. For long term storage, cryovials were transferred into a liquid nitrogen tank from -80°C storage.

2.1.7 Non-adherent cell line cryopreservation

THP1-Lucia cells were fed with fresh media the day before freezing. Cells were harvested and spun in a falcon tube. Freezing solution, containing 5% sterile DMSO and 95% FBS, was

prepared. The pellet of cells was resuspended in the freezing solution and 1ml containing $5x10^6$ cells was dispensed into 1 mL cryovial aliquots. Cryovials were transferred into a room-temperature Mr. Frosty container (Nalgene), before overnight storage at -80°C.

2.1.8 Cell line revival

1 vial of frozen down cells were briefly thawed in a water bath at 37°C, the cells were quickly transferred in 10 ml of pre-warmed serum-positive medium and centrifuged at 300xg for 2 minutes. The supernatant containing DMSO was discarded and the cell pellet was resuspended into variable volumes of pre-warmed media supplemented with serum – depending on the number of thawed cells – and transferred into a T-25 or T-75 flask.

2.2 Molecular biology methods

2.2.1 Restriction endonuclease digestion of DNA

Restriction digestion of DNA was performed either for genome linearization or for assessment of adenovirus genome structure. The digestion mix was designed to contain the desired amount of DNA with adequate amount of restriction enzyme, 10x restriction enzyme buffer and de-ionized water. The final volume of the reaction mixture was 20 or 100µl with the restriction enzyme buffer at a 1x final concentration. The choice of restriction buffer and incubation temperature were all based on manufacturer's instructions. Incubations were usually done for 1-2 hours at 37°C or room temperature (RT), according to the enzyme specificities. Restriction enzymes and buffers were purchased from New England Biolabs.

2.2.2 Agarose gel electrophoresis of DNA

Agarose gel electrophoresis was used to assess the genomic structure of the viruses, for instance a 1% Agarose gel was made with 1x TAE running buffer [40 mM Tris (pH 7.6), 20 mM acetic acid and 1mM EDTA], agarose powder (Sigma) and 5 µg/ml ethidium bromide (Sigma). Gels were submerged in 1x TAE buffer in a horizontal electrophoresis tank. DNA samples were mixed with 1/6th volume of DNA Gel Loading Dye (ThermoFisher) and then loaded into the submerged wells of the agarose gel. The 1 kb DNA ladder (New England Biolabs) were loaded in the first and last well as standards. The electrophoresis was usually run at 140 volts for half an hour to an hour, depending on the DNA fragments. After electrophoresis, the DNA bands were visualised on the GelDOC Imaging Sytem Ultraviolet M-26X Transilluminator (UVP) using the GelDOC software and photographed with the fitted camera (Canon). ImageJ software was used for further image processing.

2.2.3 Phenol/chloroform extraction of DNA

Phenol/chloroform extraction was used to remove impurities such as proteins from DNA samples. An equal volume of 1:1 (v/v) phenol/chloroform mixture (Sigma) was added to the DNA samples in an Eppendorf tube and briefly vortexed to avoid shearing the long DNA molecules. The samples were then spun in a Biofuge Fresco benchtop centrifuge (Heraeus) at 13,700xg for 2 minutes to separate the aqueous (upper) and organic phase (bottom). The upper phase containing the DNA was transferred to a new Eppendorf and mixed to an equal volume of phenol/chloroform, before repeating the mixing and centrifugation process. The upper aqueous phase was again transferred to a fresh tube followed by DNA precipitation.

2.2.4 Ethanol precipitation of DNA

The samples were first mixed with four volumes of 95% ethanol and 1/20th volume of 3M sodium acetate (Sigma). The precipitation process was carried out at -20 °C for more than 2hrs, generally an overnight incubation. The DNA was pelleted by centrifugation at 16,000xg for 10 minutes in a benchtop centrifuge (Heraeus). The supernatants were carefully removed without disturbing the DNA pellet. Finally, the pellets were air-dried for 30 minutes in a class II laminar-flow cabinet.

2.2.5 Transformation of competent bacteria with adenovirus plasmids

Competent *E. coli* XL Blue cells (Agilent) were used for transformation with plasmid DNA. 10-50 ng of plasmid DNA was added to 100 µl of defrosted competent cells, mixed gently and incubated on ice for 30 minutes. The cells/DNA mixture was then heat-shocked at 42°C for two minutes and immediately placed on ice again for two minutes. 900 µl of S.O.C medium (ThermoFisher) was added to the cell suspension and cells gently mixed. The tube was then incubated at 37°C for one hour to allow expression of the kanamycin-resistance gene encoded in the plasmid. Then 0.5 ml of the cell suspension was spread on a plate containing kanamycin LB agar. The plate was then left at room temperature for 30 minutes to allow the agar to absorb the fluid before incubating the plate upside down overnight at 37°C.

2.2.6 Large scale preparation and purification of adenovirus plasmid

For bulk preparation of plasmid DNA, a single bacterial colony was picked from plates (previous section) with a sterile 1 ml pipette tip and used to inoculate 200 mls of autoclave-sterilised LB medium (ThermoFisher) containing 100 µg/ml of kanamycin (Invitrogen). Cells were cultured at 37°C overnight in a shaker incubator. Next day, the cells were pelleted by centrifugation for 5 minutes at 3000xg (Sorvall). The resulting pellet was used in PureLink

HiPure Plasmid Purification Kit (ThermoFisher), according to manufacturer's protocol, to extract the virus plasmid DNA. During this procedure, cells and lysates were kept on ice.

2.2.7 DNA extraction using Minipreps

Viral DNA was extracted from cell lysate or supernatant samples using the GenElute Mammalian Genomic DNA Miniprep Kit (Sigma), according to the manufacturer's instructions. Briefly, samples were thawed, 200 µl of sample was treated with Lysis Solution C and Proteinase K (20 mg/ml final concentration), before incubation at 70°C for 10 minutes. After adding 200 µl ethanol, samples were transferred to pre-activated DNA binding columns and subsequently centrifuged at 9,500xg in a benchtop centrifuge (Heraeus). The liquid eluting from the column was discarded and wash solution was added to the column, before centrifugation at 9,500xg. This wash step was repeated twice before DNA was eluted in 200 µl of elution buffer, containing 10 mM tris HCl 0.5 mM EDTA (pH 8.0).

2.2.8 DNA extraction in 96 well-plate, vacuum format

DNA extraction in 96 well-plate was performed using SV mammalian DNA extraction kit (Promega) by following manufacturer's instructions, with some alterations. Briefly, proteinase K was diluted in lysis buffer to achieve a final concentration of 20 mg/ml and 100 µl was mixed to equal sample volumes and incubated at 55°C for 30 minutes. Then the samples were transferred to the binding plate located on top of a MultiScreenHTS Vacuum Manifold (Merck), after 5 minutes vacuum was applied and the eluting volume was discarded. Then, 1mL of column wash solution was added to each well of the binding plate. Again, the vacuum was applied to the plate and the eluting volume was discarded. This was repeated for a total of three washes. After the final wash, the vacuum was applied to the binding plate for 5 minutes

to dry the binding membrane. Finally, samples were eluted from the binding matrix with 210 µl of nuclease-free water.

2.2.9 DNA extraction in 96 well-plate, centrifuge format

Viral DNA was extracted from cell lysate or supernatant samples using the DNeasy 96 Blood & Tissue Kit (Qiagen), according to the manufacturer's instructions. Briefly, samples were thawed, 200 µl of sample was thoroughly mixed with 20 µl of proteinase K and 200 µl of Buffer AL by vortexing, before incubation at 56°C for 10 minutes. After adding 200 µl ethanol, samples were transferred to the DNeasy 96 plates and subsequently centrifuged using a counterbalance at 4,500xg in a Sorvall Legend XT/XTR benchtop centrifuge (ThermoFisher). The volume eluted from the column was discarded and wash solution added to the column, before centrifugation at 8,000xg. This wash step was repeated twice before a drying spin was performed for 15 minutes to remove residual contaminants from wash buffers. Finally, DNA was eluted in 200 µl of elution buffer, containing 10 mM Tris-Cl, 0.5 mM EDTA (pH 9.0).

2.2.10 Standard curve preparation for qPCR

A purified virus stock was diluted to a concentration of 1×10^{11} virus particles (vp)/ml and used to produce a top standard with 2.5×10^{10} total vp followed by 10-fold dilutions. The standard curve was extracted using the same DNA extraction method and same elution buffer as the test samples. Two µl of the eluted standards were used per every reaction, the resulting standard curve ranged from $2.5 \times 10^{8} – 2.5 \times 10^{3}$ viral particles per tube. The acceptance criteria for standard curve in this thesis were a negative slope value of around -3.3, with efficiencies from 98% upwards, a Y-intercept of 40 and a regression coefficient near one. An example of standard curve is shown in Figure 2.1.

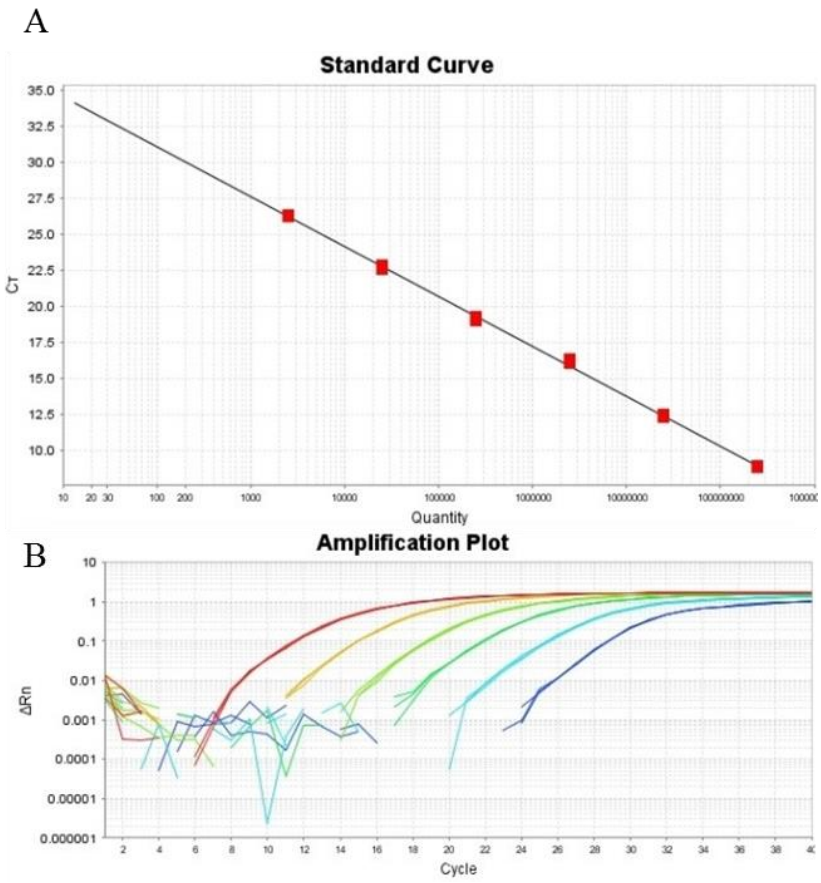


Figure 2.1 Typical standard curve for EnAd by qPCR. (A) Standard curve with corresponding CT values in triplicate. (B) Amplification curves for standard curves.

2.2.11 DNA quantification using Taqman qPCR

2.2.11.1 Primer and probes design

The TaqMan detection system was used to determine the amount of DNA or cDNA from EnAd, Ad11p, Ad5 or recombinant viruses. The primers and probes routinely used for qPCR in this thesis, were predicted with OligoArchitect software (Sigma) using the Dual-Labelled Probes options according to the recommended settings described in qPCR Technical Guide. The melting temperature of the suggested primers/probe were further assessed by nearest-neighbour method using the Oligonucleotide Properties Calculator (BioRad). The oligos were finally ordered from Eurofins Genomics UK, with probes specifically labelled with 6-carboxyfluorescein (FAM) and tetramethylrhodamine (TAMRA). Primers and probes were

empirically optimised for annealing and extension temperature based on standard curve acceptance criteria.

2.2.11.2 DNA quantification using Taqman qPCR

The primer and probes used for qPCR in this thesis are described in Table 2.2. A large mix containing the probe (0.5 pM final concentration), primers (1pM final concentration) TaqMan Fast Advanced Master Mix (LifeTech) and topped with DEPC-water (ThermoFisher), was prepared. A 96 well qPCR plate (Applied Biosystems) was aliquoted with 8 µl of the mixture as well as 2 µl of eluted DNA samples or standards. Plate was briefly votexed and pulse centrifuged, before performing the qPCR using StepOnePlus™ Real-Time PCR System (Applied Biosystems) with the amplification cycle starting at 50°C for 2 min, 95°C for 20 sec, followed by 40 cycles of 1 sec at 95°C for denaturation and 1 minute at 60°C for annealing and extension. Data were analysed using Applied Biosystems StepOnePlus™ software v2.2, with test samples compared to standards of known viral content.

Target	Oligo type	Sequence 5'→3'	Virus specificity
E1A	Forward primer	CTGCTGAGACTGGAAATGAAATATTGGA	EnAd and Ad11
	Reverse primer	CCTGAAGCGTAGGAGGCTCAA	
	Probe	**FAM**-CGGATCGTCTCCCATCAGGGCGTGCA-**TAMRA**	
E2B-pTP	Forward primer	AT GAA CTG CTC GAT CTC TTC CTC	EnAd and Ad5
	Reverse primer	GGA CTT CTA CGA GGC CAT GGA G	
	Probe	**FAM**-TCG TTC CAG ACG CGG CTG TAG ACC ACG-**TAMRA**	
L3-Hexon	Forward primer	TACATGCACATCGCCGGA	EnAd and Ad11
	Reverse primer	CGGGCGAACTGCACCA	
	Probe	**FAM**-CCGGACTCAGGTACTCCGAAGCATCCT-**TAMRA**	
E3-fusion	Forward primer	ATCCATGTCTAGACTTCGACCCAG	EnAd
	Reverse primer	TGCTGGGTGATAACTATGGGGT	
	Probe	**FAM**-ATCTGTGGAGTTCATCGCCTCTCTTACG-**TAMRA**	
L4-100k	Forward primer	CGGCGAGGAACTCAACACAAG	EnAd and Ad11
	Reverse primer	CCTCCAGACTGTCCTCCAGAC	
	Probe	**FAM**-CCTCCTCCGCCTCCTCTGCCTGACTG-**TAMRA**	
L5-Fibre	Forward primer	GCTACTGGTGCCATTACTAATGCTA	EnAd and Ad11
	Reverse primer	AGCTGTGTAGTAACAAGTTCCGTAA	
	Probe	**FAM**-AGGTTTCATGCCCAGCACGACTGCCT-**TAMRA**	
E2B-AdPol	Forward primer	CGATGAACTTATGCTAGAC	EnAd
	Reverse primer	CGGGGAAGATAGTTGTTA	
	Probe	FAM-TTCATCTGGCACGATTCTCACTTG-TAMRA	
E3-nORF	Forward primer	ACGACCAGACGGAATCTTTCAGA	EnAd and Ad11
	Reverse primer	GGTTGAAGTAGACAGAGGGAGTAAA	
	Probe	**FAM**-TGAACGGTCCCGATTCCGCCCGAGC-**TAMRA**	
E3-12.1K	Forward primer	CTGGTGACGCGGCTGAG	EnAd and Ad11
	Reverse primer	CGTGGTGTTTCCCTGGTCTC	
	Probe	**FAM**-TAGACCACTGCCGCCGCTTTCGCTGC-**TAMRA**	
E3-16K	Forward primer	GTCGTCCAGGACTCTGTTAACTT	EnAd and Ad11
	Reverse primer	CAAGCCCACCCGCAAGAA	
	Probe	**FAM**-CACTACAAGGCCCGCTTCCACCCAAGG-**TAMRA**	
E4-ORF4	Forward primer	GAGTGTGGTTGTACTTGAACTATC	EnAd and Ad11
	Reverse primer	CTGACATTCTCGTATTTTGTATAGCA	
	Probe	**FAM**-CACACTCTTCTTCGCCTTCTATCCTGCCG-**TAMRA**	

Table 2.2 Primers and probes routinely used in this thesis for qPCR and two-step RT-qPCR. Target gene and virus specificity are determined.

2.2.12 RNA extraction using Miniprep

Cellular and viral RNA was extracted using the RNeasy Mini Kit (Qiagen), according to the manufacturer's instructions. Because RNA is very sensitive to environment RNases, precautions were taken such as wiping surfaces, instruments and the use of gloves wiped with RNase zap (Thermofisher) and when possible samples were kept on ice. Supernatant was discarded from cultured cells and the cells washed with PBS. Cells were lysed with beta-mercaptoethanol (β-ME) with RLT buffer and cells were detached with a cell scrapper. Cell lysates were transferred into a QIAshredder columns (Qiagen) and spun on a benchtop centrifuge (Heraeus) at maximum speed for 2 minutes. The flow through was mixed to an equal volume of 70% ethanol and loaded into the RNeasy spin column before the column was spun at 9,500xg in the benchtop biofuge for 15 seconds. The flowthrough was discarded and RNeasy column was washed once with RW1 buffer followed by two washes with RPE buffer. RNA was finally eluted with 30 µl of RNase-free water into a new Eppendorf.

To eliminate possible DNA contaminants in the eluted RNA samples, in-solution DNase treatment was performed using the TURBO DNA-free kit (LifeTech), according to manufacturer's instructions. The clean RNA samples were used in RT-qPCR or stored at -80°C until needed.

2.2.13 RNA quantification by retro transcriptase qPCR

The mRNA expression was measured using a two-step reverse transcriptase (RT)-qPCR. During the first step RNA was reverse transcribed to cDNA and in the second step cDNA was quantified by conventional qPCR, as described in section 2.2.11.2. Extracted RNA was quantified for all samples by nanodrop before normalising the total RNA concentration to 12.5 ng/µl. A final concentration of 100 ng/µl of total RNA was mixed with SuperScript III First-Strand Synthesis SuperMix for qRT-PCR (Invitrogen) according to manufacturer's protocol,

in a sterile MicroAmp Fast Optical 96-well reaction plate (Invitrogen). The plate was sealed with the corresponding adhesive lid, the plate was gently vortexed and briefly pulsed before placing the plate into the StepOnePlus™ Real-Time PCR System (Applied Biosystems). The reverse transcription was performed accordingly: 25°C for 10 mins, 50°C for 40 mins, followed by 5 mins at 85°C with a final hold step at 4°C. Once the cDNA was obtained, unwanted RNA was digested with RNase H provided with the Kit at 37°C for 20 minutes. At this point cDNA was either stored at -80°C or 1-2 µl of each reverse-transcribed sample was used in standard qPCR, as described in the previous section.

2.2.14 Western Blot

Western blot (WB) was used to detect the phosphorylation of the CD46 cell surface receptor. As phosphorylation can be very sensitive to degradation, samples were lysed in a buffer complemented with phosphatase inhibitors and protease inhibitors. As a further precaution, lysates were manipulated at low temperature before the proteins were denatured. To decrease the background signal from other phosphorylated proteins, CD46 was initially immunoprecipitated. Phosphortyrosine was immunoblotted and developed first, before stripping the membrane for reblotting against CD46 receptor.

2.2.14.1 Cell lysis and immunoprecipitation

To retrieve CD46 from the cell surface membrane, a mild surfactant was used, along with phosphatase inhibitors cocktail to avoid losing the phosphorylation of the receptor. Accordingly, cells were harvested, pelleted and supernatant removed before lysing with freshly made Lysis Buffer (1/10 TBS (150 mM NaCl, 50 mM Tris-HCl and pH 7.6), 1/100 X-100 Triton (Sigma), 1/100 10% SDS (Sigma), 1/100 Phosphatase Inhibitor Cocktail III (Millipore), 1/100 Protease Inhibitor Cocktail II (Millipore), 1/100 100 mM Sodium Orthovanadate (NEB),

1/10 10% Sodium Deoxycholate diluted in HPLC-grade water and 1µl of Benzonase Nuclease (Sigma). Samples were mixed with monoclonal antibody raised against CD46 C-terminal (ab175096 clone, Abcam) and Pierce Protein A Agarose Beads (ThermoFisher), before incubation overnight at 4°C on a RotaMACS (Miltenyi). The following day, samples were immunoprecipitated as manufacturer's protocol recommendations.

2.2.14.2 Sample preparation and gel loading

Immunoprecipitated samples were mixed with ¼th volume of NuPage LDS Sample Buffer (LifeTech) and before boiling samples in a water bath for 10min at 70°C, samples were reduced with 1/10 NuPAGE Sample Reducing Agent (LifeTech). Meanwhile, a NUPAGE 4-12% BT GEL 1.5MM 15W (LifeTech) was conditioned, fitted in a L-Buffer Chamber Surelock tank system (LifeTech) and the chamber filled with 1x NuPAGE MOPS SDS Running Buffer (LifeTech).

First and last lane were loaded with PageRuler Plus Prestained Protein Ladder (LifeTech) and samples loaded in the middle lanes, before running the gels at 290 volts for 1 hour.

2.2.14.3 Transfer to PVDF membrane

Hybond-P PVDF membrane (Amersham) was pre-conditioned in 100% methanol (VWR) for 30 seconds. Then the membrane, filter paper and sponge pads were pre-soaked in 1x NuPAGE Transfer Buffer (LifeTech). Sponge pads, followed by filter paper, were placed in the Blot Module. Then the gel was placed on the filter paper followed by the PVDF membrane. Finally, a filter paper and more sponge pads were added, accordingly with Figure 2.2. A transfer sandwich was created, by closing the cassette which was placed in the L-Buffer Chamber SureLock tank, with the gel facing the negative electrode. The tank was filled with Transfer Buffer ensuring the sandwich was fully covered, before the transfer was carried out at 30 volts for 1 hour.



Figure 2.2 Diagram showing the sponges pad, filter papers, gel and PVDF sandwich in the Blot Module.

2.2.14.4 Immunoblot, development and reprobing

After removing the PVDF membrane from the transfer sandwich, the membrane was washed with PBST (PBS with 0.05% Tween-20 (Sigma)) and then blocked in 5% milk (Marvel) PBST, by gently rocking a benchtop shaker (The Belly Dancer, Stovall) at room temperature for 1 hour. The membrane was incubated with the Anti-Phosphotyrosine Antibody horseradish peroxidase (HRP)-conjugated (clone 4G10, Millipore), diluted in PBST to the specified concentration for 2 hours. After removing the antibody and washing with PBST for 5 minutes, and repeating the wash twice, the Enhanced Chemiluminescence reagent (ThermoFisher) was added on the membrane. The membrane was developed with the GelDOC Imaging Sytem Ultraviolet M-26X Transilluminator (UVP), assisted with the GelDOC software and photographed with the fitted camera (Canon). After developing the phosphotyrosine, the PDVF membrane was briefly washed in PBST and left soaking in Restore Stripping Buffer (ThermoFisher) for re-probing. The membrane was washed in PBST and incubated with the anti-CD46 antibody (Table 2.3) at 4°C overnight. After removing the antibody and washing with PBST for 5 minutes, and repeating the wash twice, the membrane was incubated with the appropriate secondary HRP-conjugated antibody (Table 2.3) for 1 hour at room temperature.

After removing the antibody and washing with PBST three times for 5 minutes each, the chemiluminescence was developed following the procedure explained above.

Antibody	Clone	Clonality	Species	Supplier	Dilution
Anti-human CD46	N/A	Polyclonal	Goat	R&D System	1:1000
Anti-goat-HRP	N/A	Polyclonal	Rabbit	Dako	1:1000

Table 2.3 Details of antibodies used in reprobing

2.3 Virology-related methods

The characteristics of the stocks of adenovirus used for this thesis are summarised in Table 2.4. The virus stocks were either generated from scratch (vector design, vector amplification, genome transfection and virus amplification, section 2.3.1.1 to 2.3.1.3) or simply amplifying from previously made virus stocks (section 2.3.1.4). After purification (section 2.3.1.5), virus stocks were generally characterised accordingly with methods described in section 2.3.2.

Adenovirus	Virus concentration (vp/ml)	Virus infectivity (IU/ml)	VP/IU ratio	Purity (260nm/280nm)	Features
EnAd	$3.00x10^{12}$	$1.25x10^{10}$	240.0	1.23	Chimeric E2B, large E3 deletion, short E4 deletion
Ad11p	$3.28x10^{12}$	$1.37x10^{10}$	239.4	1.23	Wildtype
Ad5	$7.40x10^{11}$	$3.10x10^{9}$	238.7	1.24	Wildtype
EnAd-Luciferase	$2.51x10^{11}$	N/A	N/A	1.25	EnAd encoding Luciferase transgene after MLP
EnAd-GFP	$3.96x10^{11}$	N/A	N/A	1.23	EnAd encoding GFP transgene in E4
Psoralen/UV CL-EnAd	$9.92x10^{11}$	$1.26x10^{4}$	$7.8x10^{7}$	1.21	EnAd DNA-inactivated by UV and Psoralen
EnAd-wtE2B	$3.26x10^{12}$	$1.33x10^{10}$	245.1	1.25	EnAd, E2B replaced with Ad11p sequence
EnAd-wtE3	$3.70x10^{12}$	$1.44x10^{10}$	256.9	1.26	EnAd, E3 replaced with Ad11p sequence
EnAd-wtE4	N/A	N/A	N/A	N/A	EnAd, E4 replaced with Ad11p sequence

Table 2.4 Purified virus stocks used in this thesis displaying assessed characteristics and features.

2.3.1 Adenovirus production

2.3.1.1 Adenovirus genome vector design and amplification

This method was used to generate the three EnAd-wtE2B, EnAd-wtE3 and EnAd-wtE4 viruses (Table 2.4), each virus had a single mutated region replaced by Ad11p wildtype sequence. The virus genome sequences were designed on ApE software (open-licence) before being sent to SGI DNA (La Jolla, CA), for synthetic generation of the genomes by Gibbs assembly. Upon receipt, the genomes were reconstituted in DEPC-water (ThermoFisher) and separately transformed into competent *E.Coli* XL Blue (Agilent), accordingly with section 2.2.5. Next day a single colony was bulk amplified for large scale isolation of plasmid (section 2.2.6). Purified plasmid was quantified by Nanodrop before it was linearised by restriction enzyme digestion, purified by Phenol/chloroform extraction and precipitated by ethanol precipitation (detailed in sections 2.2.1, 2.2.3 and 2.2.4).

2.3.1.2 Transfection of mammalian cells with adenovirus genome

Linearised ethanol-precipitated virus genomes according to methods described in section 2.2, were mixed with OptiMEM (LifeTech) and GeneJuice Transfection Reagent (Merck) (Transfection Mix), according to manufacturer's protocols. Transfection Mix was gently added on pre-seeded AD-293 cells at ~75% confluency in a T-25 flask and placed in a 37°C incubator. After 1 hr, 4 mls of pre-warmed medium supplemented with 2% FBS was added and returned into the Incubator. Cells were assessed every 24 hrs for cytopathic effect (CPE). When CPE was significant, cells were scraped, resupended into their media (Transfection crude lysate) and transferred into a falcon tube for 3 freeze-thaw cycles before storing at -80°C.

2.3.1.3 Adenovirus amplification from transfection

Transfection crude lysate was spun at 300xg for 5 minutes, before 3 different volumes of clarified supernatant (generally 1 ml, 100 µl or 10 µl) were added to give a final volume of 12 mls with 2% FBS medium and used to infect T-75 flasks with pre-seeded AD-293 at 90% confluency before placing the flasks in 37°C incubator. After 48 hrs or 72 hrs the monolayers of the 3 flasks were monitored for CPE and only the flask with more than 50% CPE was scraped and the cells were resuspended with medium, before they were transferred to a falcon tube for 3 cycles of freeze-thaw (First Amplification crude lysate).

First Amplification crude lysate was spun at 300xg for 5 minutes and 3 different volumes of clarified supernatant (generally 100 µl, 10 µl and 1 µl) were used to infect three T-75 flasks pre-seeded with AD-293 following the same method above. The flask with CPE was used as an infection test to indicate how much volume from First Amplification crude lysate was needed for Hyperflasks amplification calculated as;

1^{st}Amp.Vol.for Hyperflasks= Inoculation Volume showing CPE in infection test after 48 hrs x 46.66

The given volume was mixed with 2% FBS medium to a total 1100 ml and transferred at equal volumes into two Hyperflasks (Corning) containing pre-seeded AD-293 at 80-90% confluency. Hyperflasks were returned to the incubator and assessed every hour at 44 hrs post-inoculation until a 50-60% of CPE was reached on the monolayer.

2.3.1.4 Adenovirus amplification from purified virus stock

AD-293 cells were seeded in two Hyperflasks in medium containing 10% FBS until they reached a confluence of 80-90%. At which point, the appropriate volume of purified virus stock (purchased from ATCC, Native Antigen Company or previously produced by colleagues) needed to infect 2 x 10^7 total cells/flask at 100 particles per cell, was diluted into 1100 mls of

medium supplemented with 2% FBS. The medium in the confluent Hyperflasks was discarded, viral inoculation added before returning them to the incubator. The cells were assessed every hour after 44 hrs post-inoculation until a 50-60% of cytopathic effect was reached on the monolayers.

2.3.1.5 Adenovirus purification from Hyperflasks

Hyperflasks from section 2.3.1.3 and 2.3.1.4 at 50-60% CPE were gently knocked until all cells were detached. The cells suspensions were decanted into 4x sterile 250 mls Centrifuge Tubes with Plug Seal Cap (Corning) and spun at 300xg for 10 minutes. Supernatants were discarded and pelleted cells re-suspended and pulled together with the remaining dead-volume, before 3 freeze-thaw cycles were performed (snap freezing in liquid nitrogen and thawing in a water bath at 37°C). The last freeze step could be either stored at -80°C for later extraction or thawed. After last freeze-thaw cycle, $1/100^{th}$ volume of water saturated n-butanol was added to the lysate and incubated for 1 hour in the fridge, to enhance cell membrane lysis. The cell lysate was clarified by centrifugation at 500xg for 10 minutes; the supernatant was collected into a 15 ml tube and the cell debris discarded. Meanwhile, two gradients were prepared per purified virus in Ultraclear Ultracentrifugation 15ml tubes (Beckman) by filling them with 3 mls of 1.25 g/l Caesium Chloride, 2 mls under layer of 1.35 g/l Caesium Chloride and 2 mls over layer of 40% glycerol. The clarified cell lysate was split across both gradient tubes, in order to counterbalance each other during the ultracentrifugation. PBS was used for further adjustments to ensure equal volumes in the gradient tubes. The tubes were spun in vacuum using the Optima L-80 XP ultracentrifuge (Beckman) at 78,925xg for 1.5 hours at 10°C, with the SW40 Ti rotor (Beckman) and the corresponding swing out buckets (Beckman). The lower, slightly blue coloured, opaque virus band was removed from each tube using a sterile 21G needle (BD Biosciences) coupled to a 2 mls sterile syringe (Figure 3.6). The virus was transferred into a

pre-wet 10,000 MW Slide-A-Lyzer dialysis cassette (ThermoFisher) and left soaking into 500 mls pre-cooled PBS at 4°C. Eventually the PBS was twice replaced every 20 minutes with fresh ice-cold PBS, finishing with an overnight incubation. The virus was recovered from the dialysis cassette and transferred into a falcon tube. To digest the free DNA and preventing virus aggregates, the virus was treated with 10,000 units of Benzonase (Sigma) per every ml of dialysed virus for 1 hour at room temperature. Two CsCl-gradients were produced in Ultraclear tubes following the above procedure, however the virus was overlaid on top of a single gradient and the spare tube was exclusively filled with PBS as a balance. High speed ultracentrifugation was subsequently performed for 1.5 hours at 10°C and at 78,925xg, again using the same ultracentrifuge with the corresponding rotor and swing-out buckets. The lower virus band was removed with sterile needle/syringe. Buffer exchange of the virus preparation was then performed using Slide-A-Lyzer in 2 cycles of 20 minutes with ice-cold PBS and a final cycle of formulation buffer.

2.3.1.6 Inactivation of EnAd genome by psoralen and UV light method

EnAd was DNA-inactivated using 8-MethoxyPsoralen (Psoralen) and ultraviolet (UV) light, accordingly with a previously described method[188]. Briefly, 30 mgs of 8-MethoxyPsoralen (Sigma) was dissolved into sterile DMSO inside a class II laminar-flow cabinet. Ten microliters of 30 mg/ml Psoralen were mixed to 2 mls of EnAd purified virus stock inside a sterile T-25 flask, before the flask was tightly capped and left at room temperature for 20 minutes. The flask was then placed at the bottom of an ice-full glass-beaker and exposed to UV light for 2 rounds of 10 minutes using a Transilluminator (UVP). The flask containing the virus was moved back to sterile conditions, before the virus/psoralen mix were transferred into a pre-equilibrated PD-10 desalting column (GE-Healthcare Life Sciences) according to manufacturer's instruction. Once the 2 mls of treated virus penetrated the column, 0.6 mls of

equilibration buffer were added, as per manufacturer's recommendation. Finally, 3.5 mls of formulation buffer were added, before the eluted volume containing the inactivated virus was collected and snap frozen in liquid nitrogen.

2.3.2 Adenovirus characterisation assays

2.3.2.1 HPLC titration and evaluation of virus capsid integrity

The HPLC allows a physical quantification of virus particles based on the negative charge of EnAd virus capsid. The physical titre can either be quantified from purified virus stocks or crude virus lysate. For this, samples were mixed with 1µl of Benozonase A (Sigma) for 20 minutes at room temperature. Before loading the virus into HPLC vials, the virus/benzonase mix was spun at full speed on a benchtop biofuge for 2 minutes, whilst standard curves were prepared from a purified EnAd stock, with a known concentration. The vials were disposed in the autosampler of the HPLC (Agilent 1200 series), which had a pre-fitted Resource Q (anion exchange) column. Samples were acquired according to pre-determined settings. To elute the virus from the column a NaCl buffer was used to vary salt gradients and the virus elution was detected at 260 nm. The concentration of virus was determined by integrating the 260nm signal (DNA signal) of the virus elution peak and calculating the concentration from the standard curve. The preparation and run of HPLC was kindly performed by Magda Kieltyka and Prithvi Kodialbail (PsiOxus Therapeutics).

2.3.2.2 Evaluating the endotoxin levels in purified virus stock

Endotoxin – also known as LPS or lipoglycans – are large molecules derived from Gram-negative bacteria's wall, a ubiquitous contaminant that can induce potent immune stimulation. Endosafe®-PTS (Charles River Laboratories) and the correspondent cartridge with a detection range of 0.5 to 0.005 Endotoxin Units (EU) /ml, were used to quantify the endotoxin levels in

purified virus stocks, according to manufacturer's instruction. Briefly, virus seed stocks were diluted 1/10 in limulus amebocyte lysate (LAL) water (Charles River Laboratories). Twenty-five microliter of diluted virus were carefully loaded into the cartridge's four wells and set to analyse the endotoxin content. All purified stocks displayed in Table 2.4 (excluding the un-banded EnAd-wtE4) had less than 0.025 EU/ml. Considering that 1 EU/ml roughly equivalent to 0.1 ng endotoxin/ml with Charles River's Endosafe-PTS, the endotoxin amount in pure virus stocks were smaller than 2.5 pg/ml.

2.3.2.3 Oncolytic potency assay

MTS [3-(4,5-dimethylthiazol-2-yl)-5-(3-carboxymethoxyphenyl)-2-(4-sulfophenyl)-2H-tetrazolium] is a tetrazolium compound that is reduced to formazan – a soluble blue coloured molecule – by metabolically active cells. The amount of formazan produced can be measured by its absorption at a wavelength 490 nm. The potency assay uses this principal to determine the cell viability of treated cells relative to an untreated control. In this thesis, the commercially available CellTiter 96® Aqueous Non-Radioactive Cell Proliferation Assay (Promega) MTS subtract, was used to determine the cytotoxic effect for viruses or drugs. In general, pre-seeded 96-well plates with HT29 cells were infected with decreasing concentrations of virus and placed in a 37°C incubator. After a period of 70 hrs the supernatant was rapidly but gently exchanged with 120µl of a mixture made with 5/6 phenol red free growth medium and 1/6 of MTS reagent. Cells were cultured with the reagent mixture for 30 minutes in the Incubator, before the absorption was determined at 490 nm using a Synergy™ Multi-Mode Microplate Reader (BioTek), with a pre-shake plate reader function.

2.3.2.4 Infectivity assay by hexon staining

Infectivity assay was used to determine the amount of infectious viral particle concentrations by observing plaque forming units (PFUs) and/or cells staining positive for hexon. Pre-seeded A549 cells in a 96-well flat bottomed plate were infected with decreasing concentrations of either purified virus stocks (with a known physical virus titre) or supernatants from previously infected cells (with unknown virus titre). Each dilution was then used to infect 3 wells. Plates were incubated at 37°C in 5% CO_2 for 3 days. After 70 hours medium was removed and the cell monolayer fixed using ice-cold methanol for 30 minutes. After removing the methanol and washing with PBS, the plates were incubated with PBS containing 1% bovine serum albumin (BSA) at room temperature for 1 hour with gentle agitation. After removing the blocking buffer, plates were incubated for 1 hour at room temperature with primary anti-hexon antibody (Table 2.5) that had been diluted in PBS containing 1% BSA. After removing the primary antibody and multiple washes with PBS, plates were incubated for 1 hour at room temperature with secondary anti-mouse antibody-HRP (Table 2.5) that had been diluted in PBS containing 1% BSA. After removing the secondary antibody wells were washed with PBS multiple times and staining was performed using 3, 3'- diaminobenzidine (DAB) substrate kit (ThermoFisher). Cells that had stained positively for hexon produced a dark brown colour. Using an optical microscope (Leica) with 20X objective, positively stained cells and/or CPE were counted as one infective unit (IU). The total count was determined from wells containing between 30 and 300 IU. The average number of IU was calculated across well triplicates and the infectious particles titre (IU/mL) determined using the following equation:

$$\text{IU/ml} = \frac{\text{Dilution factor from counted well x Average IU}}{mLs\ of\ inoculum}$$

Antibody	Clone	Species	Supplier	Working dilution
Anti-adenovirus	Monoclonal B025/Ad51	Mouse	Abcam	1/800
Anti-mouse IgG-HRP	Polyclonal	Rabbit	Abcam	1/800

Table 2.5 Details of antibodies used for infectivity assay

2.3.3 Cell infection with virus

Cells were generally infected using purified virus stocks with a known concentration. In this thesis cells were generally infected using the particle titre determined by HPLC, as the physical and infectivity titre were comparable between viruses (Table 2.4). The virus stock volume needed was determined as follows:

$$\text{Virus stock volume} = \frac{Virus\ particles\ per\ cell \quad x \quad Total\ cells}{Virus\ stock\ concentration}$$

The given virus stock volume was diluted into fresh pre-warmed culture medium (pre-diluted if necessary) and thoroughly mixed. Pre-seeded cells had their culture medium replaced with the infection medium before returning the cells into the incubator. Certain experiments required the medium infection to be removed after 2-4 hrs post-infection, in which case cells were thoroughly washed with PBS before adding new pre-warmed medium and returning the cells to the incubator.

2.3.4 Drug and virus treatment studies

Drugs (Selleckchem or Biomol) were diluted into culture medium to 2-times the working concentration. Alternatively, virus was diluted to 20 vp per cell using culture medium. Equal volumes of previously prepared drug and virus dilutions were combined, before pre-seeded cells had their culture medium replaced with the drug/virus mixture. Cells were returned to the incubator at 37°C.

2.4 Procedures for immunology studies

2.4.1 Peripheral blood mononuclear cells extraction

Leukocyte cones (equivalent to one unit of blood) from healthy human donors were purchased from NHS Blood and Transplant services. Upon arrival, leukocyte cones were sprayed with 70% IPA and Trigene disinfectant, before transferring them into a class II laminar-flow cabinet. Inlet and outlet tubing of the cone were cut, before placing the cone on top of the O-ring of a T-175 flask's and allowing the cone to drain by gravity. The T-175 flask had been pre-filled with 220mls of ice-cold RPMI medium. Meanwhile six 50 mls Falcon tubes were each filled with 13ml Ficoll-Paque (GE Healthcare). Once the content of the cone had drained into the flask, the flask containing RPMI/leukocyte mixture was gently mixed, before carefully overlaying 37mls of leukocyte mixture on top of the 13 mls of Ficoll. Falcon tubes were counterbalanced in the swing-out buckets of Sorvall Stratos Centrifuge (ThermoFisher), and spun at 591xg for 35 min with no brakes.

Following the centrifuge, the tubes were transferred back into the cabinet. The band corresponding to peripheral blood mononuclear cells (PBMCs) was gently removed with a sterile Pasteur pipette and pooled together with the remaining PBMC bands from the same donor, into a new 50 mls falcon tube. PBMCs were washed by topping the 50 mls falcon tube with fresh RPMI and spinning for 5 minutes at 300xg. The supernatant was discarded and pelleted PBMCs were washed again. Finally, the wash medium was discarded, cells re-suspended into 50 mls of fresh RPMI media and PBMCs were manually counted by trypan blue method (section 2.1.3).

2.4.2 Enrichment of immune cells by magnetic-activated cell sorting

PBMCs were used to obtain CD14+ cells (Monocytes), CD4 T cells and naïve CD4 T cells by magnetic-activated cell sorting (MACS) using the Miltenyi kits shown in Table 2.6.

Cell type	Kit	Type of selection
CD14+ cells	Human CD14 Microbeads	Positive
CD4 T cells	Human CD4+ T Cell Isolation Kit	Negative
Naïve CD4 T cells	Human Naïve CD4+ T cell Isolation Kit II	Negative

Table 2.6 Details of the Miltenyi kits used to isolate CD14+ cells, CD4 T cells and naïve CD4 T cells.

The PBMCs obtained from previous section were spun at 300xg for 5 minutes. During the centrifugation, the volumes of each reagent from the isolation kit, were calculated using the pre-established cell count according to manufacturer's recommendations. Once PBMCs were pelleted, as much supernatant as possible was carefully removed by vacuum. Rapidly, cells were mixed with the appropriate volume of pre-calculated reagents following manufacturer's directions. Once cells were ready for separation, LS columns (Miltenyi) were fitted onto a QuadroMACS Separator (Miltenyi) and pre-washed with MACS Separator Buffer (Miltenyi). A maximum of $1x10^9$ cells were loaded per column and allowed to drain by gravity into a falcon tube (collection tube), which was placed underneath the column. Once all cells were inside the column, three washes were performed with MACS Separator Buffer, ensuring the full volume had drained before adding the next load. In the case of negative isolation, target cells were eluted into the collection tube. For positive isolation, the LS columns were removed from the CuadroMACS magnet and 5 mls of MACS Separator Buffer was added to the column. Using the plunger provided with the LS column, target cells were gently flushed into a new falcon tube. Finally, target cells were spun at 300xg for 5 minutes, before discarding the buffer and resuspending the cells into fresh RPMI containing 10% FBS and supplemented with 1% Pen/Strep (Gibco).

2.4.3 Mixed leukocyte reaction assay

In this thesis, multiple mixed leukocyte reaction (MLR) assay with different durations were performed, to characterise different aspects of T cell biology. However, all the assays are covered with a description of the longest MLR variant. However, the longest MLR variant is not fully representative of the mixed tumour leukocyte reaction (MTLR) assays, as tumour cells are not present in this version. Nevertheless, the culture and infection of tumour cell lines is described in section 2.1 and MTLR overlaps with the MLR on infected cancer cells.

2.4.3.1 Generation of d3iDC cells

Freshly isolated CD14+ cells were seeded in a T-175 flask at $1x10^6$ cells/ml in DC differentiation medium [RPMI 1640 medium supplemented with 10% FBS, 2mM L-Glutamine, 1% Pen/Strep (Gibco), 250 IU/ml human recombinant IL-4 (R&DSystems) and 800 IU/ml human recombinant GM-CSF (R&DSystems)]. After 3 days, day 3 immature dendritic cells (d3iDC) were harvested, spun and seeded in a T-75 flask with fresh DC differentiation medium. At this point cells were either infected with virus, treated with 100 ng/ml LPS (Sigma) or left untreated. After 2 days, the cells were harvested, washed twice with fresh RPMI medium and counted by trypan blue staining (section 2.1.3).

2.4.3.2 MLR assay

Freshly isolated CD4 T cells or naïve CD4 T cells ($6x10^6$ cells) were mixed with 48 hrs-treated d3iDC ($1.2x10^6$ cells) at a 5:1 ratio, into wells of 6 well plates, using 10% FBS RPMI medium. This was set as day 0 of the MLR.

2.4.3.3 Extended MLR assay

The MLR was monitored during the next few days for cell overgrowth by daily assessing the medium acidification. Every time medium acidification was spotted, cells were re-suspended with 1ml pipette and half the volume was transferred into a new well. Both wells were treated with one volume of 10% RPMI medium supplemented with 60 IU/ml human recombinant IL-2 (R&DSytems).

2.4.3.4 MLR polyclonal re-stimulation

After 9 days of MLR, cells were harvested and the wells were pooled accordingly. Cells were washed twice with 10% FBS RPMI and the live T cell (small refringent cells) count was established by trypan blue (section 2.1.3), before the live T cell density was normalised across conditions in 1 ml of fresh 10% RPMI. Pre-washed DynaBeads T-Activator CD3/CD28 (ThermoFisher), were added into each well at a ratio 1:1 with live T cells.

After 24 hours, cells, Dynabeads and supernatant were transferred into an Eppendorf which was exposed to a magnetic field to remove the Dynabeads. Cells and supernatants were used to assess the polarisation of CD4 T cell.

2.4.4 Antibody coating of culture plates

The corresponding antibody and matched isotype were diluted (Table 2.7) in cell culture-grade 0.01% Poly-L-lysine Solution (Sigma). Fifty microliters of the mixture were aliquoted per well in a 96-well cell culture plate and plates incubate overnight at RT. The following day, the coating solution was removed and wells thoroughly washed with PBS, before cells were added.

Antibody	Clone	Supplier	Working concentration
Ultra-pure LEAF anti-CD3	Monoclonal IgG2a OKT3	Biolegend	5 µg/ml
Ultra-pure LEAF anti-CD28	Monoclonal IgG1 CD28.2	Biolegend	2 µg/ml
Anti-CD46	Monoclonal IgG1 M177	SantaCruz	10 µg/ml
Ultra-pure LEAF IgG2a Isotype	Monoclonal MOPC-23	Biolegend	N/A
Ultra-pure LEAF IgG1 Isotype	Monoclonal MOPC-23	Biolegend	N/A

Table 2.7 Details of antibodies used for plate coating

2.4.5 Immuno-based assay to determine soluble factors

Supernatants from treated d3iDC were assessed for pro-inflammatory soluble factors using The Proteome Profiler Human Cytokine Array Kit (R&DSystems), a membrane-based sandwich immunoassay.

The membrane, which was spotted in duplicate with capture antibodies to specific target proteins, were placed on the plate provided with the kit with the reference facing up and covered with Array Buffer 4. The membrane was left to pre-wet for an hour rocking on a benchtop shaker (The Belly Dancer, Stovall). Meanwhile 0.5 ml of sample were transferred to an Eppendorf and mixed with the cocktail of biotinylated detection antibodies provided in the kit. The mixes were incubated for an hour on the MACSmix Tube Rotor (Miltenyi). Then, Buffer 4 was drained and membranes covered with the samples/antibodies mixtures. The plate containing the membranes and mixtures were left rocking on the benchtop shaker overnight in the at 4°C. Next day, the mixtures were drained and membranes washed multiple times. The streptavidin-HRP was added on the membrane and incubated for another hour on the benchtop shaker. Multiple washes were repeated before the membranes were pat-dry and laid on transparency paper. Without allowing the membranes to dry, the chemiluminescent detection reagents were added and another transparency was added on top. Finally, the signal produced was detected in the GelDOC Imaging Sytem Ultraviolet M-26X Transilluminator (UVP) and

acquired for 5 minutes with the fitted camera (Canon). The data were analysed with ImageJ software using the Gel Analyser tool.

2.4.6 Assessment of the soluble T_H cytokines from supernatant by flow cytometry

Supernatant from T cells polyclonally stimulated with Dynabead T-Activator were assessed for soluble cytokines, commonly expressed by polarised helper T cells, using the LEGENDplex Human T_H Cytokine Panel (Biolegend). This assay uses the cytometric bead assay (CBA) technology, hence requires a flow cytometer to acquire the samples.

The samples and standards were prepared in duplicates according to manufacturer's protocol and using the filter plate coupled with a MultiScreenHTS Vacuum Manifold (Merck). The only exception relative to the protocol was that supernatants were diluted $^1/_5$ instead of the recommended ½. Controls were used on the NxT Attune Acoustic Focusing cytometer (LifeTech). A SSC-H vs FSC-A dot plot was used to calibrate the voltage of these two channels, to ensure a distinguishable separation between the beads A and beads B (Figure 2.3 A). Controls were further used to calibrate the voltages in the classification channel and reporter channel, ensuring a distinct gap between the different cytokine beads and allowing a considerable dynamic range for a comfortable quantification, respectively (Figure 2.3 B and C). Once voltages were set, stained samples were placed in the auto-sampler of the cytometer for autonomous acquisition. Finally, data were analysed on the Legendplex Analysis software provided with the kit.

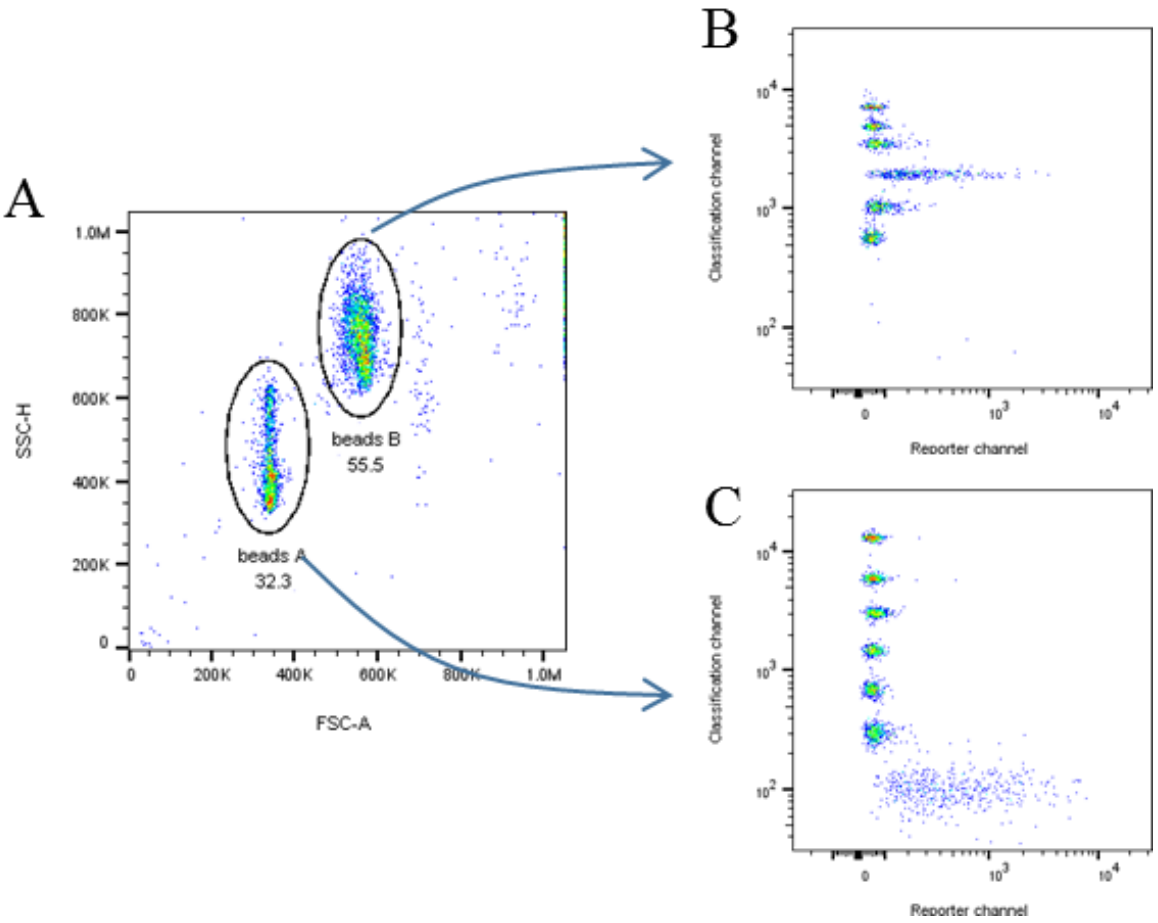


Figure 2.3 Representation of the beads from the LEGENDplex Human T_H Cytokine Panel in flow cytometry. The human T_H Cytokine Panel is a sandwich-based immunoassay that allows the quantification of 13 cytokines by flow cytometry. The assay uses 13 different capture beads (A) which have two distinctive size for a first classification. (B and C) Beads are further identified by their fluorescence intensity in the classification channel (Y axis), the reporter channel (X axis) is used to evaluate the mean fluorescence intensity of each classified bead, before extrapolating the cytokine levels from the standard curves.

2.4.7 Enzyme-linked immunosorbent assay

Supernatants were used to assessed the IL-2 concentration using an anti-human IL-2 antibody pair (R&DSystems) following manufacturer's instructions. The anti-IL-2 capture antibody (Table 2.8) was diluted into Carbonate/Bicarbonate Buffer (Sigma), according to manufacturer's recommendation. The capture antibody mix was aliquoted in 96-well ELISA plate (Nunc MaxiSorp) at 100 µl per well. The plate was covered with cling film and kept in the fridge overnight. The following day, wells were washed 3 times with PBST [PBS + 0.05% Tween-20 (Sigma)] before adding blocking buffer [PBST + 3% bovine serum albumin

(Sigma)] for one hour at room temperature. Meanwhile, human recombinant IL-2 (R&DSystems) was used to prepare a six points standard curve. After the incubation time, the blocking buffer was removed and washed 3 times with PBST, before samples and standards were added in triplicates. A triplicate of control wells received blocking buffer to determine the assay background. The plate was incubated at room temperature for 1 hour before being washed 3 times. The anti-IL-2, biotin conjugated detection antibody was diluted in blocking buffer before added on the plate and the plate was incubated for 1 hour. The plate was washed 3 times. Streptavidin-HRP conjugate (R&DSystems) was diluted 1/200 in blocking buffer before being added. The plate was incubated at room temperature for 1 hour before washing 3 times. 1-Step Ultra TMB-ELISA (ThermoFisher) was added to the wells and incubated at room temperature for 30minutes in the dark. Finally, substrate was inactivated with one equivalent volume of 1M HCl, before measuring the absorbance at 405nm (OD) on a Synergy HT plate reader. The concentration of IL-2 in each sample was determined by first subtracting the assay background from all OD values, then plotting the standard curve in GraphPad Prism 6.0 and then transforming. The concentration of IL-2 of each sample was calculated by averaging the interpolated data from the standard curve using OD values.

Antibody	Role	Clone	Supplier	Working dilution
Anti-IL-2	Capture	MAB602	R&DSystems	1/125
Anti-IL-2	Detection	BAF202	R&DSystems	1/500

Table 2.8 Details of antibodies used for IL-2 ELISA

2.4.8 Immunofluorescence staining and flow cytometry

The majority of antibodies used in immunofluorescence staining, were previously titred on target cells to maximise the signal to noise ratio (section 2.4.8.1). This was relatively simple as most of the used antibodies were directly labelled with a fluorochrome. Cell surface and vital staining reactions were carried out on ice using ice-cold reagents to prevent antibody

internalisation[189], this was less relevant in later steps of intracellular or intranuclear staining, where samples had been fixed previously. Nevertheless, staining was performed in the dark to prevent the fluorochrome from fading out.

During experimentation, fluorescence minus one (FMO) antibody mixes were prepared, containing all antibodies from a given panel, excluding one to ensure gate positions were accurate. Single stain antibody mixes were also prepared for compensation controls, along with concentration and fluorochrome matched isotype controls for each antibody being tested.

2.4.8.1 Antibody titration

All antibodies were titred against isotype controls to optimise concentrations for downstream studies. Target cells were obtained according to section 2.4.2 and 2.1. Before assessing the titration, cells were prepared accordingly with the location of the marker (surface or intracellular) described in sections below. Subsequently, the staining antibodies were serially diluted from the manufacturer's recommended staining concentration, in staining buffer according to the marker location. An isotype matched control was diluted to match the concentrations of the antibody being tested. Antibody dilutions were added to separate sample tubes of pre-prepared cells. All staining reactions were incubated in the fridge for 30 minutes. After staining, samples were washed twice with washing buffer, spun at 300xg for 5 minutes, the supernatant was discarded and the cell pellet was resuspended in each instance. After the second wash, all samples were resuspended in staining buffer and acquired with the flow cytometer. The mean fluorescence (MF) for isotype controls and positively stained samples was then determined using appropriate gates, and signal to noise ratio was determined by dividing positively stained sample MF by isotype MF at each dilution. The concentration with the greatest gap between signal to ratio was chosen.

2.4.8.2 Cell surface staining and vital staining

Pre-harvested PBS-washed cells (approximately 1x 10^5 cells per condition) were incubated with LIVE/DEAD Fixable Near-IR Dead Cell Stain Kit (LifeTech) or LIVE/DEAD Fixable Aqua Dead Cell Stain Kit (LifeTech), according to manufacturer's recommendations. Meanwhile, antibody mixes were prepared in blocking buffer (1%FBS PBS) using concentrations based on a previous titration (Table 2.9). Cells stained with live/dead stain were washed with PBS and then with blocking buffer, which followed the addition of the corresponding buffer, centrifugation at 300xg for 5 minutes, discarding of the supernatant and agitation of the cell pellet in each instance. The pelleted cells were resuspended in antibody mix and placed in the fridge for 30minutes. After staining, samples were washed twice and samples were either used for further staining or resuspended in blocking buffer and acquired on the flow cytometer.

Antibody	Clone	Species	Supplier	Working concentration
Anti-CD3	Monoclonal OKT3	Mouse	Biolegend	150ng/reaction
Anti-CD4	Monoclonal OKT4	Mouse	Biolegend	100ng/reaction
Anti-CCR7	Monoclonal 4B12	Mouse	Biolegend	300ng/reaction
Anti-CD40	Monoclonal 5C3	Mouse	Biolegend	200ng/reaction
Anti-CD80	Monoclonal 2D10	Mouse	Biolegend	200ng/reaction
Anti-CD86	Monoclonal IT2.2	Mouse	Biolegend	200ng/reaction
Anti-HLA-DR	Monoclonal L243	Mouse	Biolegend	400ng/reaction
Anti-HLA-ABC	Monoclonal W6/32	Mouse	Biolegend	400ng/reaction
Anti-CD46	Monoclonal E4.3	Mouse	BD	2µl/reaction
Anti-CAR	Monoclonal RmcB	Mouse	Milipore	5µl/reaction
Anti-DSG-2	Monoclonal 6D8	Mouse	Abcam	2µl/reaction
Anti-CD25	Monoclonal M-A251	Mouse	Biolegend	150ng/reaction
Anti-CD69	Monoclonal FN50	Mouse	Biolegend	80ng/reaction
Anti-CD45-RA	Monoclonal Hl100	Mouse	Biolegend	75ng/reaction
Anti-CD107a	Monoclonal H4A3	Mouse	Biolegend	160ng/reaction
Anti-PD-L1	Monoclonal 29E.2A3	Mouse	Biolegend	50ng/reaction

Table 2.9 Details of antibodies used for cell surface marker staining

2.4.8.3 Intracellular marker staining

The cells stained on the surface were further used for intracellular staining. Cells were briefly vortexed and rapidly resuspended in Fixation/Permeabilization solution (BD Bioscience), before placing the cells for 20 minutes in the fridge. Meanwhile, antibody mixes were prepared in 1X BD Perm/Wash buffer (BD Bioscience), using concentrations based on a previous titration (Table 2.10). Cells were then washed twice in Perm/Wash buffer, which followed the addition of Perm/Wash buffer, centrifugation at 300xg for 5 minutes, discarding of the supernatant and agitation of the cell pellet in each instance. Pelleted cells were then resuspended in antibody mix and incubated for 30 minutes in the dark. After staining, samples

were washed twice in Perm/Wash buffer, before all samples were resuspended in blocking buffer and acquired on the flow cytometer.

Antibody	Clone	Species	Supplier	Working concentration
Anti-IFN-g	Monoclonal 4S.B3	Mouse	Biolegend	200 ng/reaction
Anti-TNFa	Monoclonal Mab11	Mouse	Biolegend	100 ng/reaction
Anti-IL-4	Monoclonal 8D4-8	Mouse	Biolegend	200 ng/reaction
Anti-IL-5	Monoclonal JES1-3910	Rat	Biolegend	50 ng/reaction
Anti-IL-10	Monoclonal JES3-9D7	Mouse	Biolegend	200 ng/reaction
Anti-IL13	Monoclonal JES10-5A2	Rat	Biolegend	200 ng/reaction
Anti-IL-17A	Monoclonal BL168	Mouse	Biolegend	400 ng/reaction

Table 2.10 Details of antibodies used for intracellular marker staining

2.4.8.4 Intranuclear marker staining

The surface stained cells were further used for intranuclear staining. Cells were briefly vortexed and rapidly resuspended in Foxp3 Fixation/Permeabilization working solution (eBioscience), before placing the cells for 30 minutes in the fridge. Cells were then washed twice in 1X Permeabilization Buffer (eBioscience), followed by the addition of Permeabilization Buffer, centrifugation at 500xg for 5 minutes, discarding of the supernatant and agitation of the cell pellet in each instance. Cells were suspended in their residual volume, before FBS was added, aiming for a final 2% FBS concentration. After 15minutes of incubation in the dark, the corresponding antibodies were added to each sample using the recommended concentrations (Table 2.11), before manual mixing and incubation for another 30 minutes. After staining, samples were washed twice in Permeabilization Buffer before samples were resuspended in blocking buffer and acquired on the flow cytometer.

Antibody	Clone	Species	Supplier	Working volume
Anti-GATA3	Monoclonal L50-826	Mouse	BD	5 µl/reaction
Anti-Tbet	Monoclonal 4B10	Mouse	Biolegend	5 µl/reaction

Table 2.11 Details of antibodies used for intranuclear marker staining

2.4.8.5 Flow cytometry

Samples were vortexed briefly before being acquired through the Attune NxT Acoustic Focusing Cytometer (LifeTech), which was fitted with the 4-laser configuration (blue, red, violet and yellow). Compensation controls (single stained samples) were used first to set the channel voltages and cell-size gates. Voltages were set such that the unstained control had a mean fluorescence of approximately 1,000-2,000. Isotype and FMO controls were then analysed to set gates for populations of interest. Finally, the main study samples were acquired with the flow cytometer generally through the Auto Sampler extension, pre-determined to obtain 10,000 live events. FlowJo software (Tree Star Inc) was used to analyse the data.

2.5 Statistics

Data were analyzed using GraphPad Prism version 6.0. for Windows (GraphPad, San Diego, CA). ELISA, HPLC and CBA end point titres were normalized by Log_{10} transformation before extrapolation. Where appropriate, fold changes were calculated accordingly: (variable's value – control's value) / control's value. The student T-tests was performed to compare mean responses between unpaired data (no prior normalisation) across two observations, or between paired data across (prior normalisation against respective controls) two observations. ANOVA test analysis, as appropriate, was used to compare responses between paired data when there were more than two observations. MTS end point values were normalized by Log_{10} transformation before a non-linear sigmoidal curve was fitted. Sum of squares F test, was used to evaluate the curves' Goodness of Fit (R^2), the virus concentration to kill 50% of the cells (EC50) and to compare the LogEC50 between two sigmoidal curves by fitting a curve with

common top, bottom and hill of the curve parameters. A p value ≤ 0.05 was considered significant in T-test and ANOVA, and a p value ≥ 0.05 was accepted as comparable LogEC50 in Sum of squares F test.

3 Studying the life cycle of EnAd virus in cancer cells

3.1 Introduction

In general, oncolytic viruses have been generated by rational design with an aim to attenuate virus activity or increase selectivity in order to improve safety. EnAd was the first virus to be developed by directed-evolution and was selected for its potent cancer cell killing without altering the selectivity profile. The resulting virus had three major genomic alterations compared to the parental Ad11p virus; a chimeric E2B Ad11p:Ad3 region, a deletion in the early region 4 and a large deletion in the E3 (see Introduction). These three modifications are located in early genes, which are involved in virus cycle[190], cell control[177] and immune response[191]. On the other hand, late genes encoding structural proteins are unchanged, this is the reason why the structural capsid of EnAd is shared with the parental virus.

Two methods were employed in this chapter to try and better understand the direct anti-tumour activity of the virus. 1) Establishing the differences between parental and mutant virus biology in tumour cells, and the role each individual mutation plays. To achieve this, recombinant EnAd variants with one of the mutations replaced at a time by the corresponding Ad11p wildtype (wt) region, were used. 2) How the cellular activity contributes to the virus biology. Accordingly, cellular activity was manipulated with drugs and virus replication was screened in combination with over 300 compounds. Hit drugs were further studied in *in vitro* studies. Alternatively, potential combination therapies were suggested.

3.2 Chapter aims

1. Compare the life cycles of EnAd and Ad11p in cancer cells and relate any differences to the genetic composition of the viruses.
2. Explore the role of each mutation in EnAd by comparing its activity with three recombinant adenoviruses engineered to contain wildtype replacements of each mutant region individually.
3. Use a Selleckchem drug library to determine compounds that could enhance virus replication, both to inform on viral mechanism(s) of action and to identify potential therapeutic synergy with established drugs.

3.3 Results

3.3.1 EnAd and Ad11p molecular differences in cancer cells

EnAd was chosen as an oncolytic virus for its gain in oncolytic potency on multiple tumour cell lines, without affecting its selectivity for tumour cells compared to normal cells[6]. In this section the potency of EnAd was assessed *in vitro* on HT29 using a cytotoxicity assay and compared to Ad11p. In addition, to further understand the implications of the genetic differences between both viruses, *in vitro* assays were used to compare replication and progeny virus production, as well as viral mRNA expression.

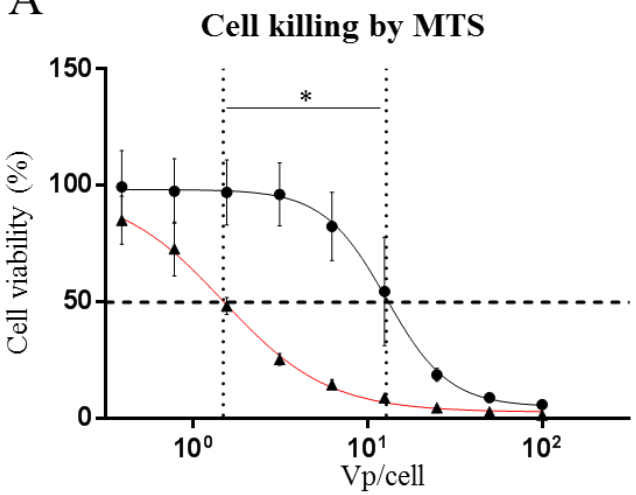
3.3.1.1 Comparison of EnAd and Ad11p oncolytic potency on HT29 cells

The oncolytic potency of EnAd on HT29 cells, compared to Ad11p virus, was determined using the MTS assay. Figure 3.1 shows that the number of EnAd particles required to kill 50% of the cells (EC50) were significantly lower than Ad11p on all cell lines tested ($p<0.0001$). Killing curves of both viruses were also statistically different ($p<0.0001$) as the sum-of-squares F test

indicated. This is consistent with previous reports describing EnAd as a more potent virus in multiple cell lines[6].

Unlike drugs, adenoviruses are capable of self-amplifying the input dose by replication and release of progeny virus capable of further replication and release. Different viruses may do this at different speeds on different cell lines. Therefore, the differences in EC50 could indicate that EnAd replicates and lyses cells faster than Ad11p. Interestingly, E2B, which is mutant in EnAd, encodes for pTP and AdPol involved in adenovirus replication[6]. To probe this further, the viral replication and progeny production were assessed.

A



B

Virus	EC50 (vp/cell)	R square
Ad11p	12.78	0.909
EnAd	1.49	0.972

Figure 3.1 Comparison of EnAd and Ad11p killing ability on HT29 determined by viability assay (MTS). HT29 cells were seeded overnight in 96 well plates at 30,000 cells/well and then infected with 5-fold serial dilutions of Ad11p (black line) or EnAd (red line). Viability (normalised to untreated control cells) was determined 3 days after infection using the MTS assay (see Materials and Methods). A) Means of 6 biological replicates with standard deviation shown. Four parameter non-linear curve fit is shown with dotted lines indicating EC50 and sum-of-squares F test was used to determine the significance of differences in killing curves between EnAd and wildtype virus (*p<0.0001). B) EC50 and R square values for each non-linear fit are shown. Representative of n>2 independent experiments.

3.3.1.2 Comparison of EnAd and Ad11p genome replication in HT29 cells

To evaluate whether differences observed in oncolytic potency between EnAd and Ad11p may derive from an improved replication capacity, a qPCR assay was developed to measure the number of virus genomes by measuring copies of Ad11p capsid gene, hexon. Virus particle uptake in HT29 cells was assessed at 3hrs post infection. As expected equivalent uptake was seen between both virus – EnAd and Ad11p capsid is the same (not shown). However, by 24 hrs post-infection EnAd showed a significant increase of 5-fold higher genome copies per input cell than Ad11p, suggesting faster replication. The differences were sustained over time – although not significantly different at 48 hrs and 72 hrs – up to complete cell depletion at 96 hours post infection (Figure 3.2). This suggested that EnAd had acquired the ability to replicate more efficiently, and subsequently higher numbers of daughter genomes were generated after HT29 cells were killed.

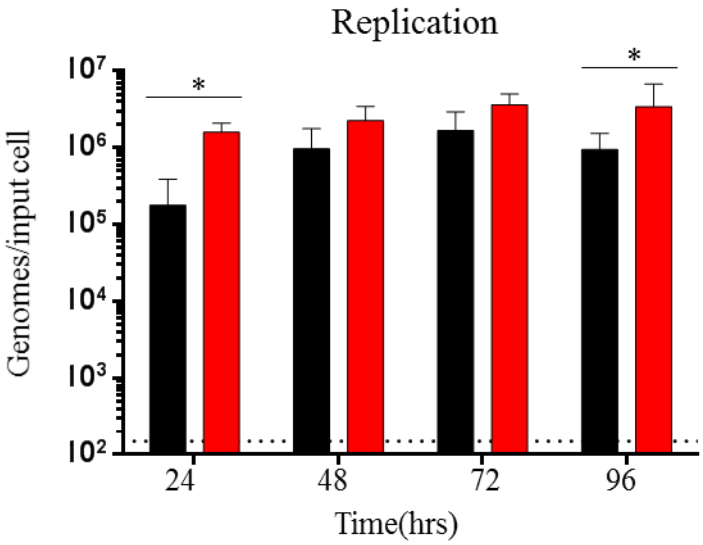


Figure 3.2 Comparison of EnAd and Ad11p replication kinetics in HT29 cell lysates by hexon qPCR. HT29 cells were infected with 100 vp/cell of Ad11p (black) or EnAd (red). Virus replication (normalised to genomes per input cells) was determined at 3, 24, 48, 72 and 96 hrs post infection using hexon qPCR assay (see Materials and Methods). Means of biological triplicates with standard deviation are shown. Dotted lines indicate virus uptake 3 hrs post infection and T test was used to determine the significance between both viruses at every timepoint (*p<0.0001). Representative of n=2 independent experiments.

3.3.1.3 Supernatant assessment to compare EnAd and Ad11p virus production in HT29 cells

Based on the previous results where EnAd was shown to replicate more efficiently than Ad11p, it was here hypothesised that more genomes could translate in additional progeny virus particles, that in turn infected more cells amplifying the cell killing effect. Virus production was investigated in supernatant (SN) of infected HT29 cell, at multiple time points by either virus genome quantification or infectious virus particles. To prevent asynchronous infection by excess virus, infection medium was replaced by fresh medium 4 hrs after infection.

Hexon qPCR showed that EnAd and Ad11p progeny was detectable in the SN only from 48 hrs post-infection onwards. About 20-fold significant difference ($p<0.0001$) in genome count were detected in 48 hrs supernatant between EnAd and Ad11p, and extended until last time point where cells had been killed by the virus (Figure 3.3 A). Virus in supernatant after 3 hrs infection was used to determine the input virus threshold (dotted line).

To ascertain whether detected genomes in supernatant corresponded to infectious virus particles, the same supernatants were used in an infectivity assay by ever increasing dilutions (see Material and Methods). In this case the virus in the 24 hrs supernatant was detectable, probably due to an increased sensitivity of this assay compared to the PCR assay. The fact that the 24 hrs timepoint were equal for both virus and under the 3 hrs input background (dotted line), suggested that these infectious particles were probably leftover input virus rather than progeny. EnAd produced significantly ($p<0.0001$) more infectious particles in supernatant than Ad11p – more than 2 logs difference – from 48 hrs onwards (Figure 3.3 B).

It was interesting to remark that viral genome kinetics (Figure 3.3 A) in the cellular SN seemed to be comparable to infectious virus particles (Figure 3.3 B). Suggesting that the virus progeny in the supernatant can be monitored by either qPCR or infectious assay. Overall, EnAd appeared to release the virus progeny from HT29 cells to the supernatant more rapidly than

parental virus, as well as the total particles. Therefore, the hypothesis exposed at the beginning of this section: “more genomes could translate in to additional virus progeny” appeared to be acceptable. But to generate new adenovirus particles, other components than genomes are needed, for instance protein expression. To probe this further, the viral transcripts were assessed.

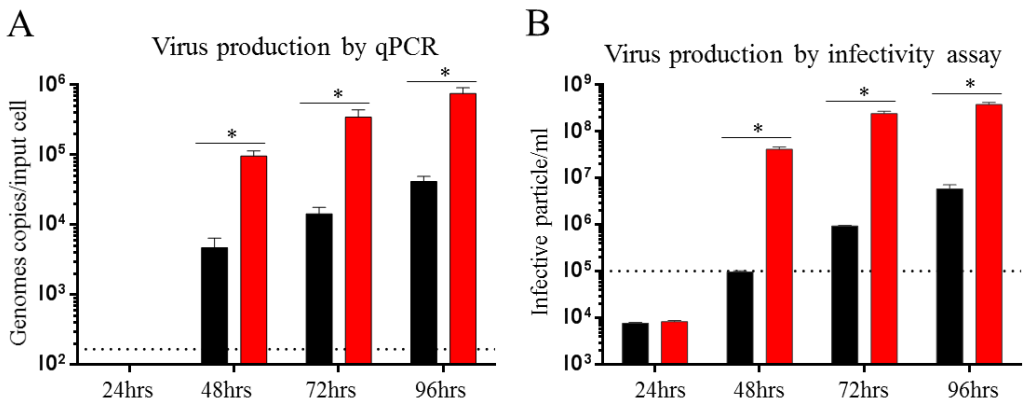
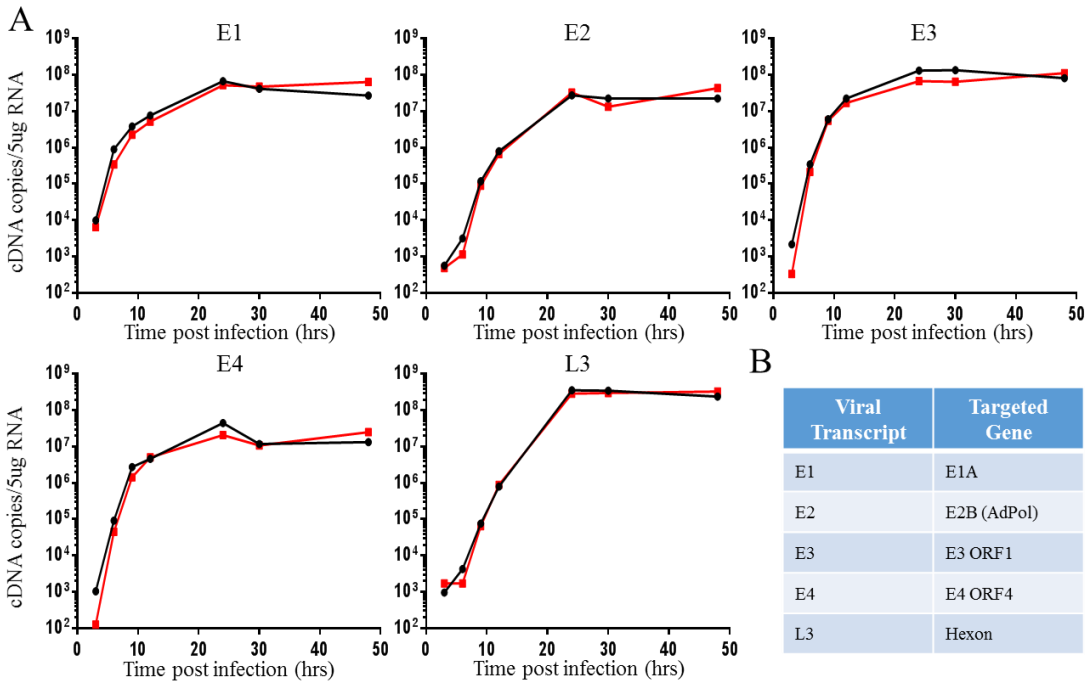


Figure 3.3 Comparison of EnAd and Ad11p virus production kinetics in HT29 cell supernatant by hexon qPCR and infectivity assay. HT29 cells were infected with 100 vp/cell of Ad11p (black) or EnAd (red) for 4 hrs before cells were washed with PBS and replaced with fresh medium. Virus in supernatant (genomes copies per input cells or infective particles/ml) was determine at 3, 24, 48, 72 and 96 hrs post infection using A) hexon qPCR assay and B) infectivity assay (see Materials and Methods). Means of technical triplicates with standard deviation are shown. Dotted lines indicate virus input at 3 hrs post infection and T test was used to determine the significance between both viruses at every timepoint (*p<0.001). Representative of n=2 independent experiments.

3.3.1.4 Comparison of the number of viral mRNA transcripts produced by EnAd and Ad11p in HT29 cells

Having shown EnAd produced greater numbers of total genomes compared to Ad11p, it was hypothesised that EnAd's increased genome copies would translate into higher numbers of total viral mRNA transcript. In turn, this would be expected to reflect more proteins available to make virus, and could explain EnAd's fast killing phenotype and earlier viral particle release. In fact, some had previously shown this correlation for a recombinant Ad5 with increased replication and progeny[192]. To compare the numbers of EnAd and Ad11p viral transcripts in HT29 cells, primers and probes were designed against consensus sequences for the four early (E) transcriptional units and the late (L) transcript. Surprisingly, E and L mRNA transcripts showed comparable levels of expression for both viruses over time (Figure 3.4 A), despite the 5-fold difference in genome copies (Figure 3.1 A).

This observation suggested that adenovirus transcripts were expressed from virus input and not from onset genomes and the level of virus mRNA transcript was not likely to be responsible for the phenotype of EnAd. However, it couldn't be disregarded that EnAd mutation had made transcripts' translation into protein more efficient. Unfortunately, the lack of available antibodies against Ad11 proteins, the protein expression could not be compared. On the other hand, if the translation efficiency was the same between EnAd and Ad11p, the genome replication would be the limiting factor for Ad11p to produce more virus progeny. A mechanism other than increased transcription of these genes, should therefore be contributing to EnAd's increased potency.



Viral Transcript	Targeted Gene
E1	E1A
E2	E2B (AdPol)
E3	E3 ORF1
E4	E4 ORF4
L3	Hexon

Figure 3.4 Comparison of EnAd and Ad11p virus transcripts kinetics in HT29 cell lysates by RT-qPCR. HT29 cells were infected with 100 vp/cell of Ad11p (black line and dots) or EnAd (red line and squares). Virus transcripts (cDNA copies normalised to 5 µg total RNA) were quantified at 3, 6, 12, 18, 24, 30 and 48 hrs post infection using E1, E2, E3, E4 and L3 RT-qPCR assay (see Materials and Methods). Means of biological duplicates are shown.

3.3.2 Investigating the role of EnAd-associated mutations in its improved oncolytic phenotype

EnAd has three genetic differences from Ad11p (see Introduction). This section explores three recombinant EnAd variants containing wildtype (wt) replacements for each mutation and their role on aspects of the virus life cycle.

3.3.2.1 Production of EnAd variants containing wtE2B, wtE3 and wtE4

Three recombinant viruses were designed using the EnAd backbone, each bearing a single substitution, resulting in EnAd-wtE2B, EnAd-wtE3 and EnAd-wtE4 (Figure 3.5). EnAd current cloning technology makes it challenging to generate these viruses[193]. The genomes were therefore designed and then out-sourced to a company for DNA synthesis by Gibson assembly.

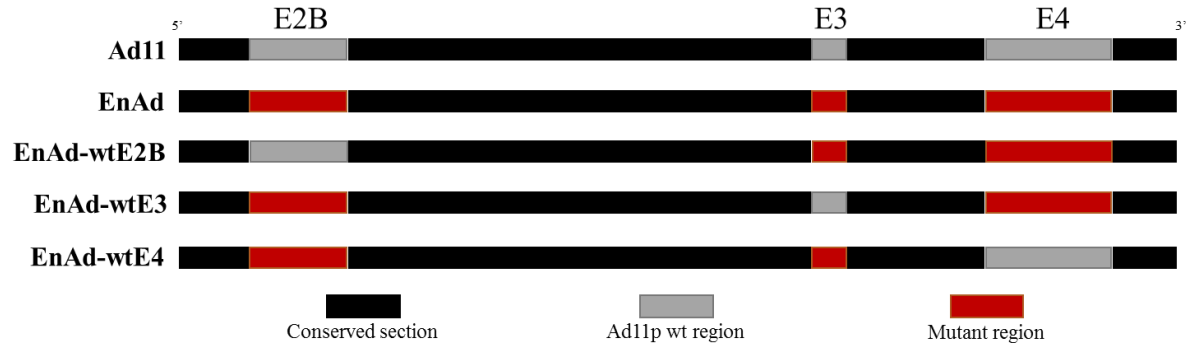


Figure 3.5 Diagram depicting the genomic differences between Ad11p and EnAd, as well as the designed recombinant virus EnAd-wtE2B, EnAd-wtE3 and EnAd-wtE4. Genome length are not to scale.

The linearised genomes were transfected onto HEK-293 cells and clarified viral lysates were used to amplify the virus (see Material and Methods). During the amplification rounds, the cytopathic effect (CPE) was determined by light microscopy to assess virus growth. The three viruses produced the expected cytopathic effect (Figure 3.6 B, C and D), however the CPE of EnAd-wtE4 (wtE4) was much slower (Figure 3.6 B) than the other two viruses (Figure 3.6 C and D).

The two hyper flasks per virus obtained at the end of the amplification process were CsCl-banded to produce purified virus stocks (see Material and Methods). After the first ultracentrifugation spin, EnAd-wtE2B and EnAd-wtE3 produced the expected pattern of incomplete virus bands on the top, and one lower dense band corresponding to fully matured virus (Figure 3.6 E). On the other hand, EnAd-wtE4 only produced incomplete bands with no visible band in the full virus region (Figure 3.6 E). This study was repeated from the transfection step and the same pattern of bands was seen reproducibly. Accordingly, it did not seem possible to produce infectious virus with the wtE4 sequence combined with the rest of the EnAd genome. This was unexpected as E4-ORF4 is generally related to regulation of cell and mRNA metabolism. Hence it was suspected that E4 mutation was responsible for EnAd's cell killing phenotype, rather than involved in production of fully-matured virus[187].

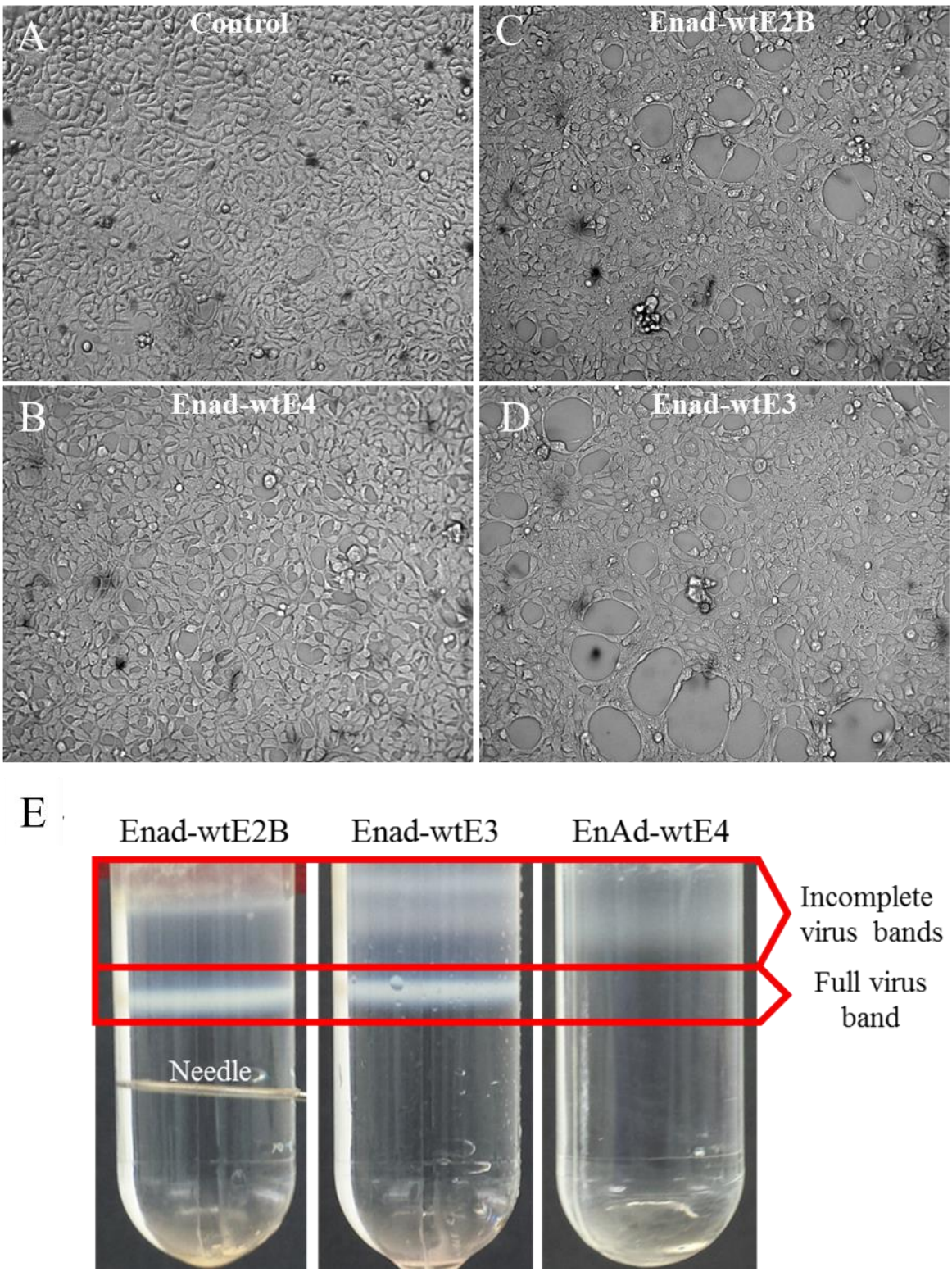
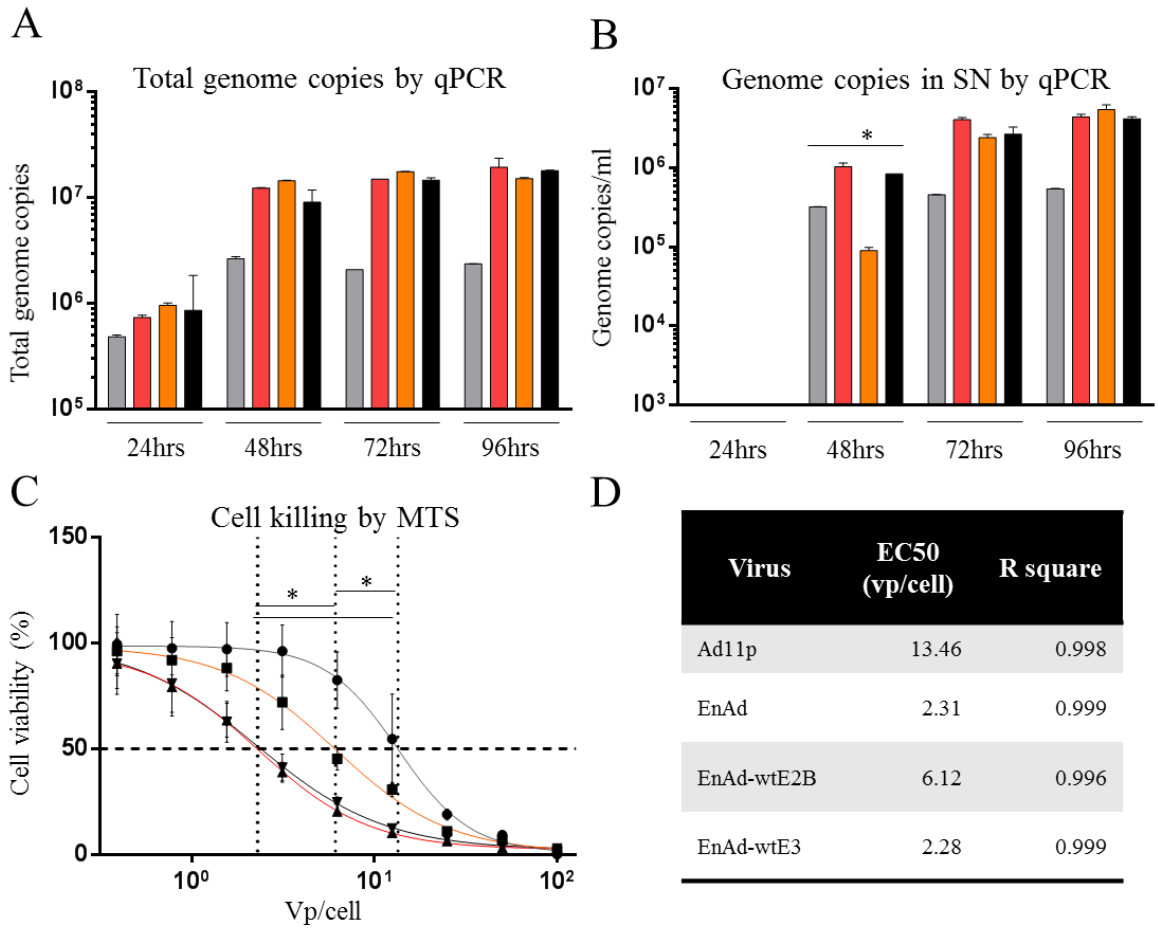


Figure 3.6 Production of EnAd variants containing wtE2B, wtE3 and wtE4. A) EnAd variant liniarised genomes were transfected into AD-293 (see Material and Methods) and CPE monitored daily. Cells transfected with (C) wtE2B, (D) wtE3 and (B) wtE4 or (A) control (mock transfection) for 5 days are shown. Transfected cells were harvested for virus amplification and purification (see Material and Methods). (E) EnAd- wtE2B, -wtE3 and -wtE4 incomplete and full virus bands in CsCl gradients are shown after first day virus purification.

3.3.2.2 Evaluation of oncolytic potency and virus production of EnAd-wtE2B and EnAd-wtE3 virus in HT29 cells

To understand the role of the genetic modification of EnAd on its improved oncolytic properties, the EnAd-wtE2B and EnAd-wtE3 purified virus stocks (produced in previous section) were used here in oncolytic potency, virus replication and progeny production assays, and compared to EnAd and Ad11p (assays used in sections above). Virus replication in HT29 cells and progeny production in supernatant over time were evaluated by hexon qPCR. EnAd-wtE3 replication and virus progeny in SN were similar to EnAd at every time point (Figure 3.7 A and B). EnAd-wtE2B virus replication followed the same kinetics as EnAd virus (Figure 3.7 A), however the virus progeny yield at 48 hrs post-infection supernatant was significantly ($p<0.0001$) 10-fold lower, eventually less than Ad11p virus (Figure 3.7 B). By 24hrs later, the virus yield had recovered to EnAd and EnAd-wtE3 levels (Figure 3.7 B). Potencies of virus cytotoxicity were also compared using an MTS-based assay on HT29 cells. EnAd-wtE3 and EnAd showed very similar EC50 values (Figure 3.7 D) and same killing curves ($p=0.0735$) by statistical analysis using the extra sum-of-squares F test (Figure 3.7 C). On the other hand, EnAd-wtE2B and Ad11p killing curves were statistically ($p<0.0001$) different to others (Figure 3.7 C), as well as their EC50 (Figure 3.7D).

Overall, these data suggested that the wtE3 had little implication for EnAd's phenotype described in HT29 in previous sections. On the other hand, the same genome replication kinetics between EnAd-wtE2B virus and EnAd, suggested that E2B mutation was not responsible for the virus improved replication. Also, EnAd-wtE2B suggested that E2B mutation was involved in the timing of virus progeny release to the supernatant. Finally, this virus suggested that both E2B and E4 mutations were involved in the fast cell killing phenotype seen with EnAd.



Virus	EC50 (vp/cell)	R square
Ad11p	13.46	0.998
EnAd	2.31	0.999
EnAd-wtE2B	6.12	0.996
EnAd-wtE3	2.28	0.999

Figure 3.7 Evaluation of genome replication, progeny production and killing ability of wtE2B and wtE3 in HT29 cells. HT29 cells were infected with 100 vp/cell of Ad11p (grey), EnAd (red) EnAd-wtE2B (orange) and EnAd-wtE3 (black). (A) Virus replication (total genomes copies) and (B) progeny released to supernatant (SN; genome copies in ml of supernatant) were determined at 24, 48, 72 and 96 hrs post infection using E1A qPCR assay (see Materials and Methods). Means of biological triplicates with standard deviation are shown. T test was used to determine the significance between viruses at every timepoint (*p<0.0001). Representative of n=2 independent experiments. Alternatively, cell HT29 cells were seeded overnight in 96 well plates at 30,000 cells/well and then infected with 5-fold serial dilutions of Ad11p (grey line), EnAd (red line) EnAd-wtE2B (orange line) and EnAd-wtE3 (black line). Viability (normalised to untreated control cells) was determined 3 days after infection using the MTS assay (see Materials and Methods). C) Means of 3 biological replicates with standard deviation are shown. Four parameter non-linear curve fit is shown with dotted lines indicating EC50 and sum-of-squares F test was used to determine the significance of differences in killing curves between EnAd and wildtype virus (*p<0.0001). D) EC50 and R square values for each non-linear fit are shown. Representative of n=2 independent experiments.

3.3.2.3 Troubleshooting the difficulties of producing EnAd-wtE4 virus

Based on previous observation that EnAd-wtE4 would not purify as expected for infectious virus particles, genome structure, virus particle numbers and cell killing studies were carried out in this section to better understand the reason for difficulty in virus production.

3.3.2.3.1 Assessment of the genomic structure of EnAd-wtE4

All three recombinant EnAd linearized genomes had been sequence-confirmed correctly. In addition, EnAd-wtE4 DNA was digested with Afl2 and Ndel restriction enzymes and run on a gel to demonstrate that it had the correct genome structure. Virtual digestion of wtE4 genome on ApE software predicted a total of eleven bands with sizes 12.5, 5.8, 5.1, 4.4, 2.5, 1.6, 2x 1.4 kb and four ranging under 0.2 kb. The observed bands for wtE4 after enzyme digestion appeared to agree with the predicted pattern (Figure 3.8), The four small bands under 0.2 kb could not be detected, although that often happens with small sized DNA bands.

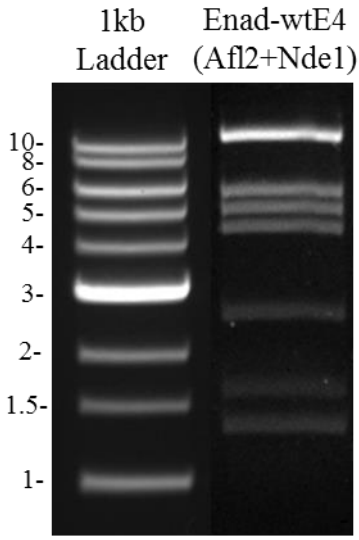


Figure 3.8 Assessment of EnAd-wtE4 genomic structure. EnAd-wtE4 genome was digested with Afl2 and Nde1 restriction enzyme (see Material and Methods). Digested product loaded on a 1% agarose gel and run for 25 minutes at 180 volts next to 1kb ladder is shown.

3.3.2.3.2 Titration of EnAd-wtE4 virus particles from crude viral lysates by HPLC

In previous section it was shown the inability to produce EnAd-wtE4 purified material. Instead, crude virus lysate (CVL) from EnAd-wtE4's amplification material was used for virus biology studies. CVL consisted of infected AD-293 cells scraped and re-suspended in their own medium. The mix was then harvested and submitted to a cycle of freeze-thaw before spinning at 300g for 5minutes and collecting the supernatant only. Colleagues in this lab had previously standardised a method to detect and quantify adenovirus from purified stock virus and CVL by high performance liquid chromatography (HPLC) fitted with an anion exclusion column. Briefly, the virus titre of a sample was determined by running a standard curve of known concentrations of virus, then the area under the curve (AUC) of the virus elution peak – which stand around 10 minutes for EnAd and Ad11p – was used to extrapolate the virus concentration (see Material and Methods).

In the present study, CVL from AD-293 cells infected with 50 µl of EnAd-wtE4, Ad11p and EnAd amplified material, was assessed at 24 hrs, 48 hrs and 72 hrs post infection. EnAd and Ad11p were largely quantifiable by 72 hrs as their AUC were 278.44 and 261.28 units respectively (Figure 3.9 A). However, EnAd-wtE4 was only visible as a tiny peak at 72 hrs, and the AUC was smaller than 40 units (Figure 3.9 A). This falls under the limit of quantification – the linearity at the bottom of the standard curve was normally lost at AUC< 55 units, or total 1.5×10^9 vp. Therefore, this method was not sensitive enough to quantify EnAd-wtE4 particles in CVL.

The previously generated 72 hrs EnAd-wtE4, Ad11p and EnAd CVLs were subject to DNA extraction and assayed by hexon qPCR. Interestingly, EnAd-wtE4 yielded 2.20×10^{11} genomes/ml, the highest concentration, whilst Ad11p and EnAd produced only 1.58×10^{11} and 3.95×10^{10} genomes/ml, respectively (Figure 3.9 B).

A clear disparity was seen in virus titres in CVLs measured by HPLC and qPCR. However, this might be related to the fact that qPCR cannot make the distinction between non-encapsidated and infectious virus DNA, whereas the HPLC only titres fully formed virus particles.

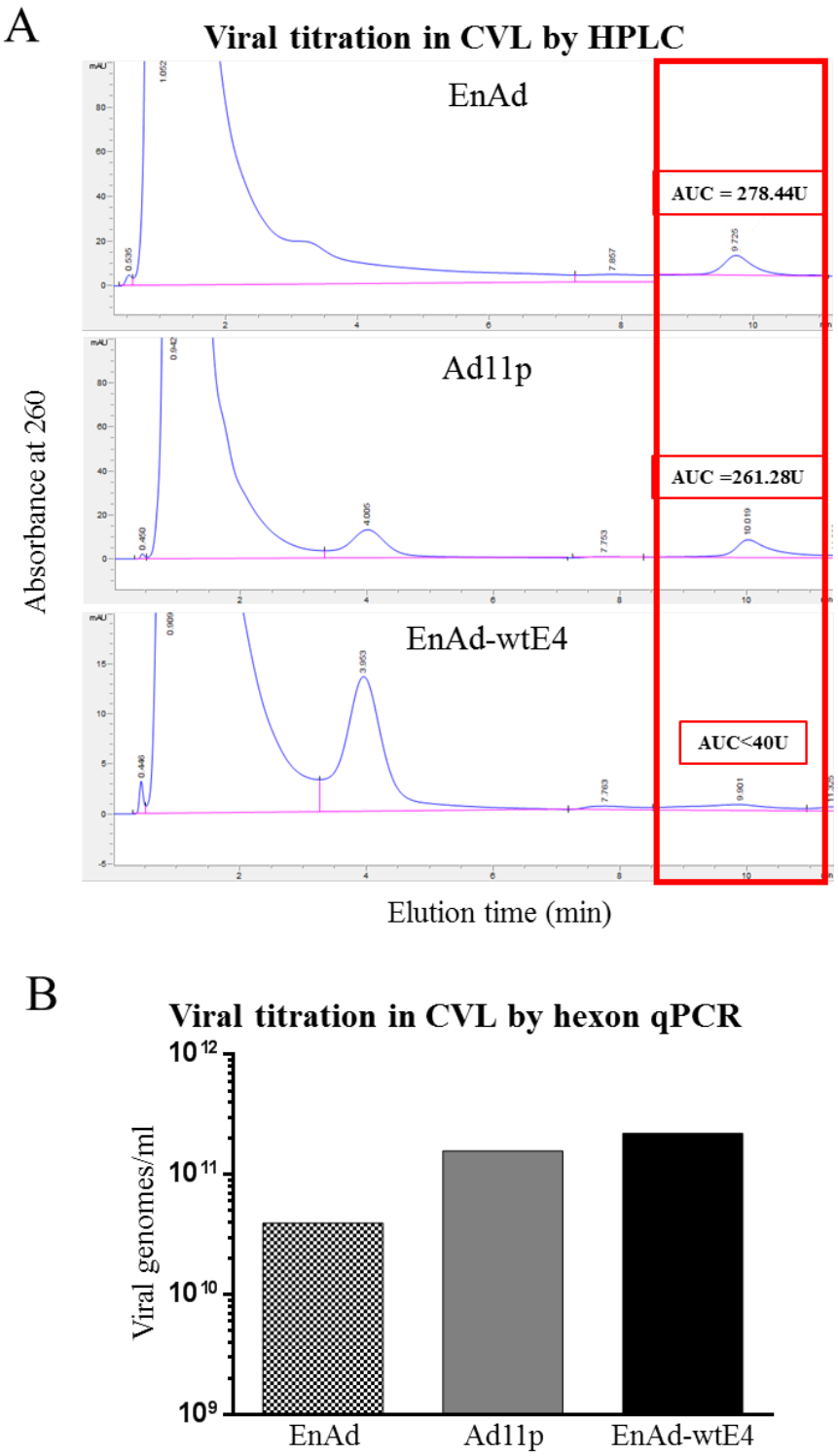


Figure 3.9 Titration of EnAd-wtE4 virus in crude virus lysate by HPLC and hexon qPCR at multiple timepoints. AD-293 cells were infected with EnAd, Ad11p and EnAd-wtE4 amplification material (see Material and Methods), CVL were harvested 24, 48 and 72 hrs later. Virus in CVL was titred by HPLC (see Material and Methods). (A) 72 hrs post-infection CVL are shown with the adenovirus elution time highlighted in red and the integrated area under the curve (AUC) for each virus. Virus was quantified in 72 hrs CVL by hexon qPCR (see Material and Methods). (B) Average of technical duplicates is shown in viral genomes per ml.

3.3.2.3.3 Assessment of oncolytic potency and virus production of EnAd-wtE4 in HT29 cells

Acknowledging that qPCR titre did not correlate with HPLC titre, genome dilutions were initially used to compare EnAd-wtE4 to Ad11p. Both virus had shown similar cell killing kinetics in amplification rounds when attempting to produce virus stock (not shown). The genome dilutions of both virus were used to compare the killing activity by MTS. Later, the cell killing was normalised to study the virus replication and progeny production.

HT29 cells were infected with decreasing doses of genomes/per cell based on titre from Figure 3.9 B. Cells were used to assess cell viability by MTS assay and virus replication by qPCR. Alternatively, SN were used to quantify infective particles by infectivity assay (see Material and Methods). All these readouts were assessed at 24, 48 and 72 hrs post infection.

Neither concentration range of the two viruses displayed significant cytotoxicity after 24hrs (not shown), but both produced a dose-dependent cytotoxicity curve after 48 hrs (Figure 3.10 A) and 72 hrs post infection (Figure 3.10 B). The cytotoxicity curve produced after 72 hrs showed better R square values – 0.995 and 0.980, respectively – and tighter EC50 confidence intervals – 37.59 to 49.97 and 57.51-111.4, respectively – than 48hrs curves; which R square ratios were 0.782 and 0.977, respectively, and EC50 intervals were 47.76 to 329.3 and 107 to 226.7 respectively.

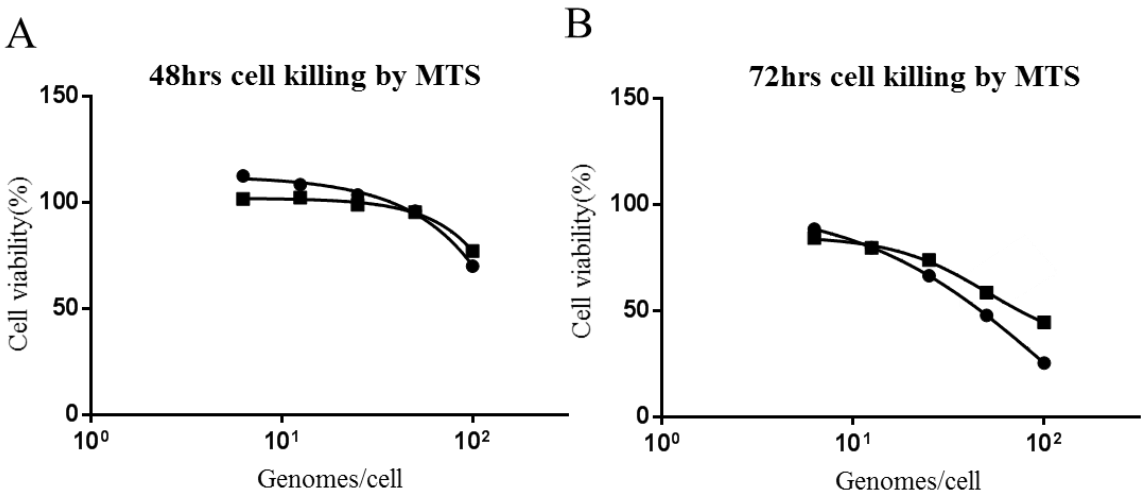


Figure 3.10 Evaluation of EnAd-wtE4 cell killing in HT29 cells at multiple timepoints. HT29 cells were infected with 2-fold serial dilutions of Ad11p (squares) or EnAd-wtE4 (dots) 72 hrs CVL using the qPCR titre from figure 3.9 B. MTS assay (see Material and Method) was used at 24, 48 and 72 hrs post-infection to assess cell viability (normalised to untreated control cells). Cell viability at (A) 48 hrs and (B) 72 hrs are shown as biological duplicate average with four parameters non-linear curve fit.

It was suspected that the high qPCR titre detected in EnAd-E4 (Figure 3.9 B) used to infect the cells, was probably not only infective particles and many non-encapsidated genomes were also measured. Consequently, virus replication and progeny virus production were compared between Ad11 and wtE4 virus, from wells with similar killing activity based on samples from Figure 3.9. Virus genomes in cell lysates appeared to be significantly higher for EnAd-wtE4 than Ad11p at both 48 hrs and 72 hrs post-infection (Figure 3.11 A). On the other hand, Ad11p produced significantly more infective particles in the supernatant than EnAd-wtE4 at both timepoints (Figure 3.11 B). At concentrations mediating similar killing activities, wtE4 virus had a poor efficiency at 48 hrs to package nascent genomes into infective particles, compared to Ad11p, giving a high genome/infectious particle ratio. This impairment was even greater at later timepoints (72 hrs), whilst the Ad11p ratio was comparable between the two timepoints (Figure 3.11 C).

The fact that EnAd-wtE4 produced increasing numbers of genome copies over time, but failed to package them into infective particles, was in line with the observation during virus purification (section 3.3.2.1) and HPLC titration (section 3.3.2.3.2) that the total number of virus particles produced was very small. This suggests that the EnAd-wtE4 virus was successfully completing the early part of its life cycle (cell entry, genome replication etc) but failing to complete virus packaging.

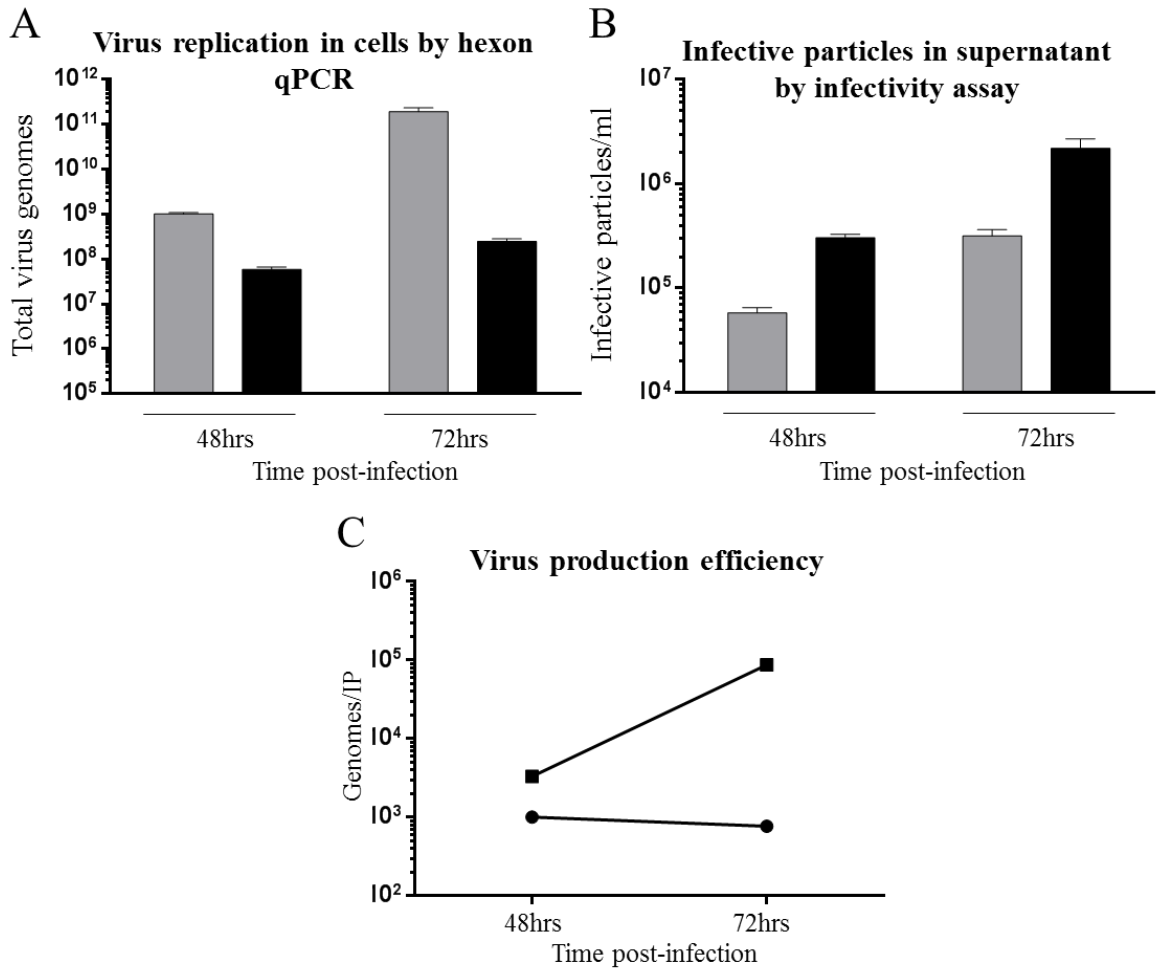


Figure 3.11 Evaluation of EnAd-wtE4 replication and progeny production in HT29 cells at 48 and 72 hrs normalised to cell killing. (A and B) HT29 cells infected with EnAd-wtE4 (grey) and Ad11p (black) with similar cell viability at 48 and 72 hrs, were used to quantify virus replication in cell by hexon qPCR and infective particles in supernatants by infectivity assay (see Material and Method). (A) Total virus genomes technical triplicates average and standard deviation are shown representative of two experiments. (B) Infective particles (IP) technical triplicates average and standard deviation are shown representative of two experiments. (C) Extensively, Ad11p (circles) and EnAd-wtE4 (square) production efficiency ratio in HT29 was calculated with virus genome in cell per infectious virus in supernatant. Production efficiency ratio is shown for 48 and 72 hrs post infection.

3.3.3 Evaluation of cellular factors involved in EnAd virus replication in cancer cells using drugs

Here it was set out to explore whether established pharmacological agents with known cellular targets could be used to further understand the cellular factors involved in EnAd replication within tumour cells. This could potentially provide an opportunity for combining drugs to increase efficacy. Accordingly, a commercially-available drug panel (Selleckchem) was screened for compounds improving EnAd replication in HT29 cells. The promising agents from the screen would then be further investigated to find optimum concentrations, and could then be used to enhance virus production.

3.3.3.1 Optimising the virus replication assay for drug screening

Prior to conducting the drug screen, the assay variables were optimised for reproducibility across biological replicates. It was decided to assay virus replication at an early time point after infection (18 hrs) prior to progeny release, thereby preventing secondary rounds of infection. Low virus concentrations were chosen (1 ppc and 10 ppc), to minimise the likelihood of a possible additive toxic effect with the drug. Replication measurements were shown to be most consistent when infecting cells with 10 ppc, so this concentration was adopted (Figure 3.12 A). To circumvent the challenge of determining optimal concentrations for each of the over 300 drugs, a fixed concentration was used across the panel. Consequently, Cisplatin – previously used in this lab for *in vivo* studies[194] – was used to establish a suitable drug concentration, and 0.1 mM Cisplatin concentration appeared to induce lower inter-replicate variation than 1 mM (Figure 3.12 B) and was adopted throughout the screen.

The order of virus and drug administration was also investigated, again using cisplatin as an example. Adding the drug before the virus was considered undesirable, because the drug might interfere with virus entry (rather than replication). Experimentally it was found that adding

virus and drug simultaneously on the cells resulted in less variation, than adding the virus one hour before the drug (Figure 3.12 C). This may have been a real pharmacological effect, or might have reflected that cells were subject to one less manipulation. Thereby, simultaneous virus and drug treatment was adopted for the panel screen.

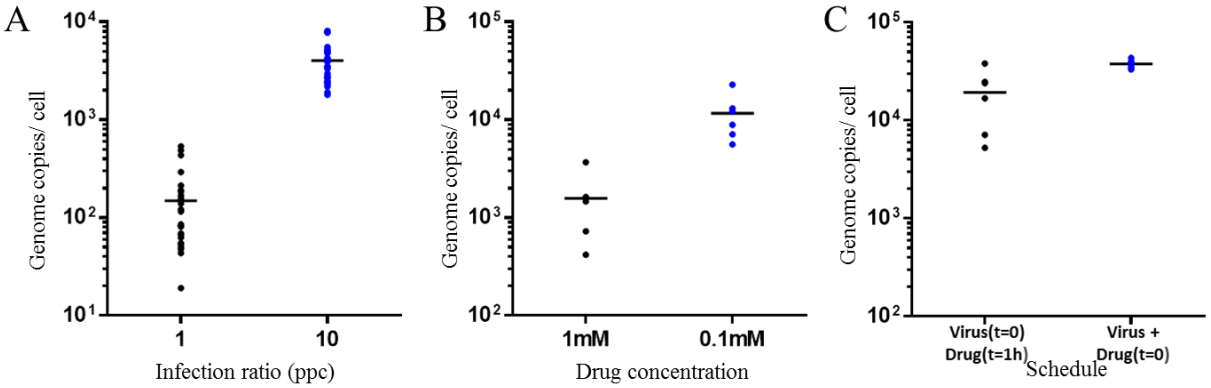


Figure 3.12 Establishing the drug screen assay variables for a consistent genome replication. HT29 cells were seeded in 96-well plates overnight, infected with EnAd for 18 hrs and DNA was extracted to assess virus replication (genome copies per input cell) in cell lysate by hexon qPCR. (A) Biological replicates (n=14) across multiple plates and the mean are shown for 1 ppc (black) or 10 ppc (blue) infection ratios. (B) Alternatively, virus replication was assessed 24 hrs post-infection in HT29 cells infected at 10 ppc and treated simultaneously with 1 mM (black dots) or 0.1 mM (blue dots) Cisplatin. Biological replicates (n=5) and mean are shown. (C) Alternatively, virus replication was investigated in different treatment schedule using 10 ppc and 0.1 mM of Cisplatin. Virus replication was evaluated in cells simultaneously treated with virus and the drug (blue dots) or cells infected with virus and 1hr later treated with Cisplatin (black dots). Biological replicates (n=5) and mean are shown.

3.3.3.2 Virus replication screening

The average genomes per cell of duplicate measurements determined by qPCR ranged from 20 to 20,000, although the top value of control samples was found to be 1740 genomes/cell (Figure 3.13). Therefore, drugs giving genome levels above the threshold of 1740 genome copies per cell indicated targets that may have enhanced EnAd genome replication (Table 3.1). However, this analysis does not account for logistical errors relating to the large scale of the experiment.

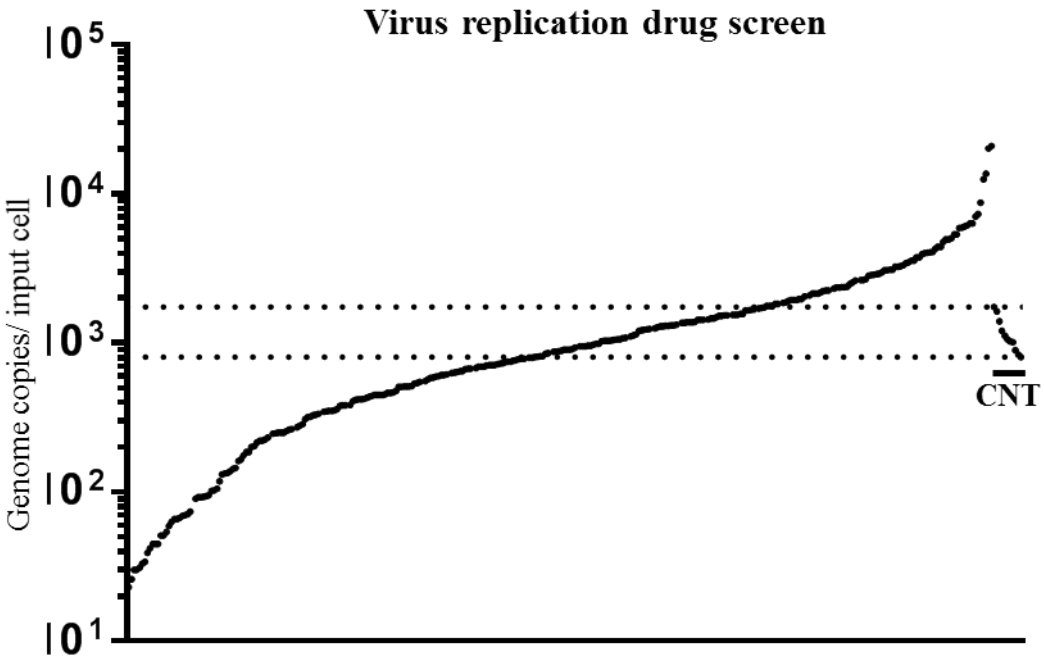


Figure 3.13 Genome copies per input cell determined by qPCR. The genome copies of each well were determined by hexon qPCR (see material and methods) and average from technical duplicate divided by input cell before ordering. The dotted lines represent the highest and lowest values of EnAd replication in cells treated with drug vehicle (DMSO) control. The individual genome copies per input cell for DMSO controls are indicated (CNT). Genome copies above and below these thresholds represent more and fewer replication than the DMSO control, respectively.

Drug Name	Genome copies/input cell	Drug Name	Genome copies/input cell
BS-181 hydrochloride	1771.00	SGX-523	2995.00
GDC-0879	1773.00	CI-1033(Canertinib)	3071.00
R406(free base)	1776.00	BMS-708163	3082.00
PIK-90	1824.00	Elvitegravir	3091.00
2-Methoxyestradiol	1828.00	NVP-ADW742	3099.00
JNJ-38877605	1852.00	R406	3245.00
XL147	1862.00	MK-2206	3249.00
Ritonavir	1867.00	KW 2449	3277.00
Trichostatin A	1908.00	Paclitaxel(Taxol)	3314.00
Allopurinol	1939.00	Docetaxel	3428.00
Eplerenone	1944.00	ZSTK474	3494.00
Tandutinib (MLN518)	1947.00	Epothilone A	3552.00
BMS-790052	1968.00	VX-680	3559.00
Masitinib(AB1010)	1977.00	Axitinib	3749.00
Fludarabine(Fludara)	2057.00	Gefitinib(Iressa)	3755.00
Quercetin(Sophoretin)	2060.00	Obatoclax Mesylate	3935.00
Dasatinib	2082.00	XL184	4001.00
Capecitabine(Xeloda)	2146.00	HMN-214	4037.00
TSU-68	2147.00	CP-724714	4047.00
ABT-751	2151.00	AZD8330	4095.00
Pramipexole	2187.00	NVP-TAE684	4269.00
PLX-4720	2232.00	XL880(GSK1363089)	4413.00
PHA-739358(Danusertib)	2240.00	WYE-354	4421.00
Sorafenib Tosylate	2247.00	PD153035 hydrochloride	4780.00
Finasteride	2277.00	MGCD-265	4956.00
WZ8040	2320.00	PD318088	4962.00
S-(+)-Rolipram	2349.00	GDC-0941	5033.00
PF-2341066	2352.00	CI-1040 (PD184352)	5334.00
Vandetanib	2366.00	Bosutinib(SKI-606)	5344.00
Erlotinib Hydrochloride	2371.00	KRN 633	5911.00
Fludarabine Phosphate	2392.00	AZD7762	5962.00
ON-01910	2489.00	BIBF1120(Vargatef)	6037.00
SP600125	2536.00	AZD6244(Selumetinib)	6139.00
TG100-115	2614.00	PD0325901	6327.00
GSK461364	2618.00	YM155	6342.00
Acetaminophen(Tylenol)	2639.00	AS703026	7033.00
MP-470	2645.00	Imatinib(STI571)	7336.00
Tadalafil(Cialis)	2689.00	AZD0530(Saracatinib)	8736.00
Imatinib Mesylate	2836.00	Vincristine Sulfate	12508.00
Aurora A Inhibitor I	2859.00	BI 2536	13599.00
ABT-737	2879.00	Cediranib(AZD2171)	20189.00
KU-0063794	2888.00	NPI-2358	20998.00
BMS-707035	2926.00		

Table 3.1 Drugs above the threshold genome copies per input cell of the virus/DMSO control. Drugs with genome copies per input cell above 1740 were identified from Figure 3.12.

3.3.3.3 Families of drugs enhancing EnAd replication

In this section, genomes fold change was calculated relative to same-plate EnAd/DMSO controls, and the average across biological triplicates was used to identify families that reproducibly improved virus replication across the independent experiments.

The most effective agent was Plinabulin, although most of the microtubule (MT) inhibitors showed the ability to enhance virus genome replication. Similarly, mTOR inhibitors (notably Everolimus) were also a successful family of agents, though not as effective as the microtubule inhibitors (Table 3.2).

Drug name	Molecular target	Interaction site (Sub-target)	Average of fold change triplicates
Everolimus	mTOR	FKBP12 (mTOR1)	3.48
WYE-354	mTOR and PI3K	PKI3 and mTOR kinase domain (mTOR1 and mTOR2)	2.28
Ku-0063794	mTOR	mTOR kinase domain (mTOR1 and mTOR2)	1.87
Rapamycin	mTOR	FKBP12 (mTOR1)	1.03
Temsirolimus	mTOR	FKBP12 (mTOR1)	0.29
Deforolimus	mTOR	FKBP12 (mTOR1)	0.13
AZD8055	mTOR	mTOR kinase domain (mTOR1 and mTOR2)	0.13
Plinabulin	MT	Colchicine-binding site of tubulin (MT destabiliser)	12.23
Vincristine	MT	Vinca-binding site of tubulin (MT destabiliser)	7.22
Paclitaxel	MT	Taxane-binding site of tubulin (MT stabiliser)	1.93
Docetaxel	MT	Taxane-binding site of tubulin (MT stabiliser)	1.53
Epothilone A	MT	Taxane-binding site of tubulin (MT stabiliser)	1.30
ABT-751	MT	Vinca-binding site of tubulin (MT destabiliser)	0.74

Table 3.2 mTOR inhibitors and MT inhibitors families improved genome replication in HT29 cells. Fold change genomes relative to EnAd/DMSO control were averaged across biological replicates. The molecular target of drugs with improved replication were identified on Selleckchem database. Families of molecular target with all drugs improving replication are shown.

3.3.3.4 Optimising the drug concentration for priority agents identified in the screen

The MT inhibitors and mTOR inhibitors mediating the highest levels of virus replication in the screen (Table 3.2), were selected for more detailed analysis. They were studied using a range of drug concentrations – 5 μM to 0.0016 μM –, to find the optimum concentration for each drug to increase the virus genomes in the cells. Cell viability was evaluated by MTS.

The MT inhibitors Vincristine and Plinabulin induced the highest virus replication approximately 5-fold increase across the concentration range 0.2-5 μM. Lower drug concentrations had no effect on virus replication. Importantly the optimal drug concentration maintained good cell viability (ranging from 80-90%) (Figure 3.14 A and B).

The mTOR inhibitors Everolimus, WYE-354 and KU-0063794 promoted a limited increase in virus replication but this only reached 1.3- to 1.8-fold (Figure 3.14 C-E). In addition, both second generation mTOR inhibitors WYE-354 and KU-0063794 showed appreciable cytotoxicity at higher concentrations (Figure 3.14 D and E), although not first generation Everolimus (Figure 3.14 C).

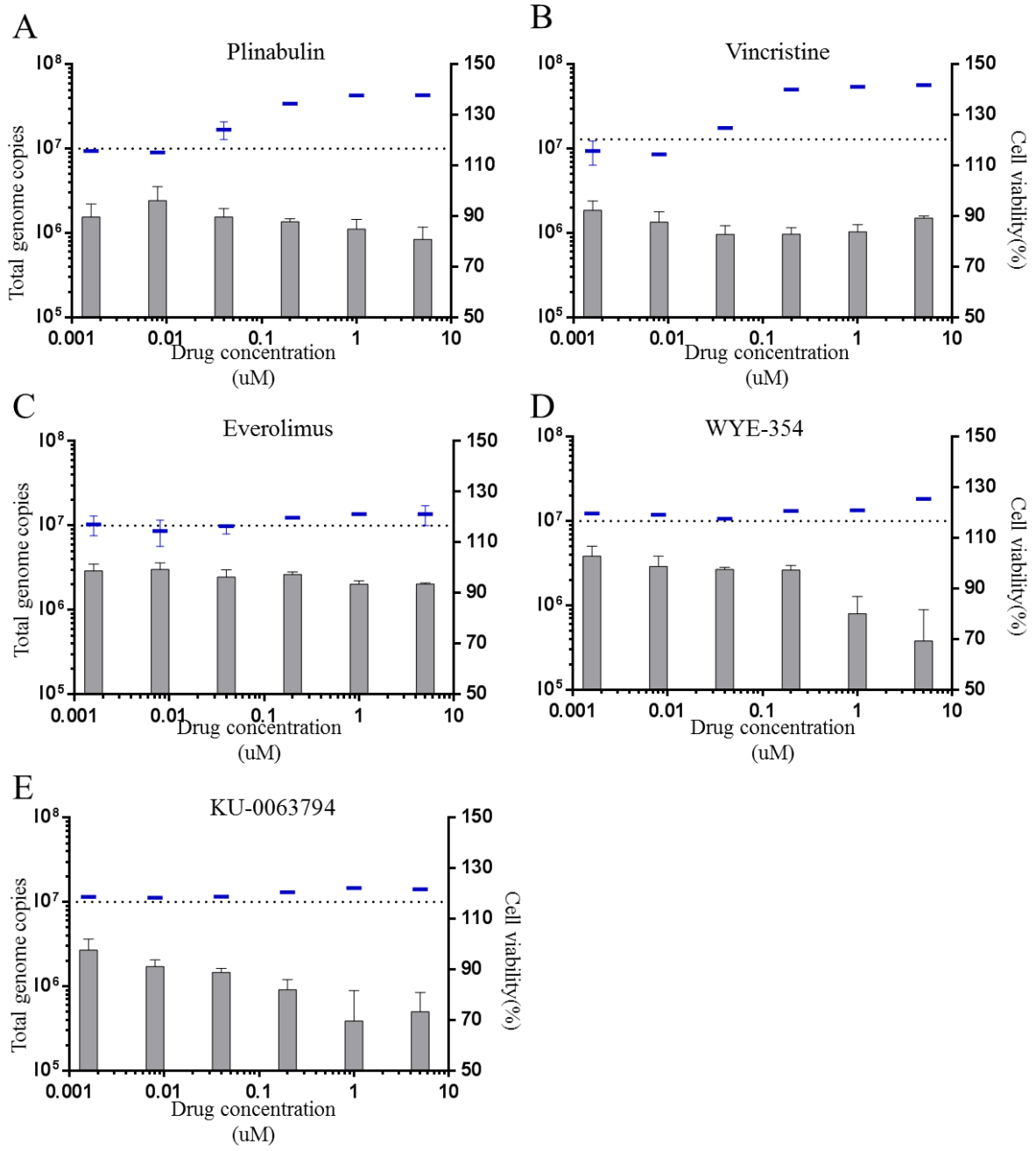


Figure 3.14 Establishing the optimal drug sub-dose with superior virus genome replication without altering HT29 viability. HT29 cells were seeded in 24 well plates overnight before infecting cells in triplicates with 10 ppc in combination with 5-fold-serial dilution (5 to 0.0016 µM range) of (A) Plinabulin, (B) Vincristine, (C) Everolimus, (D) WYE-354 or (E) KU-0063794, or only vehicle control (DMSO). iability (normalised to untreated control) was determined 24 hrs later in triplicates using MTS assay. Cell viability mean and SD are plotted against right Y axis. Cells were used in triplicates to determine the viral genome replication (total genome copies) by hexon qPCR. Virus genome replication mean and SD are plotted against left Y axis. Dotted line shows total genome for DMSO control. Representative of n=2 independent experiments.

The aim of enhancing virus replication is to increase the 'burst size' of viable particles in tumour to improve its therapeutic effect. The mTOR and MT inhibitors were therefore investigated for their ability to increase production and release of virus progeny into the cells supernatant. This was investigated using HT29 supernatants 72 hrs post-infection with 1 µM drug, measuring virus genomes by qPCR as a surrogate for release of viable virus particles.

The second generation mTOR inhibitors WYE-354 and KU-0063794 appeared to be the only agents that increased virus genomes in the supernatant significantly compared to controls ($p=0.0031$ and 0.0002, respectively). In contrast, the levels of genomes in the supernatant of cells treated with Everolimus were no different from controls. Intriguingly, both Vincristine and Plinabulin MT inhibitors performed significantly worse than the EnAd-only control ($p=0.0016$ and 0.0025, respectively) (Figure 3.15).

This observation was unexpected as it was initially hypothesised that increasing replication would lead to more progeny, and MT inhibitors had shown the best augmentation of cell-associated virus genome replication, whereas the mTOR inhibitors had only a limited effect on that readout (section 3.3.3.4). The already increased replication of EnAd relative to Ad11p could mean that viral genomes were not a limiting factor to produce more virus progeny or simply that MT inhibition impaired the EnAd biology downstream of replication.

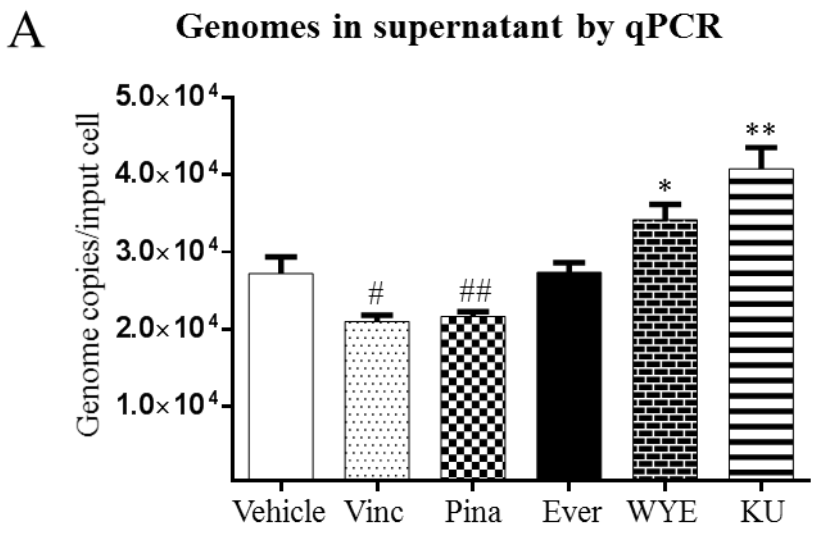


Figure 3.15 Evaluation of MT and mTOR inhibitors on EnAd progeny production in HT29 supernatant by qPCR. HT29 cells were seeded in 24 well plates overnight before being infected with 10ppc EnAd and treated with 0.1 µM drug (Table 3.1) or DMSO control (Vehicle), in four biological replicates per compound. Four hours post-treatment cells were washed to remove excess virus and cells treated again with 0.1 µM of corresponding drug for 3 days. Supernatants were spun and clarified material were used to assess virus production (genome copies per input cell) by hexon qPCR. Average and SD of four biological replicates (n=4) are shown, two-tailed unpaired T test is used to compare each drug against Vehicle control. #p=0.0016, ##p=0.0025, *p=0.0031 and **p=0.0002.

3.3.3.4.1 Assessment of priority drugs on 'virus' protein production

In a previous section it was noted that some drugs may interfere with virus replication downstream of genome production. Accordingly, here it was investigated whether late virus protein could be a more suitable indicator of the level of virus production. For this EnAd-Luciferase (EnAd-Luc) reporter tool was used in HT29 cells in combination with the shortlisted priority agents identified above. EnAd-Luc encodes the Luciferase reporter gene under transcriptional control of the virus Major Late Promoter (MLP) by incorporating its own splice acceptor. Thus, once spliced the transcript would be as follows: Tripartite leader-Luc-PA. Hence the luciferase is only expressed when the virus moves from the early part of its life cycle to the late part, where the capsid protein begins to be produced. This can be a good surrogate for the virus moving successfully throughout its life cycle towards production of infectious progeny.

All three mTOR inhibitors appeared to significantly increase the luciferase production relative to the control. Everolimus was the drug with the greatest luciferase up-regulation and both KU-0063794 and WYE-354 second generation mTOR inhibitors had a subtler increase, although all means were significantly different from vehicle controls ($p<0.0001$, <0.0001 and $=0.0047$ respectively) (Figure 3.16). In contrast, both MT inhibitors significantly ($p<0.0001$) inhibited the luciferase production compared to virus alone (Figure 3.16). Therefore, the virus surrogate protein seemed to correlate with the virus progeny production seen in section 0.

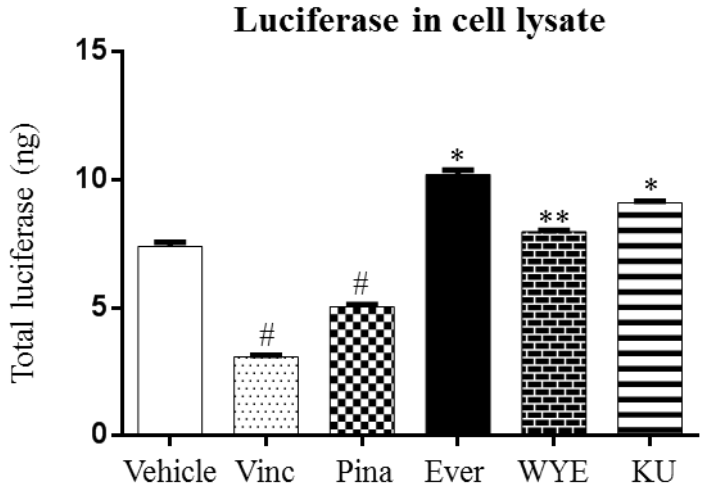


Figure 3.16 Evaluation of MT and mTOR inhibitors on luciferase expression in HT29 cells infected with EnAd-Luc. HT29 cells were seeded in 24 well plates overnight before being infected with EnAd-Luc (see Material and Methods) at 10 vp/cell with 0.1 µM of drugs (Table 3.1) or DMSO control (Vehicle), in 3 biological replicates per compound. Four hours' post-treatment cells were washed to remove excess virus and cells treated again with 0.1 µM of corresponding drug for 2 days. Supernatant was discarded and cell lysed with 1x RLB buffer for luciferase quantification in technical duplicates (see Material and Methods). Technical duplicates were averaged, biological triplicate mean and SD are shown. Two-tailed unpaired T test is used to compare each drug against Vehicle control. #p<0.0001, *p<0.0001 and **p=0.0047.

3.3.3.4.2 Assessment of priority drugs on early and late virus transcript expression

Additionally, the effects of the shortlisted (priority) drug panel on virus replication was explored by RT-qPCR, measuring production of early and late virus mRNA, using E1A mRNA and hexon mRNA as readouts. The mTOR inhibitors all showed a tendency to increase both E1A and hexon transcripts relative to the virus control. However, significant mean differences

(WYE-354 p= 0.024 and KU-0063794 p=0.0047) were only observed for E1A transcripts with second generation mTOR inhibitors relative to control (Figure 3.17 A and B). On the other hand, the MT inhibitors showed a different effect compared to the virus control, generally decreasing the number of transcript copies for either E1A and/or hexon (Figure 3.17 A and B), although this was only (p=0.044) for hexon mRNA on Vincristine-treated cells (Figure 3.17 B). Interestingly, the decreasing or increasing trend of virus transcripts compared to untreated, was replicated into virus protein surrogate (section 3.3.3.4.1) and virus progeny into the supernatant of HT29 cells (section 0).

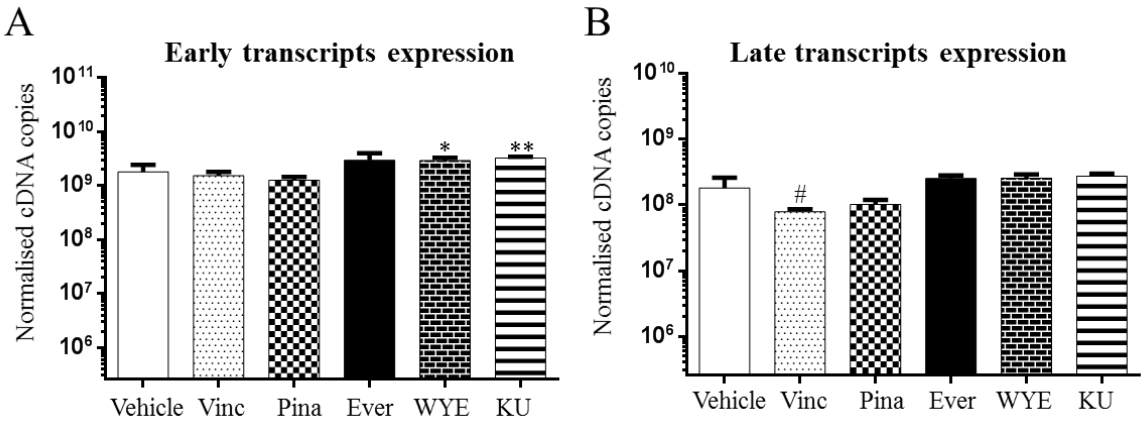


Figure 3.17 Evaluation of MT and mTOR inhibitors on early and late virus transcript expression in HT29 cells infected with EnAd. HT29 cells were seeded in 24 well plates overnight before being infected with EnAd at 10 vp/cell with 0.1 µM of drugs (Table 3.1) or DMSO control (Vehicle), in 4 biological replicates per compound. Four hours' post-treatment cells were washed to remove excess virus and cells treated again with 0.1 µM of corresponding drug for 2 days. Supernatant was discarded and cell lysed with β-ME/RLT buffer for early and late transcript quantification by RT-qPCR (see Material and Methods). Technical duplicates were averaged, biological quadruplicates mean and SD are shown. Two-tailed unpaired T test is used to compare each drug against Vehicle control. #p=0.044, *p=0.024 and **p=0.0047.

3.3.3.5 Evaluation of virus replication of priority drugs in A549 cells

Priority drugs showed in previous sections to enhance EnAd replication, were here explored in preliminary experiments using A549 cells and the same experiments as in section 3.3.3.4. However, no clear signs of replication enhancement were seen for any of the five drugs, on the contrary less replication was seen at highest drug concentration (Figure 3.18), especially with

microtubule inhibitors Plinabulin and Vincristine (Figure 3.18 A and B). Cell viability was not specially altered, ranging between 80-100% (Figure 3.18).

These preliminary data suggested that trying to artificially enhance virus potency *in vitro* might be more challenging than initially expected and needs further understanding before considering animal models.

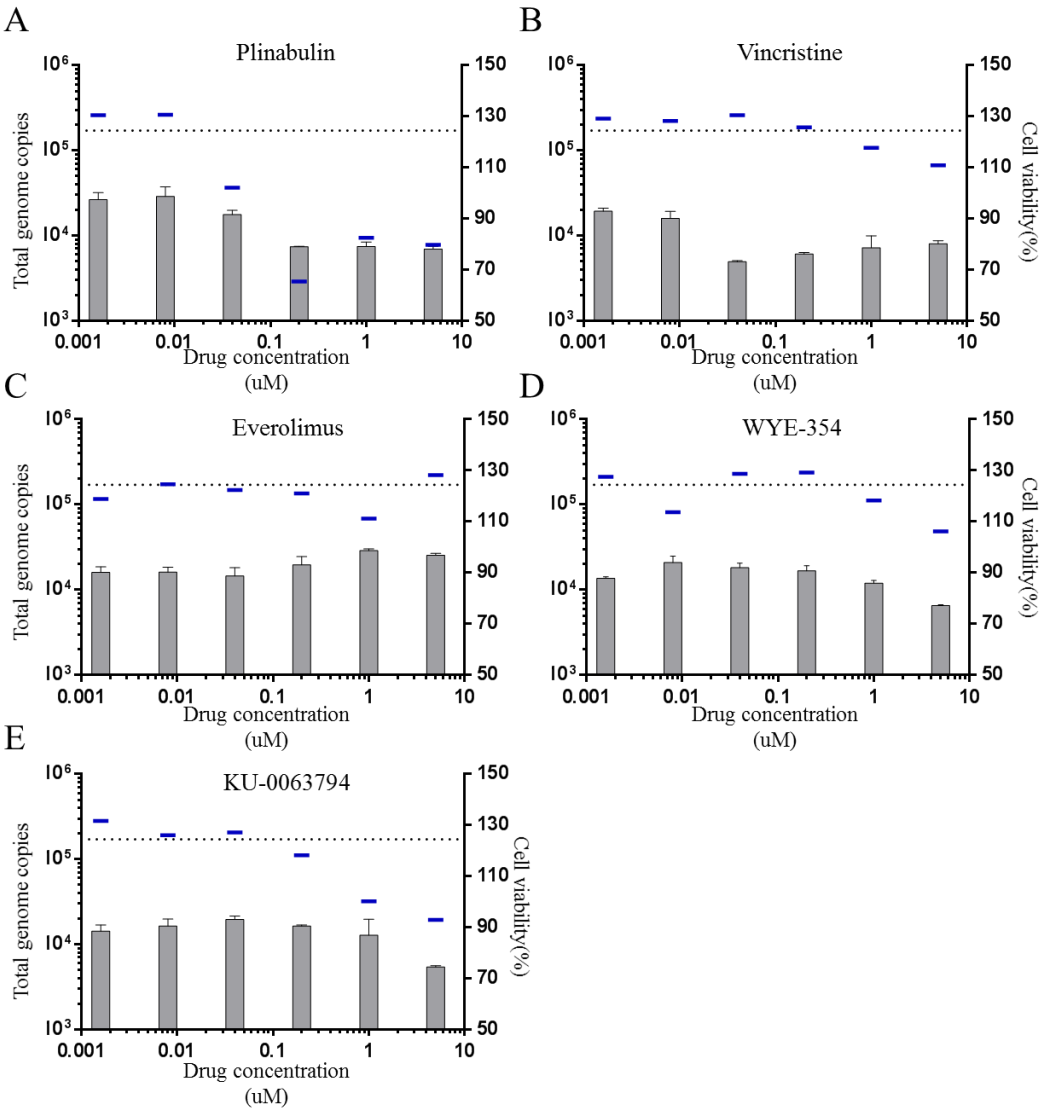


Figure 3.18 Establishing the optimal drug sub-dose with superior virus genome replication without altering A549 viability. A549 cells were seeded in 24 well plates overnight before infecting cells in triplicates with 10ppc in combination with 5-fold-serial dilution (5 to 0.0016 µM range) of (A) Plinabulin, (B) Vincristine, (C) Everolimus, (D) WYE-354 or (E) KU-0063794, or only vehicle control (DMSO). Viability (normalised to untreated control) was determined 24 hrs later in triplicates using MTS assay. Cell viability mean and SD are plotted against right Y axis. Cells were used in triplicates to determine the viral genome replication (total genome copies) by hexon qPCR. Virus genome replication mean and SD are plotted against left Y axis. Dotted line shows total genome for DMSO control.

3.4 Chapter summary

1. The genomic modifications of EnAd increase potency and enable killing of HT29 cells using fewer particles. EnAd also replicates more efficiently than Ad11p parental virus, resulting in more total genomes in HT29 cells and extra virus progeny released to the supernatant. However, no differences are seen in virus mRNA expression between EnAd and Ad11p.
2. For both EnAd and Ad11p, the number of infectious particles is directly proportional to the number of genomes in the supernatant of infected cells measured by qPCR.
3. The kinetics of replication and virus release in to the supernatant, and the cell killing activity of EnAd-wtE3 in HT29 are similar to EnAd.
4. EnAd-wtE2B shows comparable genome replication kinetics to EnAd in HT29 cells. The virus progeny released to the supernatant for EnAd-wtE2B is lower at 48 hrs post infection, however 24hours later is matched to EnAd. In addition, the wtE2B recombinant virus is less potent than EnAd to kill HT29 cells, but more active than Ad11p.
5. EnAd-wtE4 recombinant virus induces cytopathic effect, displays killing curves and virus genome is replicated in greater quantities than Ad11p on HT29 and/or Ad293 cells. However, production of fully mature and infectious virus particles is difficult and inefficient for this agent, perhaps reflecting a block in virus particle assembly.
6. In a drug screen to identify cellular factors that could increase the virus production of EnAd virus, mTOR inhibitors and MT inhibitors are the two families causing a reproducible increase in genome replication in HT29 cells. However, these drugs do not increase virus replication in A549 cells.
7. Vincristine and Plinabulin MT inhibitors increase virus replication in HT29 cells but decrease virus progeny in supernatant, late virus protein surrogate (luciferase) and E1A and hexon mRNA expression relative to controls.
8. Everolimus, WYE-354 and KU-0063794 mTOR inhibitors slightly increase virus replication in HT29 cells. In addition, they induce more virus progeny in supernatant, increase late virus

protein surrogate (luciferase) and trend upwards the virus mRNA expression relative to controls.

9. Genome replication does not necessarily correlate with more virus progeny released to supernatant. Luciferase expression as a virus protein surrogate using EnAd-Luc – and probably virus mRNA – may be better indicators of virus progeny production in drug studies.

3.5 Chapter discussion

3.5.1 Discussion of results

In this chapter EnAd was investigated for its oncolytic potency on tumour cells. The chapter was divided in two overarching sections. In the first section, the objective was to investigate the phenotypic differences between EnAd and the parental virus Ad11p, and to understand the role of the three genetic mutations. Using a drug panel, the aim of the second part of the chapter was to identify cellular factors that enhanced the virus production.

The structural proteins from the virus capsid are involved in the cell entry and trafficking to the nucleus (section 1.3.2). Since the virus capsid proteins involved in cell attachment/internalisation between EnAd and Ad11p are identical (Figure 1.5), it was not surprising to detect equal genomes of Enad and Ad11p at early timepoint (4 hrs), before the onset replication. However, differences in genome copies were detectable at later time points (from 24 hrs), well after replication onsets (Figure 3.2). After cell death, a higher total genome yield was seen for EnAd compared to Ad11p, suggesting the mutations made the virus replicate more efficiently. Additionally, EnAd produced more virus progeny rapidly detected in the supernatant at early timepoints, and maintained after cells were killed (Figure 3.3). The increase in virus progeny production was accompanied with a fast killing phenotype (Figure 3.1), suggesting EnAd had a faster virus cycle than Ad11p.

Based on these observations, it was then hypothesised that the increased bioavailability of virus DNA templates translated into more mRNA transcripts and viral proteins. This could explain the faster virus cycle. However, the viral mRNA transcripts kinetics were undistinguishable between mutant and parental virus (Figure 3.4). Therefore, the fast and early phenotype of EnAd virus would seem independent of viral gene expression. However, it is not known whether the translation kinetics are different between both viruses.

To further understand the origin of EnAd phenotype described above, three different recombinant EnAd viruses with single wildtype substitutions were designed (Figure 3.5). These viruses showed that EnAd phenotype was independent of E3 deletion, at least in *in vitro* studies where immune cells were not present (Figure 3.7). Whereas both E2B and E4 mutations seemed necessary for cell killing and fast progeny release phenotype of EnAd. Additionally, E2B mutation appeared to be dependent of the E4 short deletion to generate viable progeny (Figure 3.6, Figure 3.9 and Figure 3.11).

Adenovirus pTP and AdPol, which are encoded in E2B region, are well known for their role in replication of virus genome[93]. For that reason, it was previously assumed that the fast replication phenotype was associated to the E2B mutation, surprisingly no apparent changes in total replication were seen between EnAd and EnAd-wtE2B (EnAd which E2B was replaced by A11p E2B) (Figure 3.7). Also, EnAd-wtE2B showed an initial slow virus progeny release to the supernatant compared to EnAd and a slower oncolytic potency, but always faster than Ad11p (Figure 3.7). These unexpected results suggested that the E2B mutation was partly responsible for the fast life cycle of EnAd, but was not directly related to the fast DNA replication.

Since pTP directs the viral genome in different nuclear sub-localisation throughout the phases of the virus infection[94,96-98], it is plausible that the new mutant pTP is altering the chronology and/or nuclear organisation of the viral genome, without altering the replication rate itself. In

fact, a mutant Ad5 with altered PT displayed a fast virion release phenotype[195]. Therefore, the E2B mutation could explain the initial fast virus progeny release noted with EnAd compared to Ad11p and EnAd-wtE2B (Figure 3.7).

The E4 deletion in EnAd which stands in the upper half of the open reading frame 4, probably affects the interaction between ORF4-PP2A[196], which might translate into a deregulation of the cellular energy sensor AMPK[177]. Consequently, EnAd consumes the cell energy without control, resulting in cell blistering and cell death[187]. However, an EnAd virus which E4 was replaced by Ad11p E4 (EnAd-wtE4), showed that the E4-ORF4 mutation might have further implications in the phenotype of EnAd. This EnAd-wtE4 showed virus genome replication and induce reasonable cell killing in HT29 cells (Figure 3.9 and Figure 3.10 and Figure 3.11), however it hardly produced infectious virus (Figure 3.6 and Figure 3.11). This suggested that E4 mutation has further implications downstream of virus genome replication, for example in replication.

Since the expression of E4-ORF6 protein is dependent on the splicing acceptor located on the ORF4[173], the expression of ORF6 protein in EnAd could be adulterated. ORF6 in Ad5 associates with E1B-55k, before co-localising near the periphery of viral replication bodies[185], where the adenovirus assembly occurs[197]. However, ORF6 or E1B-55k mutations can abrogate this pattern, disseminating these proteins across the nucleus and failing to support infectious virus production[198,199]. Consequently, if the E4 deletion ablates the expression E4-ORF6, it is possible that the virus replication/packaging in the nuclear sub-location is affected. This hypothesis could explain the empty capsid phenotype seen with wtE4 combined to mutant pTP (Figure 3.6). In fact, transmission electronic microscopy (TEM) pictures provided by Professor Len Seymour, suggest that EnAd induces less structured cellular nucleus in infected cells than Ad11p or Ad5 viruses (see Appendix, part A). More investigation is needed to understand whether both E2B and E4 mutations have disorganised chronologically and spatially the

cellular nucleus in benefit of genome replication and progeny production, resulting in large virus release at early timepoints.

In the second section of this chapter, a drug panel with more than 300 agents was used to investigate cellular factors in cancer cells involved in the virus replication of EnAd. Two families of drugs, mTOR inhibitors and microtubule inhibitors, were identified (Table 3.2 and Figure 3.14). These results were consistent with previous studies[200-202]. However, only mTOR inhibitors appeared to translate to an increased progeny in the supernatant (Figure 3.15), and was correlated with an increase of late virus protein expression (Figure 3.16), and early and late virus RNA expression (Figure 3.17). Whereas MT destabilisers decreased the virus progeny and the virus gene expression, in agreement with previous publications[203]. Together, the data suggested that replication might not always be an ideal indicator of virus progeny production, whereas virus gene expression might be more suitable.

The increase of luciferase expression from HT29 cells infected with EnAd-Luc and treated with mTOR inhibitors was not surprising (Figure 3.16). During late phase of infection, adenoviruses supress the hosts cap-dependent translation to favour the translation of late viral mRNAs[204]. A mechanism termed 'ribosome shunting', loads the late mRNA transcripts directly into the 40S ribosome subunit directed by the tripartite leader[205,206]. Consequently, drug and virus may synergise to inhibit cap-dependent translation favouring late viral protein surrogate expression. However, the observation of EnAd progeny burst with mTOR inhibitor treated cells (especially with the potential loss of E4-ORF4) was confusing (Figure 3.17). mTOR inhibitors have largely been reviewed to halt translation of cap-dependent genes[207] and adenoviruses encode E4-ORF1 and E4-ORF4[177], which are known to prevent cellular protein synthesis shutdown during the early hours of the infection. It is believed that adenoviruses use this mechanism to allow the expression of cellular and early virus proteins required for controlling the cell and viral replication during the early infection[177]. Thus, mTOR inhibitors

were expected to inhibit EnAd's virus production. Possibly, the additive effect seen between EnAd and mTOR inhibitors, is explained by the mutation status of the HT29 cells. Finally, mTOR inhibitors are well known immune-suppressors[208] and might potentially interfere with immunovirotherapy (seen in Chapter 4-6), however the manipulation of the mTOR pathway appears as a good candidate to increase the oncolytic potency of EnAd.

3.5.2 Limitations and future work

The first set of data of this chapter showed that EnAd's E2B and E4 genomic modifications were essential for the oncolytic potency, fast replication and early progeny release in HT29 cell line. It was speculated that these two modifications might affect the distribution of virus components within the cellular nucleus, both complementing each other to produce EnAd's phenotype. However, several assumptions were made based on knowledge produced with other adenovirus serotypes, which should be investigated with EnAd.

Initially, confocal microscopy could be a relatively simple technique to compare the nuclear distribution of terminal protein (and precursors) in cancer cells infected with Enad, EnAd-wtE2B and Ad11p viruses. This should provide rapid evidences whether the hypothesis is possible. However, before the inexistence of antibodies against TP for these viruses, anti-TP antibodies from other serotypes should be tested[209], for instance Ad5 which has nearly 80% aa identity (Table 1.3). Alternatively, it should be assessed whether the E4-ORF4 deletion affects its own expression and these of downstream proteins, especially E4-ORF6. Based in previous reports, it was speculated that the E4-ORF4 deletion eliminated the splicing acceptor required for E4-ORF6 translation[173]. The lack of E4-ORF6 has been related with miss-localisation of E1B-55k in the cell nucleus, away from the virus replication machinery. Altogether, confirming whether E4-ORF4 and -ORF6 proteins are expressed or not could help refuting the hypothesis. However, it is likely that a prior search for antibodies against Ad11p E4-ORF4 and E4-ORF6

would be needed, as the aa identity of both proteins in Ad11p remains relatively low compared to other human adenoviruses[167].

The second set of data of this chapter identified that microtubule inhibitors and mTOR inhibitors, out of a drug panel, were capable of increasing EnAd genome replication in HT29 cells. However, further assessment using the two families of drugs, showed that an increase of virus replication was not necessarily correlated with the amount of produced virus progeny, instead mTOR inhibitors indicated that virus gene expression was a better gauge for virus production. Nevertheless, further investigation is needed to understand the mechanism by which mTOR inhibitors mediate an increase of virus gene expression. In addition, it would be interesting to reassess the drug panel, this time evaluating the gene expression or the final yield of virus progeny. Alternatively, it may be interesting to evaluate the drugs that inhibit virus replication. For instance, by overexpressing the identified cellular factors that were essential for virus replication to improve the virus potency. Also, those cellular factors, could be further investigated as biomarker indicators of EnAd activity in cancer cells.

4 Comparing the adjuvant nature of EnAd and Ad5 virus on an *in vitro* human TIDC-like model

4.1 Introduction

Dendritic cells play a key role in anti-tumour immune responses through the presentation of tumour antigens to adaptive immune cells, such as T cells, to help prime an effective T_H1 immune response. However, tumour and stromal cells present in the tumour microenvironment can inhibit the maturation and activation of tumour-infiltrating DCs (TIDC). TIDCs have impaired ability to prime T cells, due to low levels of antigen presenting and costimulatory molecules. Along with other supressing signals, TIDCs inhibit the anti-tumour immune responses, promoting disease progression[43-45]. Nevertheless, some have shown that TIDC can be stimulated with adjuvants, and overturn their phenotype to harness anti-cancer immune effector T cells[53,54].

The particulate nature of adenoviruses has led to them being characterised as pathogen recognition receptors (PRR) ligands, such as the cytosolic STING pathway and endosomal TLR9, which can directly induce innate immune cell maturation and activation via intracellular signalling[104]. In addition, the oncolytic mechanism by which EnAd directly kills tumour cells has been shown to be oncosis[187], a mode of cell death that potentially provides relevant endogenous danger signals (also known as DAMPs) that are suspected to mature, activate and recruit innate immune cells such as DCs into the tumour microenvironment[110].

It was therefore hypothesised that EnAd virus could work as an adjuvant to differentiate and activate TIDCs, that along with the tumour antigens derived from the cell lysis, should promote anti-tumour adaptive immunity in the tumour microenvironment. Day 3 immature DCs (d3iDCs) displayed an immature phenotype with poor expression of antigen presenting and costimulatory molecules (Appendix, Part B), at the same time they were inefficient primers of allogeneic T cells (Chapter 6), characteristic of tumour-infiltrating DCs[40,43-45]. Having set up this TIDC-like model (Appendix, Part B), EnAd virus was investigated for its adjuvant nature to mature and activate these cells. Further, to study the virus adjuvant effect in a more complex cellular environment, co-cultures of virus-infected tumour cell and the DC model were explored. For comparison purposes, all these experiments were performed along-side the adenovirus type 5 (Ad5), known to be agonist of many innate sensing pathways in DC[104], contributing to a strong adaptive immune response[105].

4.2 Chapter aim

Use the TIDC-like culture system (Appendix, Part B) to investigate the adjuvant effect of EnAd, as particles or as oncolytic agent infecting tumour cells, on dendritic cell maturation. Also, to assess how EnAd compares to adenovirus type 5.

4.3 Results

4.3.1 Evaluating the adjuvant effect of EnAd virus particles on d3iDC cells by immunophenotyping DC maturation markers

The previously developed d3iDC model, displayed an immature phenotype with poor expression of antigen presenting and costimulatory molecules (see Appendix, Part B), similar features with tumour-infiltrating DCs. This TIDC-like model was used in this section to

evaluate the adjuvant effect of EnAd virus particles, by assessing the expression of antigen presenting molecules class I and II (HLA-ABC and HLA-DR respectively) and costimulatory molecules (CD80 and CD86) by flow cytometry. Also, other DC markers important for T cell priming were immunophenotyped, such as maturation marker (CD83), immune checkpoint marker (PD-L1) and lymph node trafficking marker (CCR7). Altogether, the adjuvant effect of EnAd virus particles on d3iDC cells was assessed accordingly with Figure 4.1 A.

Across multiple donors, EnAd-treated DC significantly increased HLA-DR (50900 ±52137, p=0.037), CD86 (5313 ±5105, p=0.009) and PD-L1(14362 ±17498, p=0.027) median fluorescence intensity (MFI) mean (±standard variation, SD) compared to the MFI average (±SD) of untreated cells (28520 ±33746, 953.2 ±996 and 4917 ±7510, respectively) (Figure 4.1 B, D and F). Upward, but not statistically significant, trends were also seen for CD80 (606.3 ±473.8, p=0.115) and CCR7 (1674 ±1402, p=0.241) markers on EnAd-treated DC in comparison to controls (130.8 ±43.39 and 282.8 ±91.13, respectively) (Figure 4.1 E and H). Small (not-significant) differences were seen between EnAd-treated DCs in HLA-ABC (MFI 11691 ±3513, versus 10848 ±3513 for untreated controls, p=0.336) and CD83 (4432 ±3166, versus 3845 ±2250 for untreated controls, p=0.317) (Figure 4.1 C and G). It can be noticed that most of the markers presented large standard variations, which may be explained by considerable donor to donor variability in background expression.

Despite the up-regulation of the PD-L1 checkpoint molecule, the up-regulation of the costimulatory, lymph node trafficking and antigen presenting molecules by EnAd particles on d3iDC, suggested that EnAd particles in a tumour context might overall still improve the T cell priming ability of TIDC, and may contribute to an improved anti-tumour immune response.

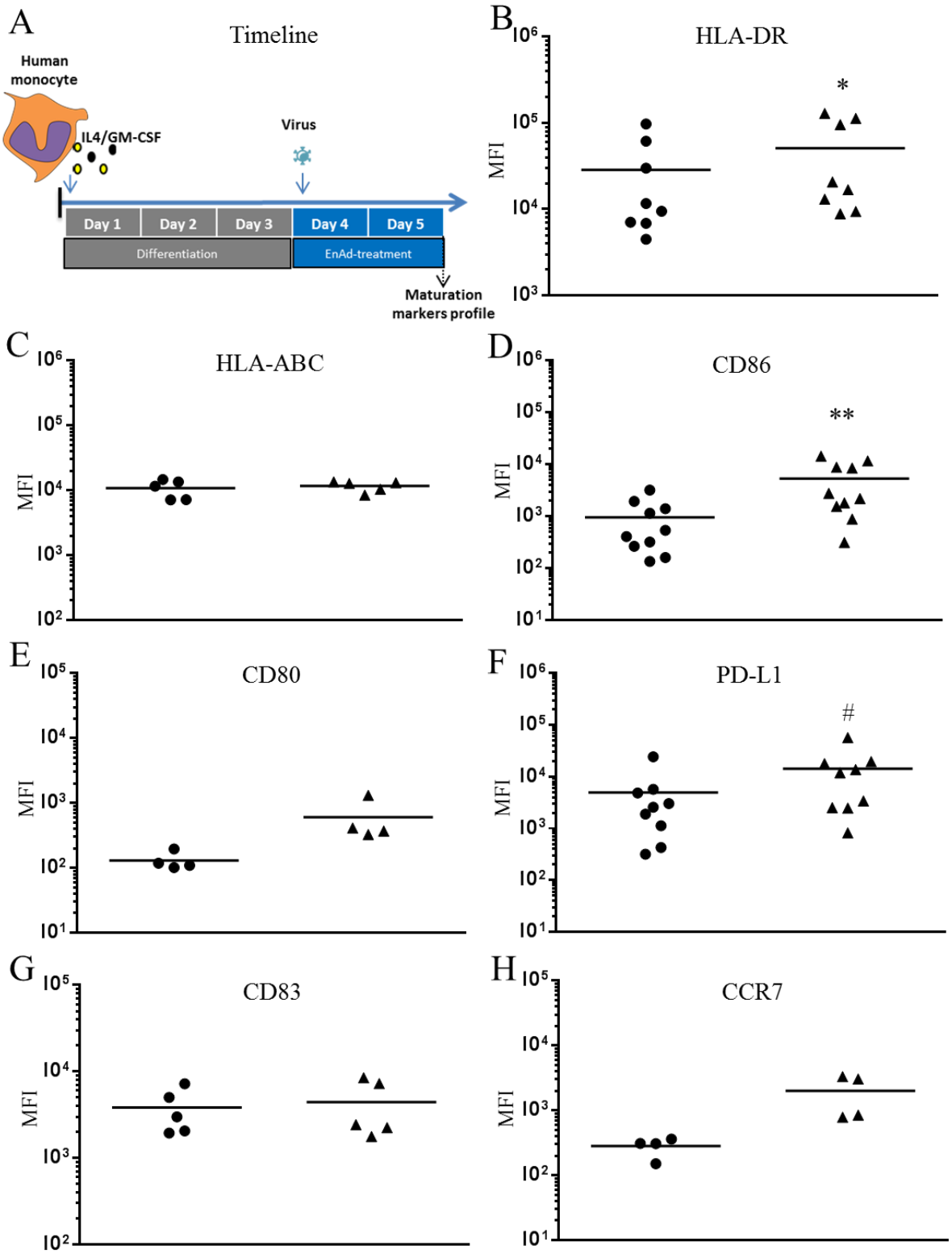


Figure 4.1 Immunophenotyping day 3 immature DC treated with EnAd particles across multiple donors. (A) d3iDC stimulated with 500 EnAd ppc or left untreated, were stained with vital dye and mAb specific for HLA-DR (B), HLA-ABC (C), CD86 (D), CD80 (E), PD-L1(F), CD83 (G) and CCR7 (H) – or matching isotype – after 48 hrs. Median fluorescence intensity (MFI) between EnAd-treated (triangles) or untreated (circles) are compared in scatter dot plots for 4 to 10 independent donors using a paired t-test. *p=0.037, **p=0.009 and #p=0.027

4.3.2 Assessment of soluble factors produced by d3iDC cells stimulated with EnAd virus particles

Upon stimulation with adjuvants, DCs produce a variety of soluble cytokines and chemokines relevant for the immune response outcome. These soluble factors have a diversity of functions, ranging from immune cell recruitment[210] to polarising the adaptive immune response[211] (further assessed in Chapter 6). Therefore, it was relevant to understand which soluble factors were induced by the virus. Using a commercially-available panel based on chemiluminescence immuno-assay Proteome Profiler (see Material and Methods), more than 30 pro-inflammatory molecules (Table 4.1) were assessed on multiple supernatants from day 3 iDC donors treated with EnAd virus or untreated (accordingly with timeframe from Figure 4.1 A).

CCL1	CCL2	CCL3/4	CCL5	CD40 ligand
C5a	CXCL1	CXCL10	CXCL11	CXCL12
G-CSF	GM-CSF	ICAM-1	IFN-g	IL-1a
IL-1b	IL-1ra	IL-2	IL-4	IL-5
IL-6	IL-8	IL-10	IL-12	IL-13
IL-16	IL-17A	IL-18	IL-21	IL-25
IL-27	IL-32a	MIF	Serpin E1	TNF-a

Table 4.1 List of soluble factors assessed in d3iDC supernatants using the Proteome Profiler Human Cytokine Array Kit (R&D Systems)

From the whole panel, only pixel density (PD) for 12 molecules were detectable; these were chemokines C-C motif ligand (CCL)-2, CCL-3/4, CCL-5, CxC motif ligand (CXCL)-10, CXCL-11 and granulocyte-macrophage colony-stimulating factor (GM-CSF), and cytokines interleukin (IL)1-ra, IL-4, IL-6 and IL-8. Additionally, other soluble factors like intercellular adhesion molecule (ICAM)-1 and migration inhibition factor (MIF) were detected. Across multiple donors, EnAd significantly induced the expression of CCL2 ($p=0.0047$), CCL3/4 ($p=0.0247$) and CXCL10 ($p<0.0001$) compared to untreated control (Figure 4.2 B, C and E).

Also, EnAd particles appeared to induce CCL5, CXCL11 and IL-6 in most of the donors, however the PD averages were not statistically significantly different from those in untreated samples (Figure 4.4 D, F and L). ICAM-1, IL-4 and IL-8 PD were detectable in both EnAd-treated and untreated cells, however EnAd tended to up-regulate these soluble factors in same donor origin, without being statistically significant (Figure 4.2 H, K and M). Finally, GM-CSF, IL1-ra and MIF showed similar pixel density between conditions (Figure 4.2 G, I and J).

It can be noticed that most of these factors are induced de novo by EnAd exposure when compared to the untreated cells. However, only CCL2, CCL3/4 and CXCL10 average from EnAd supernatants were significantly different to untreated. This was probably explained by donor to donor variability and the fact that on some occasions inducible factors were not detected in the virus supernatant, leading to large standard deviation. Interestingly, most of the factors induced by EnAd (thus being CCL2, CCL3/4, CCL5, CXCL10, CXCL11, IL-6 and IL-8) promote chemoattraction and pro-inflammation activities on immune cells, suggesting that EnAd virus particles potentially will attract immune responses to the infection site. On the other hand, IL-4 was the only cytokine seen in the model with the ability to polarise the adaptive immune response. Although IL-4 was not detected in every donor, it was further induced with EnAd.

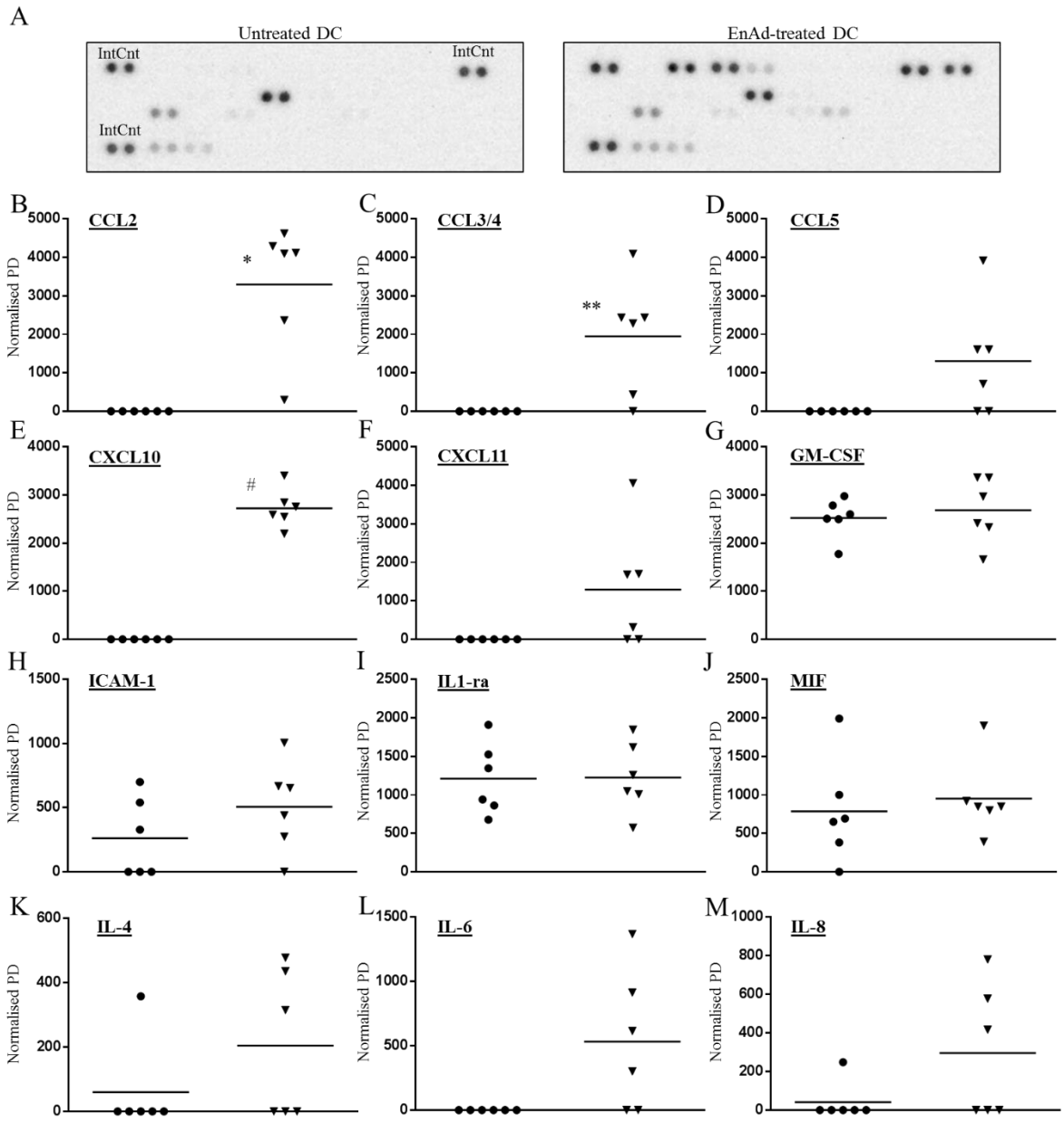


Figure 4.2 Assessment of soluble cytokines and chemokines induced by EnAd on d3iDC. d3iDC were either stimulated with 200 ppc of EnAd (triangle) or left untreated (circles) for 48 hrs. Cytokines and chemokines were evaluated on clarified supernatants using Proteome Profiler Human Cytokine Array Kit (R&D systems), according to manufacturer's protocol. (A) Light emission was acquired over 5 minutes exposure grouped per DC donor. Pixel density (PD) was measured for each dot with ImageJ, the PD of duplicate dots were averaged and normalised to internal controls (IntCnt). (B-M) The normalised PD of six different donors run in independent experiments are shown along with the mean. Statistical differences were calculated using paired t-test, *p=0.0047, **p=0.027 and #p<0.0001

4.3.3 Assessment of the EnAd particles effect on d3iDC model compared to the archetype adenovirus 5

Adenovirus type 5 belongs to adenovirus subgroup C and is probably the most studied and well known human adenovirus from the seven-identified species (A-G). Often referred as the archetypal adenovirus, it has been broadly used in multiple applications including virotherapy, gene-therapy and as a recombinant vaccine vector. Many innate sensing pathways have been described in DC to recognise different Ad5 components[104]. This may contribute to its ability to stimulate a strong pro-inflammatory response and associated strong adaptive immune response[105]. Unlike Ad5 which binds the coxsackie and adenovirus receptor, EnAd binds CD46 and desmoglein-2 as receptors, suggesting that it may trigger different responses than Ad5. In this section the effects of Ad5 and EnAd on d3iDC were assessed using the cell surface immunophenotyping and the Proteome profiler from previous sections.

4.3.3.1 Assessing EnAd and Ad5 virus particle adjuvant effect on the d3iDC by immunophenotyping DC maturation markers

Following the same assay time line as in Figure 4.1, DCs were treated with EnAd or Ad5 virus particles and the cell immunophenotype was assessed using the same marker panel from section 4.3.1. The expression levels were compared between treatments by calculating the fold change (also known as fractional differences) in median fluorescence intensity relative to correspondent untreated controls, before the average and standard deviation across multiple donors were calculated for statistical comparison. This normalisation was aimed to remove the large standard deviations, derived from the variable basal expression levels from one donor to another seen in section 4.3.1. For a better comparison, the variability from donor to donor background levels were removed by calculating the fold change in median fluorescence intensity relative to correspondent untreated controls.

The first donor assessed showed Ad5 virus particles had a very limited effect on the phenotyped markers, for instance the expression levels were very similar to untreated cells and therefore weaker than EnAd (as shown in intensity histograms, Figure 4.3 A). This was later reaffirmed with multiple donors, as the MFI fold change average in Ad5-treated cells relative to untreated was nearly zero (Figure 4.3 B-H). On the other hand, EnAd-treated DC significantly increased HLA-DR, CD86 and PD-L1 relative MFI mean compared to Ad5-treated cells (Figure 4.3 B, D and F and Table 4.2). Non-significant upward trends were seen on the relative MFI fold change average for CD80 and CCR7 markers on EnAd-treated DC in comparison to Ad5-treated cells (Figure 4.3 E and H and Table 4.2), probably becoming significant using a larger sample. Small differences were seen between EnAd-treated d3iDC's HLA-ABC and CD83 MFI fold change average and Ad5 condition, but none of these reached statistical significance (Figure 4.3 C and G and Table 4.2).

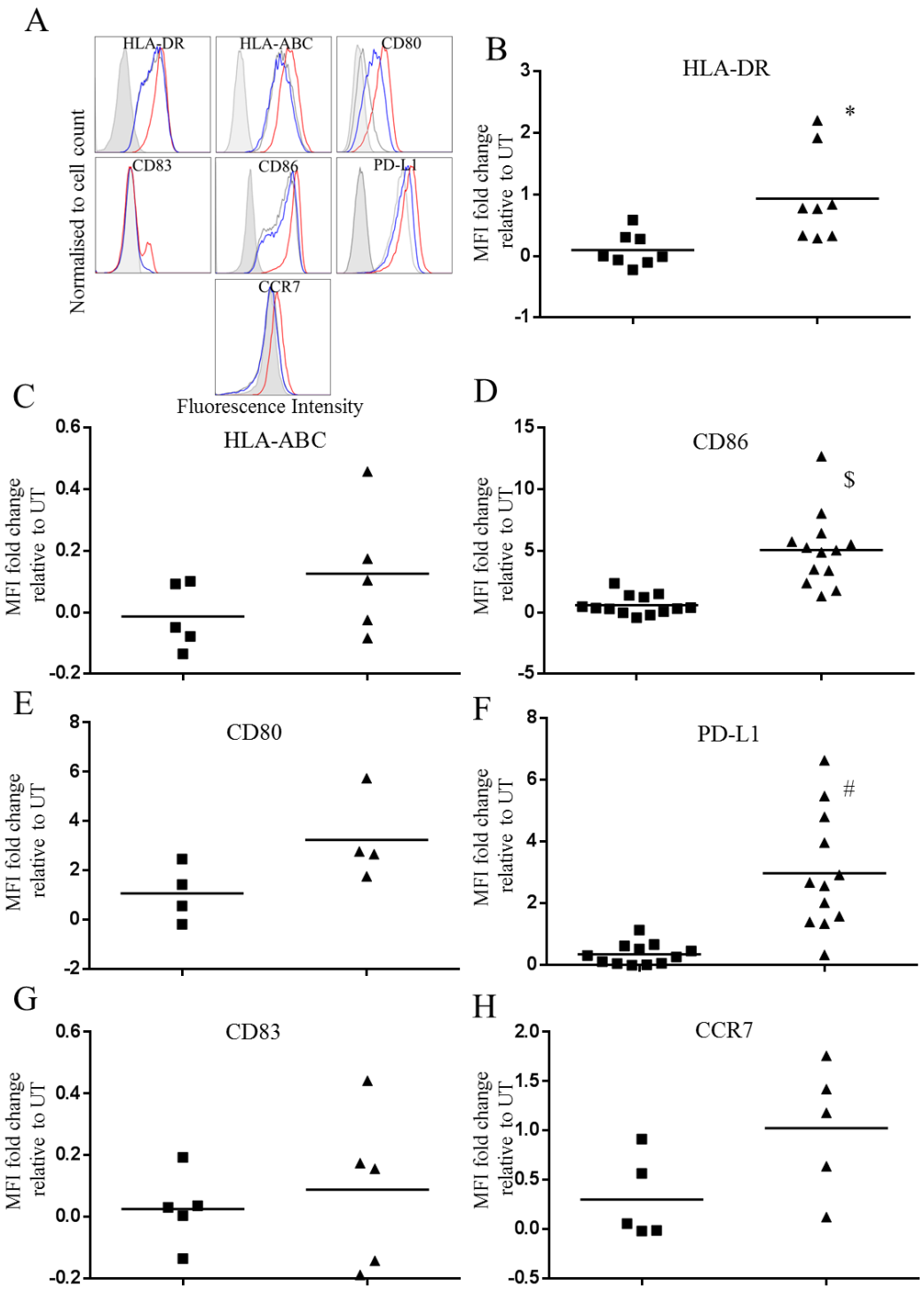


Figure 4.3 Immunophenotyping day 3 immature DC treated with EnAd or Ad5 virus particles. Accordingly with Figure 4.1 A, DC treated with 500ppc of EnAd (red line) or Ad5 (blue line), or left untreated (grey line or circles), cells were then stained with same panel as in section 4.3.1. (A) Data are reported as fluorescence intensity per normalised cell count for one representative donor of n≥4. (B-H) The MFI fold change relative to untreated control (UT) for HLA-DR (B), HLA-ABC (C), CD86 (D), CD80 (E), PD-L1(F), CD83 (G) and CCR7 (H) between cells treated with EnAd (triangle) and Ad5 (squares) virus are compared in scatter dot plots using unpaired T-test. Ad5-EnAd: *p=0.0092, $p=0.0001 and #p<0.0001.

These results showed that EnAd virus particles were a better agent to induce the up-regulation of antigen presenting molecules, costimulatory molecules and lymph node trafficking molecules than Ad5 on d3iDC. And although EnAd also up-regulated the PD-L1 expression, this raised the chances that EnAd particles in the tumour might be a better candidate to induce the up-regulation of T cell priming functions on TIDC as well, as their trafficking to the priming site, than Ad5 virus.

Marker	Ad5 fold change MFI mean ± SD	EnAd fold change MFI mean ± SD	Differences between Ad5 and EnAd relative MFI mean (*p* Value)
HLA-DR	0.098 ±0.269 (n=8)	0.935 ±0.736 (n=8)	Yes (0.0092)
HLA-ABC	-0.013 ±0.106 (n=5)	0.126 ±0.212 (n=5)	No (0.2252)
CD80	1.077 ±1.136 (n=4)	3.242 ±1.728 (n=4)	Yes (0.0812)
CD83	0.027 ±0.117 (n=5)	0.089 ±0.258 (n=5)	No (0.6345)
CD86	0.598 ±0.799 (n=13)	5.083 ±2.958 (n=13)	Yes (0.0001)
PD-L1	0.356 ±0.344 (n=12)	2.976 ±1.884 (n=12)	Yes (<0.0001)
CCR7	0.304 ±0.419 (n=5)	1.026 ±0.648 (n=5)	Yes (0.0696)

Table 4.2 Relative expression of DC markers on d3iDC from multiple donors treated with Ad5 and EnAd, and comparison between virus. MFI values from Figure 4.6 were used to calculate for each virus the MFI fold change relative (or fractional difference) to the correspondent untreated control. Fold change from multiple donors (n=4-12) were averaged, standard deviation (SD) calculated and means compared with unpaired t-test.

4.3.3.2 Comparison of soluble factors produced by d3iDC treated with same dose of EnAd and Ad5 virus particles

Following the same assay time line as in Figure 4.1, DCs were treated with EnAd or Ad5 virus particles and supernatants were assessed using the same method from section 4.3.2. The pixel density of each analyte was compared between treatments across multiple donors.

Out of the 36 studied analytes, only 12 molecules were detected in one or more treatments, coinciding with the same molecules seen in section 4.3.2. Although it was quite variable between donors, Ad5 supernatants showed a pattern much like untreated DC, with multiple

soluble factors undetectable, whilst EnAd induced prominent pixel densities. Across multiple donors, EnAd only significantly increased the PD of CCL2 ($p=0.0194$) compared to Ad5-treated DCs (Figure 4.4 A). CCL3/4 and IL-8's pixel density were also largely measured in EnAd condition, but only seen in one Ad5-treated supernatant, much similar to the untreated DCs (Figure 4.4 B and L). CXCL10 PD in Ad5-treated DC supernatants were quite variable, but the PD mean was much reduced than EnAd (Figure 4.4 D). No pixel density was seen for CCL5, CXCL11 and IL-6 with Ad5 particles, likewise untreated cells, whilst they were detectable in most donors treated with EnAd (Figure 4.4 C, E and K). ICAM-1 and IL-4 were variably detected in all three conditions. However, ICAM-1 had an increased PD in EnAd supernatants, whereas this tendency was shifted towards Ad5 with IL-4 (Figure 4.4 H, K and M). Finally, GM-CSF, IL1-ra and MIF were seen in all donors and conditions, and showed similar pixel density between conditions (Figure 4.4 G, I and J).

The significant donor to donor variability, made the Proteome Profiler assay unreliable for further investigation. However, despite the great variability between donors, EnAd virus particles induced multiple pro-inflammatory factors de novo in almost all the assessed donors, whilst they were generally unseen for the same dose of Ad5. This raised the possibility that EnAd particles in the tumour might constitute a better candidate to change the TME towards a more pro-inflammatory phenotype, attracting immune cells towards the infected cancer cells, which may synergise with cancer immunotherapy.

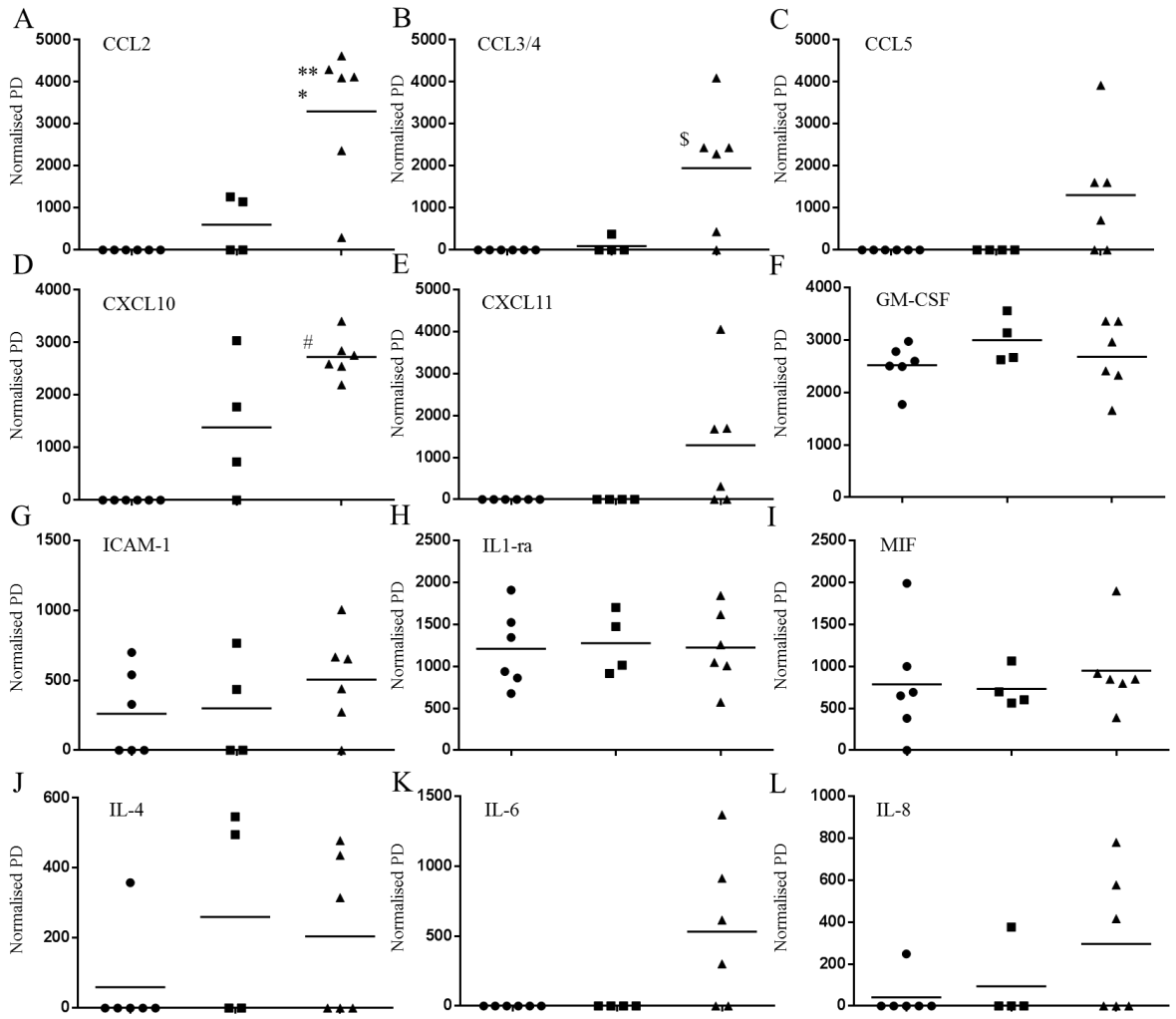


Figure 4.4 Assessment of soluble cytokines and chemokines induced by EnAd on day 3 d3iDC. Accordingly with Figure 4.3 A, supernatants from d3iDC treated with 500ppc of EnAd (triangles) or Ad5 (squares), or left untreated (circles), were evaluated on Proteome Profiler Human Cytokine Array Kit (R&D systems), according to manufacturer's protocol and settings as for Figure 4.5. (A-L) The normalised PD of four to six different donors run in independent experiments are shown along with the mean. Statistical differences were calculated using paired t-test. Untreated-EnAd: *p=0.0047, $p=0.027 and #p<0.0001. EnAd-Ad5: **p=0.0194

4.3.3.3 Transcriptome analysis of immune-related genes in d3iDC cells treated with EnAd and Ad5 virus particle

nCounter® (Nanostring® Technology) is a novel technology that uses multiplex target-specific color-coded barcode probes to study the transcriptome. In this section, a pre-built 770-wide immune-related genes panel (nCounter® PanCancer Immune Profiling for Human) was used on d3iDC from two independent donors, treated with EnAd or Ad5 virus, or left untreated

(accordingly with Figure 4.1 A). The aim was to find the type of immune responses the viruses induced, by identifying genes whose mRNA expression were altered in comparison to the untreated controls. Additionally, it was expected that differences in mRNA expression could indicate genes involved in the potent ability of EnAd particles to stimulate DC relative to Ad5. In addition, new probes specific for EnAd E1, E2 E3 and L3 mRNAs were designed and included into the previous panel to assess the viral transcript expression in d3iDC. RNA from control, Ad5 or EnAd infected-A549 cells were isolated to be used as positive controls. Due to the complexity of the technique the assay was performed externally by a contractor. However, the quality of the samples was carefully produced and previously assessed in-house by RT-qPCR (see Material and Methods), confirming no DNA contamination (not shown).

The raw transcriptome data were fed into nSolver® – Nanostring's data analysis software –, and gene expression were normalised against 4 housekeeping genes (ZNF346, TRIM39, CC2D1B and GPATCH3) picked out of 40 housekeeping genes built-in in the panel. The gene copies from EnAd and Ad5 virus treatments were normalised as fold change relative to the untreated samples and 2-fold change consistently induced by any of the two adenoviruses were identified (Table 4.3). The genes with large alterations relative to untreated could be categorised into 5 families, those being: 1) receptors, signalling molecules and transcription factors genes, 2) cytokines, chemokines and other soluble factors 3) antigen presentation and T cell priming, 4) complement factors and 5) anti-viral intra-cellular innate response. Given the previous data, the up-regulation of mRNA families 2 and 3, supported the up-regulation of pro-inflammatory factors and T cell priming molecules detected in previous sections. The expression of pro-inflammatory and other genes are dependent on cell signalling and transcription factor, probably for this reason some of category 1 genes were importantly up-regulated. Neither surprising was to see anti-viral intra-cellular innate response mRNAs up-regulated after virus exposure, as category 5 genes are a strategy for infected cells to fight the

intracellular virus. On that same line, the up-regulation of complement proteins (category 4) probably is a strategy to opsonise the extracellular infectious agent. Interestingly, Ad5 and EnAd induced the same mRNA expression pattern relative to untreated d3iDC. However, EnAd in general induced stronger mRNA expression of these altered genes (Table 4.3). Some of those strongly induced genes were CCL5, CCL8, CXCL10 and CXCL11, all involved in attraction of immune cells.

Families	Gene name	Accession number	Ad5 relative fold change	EnAd relative fold change	Families	Gene name	Accession number	Ad5 relative fold change	EnAd relative fold change
Receptors, signalling molecules and transcription factors	IRF1	NM_002198.1	6.6	10.5	Antigen presentation and T cell priming	HLA-A	NM_002116.5	1.3	4.13
	IRF2	NM_002199.3	3.2	3.0		HLA-C	NM_002117.4	1.2	3.6
	IRF7	NM_001572.3	18.1	25.8		HLA-G	NM_002127.4	1.7	4.5
	STAT1	NM_007315.2	14.0	10.5		CD80	NM_005191.3	20.7	61.7
	STAT2	NM_005419.2	9.4	10.2		CD274	NM_014143.3	4.0	5.6
	TNFSF15	NM_001204344.1	262.3	202.4		TAP1	NM_000593.5	7.8	8.7
	RIPK2	NM_003821.5	4.5	9.7		TAP2	NM_000544.3	4.5	5.0
	CD38	NM_001775.2	26.5	45.2		LAG3	NM_002286.5	24.2	26.5
	SIGLEC1	NM_023068.3	61.5	94.7	Complement	CFB	NM_001710.5	23.0	50.0
	CCR7	NM_001838.2	2.5	18.9		C1S	NM_001734.2	0.1	10.3
Cytokines, chemokines and soluble factors	CCL2	NM_002982.3	42.0	10.8		SERPING1	NM_000062.2	23.0	40.9
	CCL3L1	NM_021006.4	3.5	10.2	Anti-viral innate response	DDX58	NM_014314.3	97.2	63.0
	CCL5	NM_002985.2	93.8	1055.9		IFIH1	NM_022168.2	27.3	30.6
	CCL8	NM_005623.2	435.4	263.9		IFIT1	NM_001548.3	1784.4	1097.7
	CXCL10	NM_001565.1	6492.7	6787.1		IFIT2	NM_001547.4	1097.7	961.6
	CXCL11	NM_005409.4	1245.1	3757.8		IFITM1	NM_003641.3	508.1	688.8
	IL15RA	NM_002189.2	19.2	28.1		IFITM2	NM_006435.2	12.2	11.9
	IL6	NM_000600.1	8.4	29.8		ISG15	NM_005101.3	252.3	415.4
	TNFSF10	NM_003810.2	360.9	191.8		ISG20	NM_002201.4	248.2	422.0
	TNFSF18	NM_005092.2	24.8	25.5		IFNL1	NM_172140.1	20.5	9.3
	TNFSF8	NM_001244.3	26.8	56.0		MX1	NM_002462.2	320.5	178.4
	IDO1	NM_002164.3	107.6	708.0		OAS3	NM_006187.2	56.7	46.4
	IFNB1	NM_002176.2	121.6	75.6					

Table 4.3 Identified genes in d3iDC that across two donors were consistently 2-fold changed in mRNA expression relative to untreated control. The common name of the genes together with their accession number are shown and grouped by functionality, the relative mRNA fold change of d3iDC from one donor treated with Ad5 and EnAd are shown.

Unexpectedly, the supplementary viral panel run alongside the immune panel on nCounter, revealed the expression of the E3 mRNA transcript in two different d3iDC donors. Whilst E1, E2 and L3 viral transcripts were not detectable (Figure 4.5), on the other hand, all four E1, E2 E3 and L3 mRNA were detected in the permissive A549 cells infected with EnAd. This observation was further investigated and the results will be presented in Chapter 5.

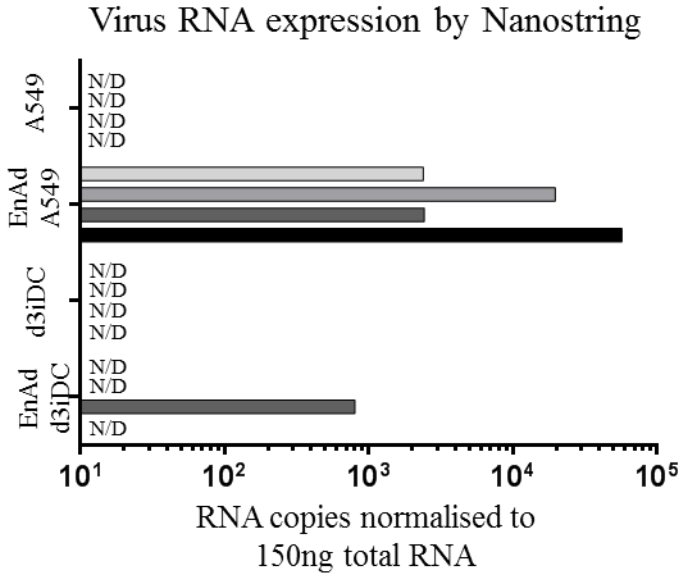


Figure 4.5 EnAd RNA transcripts expression in d3iDC. Day 3 iDC or A549 were exposed to 200EnAd ppc (EnAd-DC and EnAd-A549, respectively) or left untreated (UT-A549 and UT-DC, respectively). After 18 hrs, RNA was extracted with in-solution DNAse-treatment from lysed cells. RNA concentrations were determined by Nanodrop and adjusted to 150 ng/µl. A 800-wide pre-designed panel along with adenovirus panel for Nanostring were used to quantify copies of target-RNA in samples. Data from one donor are represented as RNA copies per cell for EnAd's E1B (light grey), E2B (grey), E3 (dark grey) and hexon (black), representative of two different donors. N/D= not detected

4.3.3.4 Assessing the adjuvant effect of EnAd and Ad5 virus particle at different doses on d3iDC model

To gain more understanding of why EnAd virus particles prompted a better maturation and pro-inflammatory phenotype on the early immature DC model than Ad5 as seen in previous sections, d3iDC were cultured with multiple concentrations of EnAd or Ad5 virus particles – ranging from 5 x 10^4 to 5 viral particles per cell. Cells were then assessed for PD-L1 and CD86 expression by flow cytometry.

Increasing doses of EnAd particles induced increasing up-regulation of PD-L1 and CD86 markers (Figure 4.6 A). On the same donor d3iDC, Ad5 also induced up-regulation of both markers at increasing doses of virus. However, more Ad5 virus particles were needed to achieve a similar fluorescence intensity as EnAd (Figure 4.6 B).

To remove the variability from donor to donor background levels and better distinguish a trend, fold change median fluorescence intensity (MFI) relative to corresponding untreated controls were calculated. EnAd virus was capable of inducing in some donors a slight relative PD-L1 MFI increase at concentrations as low as 5ppc, but this had no effect on the CD86 marker. Nevertheless, 50ppc induced a relative MFI increase on both markers and all donors when treated with EnAd virus. Extensively, consistently higher relative MFI for PDL1 and CD86 were seen across all donors at increasing doses of EnAd, suggesting a dose-response effect. Using a dose-response (stimulation) equation on both PD-L1 and CD86 relative expression across 3 donors treated with EnAd, non-linear regression curves were successfully fit with R^2=0.85 and R^2=0.823, respectively (Figure 4.6 C and D). On the other hand, d3iDC from same donors treated with Ad5 virus, only showed a small relative MFI increase on both PD-L1 and CD86 from 500ppc, and further amplified with 5000ppc. Using a dose-response (stimulation) equation on relative MFI from Ad5-treated d3iDCs, non-linear regression curves were fit on PD-L1 and CD86 with R^2=0.47 and R^2=0.66, respectively (Figure 4.6 C and D). The dose-response curves of both markers were used to statistically compare EnAd and Ad5 treatment by the extra sum-of-squares F test. PDL1 and CD86 statistical analysis showed that both viruses induced different dose-response curves (p value<0.0001) (Figure 4.6 C and D). Suggesting that less EnAd virus particles than Ad5 were needed for same adjuvant effect on DC.

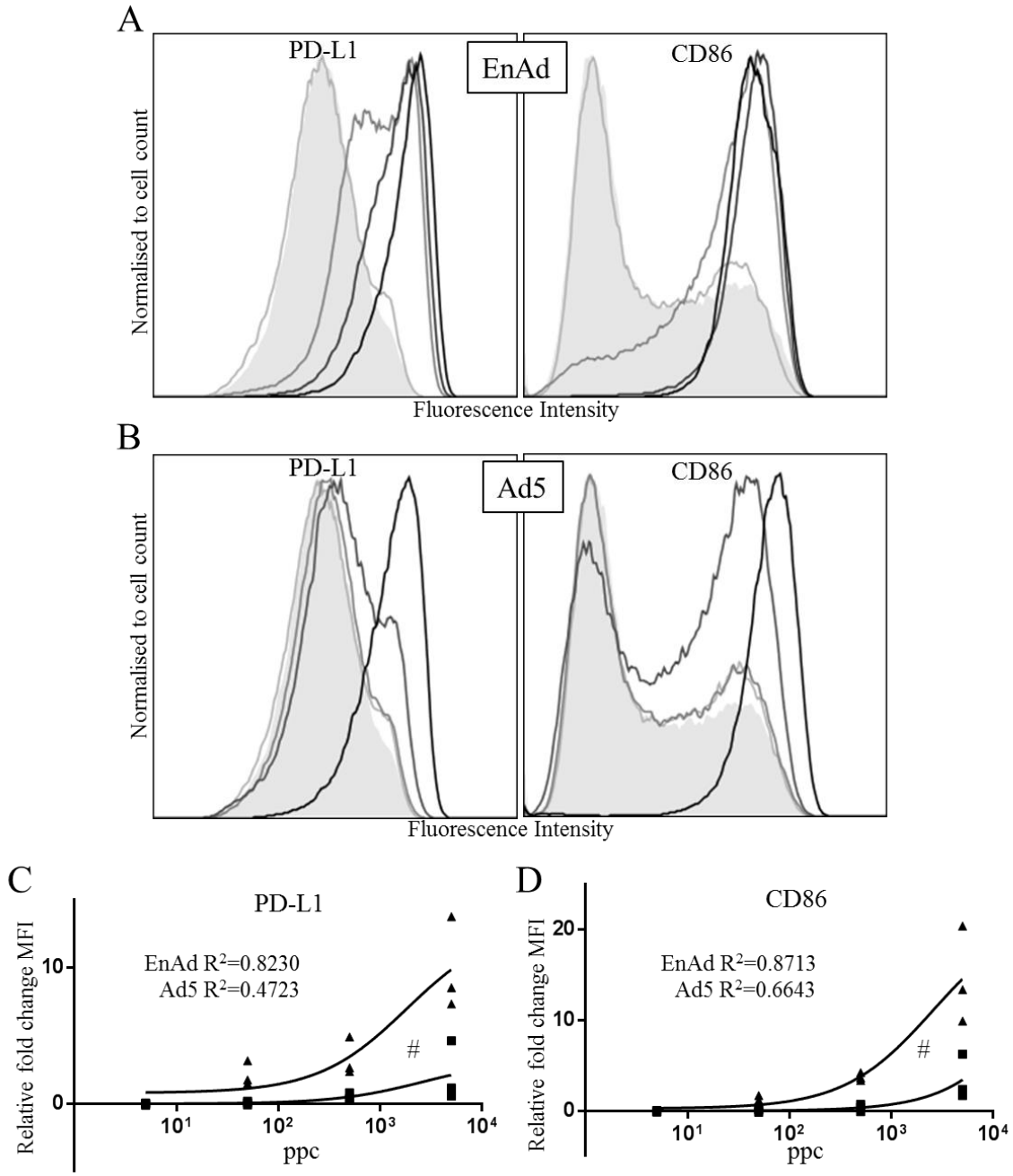


Figure 4.6 Assessment of maturation markers on d3iDC at increasing virus doses. Day 3 iDC were treated with either EnAd or Ad5 at 5ppc (light grey line), 50ppc (grey line), 500ppc (dark grey line) and 5000ppc (black line) or left untreated (solid grey). After 48 hrs, cells were stained with vital dye and monoclonal antibodies against PDL-1 and CD86, and acquired by flow cytometry. (A and B) Data are reported as fluorescence intensity per normalised cell count for one representative independent experiment of n≥3. The fold change of PD-L1 (C) and CD86 (D) MFI for EnAd and Ad5 treated-d3iDC were calculated relative to correspondent untreated control (relative fold change). The relative fold change MFI from 3 independent donors were used to fit a non-linear regression curve (dose-response equation), and to calculate goodness of fit (R^2 value) and statistical comparison of the curves by the extra sum-of-squares F test. #p value<0.0001

4.3.4 Evaluating the consequences of tumour cell virolysis on the effects of EnAd virus on d3iDC cells

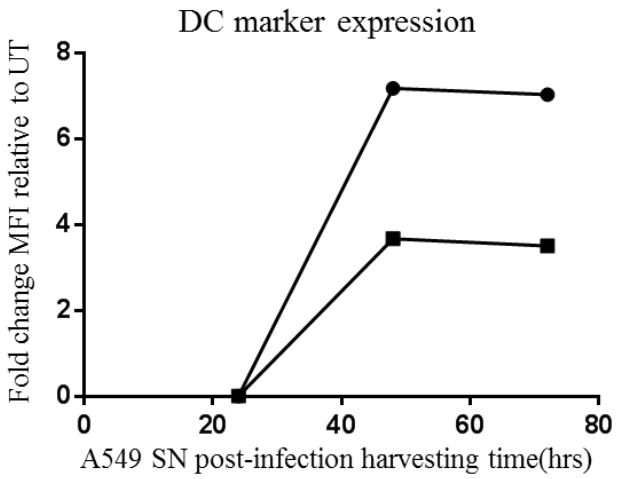
Cancer and stroma cells generate a complex tumour microenvironment that can modulate the antigen-presenting abilities of innate immune cells[49,212], likely to further contribute to the suppressive TME[52]. On the other hand, colleagues in this research group had previously demonstrated that EnAd killed A549 cancer cells by oncosis, which increased calreticulin exposure on cell surface and promoted extracellular release of adenosine triphosphate (ATP), heat-shock protein 70 (HSP70) and high-mobility group box (HMGB1)[187]. All these molecules are considered gold standard damage-associated molecular patterns produced during pathological cellular stress, which like PAMPs, they are sensed by PRR triggering the maturation of DCs[187]. In virotherapy DAMPs are believed to help harness an anti-tumour immune response. Therefore, the effect of EnAd virus particles previously described in this chapter omitted both the modulation of d3iDC from cancer cells and the DAMPs derived from the virus activity on tumour cells. To extrapolate whether EnAd and its cancer cell killing activity would overcome the modulatory stimuli from the tumour, d3iDC were immunophenotyped after exposure to the EnAd-permissive A549 cell line – described to have immuno-modulatory abilities[213-217].

In order to understand the role of soluble mediators produced by virus-infected cancer cells on d3iDC stimulation, supernatant from EnAd-infected A549 cells were harvested at multiple times points post-infection; 24hrs, 48hrs and 72hrs, and exposed for 48hrs to d3iDC, or left untreated. Then routine flow cytometry was used to immunophenotype HLA-DR and CD86 expression. The expression of HLA-DR and CD86, as fold change MFI relative to the untreated d3iDC, was not up-regulated with 24hrs supernatants. Whereas supernatant from cells infected 48hrs with EnAd, induced nearly a 4- and 7-fold increase on relative HLA-DR and CD86 MFI, respectively. The marker levels of 72 hrs supernatant were not further increased, and appeared

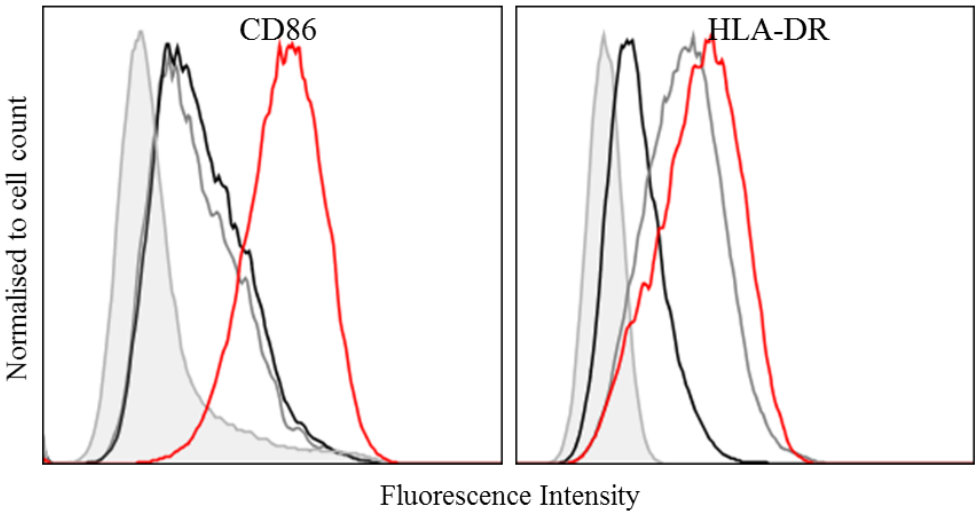
to be like the 48hrs supernatant expression (Figure 4.7 A), suggesting that EnAd activity in A549 supernatants induced DC stimulation with a maximum effect at 48hrs post-infection.

Based on these observations, the supernatant from A549 cells infected for 48hrs with EnAd virus or un-infected, were added to d3iDC for 2 days before HLA-DR and CD86 expression were analysed by flow cytometry. The first d3iDC donor again showed that exposure to the virus conditioned-medium increased the fluorescence intensity of HLA-DR and CD86. On the other hand, the fluorescence intensity from d3iDC treated with un-infected A549 supernatant, was not up-regulated when compared to un-touched d3iDC, in fact HLA-DR expression appeared to be lowered (Figure 4.7 B). After assessing multiple donors, the average of relative CD86 MFI was slightly decreased in d3iDC treated with A549 supernatant, whilst HLA-DR was markedly reduced. d3iDCs treated with supernatants from EnAd-infected A549, showed a significantly up-regulation of the relative HLA-DR and CD86 average compared to d3iDC cells treated with un-infected A549 supernatants (Figure 4.7 C). Thus, suggesting that virus PAMPs and soluble virus-induced DAMPs produced by dying cells were enough to stimulate DCs.

A



B



C

Marker	A549 SN fold change MFI mean ± SD	EnAd-A549 SN fold change MFI mean ± SD	Differences between both relative MFI means (p Value)
CD86	-0.007 ±0.581 (n=4)	6.999 ±1.543 (n=4)	Yes (0.002)
HLA-DR	-0.486 ±0.208 (n=4)	1.461 ±1.204 (n=4)	Yes (0.034)

Figure 4.7 Assessment of CD86 and HLA-DR expression on d3iDC cultured with EnAd-infected A549 supernatants. (A) SN from A549 cells infected with 100ppc of EnAd for 24, 48 and 72 hrs, were added on d3iDC. (A) CD86 (dots) and HLA-DR (squares) were monitored by flow cytometry after 48 hrs culture, and are presented as fold change MFI relative to untreated DCs, representative of 2 donors. (B and C) SN from 48 hr-infected A549 with 100ppc of EnAd (red line or EnAd-A549) or SN from non-infected A549 (black line or A549), were added on d3iDC, or left untreated (grey line). After 48 hrs, CD86 and HLA-DR – or correspondent isotype (solid grey) – were assessed by flow cytometry. (B) Data from one donor are reported as fluorescence intensity per normalised cell count, representative of 4 independent donors. (C) Extensively, the fold change CD86 and HLA-DR MFI relative to same donors untreated d3iDC were calculated for EnAd-A549 and A549 treatments. Fold change MFI mean ±SD of 4 independent donors are presented. Comparison between both SN-treatments with unpaired, two-tailed T-test, are calculated.

It was then set out to investigate which of these two components, virus or DAMPs, mediated the greater stimulation of d3iDC. Thus, EnAd-infected or uninfected A549 clarified supernatant were fractionated with a 100.000 Da molecular weight cut-off (100kDa MWCO) membrane into; flow-through fraction; enriched with molecules smaller than 100kDa MWCO (for instance DAMPs), and retentate fraction; enriched with molecules larger than 100kDa MWCO (for instance virus particles). All fractions, together with a no-fractioned EnAd-infected A549 supernatant (EnAd-SN) as well as control media (Med), were cultured on d3iDC and 48hrs later HLA-DR and CD86 immunophenotyped by flow cytometry. The virus retentate fraction appeared to induce up-regulation of CD86 and HLA-DR to similar MFI levels as un-fractioned EnAd-SN. Whereas flow-through from clarified supernatant from EnAd-infected cells displayed significantly reduced HLA-DR and CD86 MFI levels. In fact, d3iDC treated with that fraction, showed MFI levels for both markers below the medium control. Uninfected A549 supernatant flow-through presented slightly lower MFI for both HLA-DR and CD86, than either the retentate from the same condition or the medium control (Figure 4.8). This suggested that molecules larger than 100kDa, for instance adenovirus which is approximately 150MDa, might be enough adjuvant to stimulate TIDCs. Whereas DAMPs released by EnAd-infected A549 cells, which are significantly smaller than 100kDa, might not.

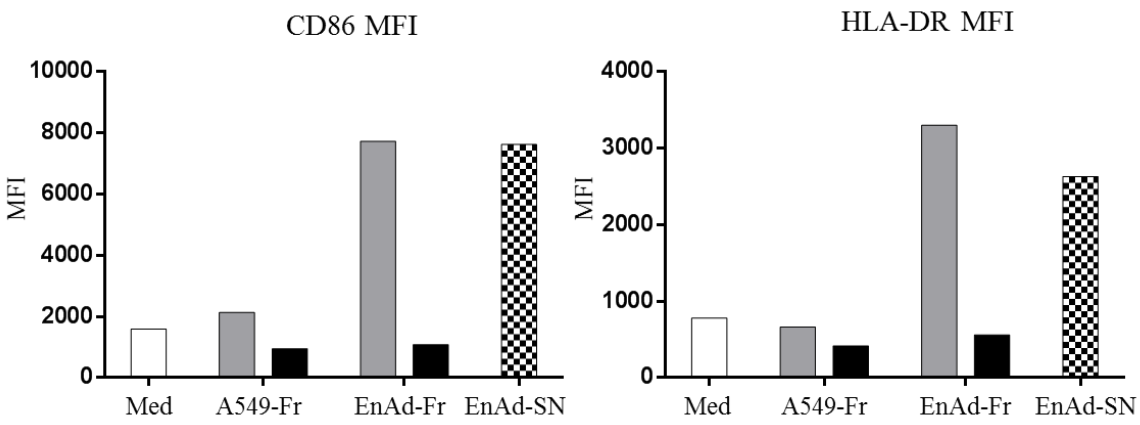


Figure 4.8 Stimulation of d3iDC with two fractions of EnAd-infected A549 supernatant split by a 100 kDa MWCO membrane. Clarified supernatants (SN) from A549 infected for 48 hrs with 100ppc of EnAd (EnAd-Fr) and non-infected (A549-Fr) were fractioned with a 100.000 molecular weight cut off (MWCO) membrane (Pierce, Protein Concentrators PES) into retentate (grey) or flow-through (black). These fractions were added to di3DC, alternatively non-fractioned EnAd-A549 SN control (EnAd-SN, square pattern) and untreated control (Med) were used. After 48 hrs, cells were stained for CD86 and HLA-DR – or correspondent isotype (solid grey) – and acquired by flow cytometry. Median fluorescence intensity (MFI) for one donor is presented, representative of 2 independent donors.

Since EnAd and Ad11p had same physical properties and similar adjuvant effect on d3iDC (shown later in Chapter 5, Figure 5.7), but had different replication kinetics in cancer cells – EnAd produced more virus progeny to the supernatant than Ad11p (shown in Chapter 3, Figure 3.3). It was hypothesised that EnAd-infected A549 supernatants would stimulate d3iDC better than the parental virus. EnAd-infected A549 supernatants appeared to induce much stronger HLA-DR and CD86 up-regulation than supernatants from A549 infected with Ad11p (Figure 4.9). These data suggested that viruses with same physical properties but producing more virus progeny to the extracellular space, were more likely to be better adjuvants of TIDC.

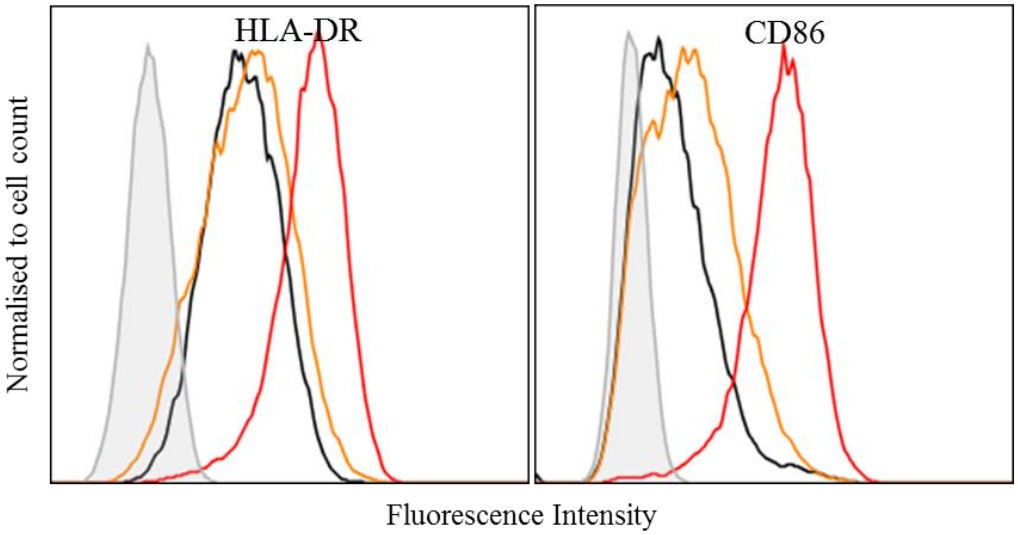


Figure 4.9 Immunophenotype of d3iDC treated with supernatants from EnAd and Ad11p infected-A549 cells. Supernatants (SN) from 48 hrs-infected A549 with 100ppc of Ad11p (orange line) or EnAd (red line), and non-infected (black line) were added onto d3iDC. After 48 hrs, DC were stained for HLA-DR and CD86 – or correspondent isotype (solid grey) – and analysed by routine flow cytometry. Fluorescence intensity for one donor is presented, representative of 2 independent donors.

The previous experiments only investigated the stimulation of d3iDC from soluble factors, missing intercellular interactions. Therefore, d3iDC stimulation was assessed in a co-culture with A549 cells. Preliminary un-infected co-cultures were used to find a suitable ratio of cancer to immune cell without altering the DC stimulation phenotype. This showed that CD86 expression on d3iDC was up-regulated with cancer cells, whilst HLA-DR was unaffected. The ratio of 1:1 induced the greatest up-regulation of CD86 relative to untreated d3iDC, whilst limited effects were seen for 1:4 and 1:16 ratios (Figure 4.10 A). During the co-culture it was observed the that d3iDC strongly adhered to the surface of the well, challenging subsequent isolation (not shown). Therefore, adding the virus into the co-culture would potentially stimulate d3iDC directly via virus particles as already studied in previous sections. Instead, pre-seeded A549 cells were infected at a low concentration of EnAd or Ad5 virus for a short period of time, or left untreated. Before adding the d3iDC to a ratio of 4 to 1 cancer cell, A549 cells were thoroughly washed with abundant PBS to remove as many free virus particles. After 48hrs co-culture, HLA-DR and CD86 expression on d3iDC were assessed by routine flow

cytometry. The data showed that EnAd-infected A549 induced up-regulation of both HLA-DR and CD86 fluorescence intensity, relative to untreated wells. In contraposition, Ad5-infected A549, despite displaying cytopathic effect, had a limited effect on both markers expression compared to un-infected condition (Figure 4.10 B). This, suggested that EnAd could up-regulate the presentation ability of DCs when in contact with tumour cells, whereas Ad5 virus could not.

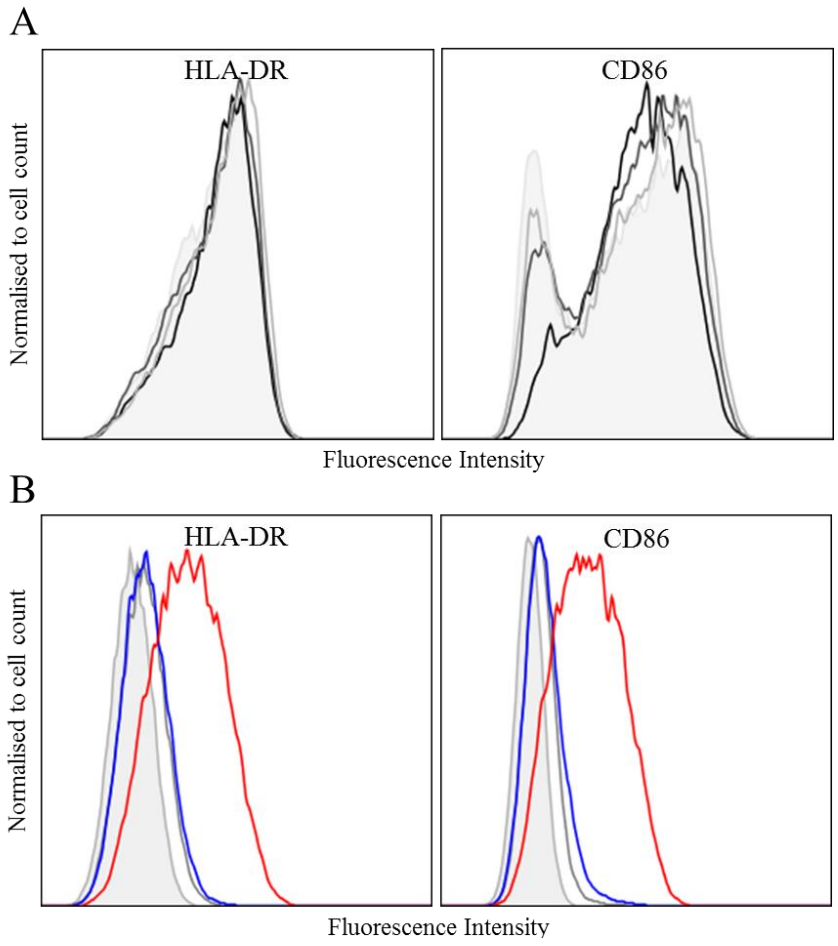


Figure 4.10 Immunophenotyping of d3iDC co-cultured with virus-infected A549 cells. (A) A549 cells were pre-seeded at different densities, later a fixed concentration of d3iDC was added, giving a A549 to DC cell ratios of 1:1 (light grey line), 1:4 (dark grey line) and 1:16 (black line) or DC alone (solid grey). After 48hrs co-culture, cells were trypsinised for 10 minutes and cells stained for CD86 and HLA-DR, as well as CD206, before acquired by flow cytometry. CD206+ and live gated cells were used to report HLA-DR and CD86 fluorescence intensity per normalised cell count, representative of 2 independent donors. (B) Pre-seeded A549 were infected with 100ppc of Ad5 (Ad5-A549, blue line) or EnAd (EnAd-A549, red line), or left untreated (UT-A549, grey line). Shortly after cells were thoroughly washed and d3iDC added at 1:4 ratio. After 48 hrs, DC were stained for vital dye, CD86 and HLA-DR – or correspondent isotype (solid grey) – and acquired by flow cytometry. B) Data from one donor are reported as fluorescence intensity of live gated cells per normalised cell count, representative of 2 independent donors.

4.4 Chapter summary

1. EnAd virus particles up-regulated a variety of DC cell-surface markers and induced the secretion of pro-inflammatory chemokines on d3iDC relative to untreated cells.
2. EnAd virus particles appeared to induce greater up-regulation of cell surface markers and inducible pro-inflammatory cytokines on d3iDC, than the same concentration of Ad5 virus. EnAd virus particles also induced greater changes in mRNA expression from immune-related genes than was shown by Ad5.
3. Both EnAd and Ad5 virus particles showed a dose-response curve on stimulation of d3iDC (measured by PD-L1 and CD86), however fewer EnAd virus particles were needed to achieve the same effect.
4. EnAd-infected A549 supernatants stimulated d3iDC via large soluble factors (greater than 100kDa MWCO). This effect was also achieved, when d3iDC were directly co-cultured with EnAd-infected A549.

4.5 Chapter discussion

4.5.1 Discussion of results

DCs play a key role at inducing and maintaining the antitumor immunity, however in the tumour their antigen-presenting function may be lost or inefficient. Tumour-infiltrating DC can modulate antigen-specific effector T cells into depletion, anergy or even regulatory T cells (Tregs)[43-45], that in turn will secrete more suppressive factors and contribute further to the immune evasion[46,49]. In this chapter it was investigated whether EnAd was a good candidate to mature tumour-infiltrating DC and help break the immune tolerance in TME by inducing pro-inflammatory responses.

Due to species-specificity of adenovirus and the lack of expression of the cellular receptors for group B virus[218], an alternative to animal models for studying EnAd was used. Human monocyte-derived immature DC (d3iDC), generated by culturing monocytes for 3 days in RMPI medium supplemented with GM-CSF and IL-4, expressed limited antigen presenting molecules and costimulatory molecules (see Appendix, Part B), a phenotype shared with TIDCs and associated with their poor T cell priming abilities[51,52]. In fact, the poor functional ability of TIDC to prime T cells, is often evaluated by assessing the T cell activation and proliferation in allogeneic mixed leukocyte reaction (MLR) assay[51,219] (see Chapter 6). Interestingly, this d3iDC cells stimulated with LPS – a TLR4-agonist– failed to produce IL-12 and IL1-beta consistently across all donors (see Appendix, Part B), cytokines not detected in LPS-stimulated TIDC[53]. Both cytokines are generally seen on pro-inflammatory day 7 monocyte-derived DC stimulated with LPS[219,220]. Consequently, d3iDC cells were considered a model with some tumour-infiltrating DCs features, adequate to investigate the adjuvant effect of EnAd virus.

The adjuvant effect of EnAd alone as a free particle on d3iDC model induced a strong up-regulation of costimulatory molecules (CD80/86) and antigen presenting molecules (HLA) as well as a small effect on migratory molecules (CCR7) (Figure 4.1). This suggested that this d3iDC would now have a restored ability to present antigens locally and in the draining lymph nodes to prime T cells. EnAd may also increase the checkpoint inhibitory function on T cells, as PD-L1 was slightly up-regulated on TIDC-like cells treated with virus (Figure 4.1), however, this might be a good opportunity for the virus to synergise with checkpoint inhibitor immunotherapy (see Chapter 6). In addition, EnAd induced the secretion of pro-inflammatory cytokines and chemokines, without detectable suppressive or anti-inflammatory molecules (Figure 4.2). Particularly interesting was to see the strong induction of CXCL10 by EnAd particles in all donors. This chemokine is known to be expressed by tumour-resident CD103+ DCs, attracting effector T cells to the tumour. However, when CD103+ DCs fail to secrete this cytokine, the anti-tumour T cell response is interrupted, contributing to immune escape[221]. The induced chemokine suggests that EnAd particles may drive a pro-inflammatory phenotype on TIDC, contributing towards an immunogenic TME[222-227]. However, TIDC-like cells treated with EnAd virus particles did not produce IL-12, a cytokine essential to induce T_H1 adaptive immune response, and instead most donors secreted IL-4, a T_H2 polarising cytokine. This suggested that EnAd may restore the T cell priming abilities of TIDC, although it might not be sufficient to polarise the adequate anti-cancer adaptive immune response (see Chapter 6).

The comparison of the effect of EnAd and Ad5 particles on d3iDC, showed EnAd reproducibly induced a stronger up-regulation of surface markers (Figure 4.3) and soluble factors (Figure 4.4). In addition, the immune-related transcriptome expression study, used to identify pathways by which EnAd was stimulating d3iDC, supported the induction of chemokines seen at the protein level, but did not identify clear pathway differences between EnAd and Ad5 (Table 4.3). The fact that Ad5 also induced mRNA for the same chemokines as EnAd but had not

induced detectable proteins for these, suggested the possibility that post-transcriptional activities may be differently stimulated by EnAd. In dose-response studies, using multiple virus concentrations, larger quantities of Ad5 virus particles were needed to achieve the same effect as EnAd (Figure 4.6), in accordance with previous reports[228]. This suggested EnAd particles were a better adjuvant candidate to stimulate TIDC-like cells at equal concentrations.

In virotherapy it is commonly accepted that the endogenous danger signals (or DAMPs), derived from the virus activity on tumour cells, together with the virus particles (or PAMPs) contribute to the activation of antigen presenting cells. However, anti-inflammatory signals found in TME can affect the adjuvant effect of the virus[49,229]. In this lab, A549 cells, which had been reported with multiple regulatory features[213-217], were shown to die by oncosis when infected with EnAd virus, releasing multiple danger-associated molecular patterns[187]. Virus-infected A549 were co-cultured with d3iDC cells, to evaluate whether EnAd virus would be capable to activate TIDCs in a tumour context. Those studies showed that the virus activity of EnAd on A549 stimulated d3iDC (Figure 4.7, Figure 4.9 and Figure 4.10). In the same timeframe Ad5 activity was not sufficient to induce d3iDC (Figure 4.10). The poor ability of Ad5 to stimulate TIDC-like cells could be a reflection of its limited generation of DAMPs in A549[187], or not enough PAMPs due to its slower life cycle[187].

Further studies to understand the implication of DAMPs and PAMPs derived from the activity of EnAd infecting A549 cells, showed that the supernatants fraction containing the larger molecules (>100kDa MWCO) bared the adjuvant effect on d3iDC cells. On the other hand, the supernatant fraction containing the smaller molecules (<100kDa MWCO) had no effect on d3iDC (Figure 4.8). Interestingly, DAMP molecules detected in EnAd-infected A549[187], such as calreticulin (46kDa)[230], ATP (0.55kDa predicted), HMGB1 (25kDa)[231] or HSP70 (70kDa)[232], are all small-sized compared to adenovirus particles (~150MDa)[65]. This finding suggested that the virus particles produced in the tumour cells by oncolytic viruses, are the

most prominent adjuvant for innate immune cells, leaving DAMPs with a minor role. This might redraw the general picture of oncolytic virus around their immune stimulation effect.

Concluding, EnAd particles might be a potent adjuvant stimulant of TIDC by inducing the secretion of factors that promote the tumour-infiltration of pro-inflammatory immune cells. Also, EnAd may induce up-regulation of antigen presenting and costimulatory molecules on TIDC that together with the tumour antigens derived from the oncolytic activity, may contribute to prime anti-tumour T cell clones. This will be investigated in detail in Chapter 6.

4.5.2 Limitations and future work

The data in this chapter supported that EnAd virus particles are a good adjuvant candidate to stimulate TIDC-like cells, inducing better rates than Ad5. However, the TIDC model was artificially differentiated from monocytes, and although tumour cells were also cultured with the d3iDC system to allow some nurturing effect, the work was exclusively performed *in vitro*. In future work, the virus particle effect could be re-assessed in a more physiological context. Human biopsies are more appealing than the animal models, as human adenovirus do not replicate well in mice cells, in which case the particle effect from the released progeny along with the DAMPs effect would be missed.

Future directions could re-assess the virus activity in human tumours arisen in abdominal or pleural cavities. These tumours generally produce large amount of fluids, generating discomfort in the patients. Therefore, they are routinely drained to alleviate the swelling, providing large amounts of samples. These samples contain cancer cells as well as they are generally rich in immunosuppressive factors and immune cells[233]. Ascites and pleural fluid are now being obtained in this lab though collaborations with public hospitals in the UK, however, this samples are exclusively used for academic research. Ascites samples have been used to evaluate the effect of virus on tumour-associated macrophages[234]. But potentially could allow

the study of EnAd adjuvant effect on the different innate cells, including the TIDC. However, the work performed under this thesis was industry-based and the use of these samples was barred. Alternatively, the running clinical trials that assessed EnAd virus at the time of this thesis, had restrictive clinical protocols. This impeded accessing cancer biopsies to evaluate the virus adjuvant effect on the innate cells. Since, new clinical trial protocols have been established, including flow cytometry and nanostring analysis pre- and post-treatment, authorising the study of EnAd activity on the innate compartment. This could help identify innate immunity shifts and allow design of future strategies that synergise with immunotherapy or even help identifying efficacy biomarkers.

5 Understanding the adjuvant effect of EnAd virus particles on the TIDC-like model

5.1 Introduction

The purpose of this chapter was to investigate the mechanism by which EnAd virus particles stimulate maturation and pro-inflammation of the immature dendritic cells model (d3iDC; see Appendix, Part B) described in Chapter 4.

Multiple adenovirus components, from proteins to nucleotides, have been described as pathogen-associated molecular pattern[104]. These PAMPs are sensed by several pathogen recognition receptor as reviewed in Hendrix *et* al[104], thus stimulating innate immune cells to promote strong pro-inflammation and consequent immunity. To overcome the strong anti-virus immune response, adenoviruses have evolved some immune-modulatory genes like, for example, the virus-associated RNA, E1A and several genes encoded in the E3 region, to prevent rapid elimination of the virus by the immune system[235-238].

Although human adenoviruses share common general macroscopic structure and genome organisation[65], EnAd and Ad5 have multiple variances that could explain the different behaviours seen on d3iDC in the previous chapter. For instance, EnAd has a fast, uncontrolled replication cycle, as well as a large deletion in the immunomodulatory E3-encoded genes. Also, the viruses engage with different cell receptors and show variable prevalence of unmethylated CpG on their genome.

EnAd and Ad5 differences are investigated in this chapter to elucidate the mechanism by which EnAd is a better adjuvant for DC stimulation. The data generated are addressed in two overarching sections: whether the effects were mediated by virus-encoded genes or by the virus

particle itself, or a combination of both. Intriguingly, genes in the E3 region of EnAd were found to be transcribed in the DC model. However, no evidence was found that cellular expression of virus genes participated in EnAd's enhanced d3iDC stimulating phenotype. Instead, DCs were found to express the adenovirus group B CD46 receptor, whilst the group C receptor CAR or DSG-2 were absent. This difference in virus particle binding was identified as the main one responsible for the improved DC stimulation by EnAd. The CD46 and virus interaction were also further studied to understand the nature of that response.

5.2 Chapter aim

Assess the mechanism whereby EnAd elicits its adjuvant effects on dendritic cell maturation.

5.3 Results

5.3.1 Investigating the mechanism by which EnAd particles induce superior stimulation on d3iDC model

The first experiments described below assessed the role of virus gene expression in stimulation of d3iDC and the later experiments focused on the effects of virus particles. As a prerequisite, the possibility of an endotoxin contamination in virus stock preparations that could have explained the results was assessed and excluded (see Materials and Methods).

5.3.1.1 Investigating whether the greater adjuvant effect of EnAd on d3iDC cells is virus gene-mediated

Since DNA, RNA and proteins from adenoviruses had all been described as PRR agonists[104], it was first hypothesised that if EnAd was non-selective and able to grow in d3iDC, the increasing concentration of virus products could trigger more stimulation. This was

investigated in d3iDC by searching for evidences of EnAd's life cycle. Later, a gene-inactivated virus and Ad11p virus were used to evaluate the role of the virus gene expression and E3 deletion in d3iDC stimulation.

5.3.1.1.1 Monitoring the genome replication of EnAd in d3iDC cells

First, virus replication was investigated by monitoring the genome copies variation every 24hrs over 4 days by qPCR. To prevent a slow up-take of virus over time, the cultured cells were exposed to 500ppc of EnAd for 4hrs before cells were thoroughly washed. The viral genome load remained steady at around 100 copies per input cell across the 4 days (Figure 5.1), seen across multiple donors. This suggested that EnAd was not replicating the genome in d3iDC, and therefore no growing concentration of viral DNA was responsible for the strong stimulation.

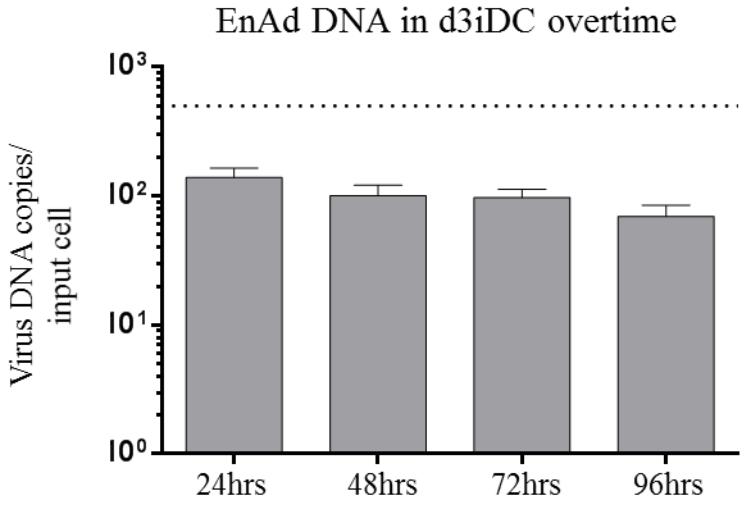


Figure 5.1 Assessment of EnAd replication in d3iDC over time. d3iDC were exposed to 500ppc EnAd, after 4 hrs cells were washed and replaced with fresh medium. Cells were harvested at 24 hrs, 48 hrs, 72 hrs and 96 hrs post infection and DNA isolated GenElute Mammalian Genomic DNA Kit (Sigma), before genome copies were quantified by hexon qPCR. Data are presented as average virus DNA copies per input cell and SD for technical triplicates. Representative of n=3 independent donors. Dotted line represents the input dose of virus.

5.3.1.1.2 Monitoring the expression of 'virus early protein' in d3iDC cells

However, the replication of adenovirus DNA is controlled by early virus genes, therefore early genes must be expressed first[239]. Accordingly, the expression of early protein was assessed next in d3iDC after 4 days of infection. For this an engineered EnAd vector encoding the green fluorescent protein (GFP) reporter gene, was used as an early virus protein surrogate. The reporter gene is spliced from the main E4 transcript of the EnAd-GFP virus (Figure 5.2 A). EnAd-GFP and EnAd were exposed to d3iDC and assessed every 24 hrs for GFP expression by flow cytometry. However, no GFP expression was seen at 24, 48 72 or 96 hours post-infection (Figure 5.2 B-D). In contrast, large numbers of GFP positive cells were found in the permissive A549 tumour cell line just at 24hrs after infection with EnAd-GFP (Figure 5.2 E). The lack of expression of early reporter gene, suggested that early protein was probably not responsible for EnAd's strong d3iDC stimulation.

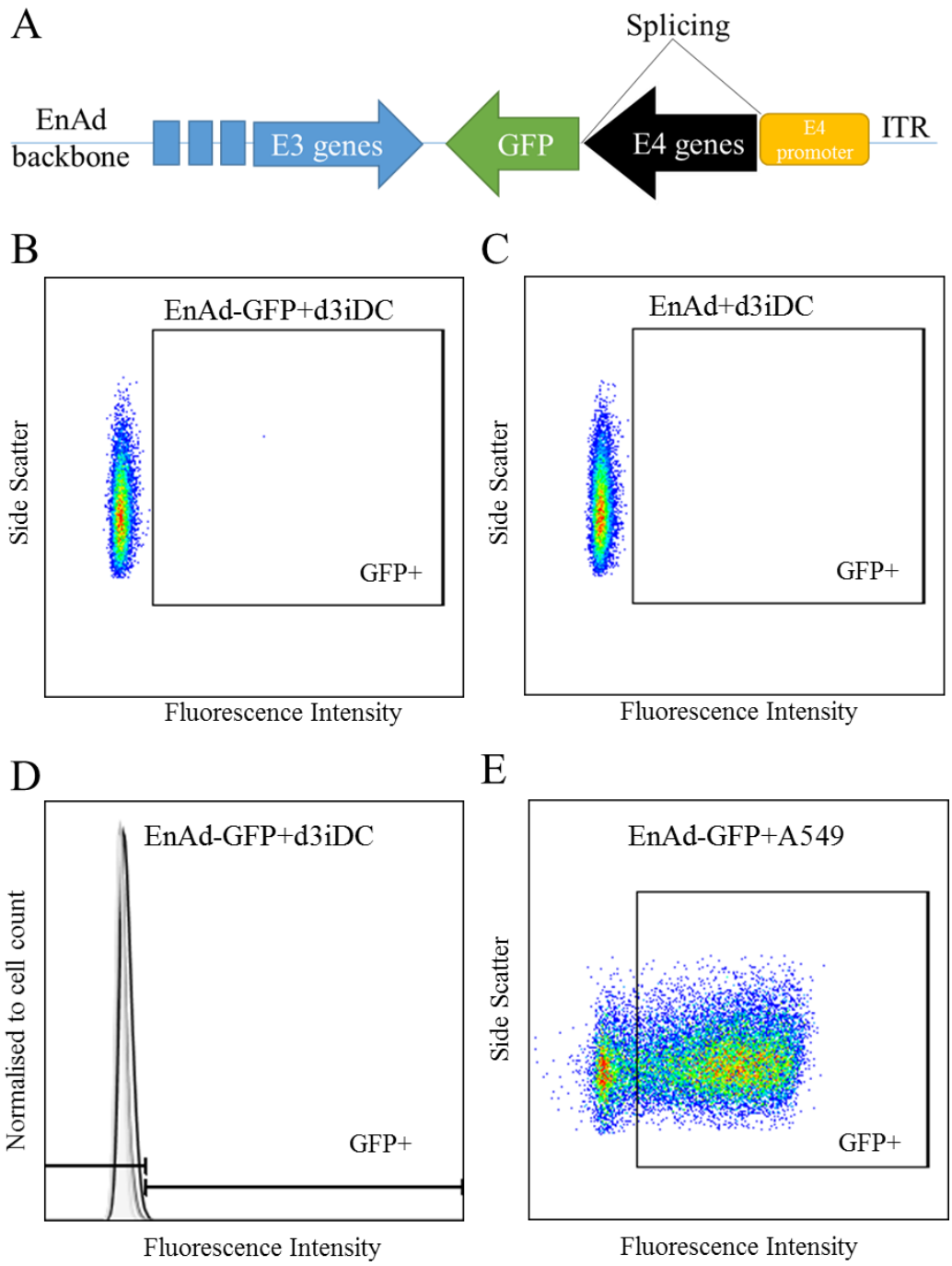


Figure 5.2 Evaluation of GFP expression in d3iDC as virus protein surrogate. (A) Representation of the right-hand side of the EnAd-GFP virus genome. Where EnAd backbone is depicted with a GFP gene and a splice acceptor after the virus E4 transcript. (B-D) d3iDC were exposed to 500ppc EnAd or EnAd-GFP virus (GFP expression is controlled by the internal E4 promoter). Four hours later cells were washed and placed into fresh medium. GFP expression was assessed by flow cytometry and is shown on d3iDC treated for 24 hrs with (B) EnAd-GFP or (C) EnAd. (D) d3iDC treated with EnAd-GFP for 24 hrs (solid grey), 48 hrs (light grey line), 72 hrs (dark grey line) and 96 hrs (black line) are overlaid in a histogram to show GFP expression overtime. (E) A549 permissive cell line were treated with 100ppc of EnAd-GFP. Cells were trypsinised after 24 hrs and assessed for GFP expression. Representative of n=2 independent donors.

5.3.1.1.3 Evaluating the mRNA gene expression of EnAd virus in d3iDC cells

EnAd RNA transcript expression in d3iDC had previously been assessed by nCounter on the virus panel in Chapter 4 (section 4.3.3.3). In Figure 4.5 it was shown that no transcripts were detected for EnAd except for E3. In fact, E3 levels analysed in two different d3iDC donors, were relatively high when compared to the replication-permissive cell line A549. Based on that, virus RNA transcripts were analysed again in d3iDC by RT-qPCR, with special interest on the EnAd E3 genes; 12.1kDa, 16kDa and fusion protein. Also, the E3 flanking genes 100K (E4) and fibre (L5) were analysed, as well as the E1A and hexon primer and probe used elsewhere. Accordingly, new TaqMan primer and probes were designed and validated for E3, E4 and L5 transcripts, see Material and Methods. Eventually, during the primer and probe design a putative new (n)ORF was detected on E3 with ApE software. This nORF started from an ATG at the base +6 downstream from the E3 TATA box and finished on the base +311 upstream of E3-12.1kDa gene (Figure 5.3).

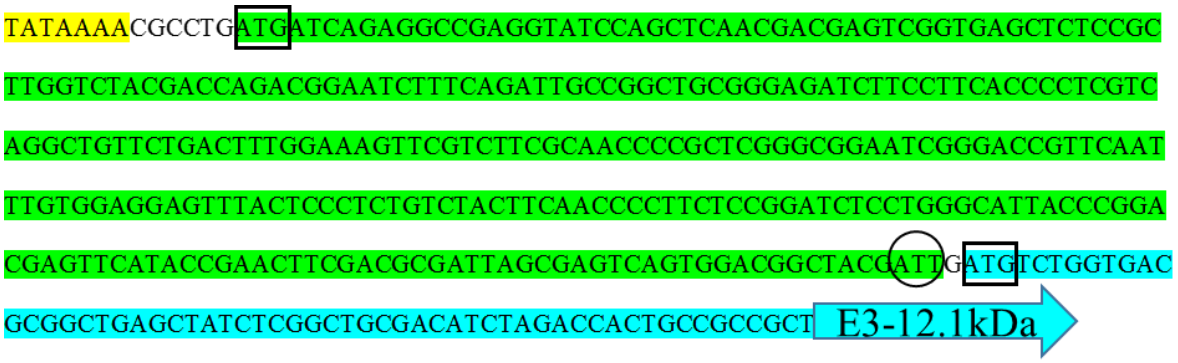


Figure 5.3 Sequence of the putative E3 nORF gene predicted by ApE software. The different features are highlighted as: yellow for TATA box, green for nORF and blue for a portion of 12.1kDA. Transcription initiation codon are indicated in boxes and stop codon in circles.

E1A, L3, L4 and L5 were under the limit of detection of the assay. On the other hand, all E3 mRNA transcripts nORF, 12.1kDa, 16kDa and fusion were detected at significant levels (Figure 5.4). On one hand, this confirmed that EnAd had no mRNA transcription in d3iDC except for E3 as previously seen by nCounter, which will be further evaluated in a section

below. On the other hand, it was fair to believe that RIG-I, a PRR previously described to sense virus ssRNA[240,241], could sense the E3 mRNA transcripts and be responsible for the improved d3iDC stimulation.

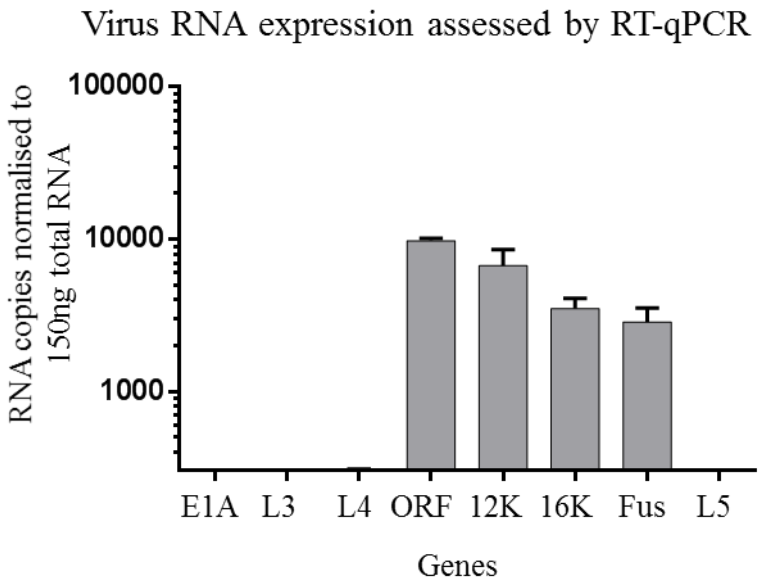


Figure 5.4 Assessment of EnAd RNA transcripts expression in d3iDC by RT-qPCR. d3iDC were infected with 500ppc EnAd. After 18 hrs, RNA was extracted with in-solution DNAse-treatment from lysed cells, concentration determined by Nanodrop and adjusted to 150 ng/µl. Two step RT-qPCR (see Material and Methods) was performed to quantify cDNA copies for EnAd's E1A, L3-Hexon (L3), L4-100k (L4), E3-ORF (ORF), E3-12.1k (12K), E3-16k (16K), E3-fusion (Fus) and L5-Fibre (L5). Data are presented as average RNA copies normalised to 150 ng of total RNA and SD for technical triplicates. Representative of n=3 independent experiments.

5.3.1.1.4 Generation of a gene-inactivated EnAd virus and use for the evaluation of the virus gene expression role for stimulation of d3iDC

To investigate whether the strong pro-inflammatory and maturation phenotype induced by EnAd on d3iDC was mediated by E3 mRNA, or other virus gene expression, it would be ideal to study the effects of a gene-inactivated EnAd.

Accordingly, a method previously described to crosslink virus DNA (leading to inactivation) through UV-activated Psoralen[188], was used (see Materials and Methods). Prior to evaluating the possible involvement of virus gene products on DC phenotype, the cross-linked (CL)-DNA EnAd virus was physically characterised to ensure its physical properties were unaltered. Using

the HPLC tittering method (see Material and Methods), the number of CL-DNA EnAd virus particles were measured and the capsid integrity compared against pure EnAd stock. It can be seen, that after Psolaren-UV inactivation, EnAd elution peak remains the same as the original pure stock (Figure 5.5 A). This suggests the virus particle structure and capsid integrity is not compromised by the psoralen treatment.

Additionally, cross-linked (CL)-DNA EnAd was assessed on A549 cells for its ability to form plaque units using a 5-days infectivity assay and to express early and late viral mRNA by RT-qPCR. The extended version of infectivity assay showed that for every 10^{12} psoralen-treated virus particle less than 10-thousand plaque forming units (PFU) were seen, whereas the same amount of untouched EnAd produced more than 10^{9} PFU (Figure 5.5 B). The psoralen-treated virus also showed no early nor late mRNA expression in A549 cells infected with 100ppc of CL-DNA EnAd, whilst large number of copies were detected with untreated EnAd virus (Figure 5.5 C).

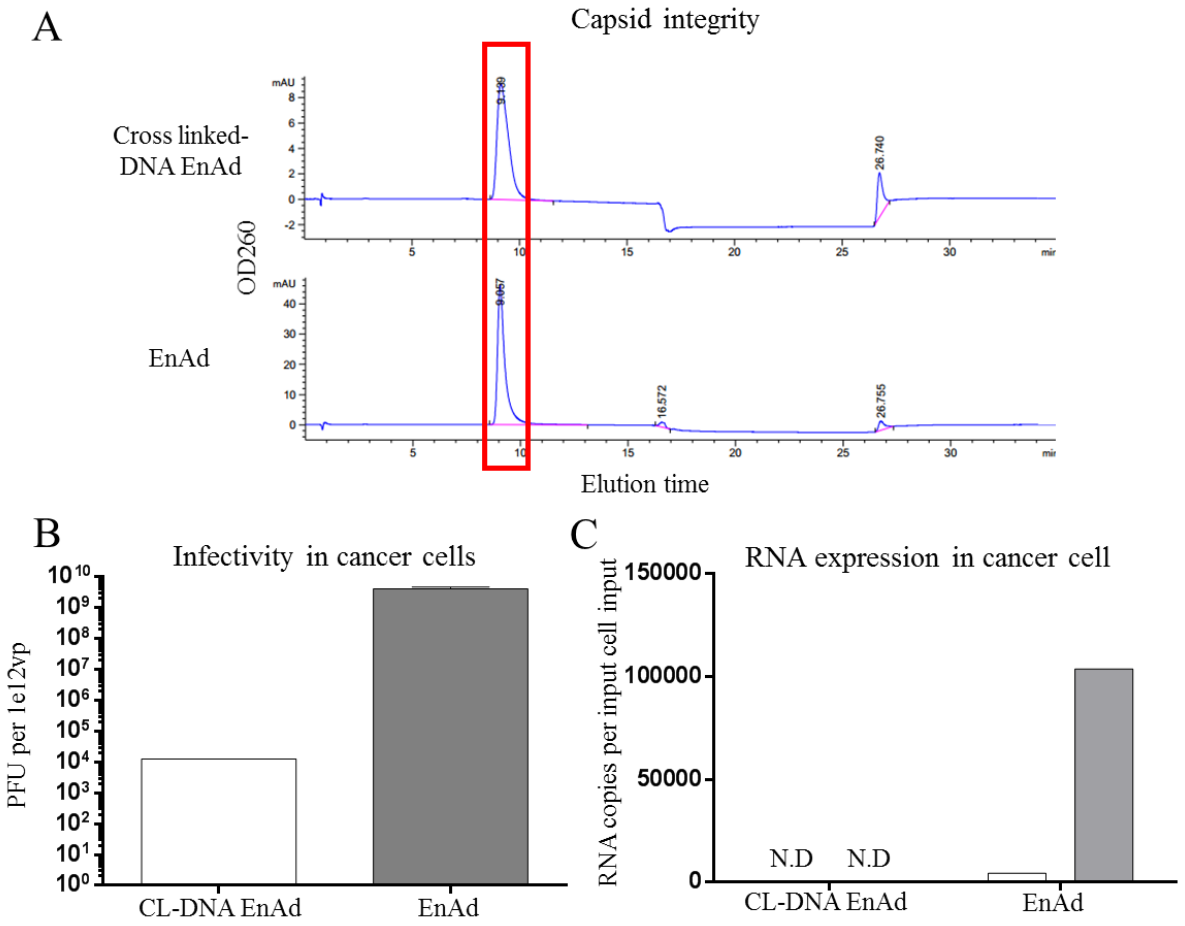
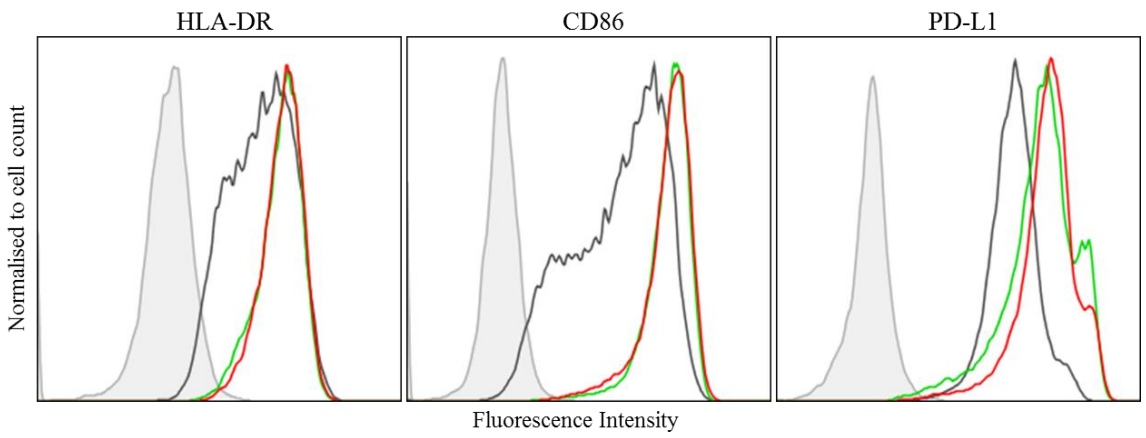


Figure 5.5 Assessment of a cross-linked (CL-)DNA Enad particles capsid integrity and life cycle. EnAd stock was mixed with 8-MethoxyPsoralen at a 0.15 mg/ml final volume, incubated in a UV-transilluminator for 2 round of 10 minutes and buffer exchanged in a desalting column. (A) Capsid integrity was assessed by comparing the elution time of OD260 peaks (red box) for CL-DNA EnAd and EnAd by HPLC (see Materials and Methods). (B) Infectivity assay (see Material and Methods), incubated for 5 days before hexon staining, was used to count PFU/well and to calculate the total PFU per 10^{12} viral particle of CL-DNA Enad (open bar) or EnAd (grey bar). Technical triplicates mean and SD were calculated. (C) Early (white) and late (grey) RNA copies were quantified by RT-qPCR in A549 cells infected for 18 hrs with 100ppc CL-DNA EnAd and EnAd. Technical duplicate averages are shown. N.D= Not-detected.

With capsid integrity apparently unchanged and the virus gene expression undetectable, the effects of CL-DNA EnAd on monocytes was compared with same virus concentration of untouched EnAd on d3iDC, by assessing the HLA-DR, CD86 and PD-L1 expression (accordingly to the timeline in Figure 4.1 A). The psoralen-treated virus appeared to up-regulate all three markers to equal MFI as the untouched EnAd particles, when assessed on the d3iDC from same donor (Figure 5.6 A).

For a better comparison of EnAd and CL-DNA EnAd, the variability from donor to donor background levels were removed by calculating the fold change in median fluorescence intensity relative to correspondent untreated controls. The relative MFIs average for HLA-DR, CD86 and PD-L1 were not significantly different between CL-DNA EnAd and untouched virus, when multiple donors were used for the comparison (Figure 5.6 B). These data suggest that E3 mRNA expression, or any virus gene expression, are not required for the maturation effects and pro-inflammatory effects of EnAd virus particles on d3iDC. Consequently, it seems likely that components of the virus capsid are probably responsible for these effects on dendritic cells.

A



B

Markers	Inactivated-EnAd fold change MFI mean ± SD	EnAd fold change MFI mean ± SD	Differences between Ad5 and EnAd relative MFI mean (*p* Value)
HLA-DR	0.857 ±0.269 (n=5)	1.156 ±0.671 (n=5)	No (0.318)
CD86	3.920 ±0.462 (n=4)	5.246 ±1.685 (n=4)	No (0.298)
PD-L1	2.023 ±1.629 (n=4)	3.485 ±1.028 (n=4)	No (0.372)

Figure 5.6 Evaluation of the effect of cross linked-DNA Enad on DC markers. d3iDC were treated with either CL-DNA EnAd (green line), untouched EnAd (red line), or left untreated (grey line). After 48 hrs, cells were stained with vital dye and monoclonal antibodies against HLA-DR, CD86 and PDL-1, and acquired by flow cytometry. (A) Representative data from one donor (of n≥4 donors) are reported as fluorescence intensity per normalised cell count. (B) The fold change in median fluorescence intensity (fold change MFI) for CL-DNA EnAd and EnAd were calculated for each donor against their correlative untreated control. The fold change MFI across donors(n≤4) were averaged, standard deviation (±SD) was calculated and both treatments compared with unpaired, two-tailed T-test.

5.3.1.1.5 Investigating whether the E3 deletion in EnAd is responsible for a stronger d3iDC stimulation

Adenoviruses encode multiple genes with immunomodulatory functions, especially in the E3 region, functioning to prevent fast clearance by an anti-viral immune response. This field has been comprehensively reviewed by Lichtenstein[107]. It was hypothesised that the nearly complete loss of E3 would mean that EnAd lacks genes that control cellular immune responses, leading to the observed effects on d3iDC. Therefore, EnAd-treated d3iDC were immunophenotyped for CD86 and HLA-DR using the same timeline described in Figure 4.1, and compared to cells treated with Ad11p (which has an intact E3 region). The flow cytometric analysis, using two independent donors, showed no-differences for HLA-DR and CD86 fluorescence intensity between EnAd- and Ad11p-treated d3iDC (Figure 5.7). This suggests that the lack of E3 genes does not account for EnAd's ability to activate the d3iDC.

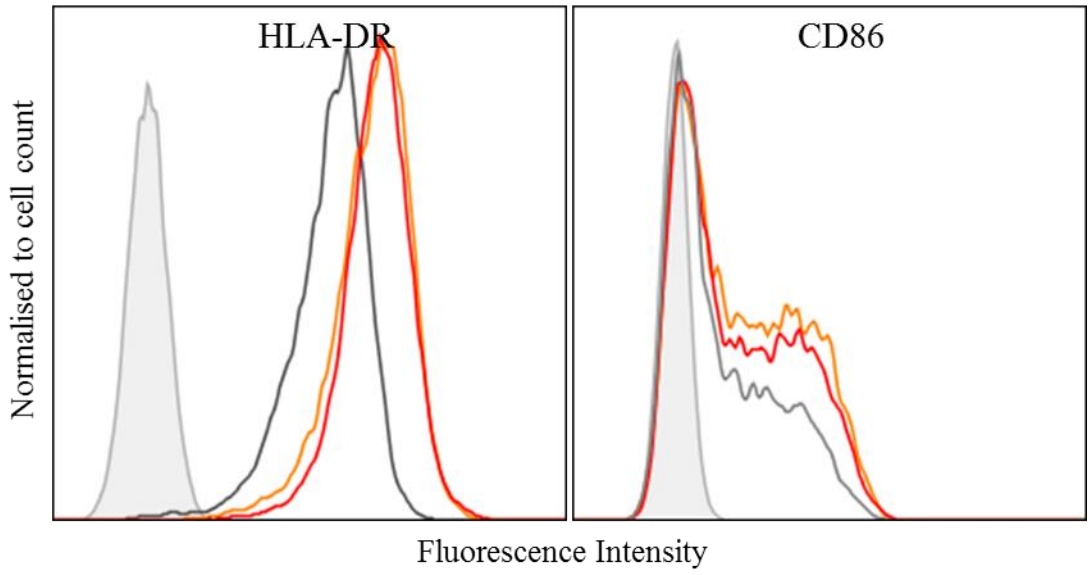


Figure 5.7 Comparison of EnAd and Ad11p virus particle effect on DC immunophenotype. d3iDC were treated with 200ppc Ad11p (orange line), EnAd-treated (red line) or left un-touched (black line). After 48 hrs, cells were stained for HLA-DR and CD86 – or correspondent isotype (solid grey) – and acquired by flow cytometry. Representative data are reported as fluorescence intensity per normalised cell count for two independent experiment.

5.3.1.2 Investigating whether the superior adjuvant effect of EnAd virus on d3iDC is virus particle-mediated

The data in the previous sections suggest that neither virus products, E3 deletion nor viral gene expression were related to the improved pro-inflammatory effect of EnAd (compared to Ad5) on d3iDC. Instead, the DNA-inactivated virus, Ad11p virus – which shares same outer capsid as EnAd– and EnAd virus particles all induced the same adjuvant effects on d3iDC, suggesting that the physical properties of the virus particles were probably responsible for the stronger DC stimulation. Adenovirus capsid proteins and DNA have previously been asserted to have immunogenic properties when sensed by pattern recognition receptors[242,243], and in some cases by direct signalling upon receptor attachment[243]. In fact, EnAd (and Ad11p) and Ad5 had capsid differences that could potentially explain the observed differential effects on DCs[244]. In this section, capsid proteins and DNA differences were investigated.

5.3.1.2.1 Investigating the contribution of the virus capsid on d3iDC stimulation

The general composition and structure of human Adenovirus particles are similar across most serotypes: the main capsid proteins like hexon, penton and fibre proteins assemble together and interact with other less-exposed minor components that hold the capsid together (cement proteins). Comparing the sequence identities of EnAd (or Ad11p) and Ad5 capsid proteins (using ExPASy software, from Swiss-Prot), displayed large protein fidelity between the two serotypes (Table 5.1). However, the fibre, which is the major component involved in initial cellular attachment, was the protein showing the least identity between these serotypes, 39.5% (Table 5.1).

Position in capsid	Virus protein	EnAd aa length	Ad5 aa length	Protein sequence identities
Cement	pIIIa	587	585	74.70%
	pVI	246	250	64.60%
	pVIII	227	227	79.70%
	pIX	139	140	50.00%
External	Penton	561	571	69.70%
	Hexon	948	952	76.70%
	Fibre	325	581	39.50%

Table 5.1 Comparison of the aa sequence of capsid proteins from EnAd and Ad5 virus. pIIIa, pVI, pVIII, pIX, penton, hexon and fibre aa sequence of Ad11p – which genomic sequence is identical to EnAd (see introduction) – and Ad5 were obtained from the national centre for biotechnology information (NCBI), corresponding with accession number: AY_598970 and AC_000008, respectively. Length and protein sequences identities were compared between both viruses using ExPASy software (SwissProt).

Fibre proteins from Ad5 and Ad11p are known to have different receptor specificity; whereas Ad5 bind the Coxsackievirus and adenovirus receptor (CAR), Ad11p (and EnAd) bind both CD46 and desmoglein-2 (DSG-2). In previous reports, another group B adenovirus Ad35, which also binds to CD46 but not DSG-2, was shown to be a better DC stimulant than Ad5[228]. It was therefore hypothesised that the greater receptor divergence could contribute to EnAd's improved stimulation effect on d3iDC. Therefore, the expression of these receptors on the surface of d3iDC model was analysed by flow cytometry. Using a FITC-conjugated anti-CD46 antibody, CD46 was shown to be highly expressed on 99.2% of d3iDC (Figure 5.8 A). On the other hand, CAR and DSG-2, stained with primary and PE-conjugated secondary antibodies, showed florescence intensity equal to cells stained only with secondary antibody, showing that both receptors were not expressed on d3iDC cells (Figure 5.8 B and C). That observation led the focus on the role of the EnAd fibre binding to CD46 in stimulation of d3iDC.

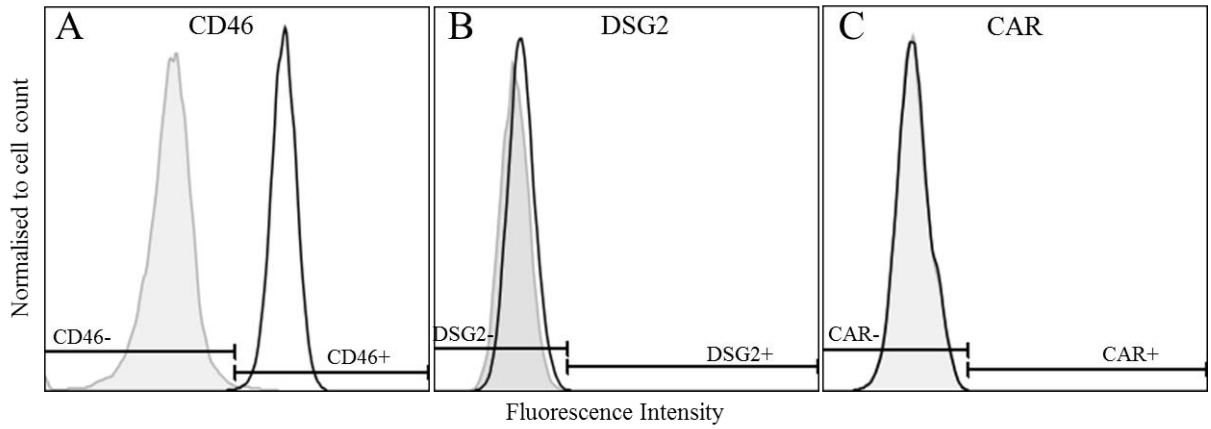


Figure 5.8 Evaluation of CD46, DSG2 and CAR expression on d3iDC cell surface. d3iDC were directly labelled with (A) monoclonal anti-CD46-FITC antibody (black line), or corresponding isotype (solid grey). Alternatively, d3iDC were labelled with (B) primary anti-DSG-2 antibody (black line) or (C) primary anti-CAR antibody (black line), followed by a secondary anti-mouse-PE antibody, cells were also stained with anti-mouse-PE antibody alone as control (solid grey) (see Material and Methods). Cells were acquired by flow cytometry and isotype staining were used to establish CD46+, DSG-2+ and CAR+ populations.

5.3.1.2.1.1 Investigating the EnAd fibre-CD46 interaction role in d3iDC stimulation

CD46 is a transmembrane protein, comprised of 4 extracellular splicing isoforms that can combine with 2 intracellular isoforms[245]. Upon CD46-crosslinking, the intracellular domain can be phosphorylated and induce a signalling cascade using intermediate proteins[246]. However this has only been shown in T cells[247]. It was therefore investigated whether EnAd signalling through CD46 could explain the strong d3iDC stimulation. A CD46-pulldown (by immunoprecipitation) and western blot (WB) was used (see Materials and Methods), detecting at least two isoforms of CD46 between 65kDA and 50kDa on d3iDC (Figure 5.9 A, Bottom). However, no phosphorylation could be detected on CD46 immune precipitated from d3iDC incubated for 5 or 20 minutes with EnAd. Equally, no phosphorylation was seen with phytohemagglutinin (PHA), a broad unspecific cross-linker of sugars from glycosylated proteins. Whereas large phosphorylation could be seen in the no-IP sample (Figure 5.9 A, Top). Others had previously induced CD46 signalling on T cells using anti-CD46 antibodies[248]. Alternatively, cell surface CD46 was cross-linked with antibodies binding to the same CD46

domain as EnAd, to investigate whether the greater d3iDC stimulation by EnAd was a result of CD46 clustering and signalling stimulated by attachment of multiple fibres of the virus. Consequently, it was first necessary to find an antibody that would bind to either CD46's short consensus repeats (SCR)1 or SCR2. These two domains are known to mediate the attachment with Ad11p fibre knob[249,250]. E4.3 (BD Biosciences PharMingen) and M177 (SantaCruz) anti-CD46 clones were identified from a previous publication[251] and tested in a competition assay with total virus genomes copies as readout. M177 significantly decreased more than 10-fold the amount of cell-associated virus genomes, whereas E4.3 clone genomes copies were the same as EnAd without Ab (Figure 5.9 B). This suggests that the M177 antibody binds to the same site as EnAd and outcompetes virus binding.

In turn, M177 clone was used to crosslink CD46 on d3iDC, and further clustered with a secondary anti-mouse IgG1 antibody (BioLegend). Additionally, cells were treated with EnAd or left untreated. After 48hrs, cells were assessed for HLA-DR, CD86 and PD-L1 expression by flow cytometry. However, cells in which CD46 had been clustered with antibodies, did not up-regulate any of the assessed DC stimulation markers, and were comparable to untreated d3iDC. Whereas EnAd-treated DCs did show increased HLA-DR, CD86 and PD-L1 expression (Figure 5.9 C). Hence, no-evidence was found to support with this approach that CD46 signalling might be involved in the greater d3iDC stimulation by EnAd.

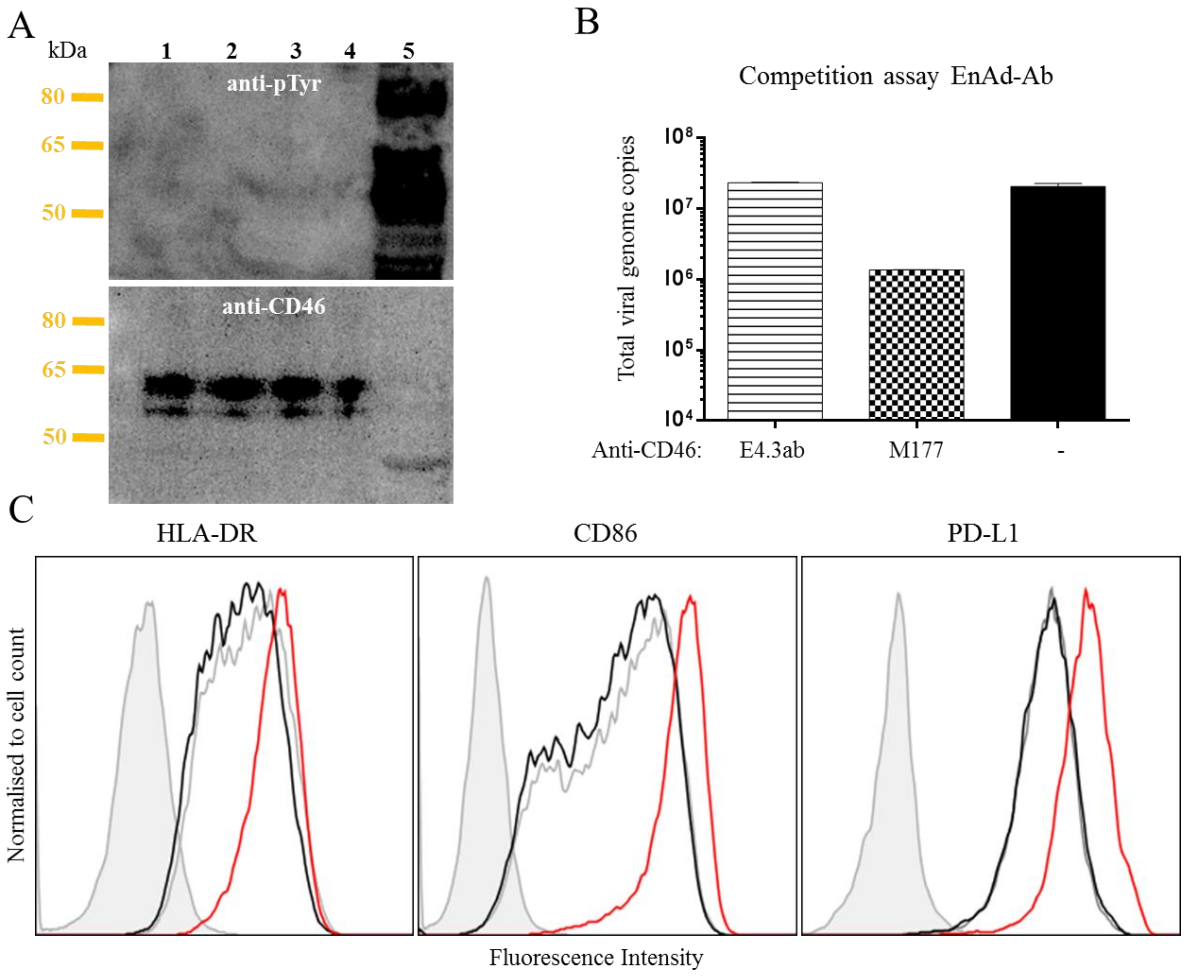


Figure 5.9 CD46 signalling involvement in day3 iDC maturation. (A) d3iDC treated for 5 (3) or 10 (4) minutes with either 500ppc EnAd, 10 µg/ml PHA (2) or left untreated (1), lysates were CD46 immunoprecipitated. Untreated lysate control (5) and immunoprecipitates were detected by western blot analysis with (top panel) anti-phosphotyrosine HRP antibody (pTyr) and, after strip-wash, with (bottom panel) anti-CD46 antibody. (B) Monoclonal anti-CD46 antibodies were used in a competing assay against EnAd. Pre-treated d3iDC with either 5µg/ml of E4.3 or M177 clone were exposed to EnAd virus. Shortly after, cells were thoroughly washed and DNA extracted to quantify total viral genome copies by qPCR. Average and SD of technical replicates were calculated. (C) DCs were treated with 1 µg M177 Ab and further crosslinked with anti-mouse IgG secondary antibody (black line), EnAd-treated (red line) or left un-touched (grey line). After 48hrs, cells were stained with vital dye and monoclonal antibodies against HLA-DR, CD86 and PDL-1 – or correspondent isotype (solid grey) – and acquired by flow cytometry. Representative data are reported as fluorescence intensity per normalised cell count for two independent experiments.

Based on the inability of M177 clone to stimulate d3iDC cells, the Ab was used in a CD46 blocking assay to prevent EnAd interacting with the receptor on the cell surface and then cell activation was assessed using the stimulation markers developed earlier. For this, the d3iDC were pre-cultured with M177 clone or its isotype, then temporarily treated with EnAd. After 48hrs, cells were assessed for HLA-DR, CD86 and PD-L1 expression by routine flow cytometry. Anti-CD46 blocking antibody appeared to be very effective to prevent the up-regulation of all three markers induced by EnAd, resulting in similar fluorescence intensity levels to un-treated d3iDC. On the other hand, cells that were pre-treated with the isotype control antibody and then with EnAd showed up-regulation of HLA-DR, CD86 and PD-L1 (Figure 5.10).

Altogether, the data indicated that EnAd virus particles achieved d3iDC stimulation following from its binding to CD46, however receptor signalling could not be demonstrated.

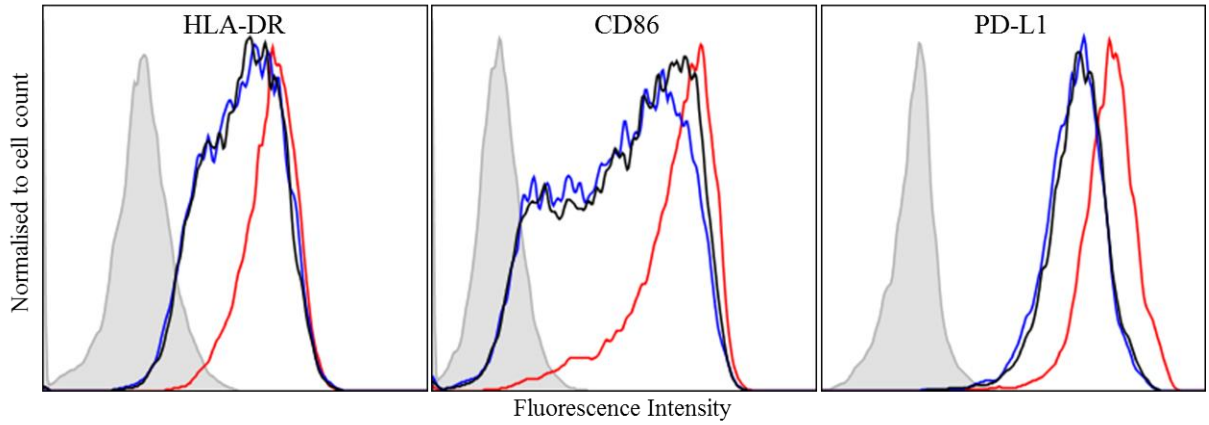


Figure 5.10 Assessment of the effect of EnAd particle on DC markers on d3iDC pre-treated with CD46 blocking antibody. Both 1 µg M177 antibody pre-treated d3iDC (blue line) and un-touched DC (red line), were briefly exposed to 500ppc of EnAd and compared to untreated DC (black line). After 48 hrs, cells were stained with vital dye and monoclonal antibodies against HLA-DR, CD86 and PDL-1 – or correspondent isotype (solid grey) – and acquired by flow cytometry. Representative data are reported as fluorescence intensity per normalised cell count for two independent experiment. Shown are representative of two independent experiment.

5.3.1.2.1.2 Assessing the adenovirus DNA as a PAMP in d3iDC

The adenovirus DNA is described as the most important pathogen-associated molecular pattern of the virus particles components. The adenovirus DNA can be recognised by multiple pathogen recognition receptors, leading to strong innate responses[104]. Based on the expression of CD46 and the lack of CAR on d3iDC surface (as seen in Figure 5.8), it was hypothesised that EnAd particles should be advantageously up-taken by d3iDC cells compared to Ad5. Subsequently higher numbers of intracellular DNA copies of EnAd should be expected, triggering more PAMPs and resulting in greater DC stimulation.

A comparative study between Ad5 and EnAd was performed to quantify the genomes associated per d3iDC. And to assess the relevance of CD46, cells were pre-cultured with M177 clone blocking antibody or its isotype. The results showed significant differences in virus-genomes associated with cells. More than 10-fold increase of EnAd genome copies were seen compared to Ad5 when cells were treated with the isotype. Additionally, the M177 significantly diminished approximately 10-fold the number of EnAd genome copies compared to cells pre-treated with isotype. Interestingly, although relatively higher without statistical significance, EnAd genome copies on cells pre-treated with M177 blocking antibody, were at similar levels to Ad5 in either M177 or isotype pre-treated cells (Figure 5.11). This suggested that EnAd had an advantageous cell-uptake relative to Ad5 thanks to CD46 receptor expression on d3iDC.

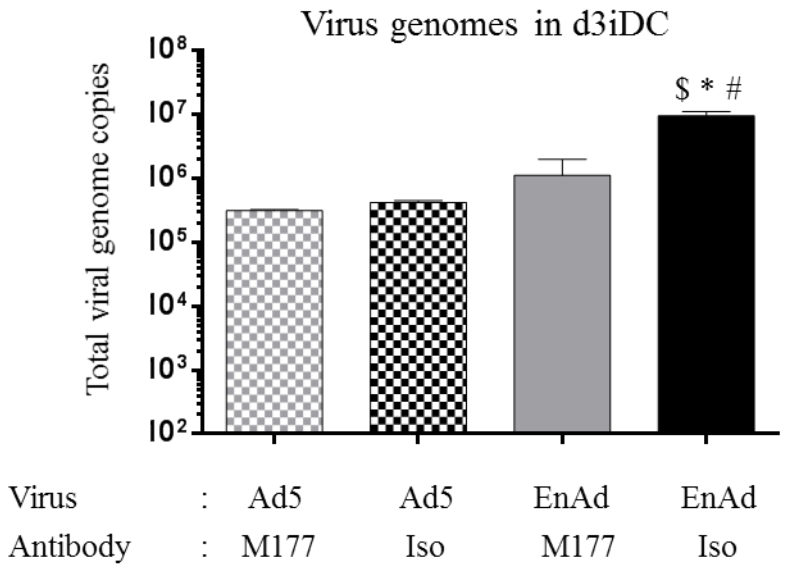


Figure 5.11 Quantification of EnAd and Ad5 genomes in d3iDC pre-treated with CD46-blocking antibody. d3iDC were pre-treated with either 1 µg M177 ab or 1 µg of correspondent isotype, later exposed to either Ad5 or EnAd. Shortly after, cells were thoroughly washed and DNA extracted to quantify total viral genome copies by qPCR. Average and SD of technical triplicates was calculated before the treatment mean were compared by one way Anova. The groups identified with ANOVA to be significantly different were individually compared with un-paired T-test. EnAd/Iso is significantly different to EnAd/M177 (#p=0.0011), Ad5/Iso (*p=0.0005) and Ad5/M177 ($p=0.0005). Representative of n=2 independent experiment.

Strangely adenovirus DNA, even though it is made in mammalian cells, is not properly methylated and so can trigger the endosomal TLR-9 pattern recognition receptor[252], stimulating strong pro-inflammatory responses. Furthermore, CpG's prevalence appears to be heterogeneous across adenovirus serotypes. Also, CpG in adenovirus can be of two sorts: stimulatory (CpG-S), which promotes the TLR9 signalling cascade, and neutralising (CpG-N), which antagonise the former. The overall CpG S to N ratio can also be variable between adenovirus and has been linked to immune-stimulatory differences between serotypes[252]. Here, putative CpG-S and CpG-N hexamers previously described by Krieg *et* al.[252] were counted and compared between EnAd and wildtype Ad5. Both Ad5 and EnAd viruses appeared to have similar total numbers of stimulant hexamers, 17 and 16 respectively. This also translated into consistent CpG-S frequency – calculated by dividing the CpG-S numbers to their respective genome length, Ad5=35.9kb and EnAd=32.0kb. On the other hand, Ad5 accounted for more

neutralising CpG than EnAd. The overall number of CpG-N and frequency in Ad5 were both 2-fold higher than EnAd (Table 5.2). Therefore, and based on previous reports, the DNA from EnAd is likely to be less neutralising of TLR9 than Ad5, probably inducing better pro-inflammatory stimulation.

Overall, the specificity of EnAd fibre for CD46 receptor, and the expression of this receptor appears to be key for a greater up-take of the virus into d3iDC compared to Ad5. Which probably use other less specific pathways, as CAR receptor was not detected. Therfore, it was speculated that EnAd provides more available virus PAMPs in the cell, and together with a less balanced CpG profile of EnAd, result into greater PRR stimulation that can explain the phenotype in d3iDC.

CpG type	Hexamer	Adenovirus 5		EnAdenotucirev	
		Number	Frequency (‰)	Number	Frequency (‰)
Neutralising	GCGCGC	55	1.5304	14	0.4347
	GCGGCG	100	2.7826	35	1.0867
	GGCGGC	101	2.8104	30	0.9314
	CGCGCG	11	0.3061	12	0.3726
	GCCGCC	27	0.7513	30	0.9314
	CGCCGC	35	0.9739	34	1.0556
	Overall	329	9.1547	155	4.8123
Stimulatory	GACGTT	13	0.3617	13	0.4036
	AACGTT	4	0.1113	3	0.0931
	Overall	17	0.4730	16	0.4968

Table 5.2 Stimulatory and neutralising CpG expression in Ad5 and EnAd virus genomes. Neutralising (N)-CpG; GCGCGC, GCGGCG, GGCGGC, CGCGCG, GCCGCC and CGCCGC, or stimulatory (S)-CpG; GACGTT and AACGTT, hexamers sequences were obtained from Krieg, A. M. *et al.* (1998)[253]. The hexamers were quantified on both DNA strands of wildtype Ad5 (AC_000008.1, NCBI) and EnAd genome sequence using the ApE software. The frequency relative to genome length – 35938bp for Ad5 and 32206bp for EnAd – were calculated for each individual hexamer and overall N-CpG or S-CpG.

5.3.2 Evaluating the role of NF-kB for the expression of EnAd E3 mRNA in d3iDC cells

The Ad5 E3 promoter has NF-1, K2, K1, AP-1 and ATF binding sites where viral or cellular factors associate for a constitutive E3 transcription during virus replication in permissive cells. All these binding sites were also found with high homology in EnAd/Ad11p E3 promoter (Figure 5.12). Interestingly, NF-kB complex binds to K1 and K2 sequence, selectively inducing E3 transcription[254]. Since NF-kB is activated by multiple PRR signalling pathways and adenovirus have been shown to promote NF-kB translocation in DCs[255], it was here hypothesised that EnAd virus was sensed by d3iDC's PRRs, with the consequent nuclear translocation of NF-kB and selective expression of the immunomodulatory E3 mRNA previously measured (Figure 4.5 andFigure 5.4).

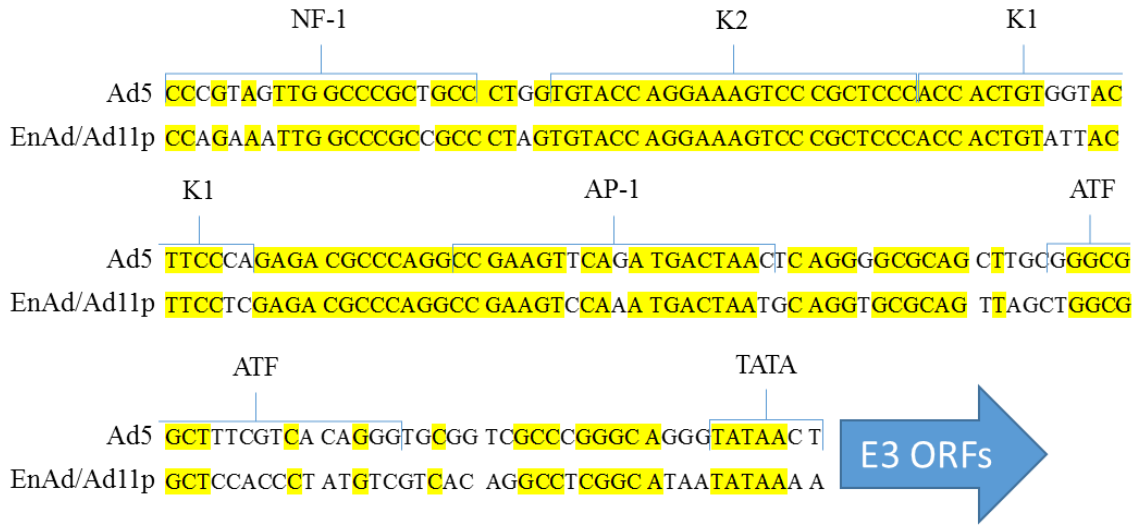


Figure 5.12 Alignment of Ad5 and EnAd (Ad11p) E3 promoter sequence. Previously described NF-1 K2, K1, AP-1, ATF binding sites and TATA box from Ad5 E3 promoter were identified on the Ad5 genome using ApE software. Ad5 E3 promoter was aligned with EnAd and Ad11p E3 promoter, and consensus base pairs are highlighted in yellow.

NF-kB is a complex of multiple proteins which are expressed from NFkB1, NFkB2, RelA RelB and c-Rel genes. These genes are inducible by a positive feedback loop, meaning that NF-kB activation induces transcription of these genes[256]. Interestingly, using the data from nCounter transcriptome study, it was found that the mRNA of REL and NFkB families were up-regulated in d3iDC treated with EnAd or Ad5 (Figure 5.13 A).

Additionally, the THP1-lucia cell line, a monocytic cell line containing a cassette with luciferase gene in which transcription is controlled by NF-kB promoters, was used to assess whether EnAd induced NF-kB activation on innate cells. Firstly, the expression of CD46 was assessed by flow cytometry. All THP1-lucia cells appeared to express CD46 receptor on the cell surface (Figure 5.13 B). Later, THP1-Lucia was cultured with EnAd virus or CD46 crosslinked with M177 antibody with a secondary antibody. Forty-eight hours later luciferase expression was assessed in the cell supernatant according to manufacturer's protocol. The luciferase expression, which was calculated as fold change relative to untreated cells, was nearly 2-fold higher than untreated or than CD46-crosslinked cells (Figure 5.13 C).

Altogether, the increase of mRNAs of NF-kB subunits and the 2-fold increase of luciferase expression mediated by EnAd in d3iDCs and THP1-lucia cells respectively, suggested that NF-kB is probably activated by the virus.

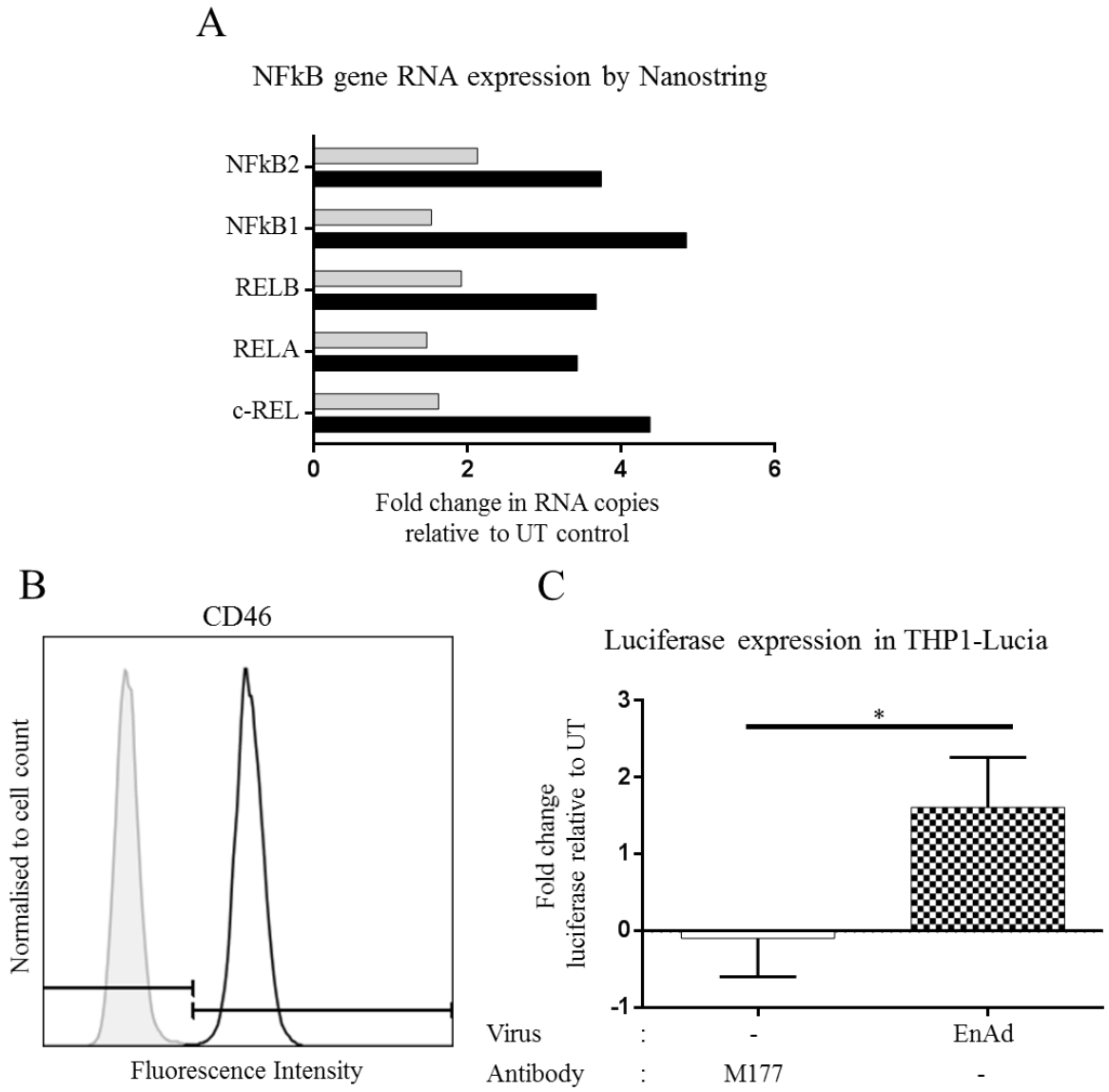


Figure 5.13 Assessment of NF-kB activation by EnAd in DC. (A) d3iDC exposed to Ad5 (grey) or EnAd (black), or left untreated. After 18 hrs, RNAs were extracted with in-solution DNAse-treatment from lysed cells. RNA concentrations were determined by Nanodrop and adjusted to 150 ng/µl. A 800-wide pre-designed panel for Nanostring was used to quantify copies of target-RNA in samples. Data from one donor are represented as fold change in RNA copies relative to untreated for Rel, RelA, RelB, NFkB1 and NFkB2 genes, representative of two different donors. THP1-Lucia monocytic cell line (Invivogen) was grown according to manufacturer's recommendation, (B) before CD46 expression was assessed by flow cytometry. (C) Alternatively, THP1-Lucia were exposed to 500ppc EnAd, 1 µg M177 antibody cross-linked with secondary antibody or left untreated in biological triplicates. Cell supernatant was assessed for luciferase levels after 48 hrs in microplate photometer in technical triplicates, according to manufacturer's protocol. Technical replicates were averaged and fold change in luciferase relative to untreated control were calculated. Fold change mean and SD for biological replicates are plotted, both treatments compared with unpaired, two-tailed T-test. Representative of n=2 experiments.

Based on the previous observation in this section, it was then interrogated whether E3 mRNA expression could be further enhanced in d3iDC by artificially enhancing NF-kB phosphorylation. Lipopolysaccharide (LPS) has previously been described as a good inducer of NF-kB translocation, upon TLR4 stimulation. Accordingly, d3iDC were treated with EnAd briefly before stimulating cells with LPS. Later cells were used for E3 mRNA quantification by RTqPCR as well as virus genome copies by qPCR. d3iDC cells treated with LPS showed a significant 5-fold increase in E3 mRNA copies compared to cells only treated with virus. Again, the flanking genes L4 and L5 were under the limit of detection (Figure 5.14 A). On the other hand, LPS treatment did not appear to change the virus the number of virus genome copies associated to cells, as same numbers were recovered either with or without LPS (Figure 5.14 B). This shows that a well-established NF-kB inducer like LPS can significantly increase the E3 expression in d3iDC, and lends support to the notion that the E3 expression documented in the absence of LPS may also be a result of NF-kB activity.

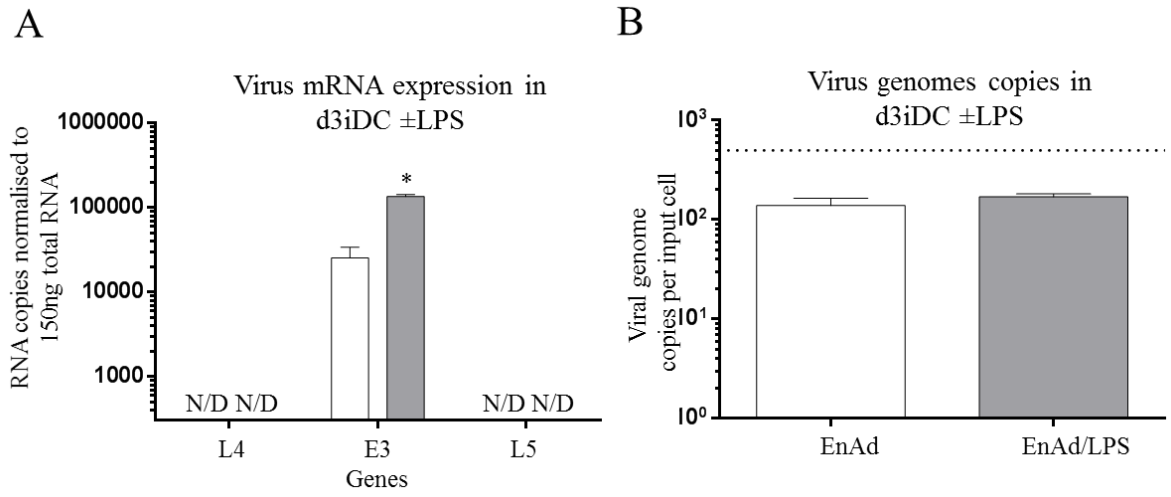


Figure 5.14 E3 expression enhancement in LPS treated DC. (A) d3iDC were exposed to 500ppc EnAd and thoroughly washed briefly after, cells were cultured in plain medium (white bars) or supplemented with 0.1 µg LPS/ml (grey bars). After 18 hrs, DNA was isolated followed by RNA extraction with in-solution DNAse-treatment. A) Two step RT-qPCR (see Material and Methods section) was performed in technical duplicates to quantify cDNA copies for EnAd's E3-12.1k (E3). Data are presented as total cDNA copies average from biological triplicates from one donor. (B) Alternatively, viral genome copies were quantified in technical duplicates by qPCR from DNA samples. Data are presented as viral genomes per input cell mean and SD for biological triplicates from one donor, both treatments compared with unpaired, two-tailed T-test. Statistical differences E3 genes no LPS/ E3 genes+LPS, *p<0.0001

5.4 Chapter summary

1. The inactivation of EnAd virus particle DNA with psoralen and UV light prevents virus growth and mRNA gene expression.
2. The stimulatory activity of psoralen/UV DNA-inactivated virus suggests no gene expression is implicated in the improved ability of EnAd to stimulate d3iDC. Neither is the E3 deletion implicated, as EnAd and Ad11p particles mediate the same levels of stimulation.
3. CD46 is expressed on d3iDC, whereas DSG2 and CAR are not. CD46 blocking antibody prevents EnAd inducing d3iDC stimulation, although no CD46 signalling could be demonstrated in these cells. EnAd virus has a 10-fold greater binding to d3iDC than Ad5, and this can be prevented with the CD46 blocking antibody.
4. Although EnAd and Ad5 had similar stimulatory CpG motifs in their genome, Ad5 accounts for 2-fold more neutralising CpG.
5. EnAd-CMV-GFP virus is taken up by d3iDC, however no-trace of virus cycle can be detected, except for a specific E3 mRNA expression. E3 is likely to be regulated by inflammation-related transcript factor NF-kB, which is induced by the virus itself.

5.5 Chapter discussion

5.5.1 Discussion of results

Based on the observation from Chapter 4, where EnAd particles appeared to be a better stimulant of d3iDC cells than Ad5, the current chapter sought to understand the underlying mechanisms responsible for the improvement. This was interrogated in two sections, whether it was mediated by virus-encoded genes or by features of the virus particle.

In the virus-encoded section, it was first hypothesised that the dysregulated life cycle of EnAd seen in chapter 3, could have rendered this virus able to replicate in DCs, hence providing a growing concentration of virus components, like DNA, RNA and proteins, largely described as PAMPs as reviewed by U.F. Greber *et* al.[104]. However, no evidence of virus DNA replication or protein expression were seen (Figure 5.1 and Figure 5.2). Additionally, most the mRNA transcripts were undetectable, with the exception of the E3 genes (Figure 5.4). It was then hypothesised that the detection of viral mRNA could be sensed by RIG-1 leading to DC stimulation. However, a DNA cross-linked EnAd, unable to express viral RNA transcripts nor replicate in permissive cell line (Figure 5.5), induced the same stimulation than EnAd on d3iDC (Figure 5.6).

Interestingly, E3 genes in adenovirus have immune-regulatory functions[107]. Thus, the selective expression in d3iDC, led to the hypothesis that the large E3 deletion in EnAd genome could render this virus less capable to control the immune response in infected d3iDC compared to other adenoviruses with whole E3. However, using Ad11p, which encodes the full E3 transcript, produced the same stimulatory effect as EnAd (Figure 5.7). Altogether, no evidence was found to support virus-encoded genes were involved in modulating the stimulation of d3iDCs, rather points the evidence towards a particle effect, as Ad11p and DNA-inactivated virus shared particle physical properties with EnAd.

Despite human adenoviruses have common capsid structure and genomic organisation[65], some differences were identified between EnAd and Ad5. In this case the most prominent difference between EnAd and Ad5 virus were their cellular receptor, CD46/desmoglein-2 and CAR respectively[244]. Desmoglein-2, likewise CAR, have specialised cell-to-cell adhesion function and have a specific distribution mostly within epithelial tissues[257,258]. Although, dermal DCs can express CAR, the majority of other DC subtypes have been described with limited or inexistent expression[259], including here the d3iDC model (Figure 5.8). On the other hand, CD46 is involved in complement inactivation to protect the host cell damage, therefore its broadly distributed across all human cells surface[245], and also found on d3iDC cells (Figure 5.8). A simple experiment using the M177 antibody – a blocking anti-CD46 antibody which binds the same SCR1 and SCR2 domain as Ad11p[249] – on d3iDC made EnAd struggle to stimulate d3iDC (Figure 5.9), likewise previously seen with Ad5. This suggested the adjuvant effect of EnAd virus particles on d3iDC was CD46 dependent.

CD46 mRNA can be processed into multiple isoforms by alternative splicing, however, only two different intracellular domains have been characterised, CYT1 and CYT2, seemingly co-expressed at once[245]. Mostly reported in T cells, each of the two domains can interact with intracellular adaptor proteins involved in signalling pathways. However, CYT2 is the only isoforms with a tyrosine that can be phosphorylated[246]. Some pathogens can induce its phosphorylation leading to signalling, for instance type IV pili of *Neisseria gonorrhoeae*[260]. Here, the western blot showed multiple isoforms were expressed in d3iDC, however no-phosphorylation was detected on CD46 upon EnAd binding nor poly-reactive PHA (Figure 5.9). Since the detection of phosphorylated proteins can sometimes be complicated, CD46 signalling involvement in d3iDC plasticity was investigated otherwise. The receptor was cross-linked using an anti-CD46 monoclonal antibody (clone M177) and further clustered with an anti-primary Ab. But neither this indirect approach seemed to suggest CD46 signalling

mediated the d3iDC stimulation (Figure 5.10), and rather other components from virus were responsible. Furthermore, the monoclonal antibody (M177) reduced EnAd's binding capacity with d3iDC to Ad5 and isotype control levels. More precisely, d3iDCs pre-treated with CD46 blocking antibody resulted in 10-fold reduction in EnAd virus associated per cell, compared to d3iDC without CD46 blockade (Figure 5.9 and Figure 5.11), matching previous reports of CD46-binding Ad35 with better uptake rates compared to Ad5[228]. It was fair to believe then that CD46 blockade on d3iDC prevented EnAd from its advantageous up take over CAR-dependent Ad5. Probably leaving EnAd to a less efficient main-stream adenovirus engulfment pathways [259], and with it fewer virus components to trigger maturation.

Multiple mechanisms have been proposed to sense adenovirus's PAMPs components, mainly DNA and RNA. Initially, recognition happens during endosomal uptake. Free viral DNA strands from disrupted capsids are sensed by TLR-9 pattern recognition receptor, which, through the MyD88 adaptor protein, leads to activation of IRF7 and IRF5 transcription factors[261]. Unmethylated CpG dinucleotides are the main TLR-9 ligand and strangely adenovirus DNA, even though it is made in mammalian cells, is not properly methylated and so can trigger the endosomal TLR-9[252]. However, it was in adenovirus the distinction between stimulatory (-S) and neutralizing (-N) CpG, was made for first time. CpG-N can override the T_H1-like function that CpG-S drives[252]. Here, although both EnAd and Ad5 virus had similar putative CpG-S numbers, it could be speculated that Ad5's weaker plasticity on d3iDC can be explained by its 2-fold higher CpG-N motif frequency (Table 5.2).

Alternatively, viable particles escape the endosomal compartment, later revealing the virus and viral DNA complexes to the cytosolic compartment. At this stage, viral DNA can be sensed via AIM2 and p204 triggering STING/TBK1 cascade that in turn promotes IRF3 dimerization and translocation to the nucleus[262]. Also, RNA polymerase III transcribes dsDNA rich in dA-dT domains, like the small virus-associated RNAs (VA-RNAs) encoded in adenovirus genome,

and generates RNA transcripts that engage the RNA-I/IPS pathway, leading to IRF3 activation[263]. Consequently, the stronger modulation of EnAd on d3iDC might simply be down to advantageous up-take kinetics due to expression of EnAd's CD46 main receptor, providing more PAMP blocks than Ad5 and feeding the various adenovirus PRR sensing pathways. This, together with the lower CpG-N frequency, should translate into the better d3iDC stimulation seen for EnAd virus particle versus Ad5 and explain why lower doses of EnAd were more effective, as shown in Chapter 4.

Infectious agents inducing strong maturation and pro-inflammatory responses on innate cells might seem counterintuitive, but the fact that EnAd was capable to express immunomodulatory E3 genes in d3iDC (Figure 5.4), likewise Ad11p and Ad5 (not shown), might explain EnAd's phenotype. In fact, Ad5 had previously been reported for selectively expressing E3 in resting T cells[264]. Again, in Ad5, several NF-kB binding sites up-stream the E3 TATA box, were identified to strongly associated with NF-kB transcription factor[264-266]. These binding sites were highly conserved in Ad11p and EnAd (Figure 5.12). It was interesting to note that NF-kB complex acts as a central mediator of the inflammatory responses, where many pathogen recognition receptor signalling converges to[267]. Consequently, it was fair to believe that adenovirus could expressed E3 transcripts in d3iDC.

Multiple PRR signalling cascades phosphorylate the inhibitor of kB (IkB) – the inhibitory unit of NF-kB complex – leading to its release from the NF-kB complex. Free NF-kB transcription factor translocates into the nucleus, activating the expression of inducible genes[256]. Some of these genes appeared to be induced by EnAd on d3iDC, such as IL-6 and ICAM (Figure 4.2), suggesting that EnAd probably induced NF-kB activation. Further evidences with the transcriptome study supported that both EnAd and Ad5 viruses might activate NF-kB, as an increase of RELs and NFKBs transcripts were seen (Figure 5.13). The transcription of these genes are induced by translocation of NF-kB, as a positive self-regulation mechanism[256].

Additionally, EnAd induced luciferase expression in THP1-Lucia reporter cells (Figure 5.13) – a cell line transfected with a luciferase cassette under NF-kB promoter. Finally, using a LPS, a TLR-2 agonist known for its ability to induce signalling cascade that phosphorylates IkBa allowing NF-kB nuclear translocation[256], enhanced 5-fold the expression of adenovirus E3 transcripts in d3iDC (Figure 5.14).

Consequently, like many other viruses appear to do[268], adenoviruses might take advantage of their nature to prime PRR on infected cells and to selectively express E3 immunomodulatory genes[107] under the master switch NF-kB. Probably, to attenuate the anti-viral immune responses. Therefore, the deletion in E3 genes should make EnAd more suitable for immunovirotherapy.

5.5.2 Limitations and future work

The data in this chapter exhibited that the CD46-mediated uptake was the underlying mechanism by which EnAd virus particles stimulated TIDC-like cells, better than Ad5. It was then supposed that the increased uptake provided more adenovirus PAMP blocks for the pathogen recognition receptors of the dendritic cells. Also, the differential expression pattern of stimulatory and neutralising CpG between Ad5 and EnAd genome, was suspected to favour EnAd stimulatory profile. Recombinant Ad5 and EnAd viruses with interchanged fibre proteins could be produced to evaluate the extent of CpG-S and -N elements in the adjuvant function. In any case, future work should address the evolutionary advantage which led group B adenoviruses to bind CD46, with the consequent strong pro-inflammatory responses.

Interestingly, different assays in this chapter showed adenovirus E3 transcripts were specifically expressed in the DC model, without any other gene nor virus products detectable. Nanostring and RT-qPCR demonstrated that all E3 mRNA transcripts were produced and could be enhanced with LPS stimulation. Altogether, it was hypothesised that adenoviruses might

express E3 genes in innate cells via NF-kB, which they induce, to modulate the anti-viral immune response. However, future work would need first to investigate if transcripts are further translated into proteins or whether they simply work as interference RNAs (iRNAs). To assess the translation of the transcripts to proteins in innate cells, western blot could be used. However, generating recombinant E3 proteins and obtaining anti-E3 serum is a laborious task. Instead, designing a recombinant EnAd virus expressing a reporter gene – luciferase or GFP – under E3, could temporarily indicate whether the E3 proteins are expressed in DCs.

From a functional perspective, Ad5 E3 genes have been shown amongst others to interact with major histocompatibility molecules[107]. Hence, if E3 genes are expressed in innate cells, full deletion of E3 region or genetic modifications in NF-kB binding sites should be contemplated to allow the anti-cancer vaccination properties of EnAd virus. Summarising, whether adenoviruses have evolved a mechanism to modulate innate cells would need further confirmation, but understanding this could be of relevance to design better strategies for oncolytic adenoviruses.

6 Evaluating the potential of EnAd-treated TIDC-like cells to functionally harness an anti-cancer adaptive immune response

6.1 Introduction

An important component of cancer immunotherapy relies on triggering innate immunity to try and generate a tumour-specific adaptive immune response, which mediates cancer cell killing. In an ideal situation, professional presenting cells, for example DCs, prime tumour peptide-specific naïve CD4 T cell via three different stimulation signals, and polarising these cells into Helper T cells type 1 (T_H1) (see Introduction). Helper T cells type 1 (T_H1) are considered the most effective to mediate anti-cancer immune functions, as they secrete cytokines that can directly inhibit the growth of cancer cell and help to activate effector cytotoxic CD8 T cell, which kill cancer cells by specific recognition of HLA-presented tumour antigens[41]. Nevertheless, as discussed in Chapter 4, tumour-infiltrating dendritic cells – and other APCs – often present defective 'signal 1 and 2' as well as a suppressive third signals. This can lead to T cell anergy or polarise T cells into regulatory phenotypes, further contributing to the suppressive TME and enhancing tumour growth[40,43-45].

In Chapter 4, it was shown that EnAd particles were a strong adjuvant inducing stimulation on d3iDC, a cell featuring common traits with tumour-infiltrating DC. The central hypothesis of this chapter is that the stimulatory effect of EnAd particles on TIDC, along with the tumour antigens derived from the virus oncolysis, may functionally prime adaptive T cell responses against tumour antigens as a component of anti-cancer immunotherapy.

A human model was needed to test this hypothesis. Using dendritic cells and T cells from the same human donor (autologous model) was excluded for both logistic and technical reasons. Logistically the timeframe to generate d3iDC from PBMCs required freezing T cells, which was not allowed under the Human Tissue Act. On the other hand, the technical reasons were that comparing d3iDC-stimulants with different physical properties – EnAd, Ad5, LPS and untreated – provided uneven 'signal one' for T cell activation (discussed in section 6.5.1).

In contrast the mixed leukocyte reaction is an allogeneic system, used in many studies to assess the functional maturation of DC. In this case overcoming the logistic and technical limitations. In an MLR, T cells stimulation happens when the TCR strongly recognises the non-self MHC from the allogeneic DC, instead of the presented epitope during autologous activation[269]. This allows the normalisation of the uneven 'signal 1' when comparing adjuvants with different antigenicity. In this way, the MLR can inform about the other signals involved in T cell activation. Therefore, a functional mixed leukocyte reaction approach was developed first to assess the effects of virus-mediated d3iDC stimulation on T cell activation and then temporally extended to allow characterisation of the effects on T cell differentiation and polarisation over several days.

Accordingly, an MLR model was set up, and EnAd-treated di3DC were compared against di3DC treated with Ad5 and LPS for their ability to prime CD4 T cell responses. The work was also extended to include di3DC exposed to A549 human lung carcinoma cells that had been pre-infected with EnAd, as tumour cells are known to be capable of directly supressing T cells by upregulating check point inhibitors[27]. In addition, immune check point inhibitor antibodies were used to assess whether these could potentiate the activity of EnAd in this system. Finally, the MLR model was extended to nine days and incorporated by a polyclonal re-stimulation step to allow qualitative evaluation of the type of polarisation induced by EnAd on the immune mediator T_H cells.

6.2 Chapter aims

1. Establish an *in vitro* model of mixed leukocyte reaction using d3iDC (developed in Appendix, part B) and CD4 T cells, to evaluate the functional ability of EnAd-treated d3iDC to prime T cells.
2. Develop an *in vitro* model of mixed tumour-leukocyte reaction to explore the effects of virus infection of tumour cells on T cell activation, using d3iDC co-cultured with virus-infected A549 cell line.
3. Extend the MLR to nine days, to enable more detailed characterisation of the effects of virus-treated DC on phenotype and polarisation of allogeneic naïve CD4 T cells.

6.3 Results

6.3.1 Mixed leukocyte reaction model development

To study the potential effect of EnAd on adaptive immunity, a mixed leukocyte reaction-based assay was developed. In this case, the MLR was designed using human d3iDC (pre-treated as described in Chapter 4, Figure 4.1) in combination with a fresh pool of CD4 T cells enriched from PBMCs from a second randomly selected donor.

Briefly, CD4+ T cells from donor one were enriched by negative selection using CD4+ T Cell Isolation Kit (MiltenyiBiotec) combined with MACS technology, from freshly isolated PBMCs (PBMCs isolation see Material and Methods). The purity of live cells was assessed by flow cytometry with anti-CD3 and anti-CD4 antibodies, as well as vital dye (accordingly with Figure 6.4), and was always shown to be above 94% purity (Figure 6.1 A and B).

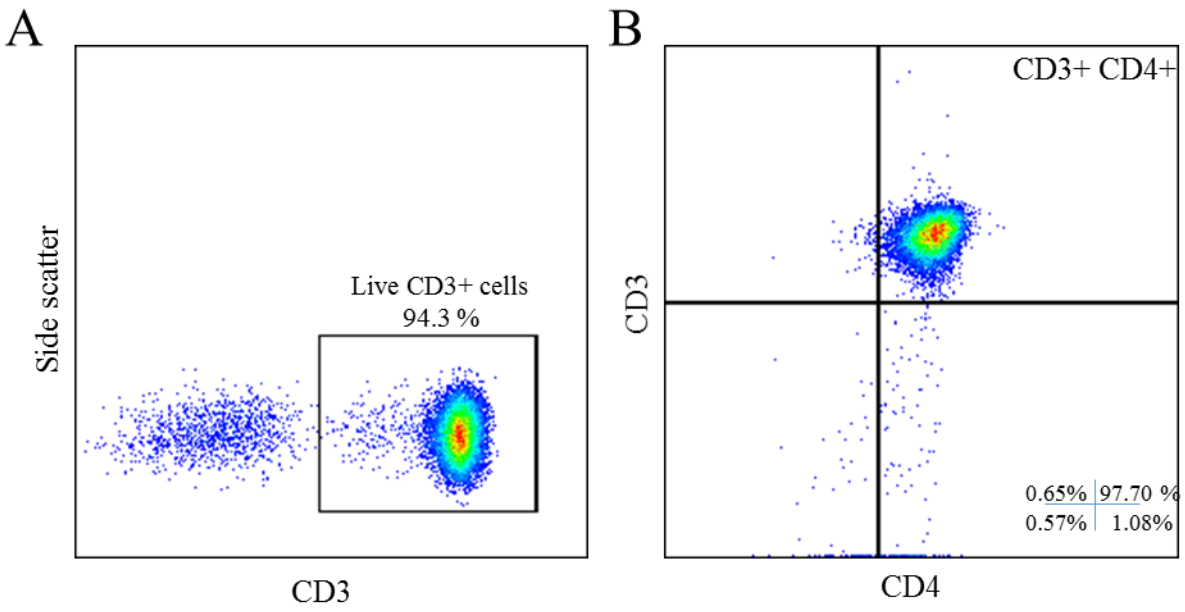


Figure 6.1 Assessment of CD4 T cells purity by flow cytometry on MACS enriched cells. Human PBMCs from leukocyte cone were isolated by Ficoll gradient (see Material and Method), before untouched CD4 T cells were enriched using the CD4+ T cell isolation kit (Miltenyi) with MACS technology (see Materials and Methods). Enriched cells were stained with vital dye and monoclonal antibody against CD4 and CD3 before assessing cell purity by flow cytometry analysis. (A) T cell purity (B) and CD4 T cell purity is shown for two different donors.

The experimental protocol for this model was to mix the enriched CD4+ cells with d3iDC previously generated from a second donor. To optimise the model, the best DC to TC ratio was evaluated aiming to achieve a big difference in T cell activation between the untreated DCs (or assay background) and stimulated DCs. LPS was used for this stimulation, as it has been extensively shown to strongly activate T cells in MLR[270]. T cell activation was assessed at three DC:TC different ratios; 1:5, 1:10 and 1:20 after 48 hrs, by IL-2 quantification, a prominent biomarker of T cell activation. IL-2 was quantified with an in-house-developed IL-2 enzyme-linked immunosorbent assay (ELISA) (see Material and Methods).

One DC to five T cell (1:5) ratio showed the biggest differential between LPS-activated and control d3iDC, resulting in about 9-fold IL-2 increase. Whilst, 1:10 and 1:20 ratios, only achieved a 4.3-fold and 6.8-fold increase respectively (Figure 6.2 A). Therefore, the 1:5 ratio was adopted from hereafter.

The MLR incubation time was also optimised for the biggest differential between treatment-induced T cell activation (LPS-treated d3iDC) and background (untreated d3iDC), again using IL-2 expression. As early as 24 hrs, more than 2-fold differential was detected between LPS-treated MLR and background, but the difference was further increased at 48hrs (Figure 6.2 B), perhaps suggesting that the background signal decreased over time. In a different experiment using different donors, MLR incubation time was evaluated at later timepoints, from day 3 to 6 post-MLR, using the same conditions. The differential between untreated and LPS-treated MLRs was maximal at day 4 (more than 3-fold), however the IL-2 levels in LPS-treated d3iDC plateaued at day 4 and trended downwards from that timepoint, being undetectable by day 6 (Figure 6.2 C). These experiments suggested it was acceptable to use IL-2 levels to assess T cell activation from day 1 to day 4 post-MLR, but after day 4 IL-2 was rapidly consumed. In the interest of reproducibility, it was decided that T cell activation would be assessed after 48hrs (Figure 6.2 D).

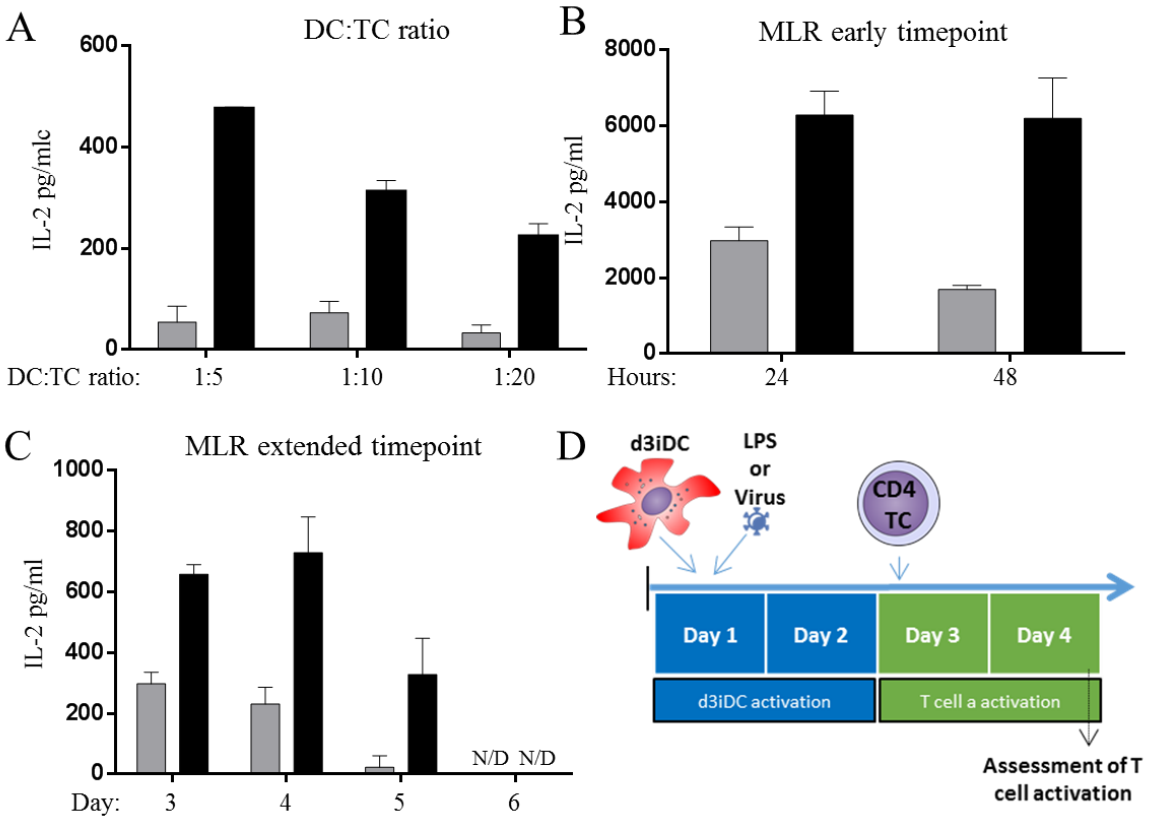


Figure 6.2 Establishing the cell ratios and timeframe for mixed leukocyte reaction using IL-2 ELISA. LPS-treated (black) and untreated (grey) d3iDC (accordingly generated to Figure 4.1 A) were mixed with freshly isolated CD4 T cells (accordingly with Figure 6.1) at increasing cell ratios. In-house developed IL-2 ELISA (see material and methods) was used to quantify the IL-2 in the supernatants of biological triplicates, before calculating the average and SD. (A) IL-2 levels for untreated and LPS condition are compared at 1:5, 1:10 and 1:20 DC to TC ratios after 48 hrs MLR. Alternatively, IL-2 was quantified on 1:5 (DC:TC) MLR ratio after (B) 24 and 48 hours or (C) after 3 to 6 days assessing IL-2 expression every 24 hrs. (D) Representation of the MLR model showing the d3iDC cells treated for 48hrs, before they were mixed with CD4 T cell at 1:5 ratio and cell activation assessed 48hrs later.

6.3.2 Comparing EnAd and Ad5 virus particles in an MLR for their ability to activate CD4 T cells via d3iDC

The allogeneic MLR model developed in section above (6.3.1) was used to assess whether the stimulation of d3iDC by EnAd particles could translate into functional CD4 T cell activation. EnAd was compared against Ad5 virus and untreated controls. Accordingly, d3iDC were treated with the same dose of EnAd or Ad5 (200ppc), or left untreated for 48 hrs. d3iDC were then thoroughly washed to remove free virus particles, mixed with freshly enriched CD4 T cells from a different donor and co-cultured in RPMI medium. Finally, T cell activation was assessed after 48hrs MLR by ELISA as well as flow cytometry, accordingly with timeline Figure 6.2 D.

Production of both IL-2 and interferon gamma (IFN-g), another marker often used to assess T cell activation, were quantified by ELISA of supernatants. The first donor displayed both IL-2 and IFN-g statistically significant upregulated when d3iDCs were treated with EnAd, well above untreated d3iDC (MLR background). In contrast, Ad5 treatment showed a limited increase against untreated d3iDC for both biomarkers (Figure 6.3 A and C). Subsequently, both cytokines were assessed across multiple donors and each condition was expressed as fold increase relative to untreated control. IL-2 and IFN-g were on average 2-fold upregulated in EnAd-treated MLR, well above and significantly different from Ad5-treated MLR (IL-2; $p= 0.0036$ and IFN-g; $p=0.0012$), which was similar to untreated (Figure 6.3 B and D). This suggested that the adjuvant effect of EnAd on d3iDC promoted a functional activation on allogeneic T cells, stronger than that achieved by Ad5.

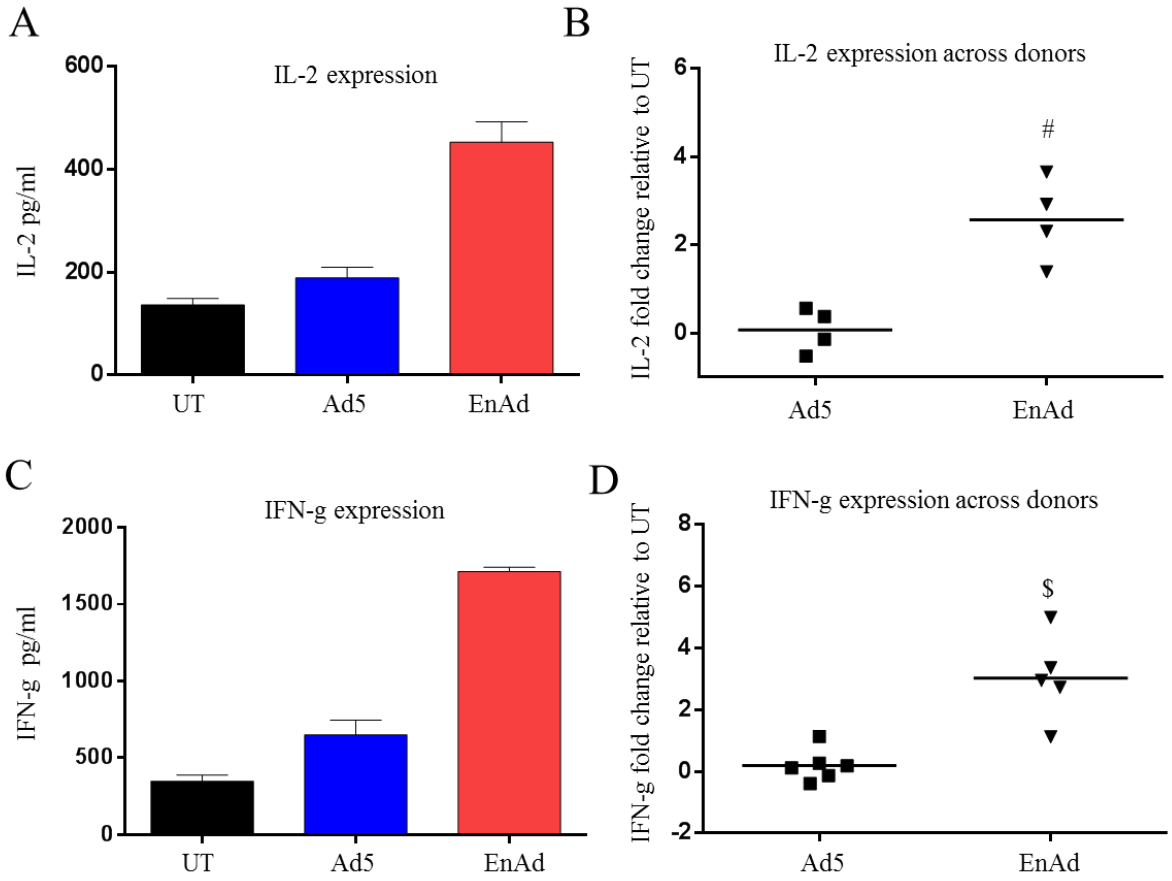


Figure 6.3 Quantification of IL-2 and IFN-g on MLR supernatants comparing EnAd and Ad5 treatments. d3iDC were treated with 200ppc of Ad5 or EnAd or left untreated before cells were washed and mixed with freshly isolated CD4 T cells, accordingly with Figure 6.2 D timeframe. Supernatants were used to quantify (A) IL-2 with in-house ELISA or (C) commercially available Human IFN gamma ELISA Ready-SET-Go kit (eBioscience) in technical duplicates, before averaging the biological triplicates of each treatment. Alternatively, the fold change in IL-2 and IFN-g for, Ad5 (squares) and EnAd (triangle) treatments were calculated relative to untreated condition (UT) from corresponding MLR combination. The fold change relative to UT of n≥4 independent experiments are shown for (B) IL-2 and (D) IFN-g, and the average of the relative fold change are compared between Ad5 and EnAd treatment with un-paired T test. The IL-2 relative fold change of EnAd is significantly different to Ad5 (#p=0.0036). The IFN-g relative fold change of EnAd is significantly different to Ad5 ($p=0.0012).

T cell activation was further investigated by flow cytometry, assessing the up-regulation of cell surface interleukin-2 receptor alpha chain (CD25), early inducible cell surface glycoprotein acquired during lymphoid activation (CD69), and lysosomal-associated membrane protein-1 (LAMP-1 or CD107), all commonly used as T cell surface activation markers. In addition, LPS-treated d3iDC was included as stimulation control for comparison. To assess the markers levels on CD4 T cells only, size and granularity differences between d3iDC and CD4 T were used to discriminate both cell types, as well as CD4 T cell specific markers following the gating strategy shown in Figure 6.4. Freshly isolated resting CD4 T cells were utilised to set the gates for each of the three activation markers.

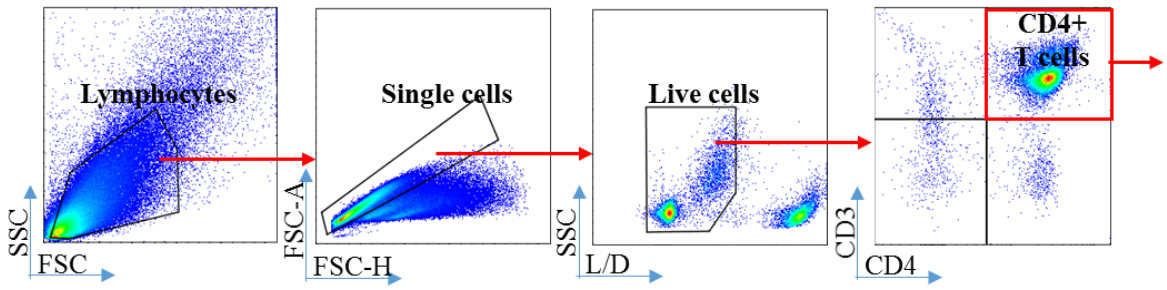


Figure 6.4 Staining and gating strategy on flow cytometry to assess the expression of specific markers on CD4 T cells. Harvested cells were stained with Live/dead fixable aqua dead cell stain (ThermoFisher), monoclonal anti-CD4 and anti-CD3 antibodies (Biolegend), as well as directly-labelled antibodies against corresponding markers, before cells were acquired on polychromatic cytometer Attune NxT (see Material and Methods). CD4 T cells were gated accordingly on SSC vs FSC plot (for T cell granularity and shape) → FSC-H vs FSC-A (for single cell) → Vital dye vs SSC (for live cells) → CD3 vs CD4 (for CD4+ T cells) → assessed marker.

The untreated MLR reaction slightly increased the percentage of CD25+ T cells compared to their resting state. However, no difference was seen across MLRs between untreated, Ad5-treated and EnAd-treated conditions; only LPS stimulation appeared to induce more CD25+ CD4 T (Figure 6.5 A). This observation was consistent across five independent MLRs, however results with LPS-treatment were not significantly different from the other treatments (Figure 6.5 B).

CD69 marker was also induced by the background allo-stimulation compared to d3iDC. However in this case, EnAd-treatment induced additional CD69 expression, to the largest percentage of CD69+ CD4 T cells compared to either Ad5 and LPS treatment (Figure 6.5 A). In fact, the average CD69+ percentage expression across five independent MLR combinations was significantly different between EnAd-treated and untreated condition ($p=0.0463$), but not significantly different between EnAd-treated and LPS ($p=0.067$) nor EnAd-treated and Ad5-treated ($p=0.0883$) (Figure 6.5 C).

CD107 was also induced by the MLR itself in comparison to resting cells, however virus treatments and especially EnAd lead to an apparent increase in the percentage of CD107+ population (Figure 6.5 A). This can be seen most clearly when multiple combination MLRs are assessed, although the percentage of CD107+ average from EnAd-treated MLR was not significantly different from untreated ($p=0.109$), LPS-treated ($p=0.061$) nor Ad5-treated ($p=0.152$) (Figure 6.5 D).

Altogether, CD69 and CD107 T cell activation markers suggested that EnAd-treated d3iDC induced T cell activation in the MLR assay, the CD25 marker was un-altered. This may be a time-dependent effect with CD25 being induced later[271]. However, apart from CD69, the flow cytometry data were not as statistically conclusive as seen with IL-2 and IFN-g cytokines. It may be that the lack of relative normalisation on flow cytometry data, demanded larger samples to over-come the donor to donor variability.

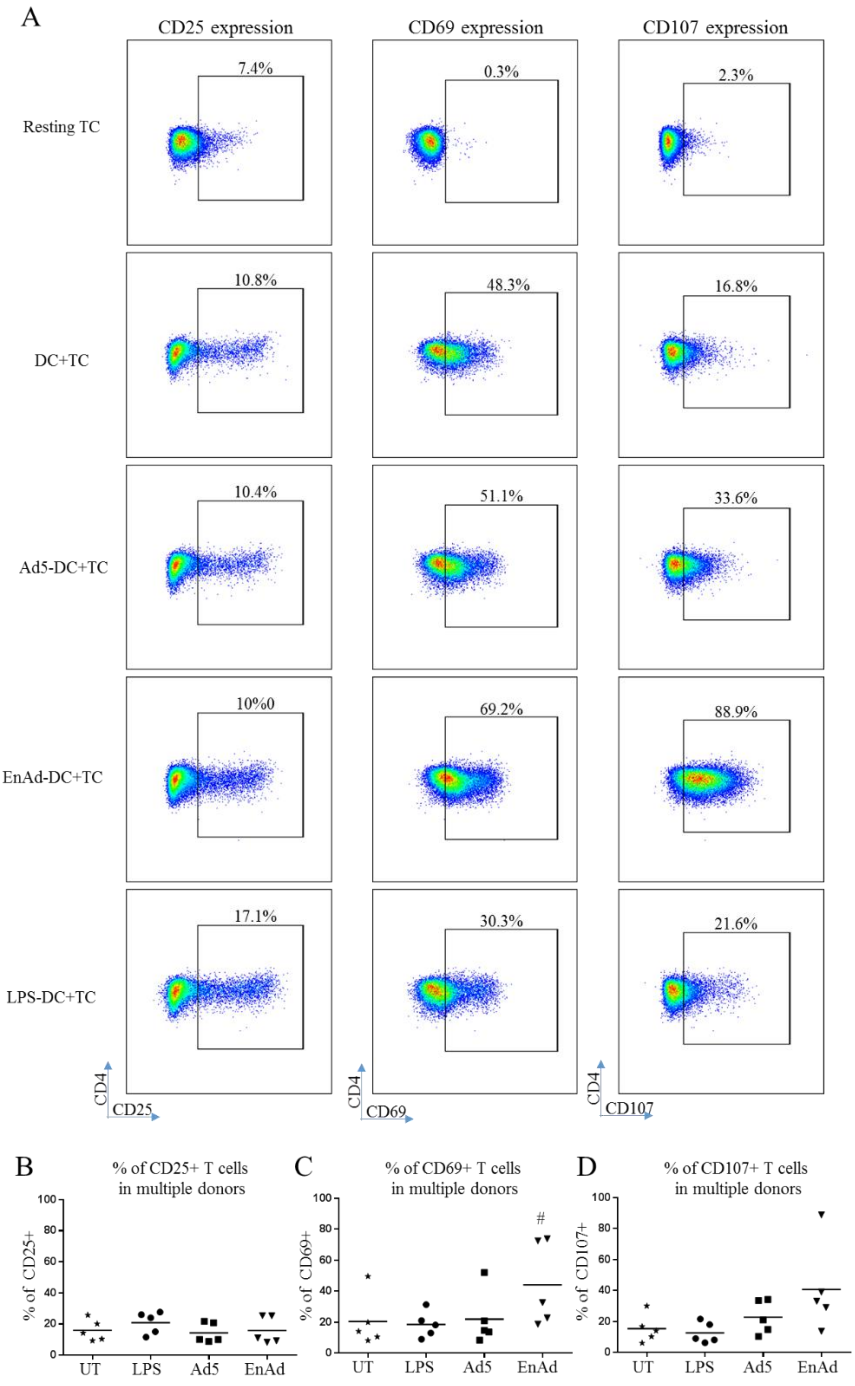


Figure 6.5 Assessment of CD25, CD69 and CD107 expression on CD4 T cells from MLR exposed to d3iDC treated with EnAd, Ad5 and LPS, or untreated. d3iDC were treated with 200ppc of Ad5 or EnAd, 100 ng/ml LPS or left untreated before cells were washed and mixed to freshly isolated CD4 T cells (or resting alone), accordingly with Figure 6.2 D timeframe. Cells were harvested and stained with directly labelled monoclonal anti-CD25, anti-CD69 and anti-CD107 antibodies (Biolegend), in addition to Figure 6.4's staining, before following the CD4 T cell gating strategy. The gating to determine the percentage of CD4 T cells that are CD25+, CD69+ and CD107+, were established based on resting T cell. (A) Percentage of CD4 T cells CD25+, CD69+ and CD107+ are shown for a same MLR combination treated with Ad5, EnAd, LPS and untreated d3iDC, or resting CD4 T cells. The percentage of CD4 T cells CD25+, CD69+ and CD107+ in n≥4 independent MLR combinations are shown, and averages are compared between d3iDC treatments using paired-t Test. The average of CD69+ T cells for EnAd is significantly different to untreated (#p=0.0463).

6.3.3 Evaluating whether PD-L1 blockade can further enhance the T cell activation mediated by EnAd-treated d3iDC in an MLR assay

In the previous section it was shown that d3iDC treated with EnAd stimulated activation of CD4 T cells. This was likely mediated by the strong up-regulation of HLA and costimulatory molecules that EnAd promoted on d3iDC, as shown in Chapter 4. In Chapter 4 it was also shown that EnAd induced d3iDC to strongly up-regulate the programmed-death ligand 1. PD-L1 binds to programmed death-1, a well-known T cell immune checkpoint involved in negative regulation of T cell functions[27]. Therefore, it was hypothesised that PD-L1 blockade might improve the ability of EnAd-treated d3iDC to stimulate T cells. To test the concept, large concentrations of virus particles were used to stimulate d3iDC, as PD-L1 was up-regulated in a dose dependent-manner (Figure 4.6), and it was thought this would amplify the difference between anti-PD-L1 blocking antibody and isotype or no antibody.

Using the MLR assay developed above, d3iDC were treated with 5000ppc of EnAd or Ad5, 100 ng/ml LPS, or left untreated for 48hrs. Anti-PD-L1 blocking antibody (as well as isotype antibody or no antibody) was added at the time of mixing CD4 T cells with the dendritic cells. IL-2 and IFN-g were quantified by ELISA 2 days post-MLR.

Once again EnAd-treatment of the MLR induced a strong secretion of IL-2 and IFN-g compared to the untreated control. The addition of PD-L1 blocking antibody enhanced the absolute levels of both IL-2 and IFN-g, whilst the isotype showed no effect. Ad5-treated d3iDC also promoted IL-2 and IFN-g secretion, which was further enhanced with the PD-L1 antibody. LPS–treatment induced only a poor IL-2 and IFN-g secretion relative to untreated d3iDC. Nevertheless, here again anti-PD-L1 promoted further expression (Figure 6.6 A and B). Overall, T cell stimulation in the MLR appeared to be enhanced with anti- PD-L1 blocking antibody independently of the DC treatment, averaging 1.44- and 1.26-fold increase relative to the corresponding isotype controls, in IL-2 and IFN-g respectively (Figure 6.6 C and D). The

fact that in this experiments Ad5 induced such a strong T cell activation was because in previous sections d3iDC were triggered with 200ppc instead of the 5000ppc used here. In Chapter 4 it was shown that Ad5 virus also induced DC stimulation in a dose-response manner, despite being weaker than EnAd (Figure 4.6).

Nevertheless, these data suggested that anti-PD-L1 blocking antibody could enhance the stimulatory effect produced by EnAd virus in the MLR, potentially promoting a stronger cancer immunotherapy.

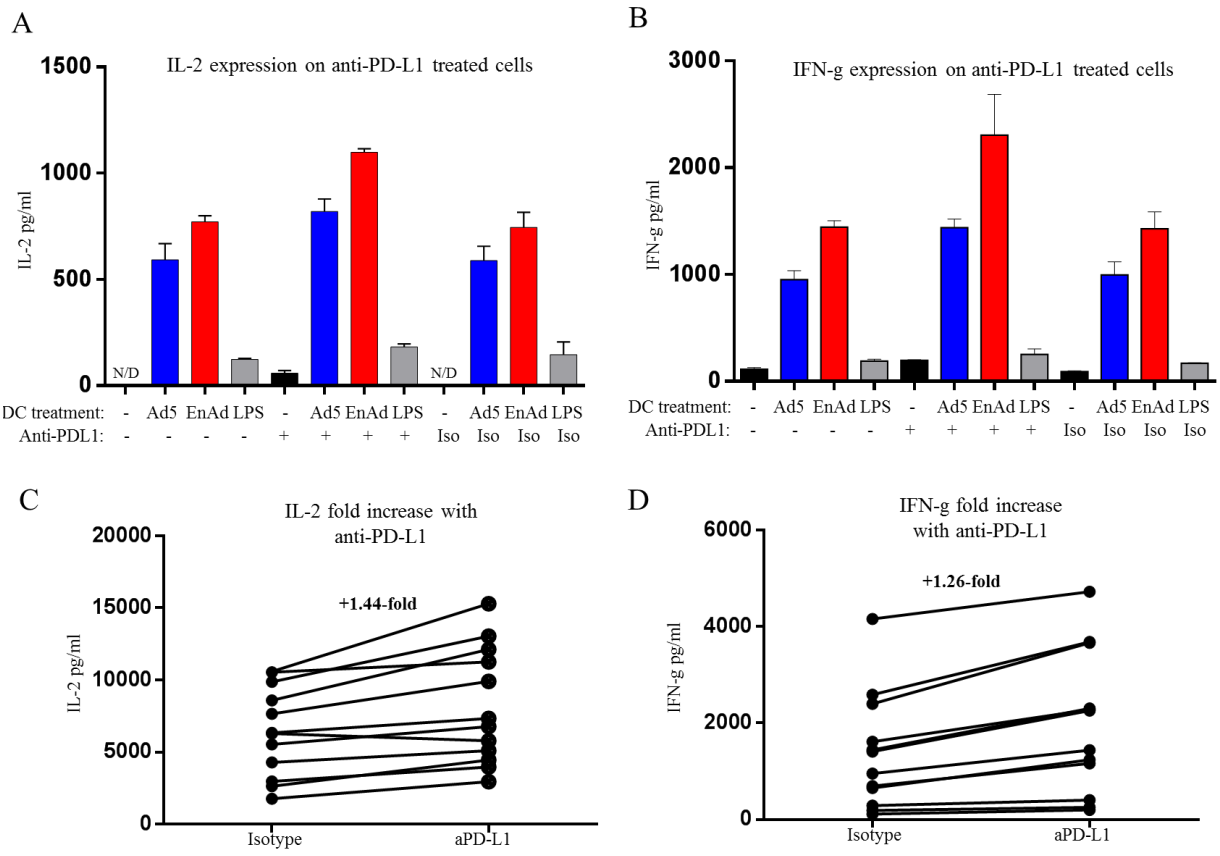


Figure 6.6 Evaluating the IL-2 and IFN-g expression on MLR supernatants treated with anti-PD-L1 blocking antibody. d3iDC were treated with 5000ppc of Ad5 or EnAd, 100 ng/ml LPS or left untreated before cells were washed and mixed with freshly isolated CD4 T cells, accordingly with Figure 6.2 D timeframe. At the same time, ultra-LEAF purified anti-human PD-L1 antibody or corresponding isotype (Biolegend) were added to some wells. (A) IL-2 in-house ELISA or (B) human IFN gamma ELISA Ready-SET-Go kit (eBioscience) were used to quantify the cytokine levels in supernatants in technical duplicates. Average of biological triplicates and SD for each treatment are shown. (C) IL-2 and (D) IFN-g levels from isotype wells are paired to their equivalent MLR treatment with anti-PD-L1, the PD-L1 fold change relative to the isotypes are calculated and averaged across. Shown are representative of three independent experiment.

6.3.4 Evaluating the potential of EnAd to activate T cells within the tumour context

In previous sections, EnAd was shown to be capable of inducing T cell activation via its adjuvant effects on tumour infiltrating-like DC. However, T cell activation was assessed only in a very defined reductionist context and chronological order. This approach can be criticised on several levels, for example it excludes study of multiple signals that could interplay with T cell activation in the tumour, for instance; PD-L1 up-regulation on tumour cells. In fact, colleagues in this lab and others had previously shown that A549 cells express low levels of PD-L1 on their surface, and can be up-regulated by virus and IFN-g[272]. Another aspect missing in previous experiments was the interaction between the virus progeny produced in tumours and T cell, especially since previous reports showed that adenovirus type 35 (Ad35) suppressed T cell activation via CD46 engagement[273]. The purpose of this section was to extrapolate whether EnAd could promote TIDC to functionally activate T cells in a tumour context, and overcome the suppressive signals from tumour cells and the virus.

6.3.5 Assessing the ability of EnAd virus to activate CD4 T cells via d3iDC when pre-infected in A549 cell

The co-culture of infected-A549 and d3iDC used in Chapter 4 (section 4.3.4, Figure 4.10) was considered a good starting point to evaluate whether EnAd could promote TIDC to functionally activate T cells in a tumour context. After previous optimisation, it was proposed to perform the MLR in the same well as the virus-treated tumour cells without a prior DC-isolation, by adding the allogeneic CD4 T cells 2 days after the infected-A549-d3iDC co-culture was set (or mixed tumour-leukocyte reaction, MTLR). T cell activation would then be assessed 24hrs later (Figure 6.7 A). This experimental layout was thought to be arguably more clinically relevant,

as it is highly likely that virus particles produced *in vivo* will encounter the T cells within the tumour.

To evaluate whether the viruses could have a direct effect on the analysed markers independently of d3iDC, co-cultures were prepared excluding the DC fraction. In fact, IL-2 in supernatant was beneath the limit of detection for EnAd-infected and Ad5-infected A549 cells as well as uninfected A549 cells control, when d3iDC were left out. On the other hand, the inclusion of allogeneic d3iDC (MTLR) induced IL-2 expression independently of treatment, suggesting that T cell activation was dependent on DC mediation. Interestingly, d3iDC from the EnAd-infected A549 well promoted a more than 3-fold increase of IL-2 in comparison to un-infected A549. But both Ad5 and LPS led to a decreased in IL-2 levels relative to uninfected A549 (Figure 6.7 B).

Likewise, IFN-g was undetectable in the controls without d3iDC, but was detectable when d3iDC were added, except for the MTLR treated with Ad5, where no IFN-g was seen. A high expression of IFN-g was measured in the MTLR treated with EnAd, more than 5-fold increased relative to uninfected A549 cells. LPS treatment of the MTLR also promoted a limited increase of IFN-g relative to untreated A549 (Figure 6.7 C).

In addition, T cell activation was assessed by cell surface CD69 staining using the same methodology described in section 6.3.2. Interestingly, a relatively high percentage (42.8%) of CD4 T cell expressed CD69 just by being exposed to A549, without the intermediation of d3iDC (A549+CD4). This was increased by EnAd, as EnAd-infected A549+CD4 displayed 14 points more CD69+ T cells than the uninfected control. More interesting was that T cells that had been co-cultured with Ad5-infected A549 only, showed an impaired percentage of CD69+ T cells, resulting in more than 2-fold reduction compared to controls (A549 + CD4). This was also seen in fully constituted MTLR, as Ad5-infected A549+d3iDC+CD4 showed a drop in CD69+ expression in CD4 T cells of 15 points relative to uninfected-A549+d3iDC+TC

(55.6%). On the other hand, EnAd- and LPS-MTLR, triggered the expression of CD69 to nearly 80% of the CD4 T cell population (Figure 6.7 D). CD69 displayed a high background in this assay, suggesting that it might well be a sensitive marker. In fact, EnAd appeared to further up-regulate CD69 without d3iDC intermediation. This may be related to a CD46-engagement by EnAd fibre, which will be considered in the following section.

Overall, the soluble IL-2 and IFN-g and surface marker CD69 suggest that EnAd virus can induce CD4 T cell activation via d3iDC above suppressive signals from A549 cells and derived from CD46 engagement. In contrast, Ad5 virus appears to supress all T cell activation markers well below the untreated MTLR background. Thus, this may well indicate that EnAd could be a good candidate to stimulate tumour-infiltrating DC and locally stimulate adaptive immunity, whilst in that same context, the wildtype Ad5 might supress it.

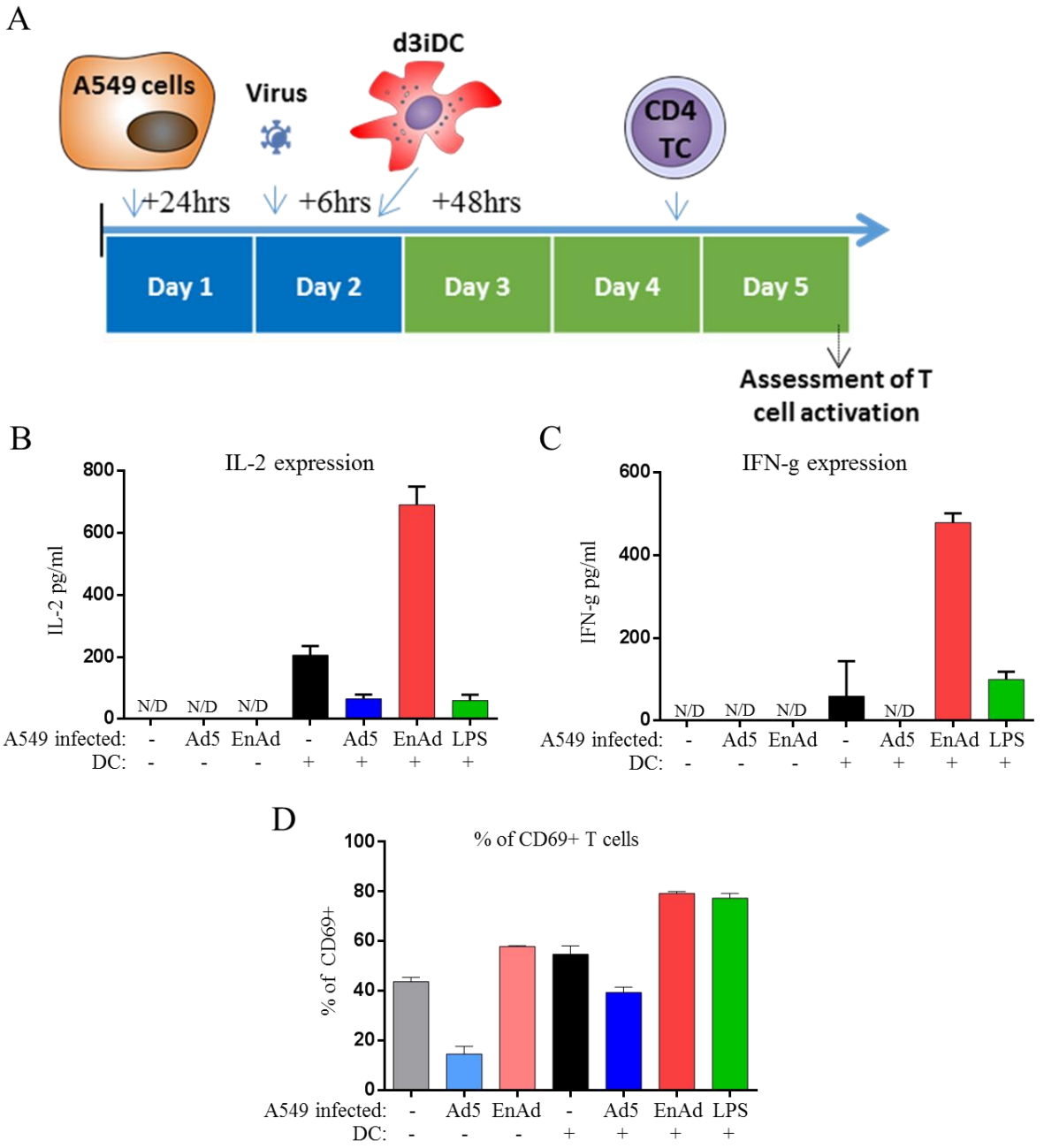


Figure 6.7 Comparing T cell activation in a mixed tumour-leukocyte reaction treated with EnAd, Ad5 and LPS. (A) Pre-seeded A549 were infected with 100ppc EnAd or Ad5, after 6 hrs cells were thoroughly washed and d3iDC were added in some wells, and few more were treated with 100 ng LPS/ml. After 2 days, freshly isolated CD4 T cells from a second donor were added, before T cell activation was assessed on supernatants by (B) IL-2 and (C) IFN-g ELISA, or (D) CD69 expression on CD4 T cells by flow cytometry (accordingly with Figure 6.5). Average of biological triplicates and SD for each treatment are shown, representative of n=3 independent experiments.

6.3.6 Investigating the role of EnAd virus particles on CD4 T cell stimulation

Based on previous reports[273] and results from the previous section (Figure 6.7), this section dissected the effect of CD46 engagement on T cell activation. Accordingly, EnAd virus particles were tested either alone or combined with TCR ligation (anti-CD3). For this, a large concentration of virus, $1x10^5$ EnAd particles per cell, was added to freshly isolated CD4 T cells. Anti-CD28 (aCD28.2), anti-CD46 (aCD46) antibodies and corresponding isotypes (iso), were bound to the cell culture plates by overnight poly-L-lysine coating (see Materials and Methods), as a costimulatory ligand and CD46 crosslinking controls respectively. EnAd, anti-CD28 and anti-CD46 permutations were also combined with plate-bound anti-CD3 antibody (aCD3). Alternatively, CD4 T cells were left untreated. Twenty-four hours later, supernatants were used to assess IL-2 and IFN-g, and cells were evaluated for CD69 expression.

Neither EnAd virus particles or anti-CD46 antibody alone promoted IL-2, IFN-g nor CD69 expression, resulting in equivalent levels to untreated or isotype controls. Only, costimulatory signal alone (anti-CD28 antibody) led to a slight up-regulation for all three activation markers (Figure 6.8 A, C and E). Therefore, CD46 engagement alone by EnAd virus or antibody had no effect on resting T cells.

Interestingly, when anti-CD46 or EnAd virus particles were combined with TCR ligand anti-CD3, the percentage of CD69+ cells were increased to similar levels achieved by combining costimulation (anti-CD28) and anti-CD3 (Figure 6.8 F). On the other hand, IL-2 and IFN-g levels were equivalent to those induced by TCR ligand (Figure 6.8 B and D). The IL-2 and IFN-g data showed that engagement of CD46 with antibody or EnAd virus particles did not supress nor activated the T cell activation induced by TCR singling, contradicting previous report with group B adenovirus 35[273]. However, CD69 marker appeared to be sensitive to EnAd when TCR was also engaged, aligning with the data seen in MTLR assay (section 6.3.5). Hence, CD69 assessment might not be ideal to characterise T cell activation in MTLR setting.

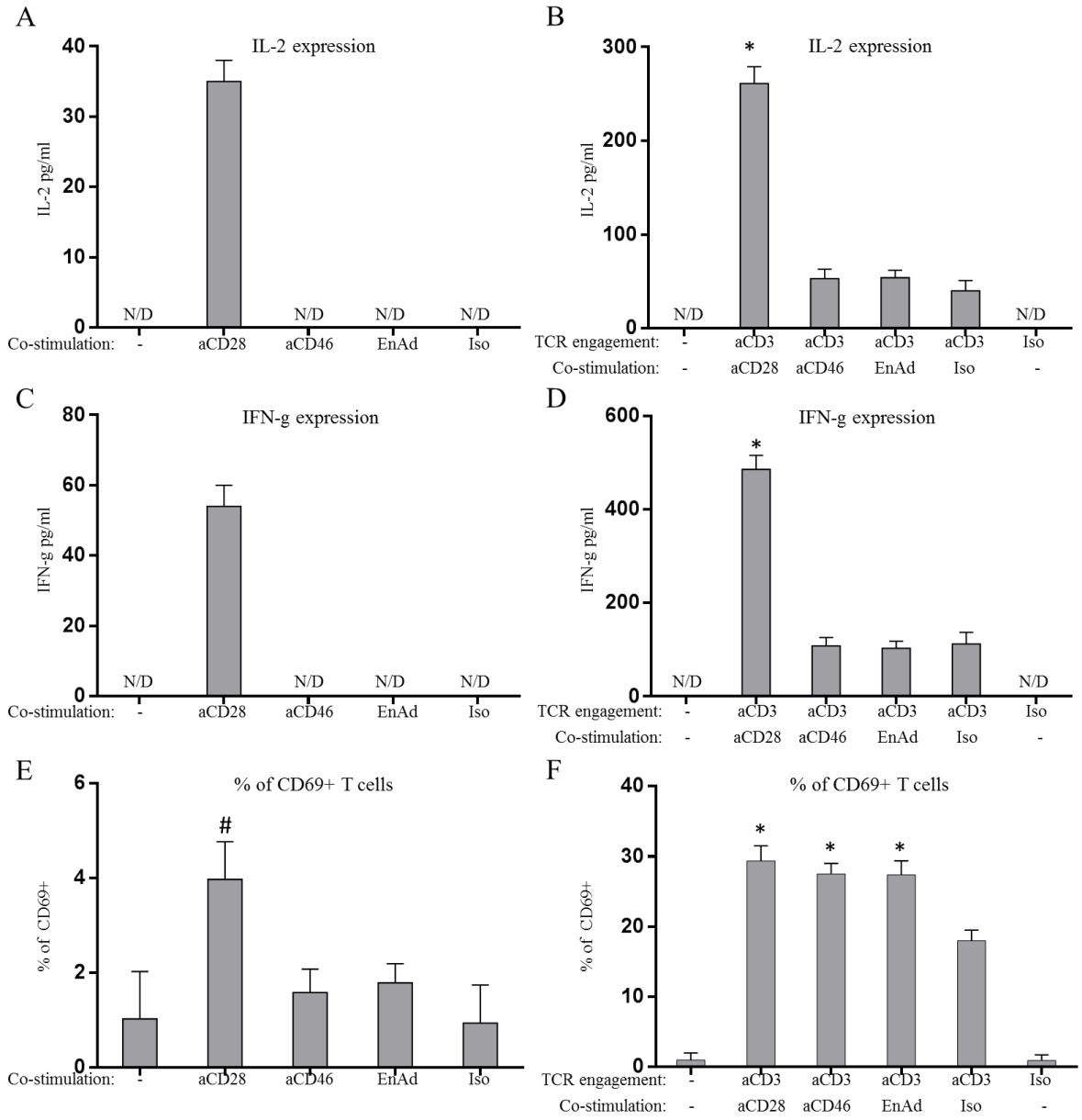


Figure 6.8 Evaluation of EnAd virus particles as stimulant or costimulant of CD4 T cells. Freshly isolated CD4 T cells were cultured in triplicates with 50000 EnAd ppc, untreated or in wells that had been pre-coated with 5 µg/ml of monoclonal anti-CD28 (Biolegend), anti-CD46 (SantaCruz Biotech) or isotype control (Biolegend) antibodies (see material and methods). Twenty-four hours later, (A) IL-2 and (C) IFN-g were quantified in supernatants by ELISA or (E) % of CD4 T cells CD69+ determined by flow cytometry. Alternatively, the same CD4 T cells and the same iteration of treatments were used, but this time all triplicate wells were pre-coated with 5 µg/ml of anti-CD3 antibody (Biolegend), in exception of the isotype and untreated controls. (B) IL-2, (D) IFN-g and (F) CD69+ were equally assessed after 24 hrs. Average of biological triplicates and SD for each treatment are shown.

6.3.7 Evaluating whether EnAd and Ad5 virus particles can potentially prime anti-cancer adaptive immune responses using a 9 days MLR assay

In previous sections, it was shown that EnAd could activate T cells via dendritic cell processing, both as a free virus particle and also following infection of A549 cells. This suggests that EnAd, along with the tumour antigens released by the oncolytic activity, may be able to prime an adaptive immune response. Once antigen-specific naïve CD4 T cells are primed, clonal expansion begins and over the following days cells differentiate into memory phenotypes, which are responsible for fast responses following future antigen exposure. However, in order to prime anti-tumour cellular immunity, CD4 T cells must also polarise into T_H1 during the differentiation.

T cell activation 'signal 2' or the lack of it contribute towards the polarisation, but cytokines (signal 3), normally provided by the antigen presenting cells, play the pivotal role. For instance, IL-12 is the most prominent T_H1 polarising cytokine, which has not been found to be secreted by TIDC[53]. Equally, IL-12 was not detected in d3iDC treated with EnAd virus particles, as shown in Chapter 4 (section 4.3.3.2). Instead, traces of IL-4, known to polarise naïve T cells into T_H2, were found in some d3iDC treated with EnAd, Ad5 or untreated (section 4.3.3.2). T_H2 induces antibody isotype switch (to IgE) and is generally involved in humoral responses against parasites and inhibiting anti-tumour cellular immunity[211]. Therefore, it was assumed that EnAd-stimulated d3iDC would most likely mediate a compromised polarisation of the anti-tumour adaptive immune response. A model was therefore developed to evaluate whether EnAd as a particle may stimulate TIDC to prime proliferation and differentiation of naïve CD4 T cells, as well as to evaluate the type of polarisation achieved. The previously developed MLR model (section 6.3.1) was followed, except that d3iDC were co-cultured with freshly isolated naïve CD4 T cells and for an extended period of time. Cells were fed by adding medium supplemented with recombinant IL-2 whenever there were signs of acidification. After 9 days,

when primed T cells usually return to a basal state, CD4 T cells were assessed for proliferation and differentiation. Cell density was determined by trypan blue and normalised for polyclonal re-stimulation with Dynabeads T-Activator CD3/CD28 (ThermoFisher), to simulate the activation of antigen-experienced CD4 T cells and assess their polarisation (Figure 6.9 and Material and Methods).

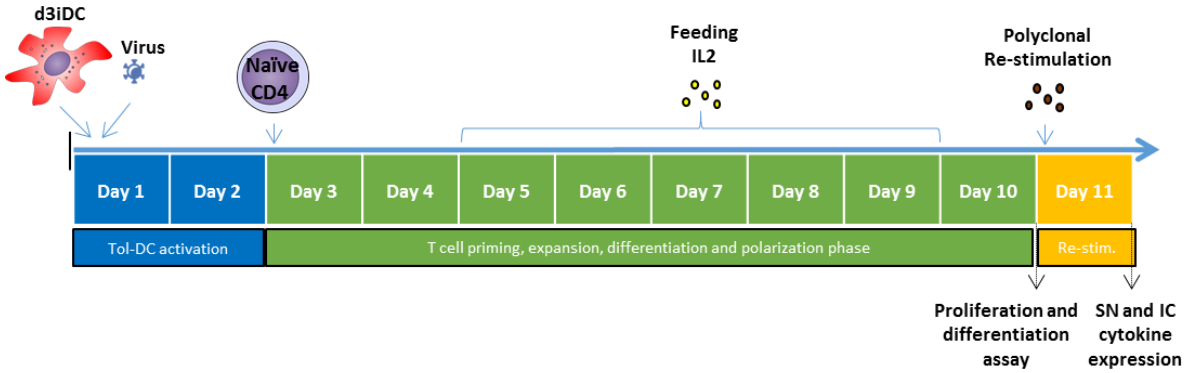


Figure 6.9 Representation of the extended MLR model used to assess the proliferation, differentiation and polarisation of naïve T cells. d3iDC cells are treated for 48hrs, before they are mixed with naïve CD4 T cell (naive CD4+ T cell isolation kit II, Miltenyi) at 1:5 ratio. MLR is monitored and fed with fresh medium supplemented with 30 units recombinant IL-2/ml (R&D Systems) when acidification and proliferation is noted. After 9 days, cell proliferation and differentiation assays are performed by flow cytometry, before cells are counted with trypan blue and cell concentration adjusted for T cell polyclonal activation with DynaBead T-activator CD3/CD28 (ThermoFisher), according to the manufacturer's protocol. Twenty-four hours later CD4 T cell polarisation was assessed by flow cytometry.

6.3.7.1 Assessing EnAd- and Ad5-treated d3iDC for their ability to induce differentiation of naïve CD4 T cells 'primed' in a 9 days MLR assay

The memory/naïve phenotype of CD4 cells was determined by flow cytometry after 9 days of MLR (Figure 6.9), using the CD4 T cell panel and the gating strategy from section 6.3.2, combined with CCR7 and CD45-RA markers. CD45 is found on human T cells in two different splicing isoforms dependent on differentiation status. CD45-RA, the naïve isoform, is switched to CD45-RO when cells differentiate into memory phenotypes. On the other hand, CCR7 is a chemokine receptor involved in lymph node trafficking, where naïve T cells will be primed[274]. Hence, double CCR7+CD45RA+ is generally used to identify naive T cells, as seen on freshly

isolated naïve CD4 T cells (Figure 6.10 A). Upon priming, naïve CD4 T cells become effector memory (or CCR7-CD45RA-) or central memory (or CCR7+CD45RA-).

LPS treatment promoted differentiation of about 40% of naïve T cells, giving similar proportions of central and effector memory cells (Figure 6.10 C). In contrast EnAd promoted slightly greater overall differentiation (about 50%), with about three quarters of differentiated cells showing a CCR7-CD45RA- (effector memory) phenotype (Figure 6.10 E). On the other hand, Ad5 and untreated d3iDC did not promote much T cell differentiation, and CD4 T cells mostly remained naïve (Figure 6.10 B and D).

Memory T cells (identified as all the CD45RA- T cells) and naïve T cells (CCR7+CD45RA+) were calculated as a proportion of total live CD4+ T cells, and the effects of the treatments were compared across seven independent experiments (different donor combinations). Untreated or Ad5-treated d3iDC showed very little effect on CD4 T cell differentiation, as after 9 days very few of the T cells had differentiated into memory cells (12-15%, Figure 6.10 F and G). In contrast, treatment of d3iDC with EnAd particles appeared to promote differentiation of naïve T cells into memory phenotypes (typically 30%, although there was substantial variation between donors). A small increase in the proportion of memory phenotype and a decrease in naïve type was also seen following treatment with LPS, but this was not significantly different to any other treatment.

Overall, these data suggest that EnAd virus particles may stimulate TIDC in a way that primes naïve CD4 T cells and induces differentiation into memory phenotypes, whereas the same dose of Ad5 virus seemed unable to do this.

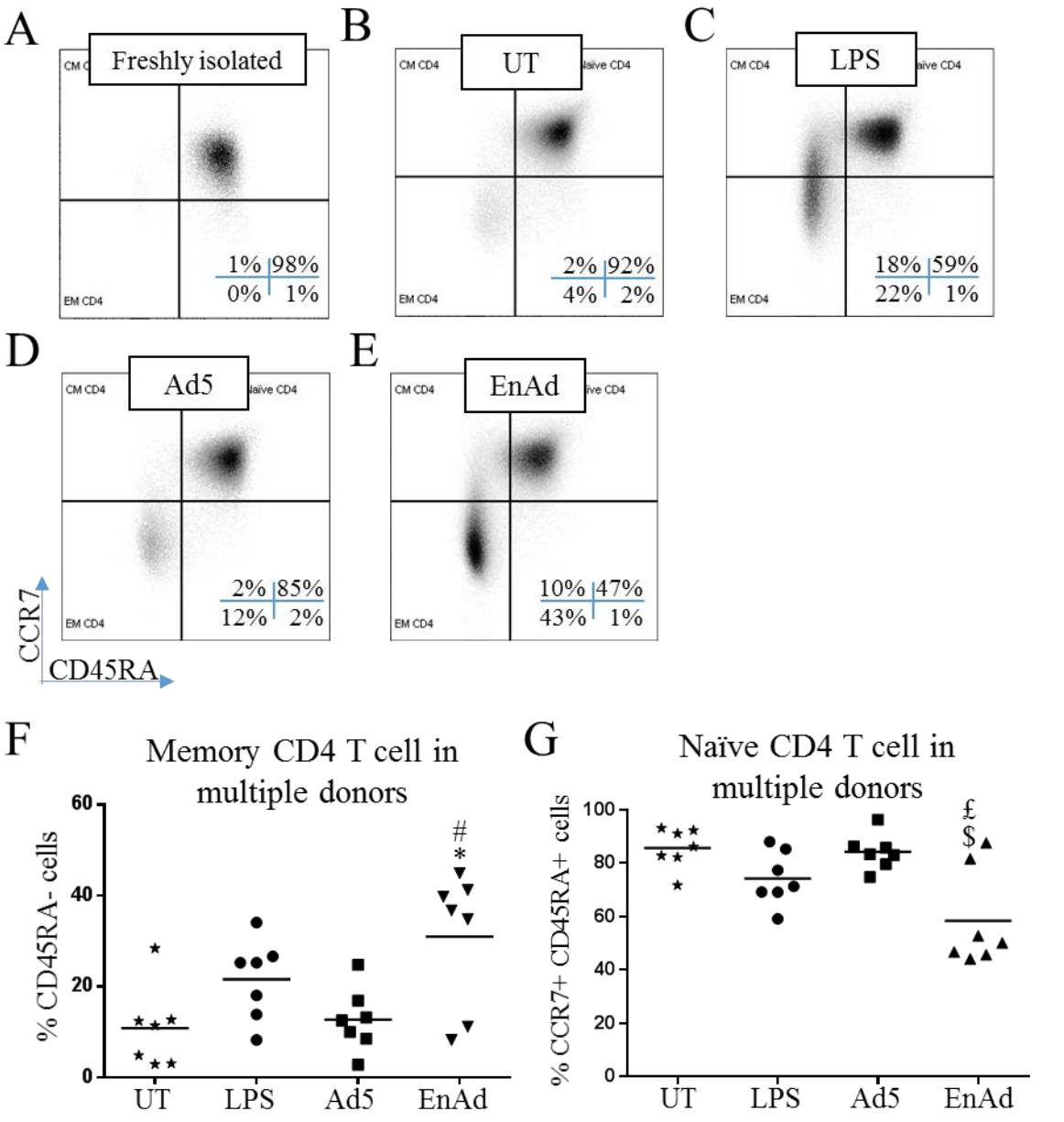


Figure 6.10 Comparison of naïve CD4 T cells differentiation after 9 days MLR with d3iDC treated with EnAd, Ad5 and LPS, or left untreated. d3iDC were treated with 500ppc of (D, square) Ad5 or (E, triangle) EnAd, (C, circle) 100 ng/ml LPS or (B, star) left untreated before cells were washed and mixed to freshly isolated naïve CD4 T cells, accordingly with Figure 6.9 timeframe. MLR cells harvested after 9 days or (A) the corresponding freshly isolated naïve CD4 T cells, were stained with directly-labelled monoclonal anti-CCR7 and anti-CD45RA antibodies (Biolegend), in addition to the Figure 6.4 staining. Cells were acquired on flow cytometry, live CD4+ T cells were gated accordingly with Figure 6.4 strategy and gated cells were dot plotted in a CCR7 vs CD45RA graph. The percentage of (F) memory (CD45RA-) and (G) naïve (CCR7+CD45RA+) live CD4+ T cells were assessed for 7 independent MLR combinations, and the treatment's average were compared using paired-t Test. The average of % CD45RA- for EnAd condition is significantly different to untreated (#p=0.0166) and Ad5 (*p=0.016). The average of % CCR7+CD45RA+ for EnAd condition is significantly different to untreated (£p=0.0144) and Ad5 ($p=0.017).

6.3.7.2 Evaluating the proliferation of naïve CD4 T cells exposed to EnAd- and Ad5-treated d3iDC cells over the course of 9 days of MLR assay

Induction of T cell proliferation was assessed in the MLR after 9 days by flowcytometry quantification of total living CD4+ T cells (Figure 6.9). Interestingly, treatment with EnAd particles stimulated almost 10-fold more living CD4 T cells (Figure 6.11 D) compared to untreated controls (Figure 6.11 A), whilst Ad5 and LPS treatments had only small effects (Figure 6.11 C and B).

The total number of viable CD4 T cells was also used to calculate the proliferation ratio across seven independent experiments, by dividing the output of living CD4+ T cells against the starting input. Thus, any value of one or above meant the cells had proliferated, as naive CD4 T cell are sensitive to *in vitro* culture and die if un-primed[275]. Accordingly, a value less than one probably reflected little or no proliferation, suggesting no T cell priming. All independent MLR combinations that were treated with EnAd had a ratio above one, with an overall average across independent experiments of 1.71, meaning that EnAd-treated d3iDC promoted a growth of CD4 T cells relative to input. LPS treatment displayed a ratio average of 0.97, while Ad5-treated and untouched d3iDC displayed averages of 0.64 and 0.53, respectively (Figure 6.11 E). This is consistent with EnAd-treatment yielding effective priming of naïve T cells, with Ad5 showing little effect.

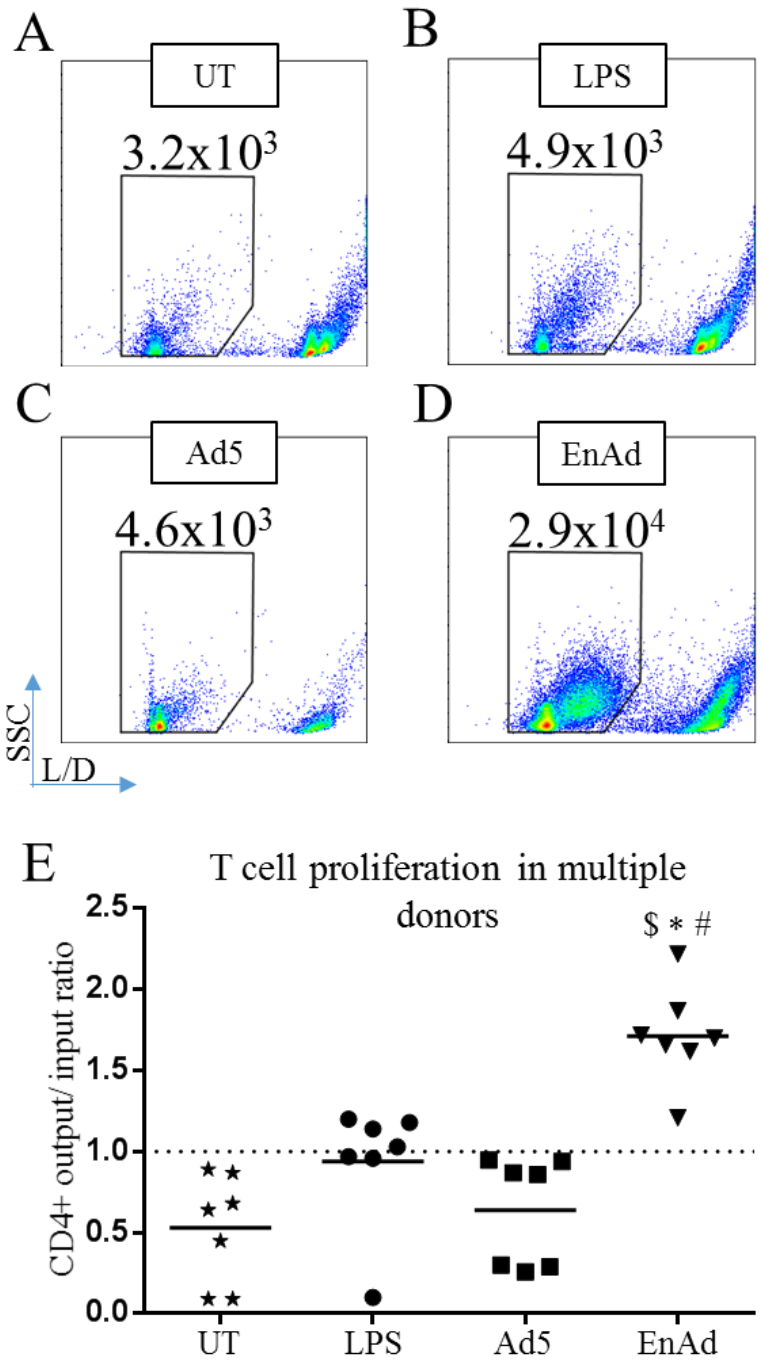


Figure 6.11 Comparison of live CD4 T cells and proliferation after 9 days MLR with d3iDC treated with EnAd, Ad5 and LPS, or left untreated. The live CD4T cells from (C) Ad5, (D) EnAd, (B) LPS or (A) untreated condition, obtained by flow cytometry assay corresponding to Figure 6.10, are shown for one MLR combination. Alternatively, the T cell proliferation ratios were calculated dividing the total live CD4+ T cells output (obtained in the flow cytometry assay corresponding with Figure 6.10) by the live CD4+ T cell input (obtained during purity assessment of freshly isolated CD4 cells before MLR) for each condition. (E) The proliferation ratio average of 7 independent MLR combinations are shown for EnAd (triangle), Ad5 (square), LPS (circle) or untreated (star) conditions. The proliferation ratio averages are compared between treatments using paired-t Test. EnAd's proliferation ratio average is significantly different to untreated ($p=0.0021), LPS (*p=0.0173) and Ad5 (#p<0.0001).

6.3.7.3 Studying EnAd- and Ad5-treated d3iDC for their effect on the polarisation of naïve CD4 T 'primed' in a 10 days MLR assay

As previously mentioned, the properties of polarised helper T cells direct the type of adaptive immune response obtained. Each of the T_H types produces a measurable set of cytokine mediators that can be used to determine the polarisation. Up to date, the most relevant Th types and corresponding secreted cytokines are: IFN-g and TNF-a for T_H1; IL-4, IL-5, IL-10 and IL-13 for T_H2; IL-10 and transforming growth factor beta (TGF-b) for regulatory T cells and IL-17 for T_H17. An extended version of T_H and cytokines can be seen on Table 6.1.

The aim of this section was to investigate how EnAd-treated DC would polarise naïve CD4 T cells (and to infer the type of adaptive response that would ensue), and to compare it to Ad5 or LPS treatment as well as untreated d3iDC. However it was suspected that the polarising T_H2 IL-4 detected in d3iDC would polarise the adaptive response towards T_H2, especially when the T_H1 polarising IL-12 was not seen in EnAd-treated d3iDC (Chapter 4, section 4.3.3.2). Commonly the polarisation of primed CD4 T cells is investigated after cells are polyclonally re-stimulated. Accordingly, the 9 day MLR assay CD4 T cells were polyclonally stimulated with DynaBeads for 24hrs before assessing the polarisation (see Figure 6.9 and Materials and Methods). Harvested cells were stained with CD4 T cell staining panel (shown in Figure 6.4), and combined with intracellular staining with monoclonal antibodies against IFN-g, TNF-a, IL-4, IL-5, IL-10, IL-13 and IL-17 (see Material and Methods). Cells were acquired on flow cytometry and gated on live CD4+ T cells. Cytokine+ events were used to calculated the percentage of live CD4+ T cells positive for each polarisation marker. This was repeated in multiple independent experiments using cells from different donors (n=8).

Interestingly, only IFN-g and TNF-a staining appeared to be measurable, independent of the treatment and across donors. In contrast the other cytokines were generally very low or not found (Figure 6.12 A). When comparing between treatments across multiple independent MLR

combinations, treatment with EnAd showed a significantly higher average of IFNg+ cells (25.68%) than untreated (7.19%), Ad5-treated (9.67%) and LPS-treated (7.65%) (Figure 6.12 B). Treatment with EnAd also induced a significantly higher average of TNF-a+ cells (8.84%) in comparison to untreated (2.66%) and Ad5-treated (3.24%), whereas the TNF-a+ average was also increased with LPS treatment (7.01%) (Figure 6.12 C). The high numbers of IFN-g+ and TNF-a+ cells in all treatments and across donors, suggested that this assay was T_H1 biased, despite the T_H1 polarising cytokine IL-12 was not being detected in d3iDC (Figure 4.4). This was surprising as T_H2 cytokines (IL-4, IL-5, IL-10 and IL-13) were expected, since IL-4 cytokine had been previously detected in d3iDC (Figure 4.4). Nevertheless, treatment with EnAd gave a greater proportion of T_H1 cytokine+ cells relative to Ad5-treated and untreated conditions, whilst the proportions of cells positive for other T_H cytokines remained low or undetectable.

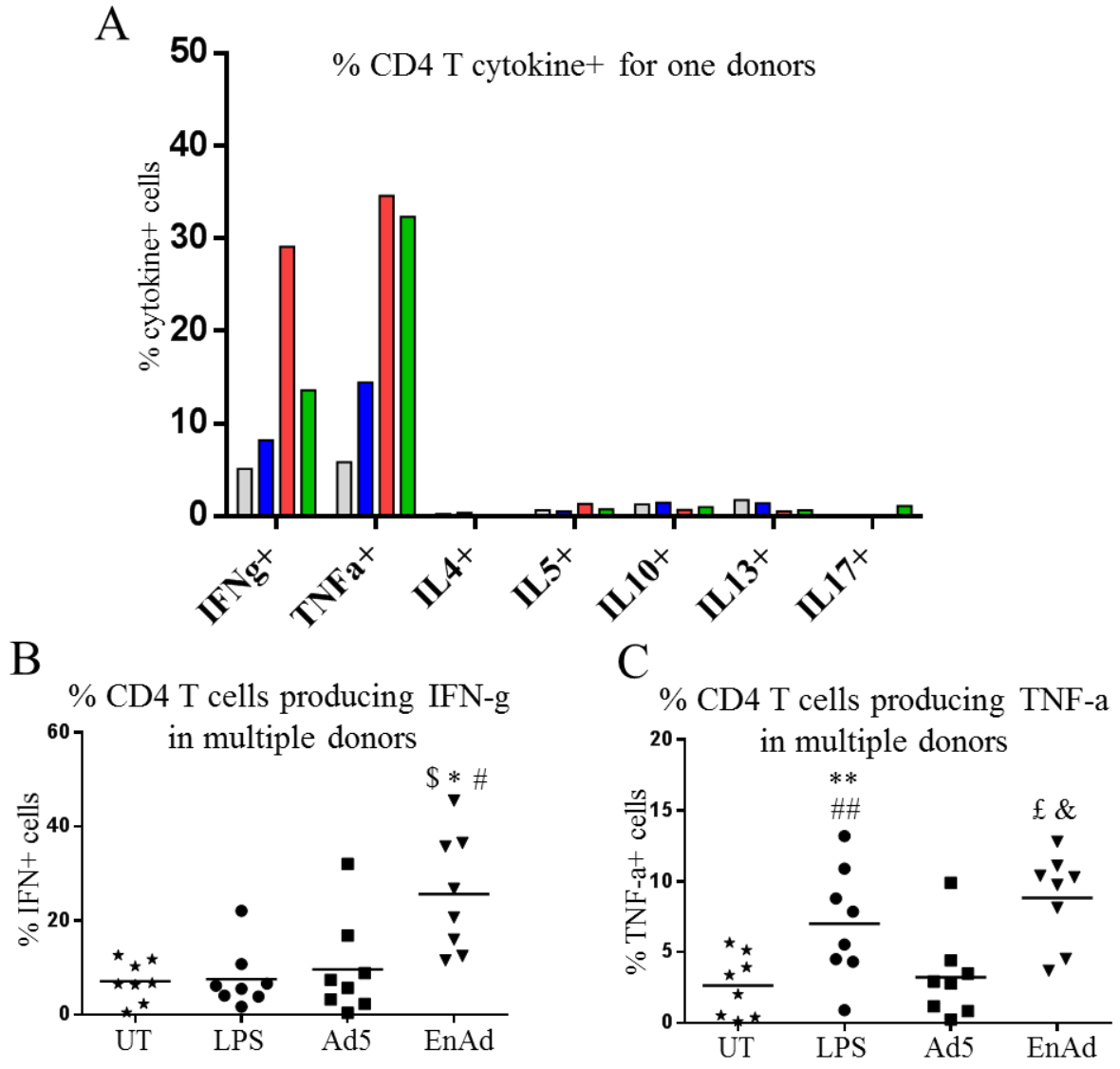


Figure 6.12 Comparison of intracellular cytokine expression on polyclonally re-stimulated CD4 T cells after 9 days in MLR with d3iDC pre-treated with Ad5, EnAd, LPS or untreated. d3iDC were treated with 500ppc of (blue) Ad5 or (red) EnAd, (green) 100 ng/ml LPS or (grey) left untreated, later cells were washed and mixed to freshly isolated naïve CD4 T cells, before T cells were re-stimulated with Dynabead T-activator, accordingly with Figure 6.9 timeframe. One day later supernatants were snap frozen and cells were harvested for intracellular staining (see material and methods) with directly-labelled monoclonal anti-IFN-g, anti-TNF-a, anti-IL-4, anti-IL-5, anti-IL-10, anti-IL-13 and anti-IL-17 antibodies (Biolegend), in addition to the staining from Figure 6.4. Cells were acquired on flow cytometry, live CD4+ T cells were gated accordingly with Figure 6.4 strategy and used to assessed the percentage of cytokine+ CD4 T cells. (A) The proportions of cytokine+ CD4 T cells of one donor is shown for all assessed cytokines, representative of 8 independent MLR combinations. The percentage of live CD4+ T cells (B) IFN-g+ and (C) TNF-a+ are shown for EnAd (triangle), Ad5 (square), LPS (circle) or untreated (star) conditions for 8 independent MLR combinations. The % of cytokine+ averages are compared between treatments using paired-t Test. The % of IFN-g+ average of EnAd condition is significantly different to untreated ($p=0.0049), LPS (*p=0.0113) and Ad5 (#p=0.0067). The % of TNF-a+ average of EnAd condition is significantly different to untreated (£p=0.0006) and Ad5 (&p=0.0015). The % of TNF-a+ average of LPS condition is significantly different to untreated (£p=0.0054) and Ad5 (&p=0.0274).

The second method used to assess T cell polarisation was a commercially available 13-multiplexed bead immunoassay (LEGENDplex Human T_H Cytokine Panel, Biolegend) that allows flow cytometric quantification of soluble cytokines from specific helper T cell types (Table 6.1).

T_H type	T_H 1	T_H 2	T_H 9	T_H 17	T_H 22	Treg
Markers	IL-2 IFN-g TNF-a	IL-4 IL-5 IL-13 IL-10	IL-9	IL-17A IL-17F IL-21 IL-6	IL-22	IL-10

Table 6.1 The 13 cytokines measured with the 13-LEGENDplex Human T_H Cytokine Panel (Biolegend) and the corresponding helper T cell type known to express them.

Supernatants from 24hrs polyclonal re-stimulation were assayed according to the manufacturer's protocol (see Materials and Methods). The raw cytokine values showed a large secretion of three cytokines in particular and independent of treatment; IL-2, IFN-g and TNF-a. Whilst, most of the other cytokines showed lower levels near the limit of detection – for instance IL-4, IL-5, IL-6, IL-10 and IL-13 – or under the limit of quantification – IL-9, IL-17A, IL-17E, IL-21 and IL-22 – (Figure 6.13 A). This further supported the notion that the assay was T_H1 deviated, although there was also considerable inter-donor variation. Therefore, the cytokines quantified above the limit of detection were normalised against the corresponding total number of live CD4+ T cells quantified in the intracellular staining shown above (Figure 6.12). The cytokine normalisation to CD4 T cells revealed that EnAd significantly up-regulated the average of IFN-g and IL-4 cytokines per cell relative to untreated control, as well as Ad5 and LPS conditions (Figure 6.13 B and E). Whilst no other significant differences were seen for the other quantifiable cytokines, these being IL-2, IL-5, IL-6, IL-10, IL-13 and TNF-a (Figure 6.13 C-D and F-I).

The increase in supernatant of IL-4 by EnAd virus was unexpected, since intracellular IL-4 was generally undetected (Figure 6.12 A). It was also unexpected because IFN-g (T_H1 cytokine) and IL-4 (T_H2 cytokine) have been reported to be mutually exclusive in helper T cells[211]. However, when a ratio of IFN-g/IL-4 was calculated using the average of cytokine concentration/cell between MLR combinations, EnAd treatment was inclined towards IFN-g (144.06 units of IFN-g per IL-4) whilst untreated cells leaned towards IL-4 (115.23 unit of IFN-g per IL-4). Thus, suggesting that EnAd promoted more IFN-g expression for every IL-4 in this system despite the lack of T_H1 polarising cytokine IL-12. Alternatively, it was possible that the detected soluble IL-4 was produced by the d3iDC – present throughout the duration of the experiment. As in Chapter 4 it was shown that EnAd virus induced on d3iDC the secretion of IL-4 cytokine (Figure 4.4), which could justify why intracellular IL-4 was unseen in T cells (Figure 6.12).

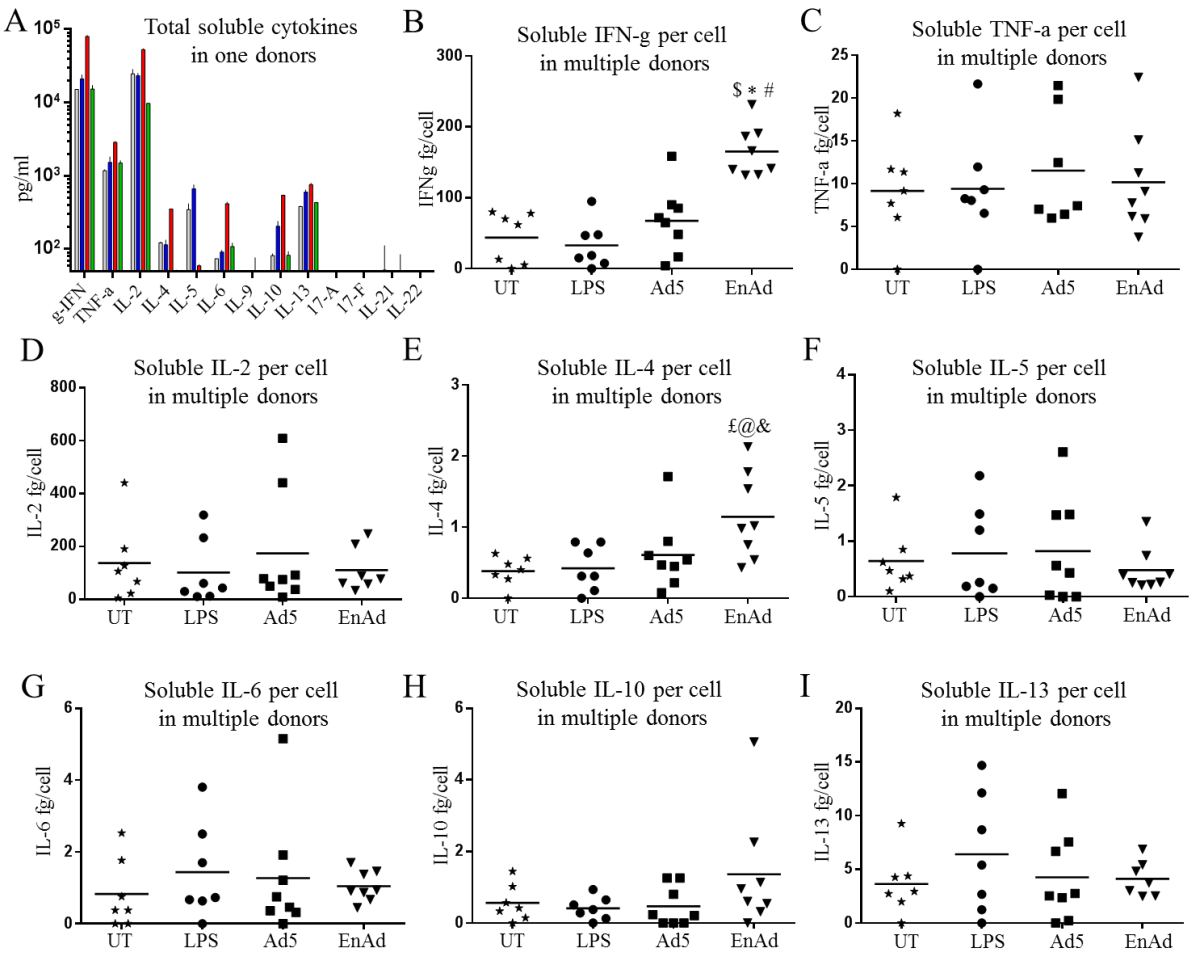


Figure 6.13 Comparison of soluble cytokine expression on polyclonally re-stimulated CD4 T cells after 9 days in MLR with d3iDC pre-treated with Ad5, EnAd, LPS or untreated. The frozen supernatant generated in re-stimulation MLR shown in Figure 6.12, were used to quantify soluble cytokines with 13-LEGENDplex Human Th Cytokine Panel (Biolegend), according to manufacturer's protocol. (A) The total measured cytokines for EnAd (red), Ad5 (blue), LPS (green) and untreated (grey) conditions for one MLR combination is shown. Alternatively, only the cytokines detected above the limit of detection were normalised per live CD4+ T cells output, accordingly quantified by flow cytometry in Figure 6.12. The femtograms per live CD4+ T cells for (B) IFN-g, (C) TNF-a, (D) IL-2, (E) IL-4, (F) IL-5, (G) IL-6, (H) IL-10 and (I) IL-13 are shown for EnAd (triangle), Ad5 (square), LPS (circle) or untreated (star) conditions across 8 independent MLR combinations. The cytokine fg/cell averages are compared between treatments using paired-t Test. The IFN-g average for EnAd condition is significantly different to untreated ($p=0.0006), LPS (*p=0.0002) and Ad5 (#p=0.0023). The IL-4 average for EnAd condition is significantly different to untreated (£p=0.0186), LPS (@p=0.0142) and Ad5 (&p=0.0221).

6.3.7.3.1 Intranuclear staining of T-bet and GATA3 transcription factors to evaluate the polarisation bias of the 10 days MLR assay

Whilst the intracellular staining in previous section suggested that EnAd-treated d3iDC polarised naive CD4 T cells into T_H1 phenotype, the soluble cytokines added ambiguity as mutually exclusive T_H1 cytokine and T_H2 cytokine were simultaneously upregulated following treatment with EnAd. It was therefore hypothesised that the soluble IL-4 was produced by d3iDC and the MLR model was biased towards T_H1 polarisation, even though the T_H1 polarising cytokine IL-12 was not detected in the system. In this section, intranuclear staining (see Materials and Methods) of transcription factor GATA-binding-protein-3 (GATA3) and T-box-expressed-on-T-cells (T-bet), were used in combination with the CD4 T cell gating strategy (Figure 6.4), on CD4 T cells after being polyclonally re-stimulated for 24hrs, accordingly with experiment layout (Figure 6.9). GATA3 is a transcription factor involved in T_H2 phenotype, whereas T-bet is a transcription factor that promotes T_H1 features[276]. Both transcription factors determine the expression of the previous assessed cytokine markers and was thought it would help better identify the T_H type.

Interestingly, the MLR with untreated d3iDC lead to 9% single GATA3+, 2% single T-bet+, 5% double T-bet+GATA3+ CD4 T cells, and the remaining double negative (Figure 6.14 A). In other words, the MLR process (without any virus) polarised cells into a ratio of two T_H2 cells for every T_H1 cell, with the majority of polarised cells being single GATA3+. In contrast d3iDC that had been exposed to EnAd, 2% cells were single GATA3+, 2% single T-bet+, 34% double T-bet+GATA3+ and the rest double negative (Figure 6.14 B). This provides evidence that EnAd-treatment of d3iDC raised the proportion of polarised CD4 T cells although to a similar proportion between T_H1 and T_H2, as most cells were double positive T-bet/GATA3. Given that the untreated condition suggests that d3iDC might have an underlying T_H2 polarisation, probably mediated by the IL-4 produced by d3iDC. Treatment with EnAd may

non-specifically activate cells and promote a T_H1 bias on top of it T_H2-biased background, resulting in this ambivalent polarisation.

Although it appears that EnAd may favour a T_H1 polarisation via d3iDC independently of IL-12 cytokine, considerable further assessment is needed before it would be possible to assert EnAd leads to T_H1 polarisation via TIDCs.

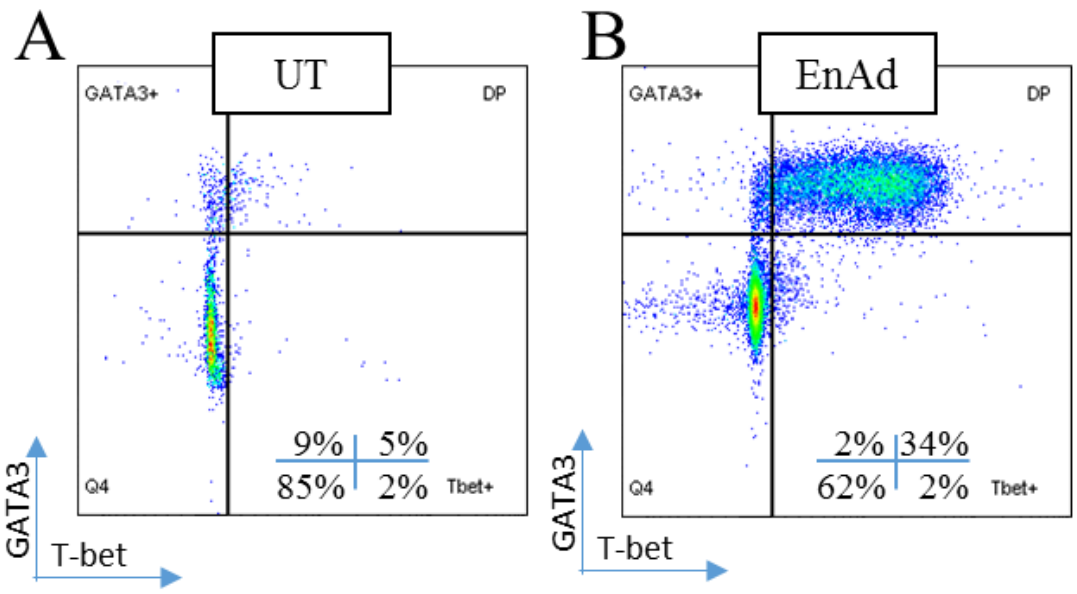


Figure 6.14 Assessemnt of GATA3 and T-bet transcription factors on polyclonally re-stimulated CD4 T cells after 9 days in MLR with EnAd-treated or untreated d3iDC. (B) EnAd-treated and (A) untreated d3iDC were used accordingly with the same MLR model described in Figure 6.12. After 24hrs of polyclonal stimulation with Dynbead T-activator, cells were harvested for intranuclear staining (see Material and Methods) with directly-labelled monoclonal anti-GATA3 and anti-T-bet antibodies, in addition to the staining from Figure 6.4. Cells were acquired on flow cytometry, live CD4+ T cells were gated accordingly with Figure 6.4 strategy. The gated live CD4+ T cells are shown in a GATA3 vs T-bet dot plotted with the percentage for GATA3+, double positive, Tbet+ and double negative for one MLR, representative of three independent combination MLR.

6.4 Chapter summary

1. Small doses of EnAd virus particles mediate a powerful activation on allogeneic CD4 T cell via d3iDC in a mixed leukocyte reaction. Whereas the same concentration of Ad5 virus particle results in a poor T cell activation, similar to untreated d3iDC. T cell activation can be further enhanced with anti-PD-L1 blocking antibody, independently of d3iDC's treatment.
2. EnAd-infected A549 cancer cell line largely activate CD4 T cell via d3iDC. In contrast, Ad5 virus appeared to inhibit T cell activation below the allogeneic stimulation background.
3. Free EnAd particles alone do not appear to induce T cell activation. However, CD69 T cell activation marker is sensitive to EnAd and anti-CD46 antibody when TCR is crosslinked, but IL-2 and IFN-g activation markers remain un-affected.
4. EnAd-treated d3iDC promoted a strong proliferation of naïve CD4 T cells and differentiation into memory phenotypes in an MLR assay. The same concentration of Ad5 virus particles failed to induce proliferation or differentiation of naïve CD4 T cells.
5. The extended (9 days) MLR model with polyclonal re-stimulation shows an ambivalent underlying polarisation bias on CD4 T cells, and EnAd treatment induces a dual T_H1/ T_H2 polarisation compared to the other treatments. However, most of the T_H1 markers assessed are strongly detectable following treatment with EnAd, whilst only secreted IL-4 and transcription factor GATA3 are seen for T_H2 markers.

6.5 Chapter discussion

6.5.1 Discussion of results

The aim of this chapter was to investigate whether the strong adjuvant effect EnAd promoted on TIDC-like cells, shown in Chapter 4, was functional to prime T cells. In addition to compare the effects of EnAd with Ad5 virus and LPS stimulation. Moreover, the polarisation of adaptive immune response was also investigated, to extrapolate whether it could promote and synergise with cancer immunotherapy.

Comparing the activation of adaptive immunity by APC treated with different adjuvants, with inherently different antigenic composition, can be difficult for multiple reasons; 1) antigen-experienced T cells can be found in individuals that have been previously exposed to the antigen, which are activated when re-exposed to the antigen[277]. For instance, studies describing the frequency of neutralising antibodies in humans for multiple human adenovirus suggest that a large number of population have been exposed to Ad5 whilst a limited number have to Ad11p[106]. It is likely that in an autologous model Ad5 results in a better T cell stimulation. 2) Within the genetic diversity of MHC, some polymorphisms have been shown to preferentially present specific antigens and unable to present others[278], this could well lead to one virus having particular peptides presented that are missing on the other virus. 3) LPS is a polysaccharide without protein antigens (as well as untreated condition), hence the adjuvant properties are hardly comparable to viruses. These outlined reasons provide un-comparable TCR 'signal 1' across treatments to purely assess the adjuvant role. Alternatively, in an allogenic recognition, TCR strongly recognises non-self MHC independently of epitope[269], providing a normalised T cell activation signal 1 across adjuvant treatments.

Hence, it was not surprising to discover that d3iDC treated with small dose of EnAd strongly activated CD4 T cells relative to the MLR background (Figure 6.3, Figure 6.5 and Figure 6.6),

as Chapter 4 showed that EnAd up-regulated HLA-DR (or 'signal 1') on the skewed DCs, as well as the costimulatory molecules (or 'signal 2'). In the same manner, it was not surprising to see a poor T cell activation with the same Ad5 dose because this virus already had a poor effect on the up-regulation of ligands for 'signal 1' and 'signal 2' on d3iDC (seen in Chapter 4) (Figure 6.3, Figure 6.5 and Figure 6.6). Better T cell activation rates were achieved using higher concentration of Ad5 virus (5000ppc) (Figure 6.6), also in accordance with the dose-response described in Chapter 4 (Figure 4.6).

In addition to the up-regulation of TCR ligand and positive costimulatory molecules EnAd virus also upregulated the programmed-death ligand 1 on d3iDC cells (Figure 4.1 and Figure 4.3). PD-L1 is the ligand of immune checkpoint programmed death-1 expressed on T cells, well known for inducing tolerance of effector cells in the peripheral tissues. PD-L1 is reportedly up-regulated in the tumour, contributing towards the immune evasion by tumour cells[27]. In fact, PD-1/PD-L1 inhibitors are currently showing therapeutic effects in cancer patients[2]. Accordingly, an anti-PD-L1 blocking antibody was used in the MLR system to further activate T cells, which was achieved independently of the treatment given to d3iDCs (Figure 6.6), probably due to the basal PD-L1 levels seen in d3iDC. Alternatively, PD-L1 was previously shown on A549 cells by colleagues and others[272]. In this chapter, an *in vitro* MTLR model using A549 cells suggested that EnAd might activate T cells through DC, even in the presence of suppressive signals from the tumour (Figure 6.8). In any case, it is sound to combine the vaccination properties of EnAd with antibodies against PD-1/PD-L1 axis. In fact, this work contributed to set ground for a clinical trial, in which EnAd is combined with Bristol-Myers Squibb's anti-PD-1 Nivolumab (clinical trials identifier: NCT02636036).

Nevertheless, the stimulation of T cell in presence of free EnAd virus particles like in the MTLR model (Figure 6.7) or in direct interaction studies (Figure 6.8) appeared controversial. In a previous report, human adenovirus type 35 supressed T cell activation via CD46

engagement[273]. Recent preliminary studies in which polyclonally stimulated CD4 T cells were then exposed to EnAd or Ad5 virus particles or no-virus, resulted with the same T_H cytokine profile (not shown). Subtle differences between Ad35 and Ad11p fibre knob shown by X-ray crystallography, were predicted to translate in slightly different virus-CD46 interactions[250]. In another report, single point mutations were introduced in Ad35 fibre knob, which resulted in either further supressing or enhancing the T cell activation, depending on the mutation. Altogether, it is plausible that the fibre knob differences between both virus yield different effect on T cell activation[279].

Intriguingly, Ad5 supressed T cell activation compared to the background activation of the MTLR assay (Figure 6.8). In fact, in Chapter 4 it was already shown that Ad5 infecting A549 was quite poor in up-regulating HLA-DR and costimulatory molecules on the skewed DC (Figure 4.10). Nevertheless, in this chapter, the inhibition of T cell activation with Ad5 appears to be mediated by A549 cells and independent of dendritic cells (Figure 6.8). Perhaps this can be explained by the expression of specific Ad5 virus genes in A549, for instance E3 immunomodulatory genes which can inhibit anti-viral immune responses[107], and which are largely deleted in EnAd (see Introduction). Although further investigation would be needed, EnAd E3 deletion might be a relevant feature to drive anti-tumour immunity, although it might simultaneously be detrimental to the virus infection.

After naïve CD4 T cells are successfully primed for a specific epitope, cells clonally expand and differentiate into effector and central memory cells. Both proliferation and differentiation were found in naïve CD4 T cells that had been cultured with EnAd-treated d3iDC (Figure 6.10 and Figure 6.11). Nevertheless, T cell proliferation was weak and nearly all CD4 T cells had retained the initial naïve phenotype when the MLR was performed with untreated d3iDC or Ad5-treated (Figure 6.10 and Figure 6.11). Poor ability to stimulate proliferation and differentiation on T cells can be considered a sign of tolerogenicity, often associated with the

tumour infiltrating DC[40,43-45]. Accordingly, this could be interpreted as another feature – along those mentioned in Appendix, Part B – d3iDC and TIDC cells share. Evermore, this would weaken the position of Ad5 virus as TIDC stimulant to prime vaccination in a cancer environment.

In addition to influencing T cell activation, proliferation and differentiation, dendritic cells also secrete specific cytokines (signal 3) that polarise helper CD4 T cells (Th) into different types. Polarised helper CD4 T cells will then mediate the subsequent effector immune response. Typically, when antigen presenting cells sense viruses they express IL-12, which is needed for polarising CD4 cells into T_H1 and mediate the cellular immunity to kill the infected cells, which is equally needed in anti-cancer immune response[41]. However, IL-12 was not detected on EnAd-treated d3iDC, and instead IL-4 T_H2 polarising cytokine was found in some donors (shown in Chapter 4). T_H2 is generally related with humoral responses against parasites and the inhibition of the anti-tumour cellular immunity[211].

An extended version (9 days) of MLR system was used to understand the type of polarisation the skewed DC would promote, and whether the virus could change it. However, characterising the polarisation of CD4+ T cells with this model was confusing due to the ambivalent expression of IFN-g and TNF-a T_H1 markers and GATA3 T_H2 marker in the MLR with untreated d3iDC (Figure 6.12, Figure 6.13 and Figure 6.14). Although, this has also been reported by others when using immature DC[270,280], T_H1 and T_H2 are generally considered to be mutually exclusive. Interestingly, this ambivalence was further increased following EnAd treatment, but all the assessed T_H1 markers (IFN-g, TNF-a, T-bet) were generally strongly expressed, whilst only one subset of T_H2 markers (soluble IL-4 out of IL-5, IL-10, IL-13 and intracellular IL-4) was found (Figure 6.12, Figure 6.13 and Figure 6.14), which was suspected to be secreted by the d3iDC. Nevertheless, the high levels of secreted IFN-gamma with EnAd

were re-comforting, as this cytokine can directly supress tumour growth, activate cytotoxic CD8 T cells, and inhibit immune-suppressive cells, as extensively reviewed by Parker *et* al.[281]. Despite MLR not being the most suitable model to characterise the polarisation of the immune response, it is likely that EnAd promotes cellular immunity, like most cytopathic viruses do[55]. Overall, EnAd might be a better adjuvant candidate than Ad5 to stimulate TIDCs, and together with the tumour antigens derived from its oncolytic activity, may functionally prime the right mediators for an anti-tumour immune response and potentially synergise with other immunotherapy strategies. However, further research is needed to fully understand how EnAd can promote T_H1 response without IL-12, and evaluate whether this cytokine or others should be encoded in the genome of EnAd.

6.5.2 Limitations and future work

In this chapter, it was shown that EnAd-treated TIDC-like cells primed naïve CD4 T cells in an MLR assay, better than Ad5 or LPS treatment or untouched cells. However, the MLR model was not very effective to indicate the type of polarisation induced by EnAd adjuvant treatment. Future experiments should aim to investigate the polarisation of naïve CD4 T cells using an *in vitro* autologous human system. Maybe by sourcing the TIDC-like cells from other means in which same donor CD4 T cells can be maintained without infringing the Human Tissue Act. For instance, isolating TIDCs directly from ascites or pleural fluids[233]. Plasmacytoid DCs, which are known to have tolerogenic functions and are easily isolated from PBMCs[282], could alternatively be used.

It is possible that EnAd virus particles only mature the TIDC cells, without prompting a switch on the secreted cytokines needed for a T_H1 polarisation, as seen in Chapter 4. In such case, it might be interesting to encode the T_H1-polarasing IL-12 cytokine within the genome of EnAd. Following this strategy, other immunomodulatory agents known to favour T_H1 adaptive

immune responses, such as IFN-g cytokine or molecules to deplete soluble IL-10[283], might raise as promising payloads too.

In this chapter, it was also described that anti-PD-L1 blocking antibody improved the priming of T cell mediated by EnAd-treated dendritic cells. However, the suppression of effector T cells derived from the PD-L1/PD1 interaction is generally associated to peripheral tissues, for instance the direct suppression of CTLs by cancer cells[27]. Consequently, in the future it might be interesting to arm EnAd with either anti-PD1 or anti-PD-L1 blocking antibodies to further unleash the anti-cancer immune response potentially induced by the virus. On the other hand, since CTLA-4 is an immune checkpoint of the T priming phase in the lymph nodes[284], anti-CTLA-4 blocking antibodies might be better off given in combination treatment with EnAd, rather than expressed by the virus in the tumour.

CD46 is often referred as the 'pathogen magnet' for being the receptor of numerous pathogens[247]. Some have shown that CD46 can supress T cell activation[247,285], a fact that would justify why some many pathogens interact with this receptor. However CD46 engagement is controversial, as other reports claim that CD46 is a T cell costimulatory molecule[248]. In adenovirus field, a previous report showed that group B Ad35 supressed T cell activation via CD46[273], however, this was not seen with EnAd virus in this chapter. The unclear evolutionary advantage for multiple pathogens to bind to this receptor, entails further investigation on the direct interaction between EnAd and T cells, to ensure EnAd will not spoil cancer immunotherapy.

7 Discussion

7.1 Summary and discussion of results

7.1.1 Assessing the virus and cellular factors involved in the oncolytic activity of EnAd

This thesis describes the increased oncolytic potency, more efficient replication and extra virus progeny production of EnAd compared to Ad11p virus, in colorectal carcinoma HT29 cells. Recombinant EnAd viruses with single replacements of mutated regions with Ad11p wildtype sequence were used to explore the roles of the three mutant regions. EnAd containing a wild type E3 region showed properties indistinguishable from the parental virus, suggesting that the loss of E3 genes is not important in driving the potency of EnAd, neither does the smaller genome size of EnAd seem to be of central importance. However, the other two genetic mutations did influence virus activity, though not as initially predicted. Notably EnAd-wtE2B (which is modified to contain the E2B region of the wild type Ad11p virus and encodes a hybrid DNA polymerase the terminal protein) showed comparable genome replication kinetics to EnAd itself, although the progeny virus production was initially slower and its oncolytic potency was reduced relative to EnAd virus. On the other hand, EnAd-wtE4 recombinant virus (containing the Ad11p wild type E4 region) displayed reasonable cell killing and virus genome replication in transformed cell lines, yet it was inefficient at producing fully mature and infectious virus particles. These observations suggested that neither the E2B nor E4 mutations was sufficient on its own to drive the potent EnAd phenotype, indeed both changes alone seemed to attenuate virus activity. Taken together, these data suggest that the individual changes are not sufficient to explain the increased potency of EnAd, although when present together they appear to complement each other in contributing to the improved oncolytic

phenotype of EnAd. This may rely on the interplay of virus mechanisms that have not yet been delineated, and further interrogation of the activity of the recombinants could yields additional mechanistic insights.

A chemical drug panel was used in combination with EnAd, aiming to find agents and/or cellular targets with the potential to increase the EnAd virus production. The main output from this study was the observation that several mTOR inhibitors and microtubule inhibitor families increased EnAd genome replication in HT29 cells. These two families of compounds were further used to evaluate the effects on virus gene expression (virus mRNA and virus protein) and virus production. Despite Vincristine and Plinabulin MT inhibitors caused a significant increase in virus replication, both agents resulted in decreased virus progeny production, virus protein and mRNA expression. On the contrary, Everolimus, WYE-354 and KU-0063794 mTOR inhibitors slightly increased the virus replication, but also augmented the virus progeny production and the virus gene expression. Therefore, the virus genome replication does not necessarily correlate with more virus progeny. These data may also indicate that the late virus gene expression (encoding capsid proteins) might be a better indicator for infectious EnAd virus production.

7.1.2 The adjuvant effect of EnAd virus on TIDC-like cells

The oncolytic activity of viruses is believed to release PAMPs and DAMPs that can activate tumour-associated antigen presenting cells. In conjunction with tumour antigens, also released by oncolysis, this may allow stimulation of an anti-cancer immune responses. However, APCs within tumours, such as tumour-infiltrating DCs (TIDCs), have been shown to poorly present tumour antigens and sometimes contribute to immune suppression. With this in mind, EnAd was tested as an adjuvant to determine whether it could stimulate TIDC to functionally prime anti-cancer immune responses. As a benchmark it was compared against adenovirus type 5,

considered the adenovirus archetype and which has already seen extensive development as an oncolytic agent.

Relatively low doses of EnAd virus particles showed considerable adjuvant effects on a TIDC-like model – d3iDC, generated from human monocytes isolated from PBMCs – by up-regulating cell-surface markers such as antigen presenting molecules (HLA-DR), costimulatory receptors (CD80/86) and lymph-node trafficking molecules (CCR7). Also, EnAd promoted the secretion of pro-inflammatory factors and chemokines such as IL-6, ICAM, CCL2, CCL3/4, CCL5 and CXCL10, and the adaptive immune polarising cytokine IL-4. This suggest that tumour-infiltrating DCs encountering EnAd virus particles, might promote pro-inflammatory TME conditions, attracting immune cells to the tumour. At the same time TIDCs may then be more competent to prime CD4 T cells. Interestingly, EnAd virus particles appeared to induce a greater adjuvant effect on TIDC-like cells than the same concentration of Ad5 virus, although both induced a dose-response curve.

Tumour cells are thought to nurture the TIDC into an immune-suppressive phenotype. The cancer cell killing mechanism of EnAd, oncosis, is known to release large quantities of DAMPs[187]. These danger signals are broadly considered as an important part for the immune-virotherapy by stimulating the local innate cells. An *in vitro* co-culture of TIDC-like cells and EnAd-infected A549 cancer cells suggested that the consequences of EnAd oncolysis (progeny virus particles and DAMPs) was a strong TIDC adjuvant which might be capable of overcoming the potential modulation provided by tumour cells. In further studies, it appeared that the DAMPs probably only had a minor role on the stimulation of TIDC-like cells, at least in this experimental system, and EnAd virus particles held most of the adjuvant effect.

Overall, EnAd virus particle released from infected cancer cells are likely to stimulate TIDCs into a new phenotype, which might be more competent to prime T cells. However, it is possible that EnAd only can promote maturation and pro-inflammation on TIDCs, but fail to polarise a

T_H1 adaptive immune response against the tumour, as EnAd-treated TIDC-like cells only secreted T_H2 polarising cytokine IL-4, whilst T_H1 polarising cytokine IL-12 was unseen.

7.1.3 The mechanism underlying the adjuvant effect of EnAd virus particles

Adenovirus type 5 activates strong immune responses and has been widely used as a vaccination platform[60]. In this thesis, it was seen that the group B oncolytic adenovirus EnAd was a better adjuvant of TIDC-like cells than Ad5.

The strong stimulation induced by EnAd particles on TIDC-like cells was clearly associated with its ability to bind CD46, rather than reflecting the expression of virus genes. On one hand, CD46 molecules were found to be expressed on the TIDC model, whilst CAR (the receptor for Ad5 and other group C adenoviruses) was untraceable. On the other hand, a CD46 blocking antibody prevented the adjuvant effect of EnAd. Yet, multiple experiments could not link the better stimulation of d3iDC to a CD46 signalling upon the virus attachment. Instead, the adjuvant effect in TIDC-like cells was thought to be associated to a significant virus uptake via CD46, as the blockade of this pathway placed EnAd uptake to equal levels of Ad5.

This is the first time that CD46 expression on dendritic cells has been implicated in the advantageous uptake of group B adenovirus particles compared to Ad5. It was therefore speculated that the advantageous uptake of EnAd translated into more PAMPs per cell, triggering the multiple pathogen recognition receptors within dendritic cells that are known to recognise adenovirus[104] and underpinning the efficient adjuvant effect seen with EnAd virus particles. In addition, Ad5 genome was shown to contain twice as much neutralising CpG than EnAd. CpG-N are TLR9 antagonists that counteract the unmethylated CpG (TLR9 agonists) also found on the adenoviruses genomes[252]. This was considered another potential mechanism that could improve the adjuvant profile of EnAd virus.

More interesting was to discover that adenovirus might express immunomodulatory E3 genes in dendritic cells, despite having all remaining virus genes silenced as well as any virus cycle-related activity. This expression mechanism may have been regulated by inflammation-related transcription factor NF-kB, which EnAd virus particles were found to trigger in the dendritic cell model. It is well known that the adenovirus E3 transcription promoter encodes several binding sites for NF-kB[172]. In fact, Ad5 had previously been shown to express E3 genes in T cells through NF-kB, thought to modulate the adaptive immune response[264]. It is reasonable to believe that adenovirus can use this mechanism to express the E3 proteins within innate immune cells and control the anti-viral immune response from earlier phases, although at this stage this is simply an unproven hypothesis.

7.1.4 Evaluating whether EnAd can sway T_H1 adaptive immune response

The cytokines, antibody isotype and effector cellular immunity mediated by T_H1, have been shown to be the most appropriate for an effective anti-tumour immune response[41]. With that in mind, this thesis questioned whether the previously described adjuvant effect of EnAd virus particles on tumour-infiltrating DCs, could help prime naïve CD4 T cells and polarise a T_H1 adaptive immune response. At the same time, EnAd was compared to other treatments. Due to the diverse nature of the adjuvants compared (potentially producing different 'signal 1' on T cell) and the Human Tissue Act limitations (storing CD4 T cells during the generation of TIDC-like cells), a mixed leukocyte reaction model was used instead to address this question.

Small doses of EnAd virus particles mediated a powerful activation on allogeneic CD4 T cell via TIDC, whereas the same concentration of Ad5 virus particle resulted in a poor T cell activation, similar to untreated TIDC-like cells. More interestingly, EnAd promoted the activation of CD4 T cells via the dendritic cells in a mixed tumour leukocyte reaction, overcoming suppressive signals from cancer cells[3] or the interaction with CD46 receptor[273],

whereas Ad5 had the opposite effect and supressed the activation of T cells. In addition, T cell activation could be further enhanced with anti-PD-L1 blocking antibody.

Separately, in an extended 9 days MLR, EnAd-treated TIDC-like cells promoted a strong proliferation of naïve CD4 T cells and functional differentiation into memory phenotypes. However, the same concentration of Ad5 virus particles failed to induce proliferation or differentiation, resulting in similar effect of untreated TIDC-like cells. This suggested that tumour infiltrating DC encountering EnAd virus particles, will probably functionally prime naïve CD4 T cells, whereas Ad5 virus particles are unlikely to be effective.

A final experiment to evaluate the polarisation of naïve CD4 T cells, using a 10 days MLR model with polyclonal re-stimulation, showed an ambivalent T_H1/T_H2 underlying polarisation bias on T cells. EnAd-treated TIDC-like cells further induced a dual T_H1/T_H2 polarisation compared to the other treatments. However, most of the T_H1 markers (secreted and intracellular IFN-g, intracellular TNF-a and intranuclear T-bet) assessed were strongly detectable following treatment with EnAd, whilst only secreted IL-4 and transcription factor GATA3 were induced as T_H2 markers. Nevertheless, TIDC-like cells treated EnAd were never seen to express IL-12 cytokine, which is required for T_H1 polarising cytokine[40]. Instead, IL-4 was more commonly seen in the supernatant of EnAd-treated d3iDCs.

In summary, EnAd virus may stimulate tumour infiltrating dendritic cells in such a manner that they will be able to functionally prime CD4 T cells, which is likely to synergise with immune checkpoint inhibitors therapy. However, it is uncertain whether EnAd can change the inherent suppressive cytokines of TIDCs into cytokines that harness a T_H1 adaptive immune response.

7.2 Final discussion and future directions

7.2.1 Future directions

A logical initial extension of this work would be to gain further understanding on the mechanism leading to the improved oncolytic phenotype of EnAd in cancer cells. Probably by assessing the two mutant regions, E2B and E4, responsible for the phenotype of EnAd, for example assessing whether the expression and nuclear distribution of the altered proteins such as pTP, E4-ORF4 and E4-ORF6 are affected. The mutant regions appeared to readily upgrade the virus genome replication in cancer cells without improving virus gene expression. In fact, improving the virus gene expression with mTOR inhibitors, resulted with more virus progeny production in cancer cells, whilst microtubule inhibitors supressed both. With that in mind, it would be interesting to reassess the drug panel, used in this thesis, using virus late gene expression or infectious virus production as readouts. This could help identify drugs that could potentially enhance the virus activity and replication in the tumour. Alternatively, it could be used to identify cellular factors that are essential for virus growth, as possible bioindicators of virus activity or to improve the virus production by overexpressing these cellular factors.

This thesis demonstrates that EnAd virus particles are strong adjuvants for tumour infiltrating dendritic cells, converting TIDCs into functional cells that prime helper CD4 T cells. Despite not being very conclusive, data also suggested there might be a T_H1 polarisation of the adaptive immune response, which is critical to endorse a cancer immunotherapy. It was presumed that the mixed lymphocyte reaction model used to assess the polarisation of the helper T cells was the probable source for the ambivalent results. Future experiments should seek a new system that permits to investigate the adjuvant effect of EnAd virus on physiological TIDC, at the same time it allows the assessment of the polarisation of adaptive immunity on autologous cells. Suggested systems, are human ascites or pleural fluid from abdominal and pleural clinical

cancers, which are perhaps more accessible and are known to contain immune cells with interesting phenotypes[233]. Alternatively, plasmacytoid DC isolated from PBMCs are known to have regulatory features[282]. This could help understand whether EnAd particles in the tumour directly promote anti-tumour immune responses or whether it is necessary to encode a transgene payload responsible for actively driving a T_H1 polarisation.

In this thesis, the uptake of EnAd virus particles into the dendritic cells model via CD46 receptor was identified as the main mechanism by which EnAd presented better adjuvant properties compared to adenovirus 5, for which the CAR receptor was not expressed on the DC model. CD46 is also known to have a controversial costimulation/inhibition function on T cells. However, preliminary studies in which polyclonally stimulated CD4 T cells were exposed to EnAd virus particles did not shed much light on the implications of engaging CD46 on this cell type. In principle, it seems irrational that group B adenovirus have evolved to use CD46 as the main cellular receptor, with the consequent stronger stimulation of innate cells but lacking a mechanism that regulates the anti-viral immune response. The diversity of pathogens binding to the same receptor, suggests that CD46 might have further immunological implications[247]. Future work to understand the mechanistic and immunological implications of using CD46 as a cellular receptor, will be important to maximise the value of EnAd as an immunoncolytic agent.

Finally, it was shown that EnAd, and possibly other human adenoviruses, might express exclusively the immunomodulatory E3 genes in dendritic cells, or other innate cells, perhaps to dampen the anti-viral immune response. Although additional work is needed to confirm E3 mRNA or E3 proteins are functional in these cells, it might be necessary to remove the remaining genes encoded in the E3 region of EnAd in order to maximise its cancer vaccine activity. Although this deletion might negatively impact on the persistence of the virus in the tumour, it should help achieve better anti-tumour immune responses, while at the same time it

generates more space in the virus genome for encoding transgenes. Alternatively, the potential dual expression ability of adenovirus, may lead to new strategy opportunities in which transgenes are expressed depending upon the infected cell type.

7.2.2 Final conclusions

This thesis describes the potent oncolytic properties, fast replication and improved virus progeny production in cancer cells of EnAd compared to Ad11p, the main parental virus. At the same time, it identifies the two mutant regions, chimeric E2B and small deletion in E4-ORF4, responsible for this new phenotype. These mutations have considerably boosted the genome replication of EnAd compared to the parental virus, without changing the virus gene expression. Hence mTOR inhibitors, which appeared to ameliorate the virus gene expression, resulted in more virus progeny production. The combination of mTOR inhibitors, currently used in cancer patients, with EnAd might improve the virus activity and replication in the tumour.

The third and last mutation, a large deletion in E3 region which encodes immunomodulatory genes, was shown to have no direct implication in the new oncolytic phenotype of EnAd. Although E3 deletion might have a major role in the second mechanism of the oncolytic virus, the immune-mediated cell killing, in which this thesis centres much of its interest. In fact, EnAd appears to specifically express the transcripts of the remaining E3 genes in dendritic cells, perhaps via the NF-kB promoter encoded upstream of E3. Of note, this strategy is probably a broader adenovirus feature; once the adenovirus is sensed though pathogen recognition receptors in innate immune cells and NF-kB signalling activated, they modulate the anti-virus immune response with E3 proteins.

Finally, based on the premises that innate cells in tumour have compromised phenotype and inhibit anti-tumour immune responses, such as tumour infiltrating DC. EnAd virus particles

are shown to be a strong adjuvant on TIDC-like cells, promoting the secretion of pro-inflammatory factors, restabilising their ability to prime T cells, and potentially driving anti-tumour immune responses. However further investigation is needed to elucidate whether T_H1 polarisation is induced by the virus or whether this should be mediated via the expression of specific transgene. Nevertheless, EnAd appears to be an improved adjuvant agent than Ad5, which has been largely used as vaccine or oncolytic platform. The differences between both viruses are more notably when infecting tumour cells. This is mediated exclusively by the virus particles in the case of EnAd, with little effect left on endogenous danger signals.

In conclusion, this thesis describes the improved oncolytic activity of EnAd virus and its strong adjuvant effect on compromised immune cells characteristically found in tumours. This brands EnAd as a very interesting multifaceted anti-cancer platform, with the potential to synergise with other immunotherapeutics, such as check point inhibitors, and locally deliver multiple payloads. Further development of this technology will likely deliver significant therapeutic effects in patients with cancer.

8 Bibliography

1 Rosenberg, S. A. Progress in human tumour immunology and immunotherapy. *Nature* **411**, 380-384, doi:10.1038/35077246 (2001).

2 Voena, C. & Chiarle, R. Advances in cancer immunology and cancer immunotherapy. *Discov Med* **21**, 125-133 (2016).

3 Topalian, S. L. *et al.* Safety, activity, and immune correlates of anti-PD-1 antibody in cancer. *N Engl J Med* **366**, 2443-2454, doi:10.1056/NEJMoa1200690 (2012).

4 Marcato, P., Dean, C. A., Giacomantonio, C. A. & Lee, P. W. Oncolytic reovirus effectively targets breast cancer stem cells. *Mol Ther* **17**, 972-979, doi:10.1038/mt.2009.58 (2009).

5 Coukos, G. *et al.* Oncolytic herpes simplex virus-1 lacking ICP34.5 induces p53-independent death and is efficacious against chemotherapy-resistant ovarian cancer. *Clin Cancer Res* **6**, 3342-3353 (2000).

6 Kuhn, I. *et al.* Directed evolution generates a novel oncolytic virus for the treatment of colon cancer. *PLoS One* **3**, e2409, doi:10.1371/journal.pone.0002409 (2008).

7 Garcia-Carbonero, R. *et al.* Phase 1 study of intravenous administration of the chimeric adenovirus enadenotucirev in patients undergoing primary tumor resection. *J Immunother Cancer* **5**, 71, doi:10.1186/s40425-017-0277-7 (2017).

8 Luqmani, Y. A. Mechanisms of drug resistance in cancer chemotherapy. *Med Princ Pract* **14 Suppl 1**, 35-48, doi:10.1159/000086183 (2005).

9 Kim, A. Y., Kwak, J. H., Je, N. K., Lee, Y. H. & Jung, Y. S. Epithelial-mesenchymal Transition is Associated with Acquired Resistance to 5-Fluorocuracil in HT-29 Colon Cancer Cells. *Toxicol Res* **31**, 151-156, doi:10.5487/TR.2015.31.2.151 (2015).

10 Johnston, S. L. Biologic therapies: what and when? *J Clin Pathol* **60**, 8-17, doi:10.1136/jcp.2005.032300 (2007).

11 Berndt, N., Karim, R. M. & Schonbrunn, E. Advances of small molecule targeting of kinases. *Curr Opin Chem Biol* **39**, 126-132, doi:10.1016/j.cbpa.2017.06.015 (2017).

12 Callahan, M. K., Flaherty, C. R. & Postow, M. A. Checkpoint Blockade for the Treatment of Advanced Melanoma. *Cancer Treat Res* **167**, 231-250, doi:10.1007/978-3-319-22539-5_9 (2016).

13 Kurzrock, R., Kantarjian, H. M., Druker, B. J. & Talpaz, M. Philadelphia chromosome-positive leukemias: from basic mechanisms to molecular therapeutics. *Ann Intern Med* **138**, 819-830 (2003).

14 Hoption Cann, S., van Netten, J. & van Netten, C. Dr William Coley and tumour regression: a place in history or in the future. *Postgraduate medical journal* **79**, 672-680 (2003).

15 Wiemann, B. & Starnes, C. Coley's toxins, tumor necrosis factor and cancer research: a historical perspective. *Pharmacology & therapeutics* **64**, 529-564, doi:10.1016/0163-7258(94)90023-X (1994).

16 McCarthy, E. The toxins of William B. Coley and the treatment of bone and soft-tissue sarcomas. *The Iowa orthopaedic journal* **26**, 154-158 (2005).

17 Burnet, M. Cancer; a biological approach. I. The processes of control. *British medical journal* **1**, 779-786, doi:10.1136/bmj.1.5022.779 (1957).

18 Dunn, G. P., Old, L. J. & Schreiber, R. D. The immunobiology of cancer immunosurveillance and immunoediting. *Immunity* **21**, 137-148, doi:10.1016/j.immuni.2004.07.017 (2004).

19 Goedert, J. J. *et al.* Spectrum of AIDS-associated malignant disorders. *Lancet* **351**, 1833-1839 (1998).

20 Pardoll, D. Does the immune system see tumors as foreign or self? *Annu Rev Immunol* **21**, 807-839, doi:10.1146/annurev.immunol.21.120601.141135 (2003).

21 Old, L. J. & Boyse, E. A. Immunology of Experimental Tumors. *Annu Rev Med* **15**, 167-186, doi:10.1146/annurev.me.15.020164.001123 (1964).
22 Burnet, F. M. The concept of immunological surveillance. *Prog Exp Tumor Res* **13**, 1-27 (1970).
23 Thomas, L. On immunosurveillance in human cancer. *Yale J Biol Med* **55**, 329-333 (1982).
24 Dunn, G., Old, L. & Schreiber, R. The three Es of cancer immunoediting. *Annual review of immunology* **22**, 329-360, doi:10.1146/annurev.immunol.22.012703.104803 (2004).
25 Heath, W. *et al.* Cross-presentation, dendritic cell subsets, and the generation of immunity to cellular antigens. *Immunological reviews* **199**, 9-26, doi:10.1111/j.0105-2896.2004.00142.x (2004).
26 Chen, H. *et al.* A functionally defective allele of TAP1 results in loss of MHC class I antigen presentation in a human lung cancer. *Nature genetics* **13**, 210-213, doi:10.1038/ng0696-210 (1996).
27 Topalian, S. *et al.* Safety, activity, and immune correlates of anti-PD-1 antibody in cancer. *The New England journal of medicine* **366**, 2443-2454, doi:10.1056/NEJMoa1200690 (2012).
28 Hanahan, D. & Weinberg, R. A. Hallmarks of cancer: the next generation. *Cell* **144**, 646-674, doi:10.1016/j.cell.2011.02.013 (2011).
29 Condamine, T., Ramachandran, I., Youn, J. I. & Gabrilovich, D. I. Regulation of tumor metastasis by myeloid-derived suppressor cells. *Annu Rev Med* **66**, 97-110, doi:10.1146/annurev-med-051013-052304 (2015).
30 Talmadge, J. E. & Gabrilovich, D. I. History of myeloid-derived suppressor cells. *Nat Rev Cancer* **13**, 739-752, doi:10.1038/nrc3581 (2013).
31 Marvel, D. & Gabrilovich, D. I. Myeloid-derived suppressor cells in the tumor microenvironment: expect the unexpected. *J Clin Invest* **125**, 3356-3364, doi:10.1172/JCI80005 (2015).
32 Beatty, G. L. & Gladney, W. L. Immune escape mechanisms as a guide for cancer immunotherapy. *Clin Cancer Res* **21**, 687-692, doi:10.1158/1078-0432.CCR-14-1860 (2015).
33 Mauti, L. A. *et al.* Myeloid-derived suppressor cells are implicated in regulating permissiveness for tumor metastasis during mouse gestation. *J Clin Invest* **121**, 2794-2807, doi:10.1172/JCI41936 (2011).
34 Mellman, I., Coukos, G. & Dranoff, G. Cancer immunotherapy comes of age. *Nature* **480**, 480-489, doi:10.1038/nature10673 (2011).
35 Hamid, O. *et al.* Safety and tumor responses with lambrolizumab (anti-PD-1) in melanoma. *N Engl J Med* **369**, 134-144, doi:10.1056/NEJMoa1305133 (2013).
36 Kalos, M. & June, C. H. Adoptive T cell transfer for cancer immunotherapy in the era of synthetic biology. *Immunity* **39**, 49-60, doi:10.1016/j.immuni.2013.07.002 (2013).
37 Rosenberg, S. A., Restifo, N. P., Yang, J. C., Morgan, R. A. & Dudley, M. E. Adoptive cell transfer: a clinical path to effective cancer immunotherapy. *Nat Rev Cancer* **8**, 299-308, doi:10.1038/nrc2355 (2008).
38 Halama, N. *et al.* The localization and density of immune cells in primary tumors of human metastatic colorectal cancer shows an association with response to chemotherapy. *Cancer Immun* **9**, 1 (2009).
39 Schreiber, R. D., Old, L. J. & Smyth, M. J. Cancer immunoediting: integrating immunity's roles in cancer suppression and promotion. *Science* **331**, 1565-1570, doi:10.1126/science.1203486 (2011).
40 Bakdash, G., Sittig, S. P., van Dijk, T., Figdor, C. G. & de Vries, I. J. The nature of activatory and tolerogenic dendritic cell-derived signal II. *Front Immunol* **4**, 53, doi:10.3389/fimmu.2013.00053 (2013).
41 Kennedy, R. & Celis, E. Multiple roles for CD4+ T cells in anti-tumor immune responses. *Immunol Rev* **222**, 129-144, doi:10.1111/j.1600-065X.2008.00616.x (2008).
42 Garg, A. D. *et al.* Trial watch: Dendritic cell-based anticancer immunotherapy. *Oncoimmunology* **6**, e1328341, doi:10.1080/2162402X.2017.1328341 (2017).

43 Gabrilovich, D. Mechanisms and functional significance of tumour-induced dendritic-cell defects. *Nat Rev Immunol* **4**, 941-952, doi:10.1038/nri1498 (2004).
44 Maldonado, R. A. & von Andrian, U. H. How tolerogenic dendritic cells induce regulatory T cells. *Adv Immunol* **108**, 111-165, doi:10.1016/B978-0-12-380995-7.00004-5 (2010).
45 Mahnke, K., Johnson, T. S., Ring, S. & Enk, A. H. Tolerogenic dendritic cells and regulatory T cells: A two-way relationship. *Journal of Dermatological Science* **46**, 159-167, doi:10.1016/j.jdermsci.2007.03.002 (2007).
46 Janco, J., Lamichhane, P., Karyampudi, L. & Knutson, K. L. Tumor-Infiltrating Dendritic Cells in Cancer Pathogenesis. *The Journal of Immunology* **194**, 2985-2991, doi:10.4049/jimmunol.1403134 (2015).
47 Ma, Y., Shurin, G. V., Gutkin, D. W. & Shurin, M. R. Tumor associated regulatory dendritic cells. *Semin Cancer Biol* **22**, 298-306, doi:10.1016/j.semcancer.2012.02.010 (2012).
48 Ma, Y., Shurin, G. V., Peiyuan, Z. & Shurin, M. R. Dendritic cells in the cancer microenvironment. *J Cancer* **4**, 36-44, doi:10.7150/jca.5046 (2013).
49 Shurin, G. V., Ma, Y. & Shurin, M. R. Immunosuppressive Mechanisms of Regulatory Dendritic Cells in Cancer. *Cancer Microenvironment* **6**, 159-167, doi:10.1007/s12307-013-0133-3 (2013).
50 Shurin, M. R., Naiditch, H., Zhong, H. & Shurin, G. V. Regulatory dendritic cells: new targets for cancer immunotherapy. *Cancer biology & therapy* **11**, 988-992, doi:10.4161/cbt.11.11.15543 (2011).
51 Krempski, J. *et al.* Tumor-infiltrating programmed death receptor-1+ dendritic cells mediate immune suppression in ovarian cancer. *J Immunol* **186**, 6905-6913, doi:10.4049/jimmunol.1100274jimmunol.1100274 [pii] (2011).
52 Harimoto, H. *et al.* Inactivation of tumor-specific CD8(+) CTLs by tumor-infiltrating tolerogenic dendritic cells. *Immunol Cell Biol* **91**, 545-555, doi:10.1038/icb.2013.38 (2013).
53 Vicari, A. P. *et al.* Reversal of tumor-induced dendritic cell paralysis by CpG immunostimulatory oligonucleotide and anti-interleukin 10 receptor antibody. *J Exp Med* **196**, 541-549 (2002).
54 Guiducci, C., Vicari, A. P., Sangaletti, S., Trinchieri, G. & Colombo, M. P. Redirecting in vivo elicited tumor infiltrating macrophages and dendritic cells towards tumor rejection. *Cancer Res* **65**, 3437-3446, doi:10.1158/0008-5472.CAN-04-4262 (2005).
55 Rouse, B. T. & Sehrawat, S. Immunity and immunopathology to viruses: what decides the outcome? *Nat Rev Immunol* **10**, 514-526, doi:10.1038/nri2802 (2010).
56 Rowe, W. P., Huebner, R. J., Gilmore, L. K., Parrott, R. H. & Ward, T. G. Isolation of a cytopathogenic agent from human adenoids undergoing spontaneous degeneration in tissue culture. *Proc Soc Exp Biol Med* **84**, 570-573 (1953).
57 Rosen, L. A hemagglutination-inhibition technique for typing adenoviruses. *Am J Hyg* **71**, 120-128 (1960).
58 Harwood, L. M. & Gallimore, P. H. A study of the oncogenicity of adenovirus type 2 transformed rat embryo cells. *Int J Cancer* **16**, 498-508 (1975).
59 Green, M., Mackey, J. K., Wold, W. S. & Rigden, P. Thirty-one human adenovirus serotypes (Ad1-Ad31) form five groups (A-E) based upon DNA genome homologies. *Virology* **93**, 481-492 (1979).
60 Majhen, D. *et al.* Adenovirus-based vaccines for fighting infectious diseases and cancer: progress in the field. *Hum Gene Ther* **25**, 301-317, doi:10.1089/hum.2013.235 (2014).
61 Nemerow, G. R., Stewart, P. L. & Reddy, V. S. Structure of human adenovirus. *Curr Opin Virol* **2**, 115-121, doi:10.1016/j.coviro.2011.12.008 (2012).
62 Vellinga, J., Van der Heijdt, S. & Hoeben, R. C. The adenovirus capsid: major progress in minor proteins. *J Gen Virol* **86**, 1581-1588, doi:10.1099/vir.0.80877-0 (2005).
63 Crawford-Miksza, L. & Schnurr, D. P. Analysis of 15 adenovirus hexon proteins reveals the location and structure of seven hypervariable regions containing serotype-specific residues. *J Virol* **70**, 1836-1844 (1996).

64 Bradley, R. R. *et al.* Adenovirus serotype 5-specific neutralizing antibodies target multiple hexon hypervariable regions. *J Virol* **86**, 1267-1272, doi:10.1128/JVI.06165-11 (2012).
65 Russell, W. C. Adenoviruses: update on structure and function. *J Gen Virol* **90**, 1-20, doi:10.1099/vir.0.003087-0 (2009).
66 Nicklin, S. A., Wu, E., Nemerow, G. R. & Baker, A. H. The influence of adenovirus fiber structure and function on vector development for gene therapy. *Mol Ther* **12**, 384-393, doi:10.1016/j.ymthe.2005.05.008 (2005).
67 Smith, T. A. *et al.* Adenovirus serotype 5 fiber shaft influences in vivo gene transfer in mice. *Hum Gene Ther* **14**, 777-787, doi:10.1089/104303403765255165 (2003).
68 Zhang, Y. & Bergelson, J. M. Adenovirus receptors. *J Virol* **79**, 12125-12131, doi:10.1128/JVI.79.19.12125-12131.2005 (2005).
69 Rux, J. J. & Burnett, R. M. Adenovirus structure. *Hum Gene Ther* **15**, 1167-1176, doi:10.1089/hum.2004.15.1167 (2004).
70 Tomko, R. P., Xu, R. & Philipson, L. HCAR and MCAR: the human and mouse cellular receptors for subgroup C adenoviruses and group B coxsackieviruses. *Proceedings of the National Academy of Sciences of the United States of America* **94**, 3352-3356 (1997).
71 Roelvink, P. W. *et al.* The coxsackievirus-adenovirus receptor protein can function as a cellular attachment protein for adenovirus serotypes from subgroups A, C, D, E, and F. *J Virol* **72**, 7909-7915 (1998).
72 Howitt, J., Bewley, M. C., Graziano, V., Flanagan, J. M. & Freimuth, P. Structural basis for variation in adenovirus affinity for the cellular coxsackievirus and adenovirus receptor. *The Journal of biological chemistry* **278**, 26208-26215, doi:10.1074/jbc.M301492200 (2003).
73 Walters, R. W. *et al.* Basolateral localization of fiber receptors limits adenovirus infection from the apical surface of airway epithelia. *The Journal of biological chemistry* **274**, 10219-10226 (1999).
74 Coyne, C. B. & Bergelson, J. M. CAR: a virus receptor within the tight junction. *Adv Drug Deliv Rev* **57**, 869-882, doi:10.1016/j.addr.2005.01.007 (2005).
75 Sachs, M. D. *et al.* Integrin alpha(v) and coxsackie adenovirus receptor expression in clinical bladder cancer. *Urology* **60**, 531-536 (2002).
76 Gaggar, A., Shayakhmetov, D. M. & Lieber, A. CD46 is a cellular receptor for group B adenoviruses. *Nat Med* **9**, 1408-1412, doi:10.1038/nm952 (2003).
77 Wang, H. *et al.* Desmoglein 2 is a receptor for adenovirus serotypes 3, 7, 11 and 14. *Nat Med* **17**, 96-104, doi:10.1038/nm.2270 (2011).
78 Niehans, G. A., Cherwitz, D. L., Staley, N. A., Knapp, D. J. & Dalmasso, A. P. Human carcinomas variably express the complement inhibitory proteins CD46 (membrane cofactor protein), CD55 (decay-accelerating factor), and CD59 (protectin). *Am J Pathol* **149**, 129-142 (1996).
79 Wickham, T. J., Mathias, P., Cheresh, D. A. & Nemerow, G. R. Integrins alpha v beta 3 and alpha v beta 5 promote adenovirus internalization but not virus attachment. *Cell* **73**, 309-319 (1993).
80 Meier, O. & Greber, U. F. Adenovirus endocytosis. *J Gene Med* **6 Suppl 1**, S152-163, doi:10.1002/jgm.553 (2004).
81 Wang, K., Huang, S., Kapoor-Munshi, A. & Nemerow, G. Adenovirus internalization and infection require dynamin. *J Virol* **72**, 3455-3458 (1998).
82 Kalin, S. *et al.* Macropinocytotic uptake and infection of human epithelial cells with species B2 adenovirus type 35. *J Virol* **84**, 5336-5350, doi:10.1128/JVI.02494-09 (2010).
83 Wiethoff, C. M., Wodrich, H., Gerace, L. & Nemerow, G. R. Adenovirus protein VI mediates membrane disruption following capsid disassembly. *J Virol* **79**, 1992-2000, doi:10.1128/JVI.79.4.1992-2000.2005 (2005).
84 Bailey, C. J., Crystal, R. G. & Leopold, P. L. Association of adenovirus with the microtubule organizing center. *J Virol* **77**, 13275-13287 (2003).
85 Leopold, P. L. & Crystal, R. G. Intracellular trafficking of adenovirus: many means to many ends. *Adv Drug Deliv Rev* **59**, 810-821, doi:10.1016/j.addr.2007.06.007 (2007).

86 Shayakhmetov, D. M. *et al.* The interaction between the fiber knob domain and the cellular attachment receptor determines the intracellular trafficking route of adenoviruses. *J Virol* **77**, 3712-3723 (2003).
87 Shayakhmetov, D. M. *et al.* Genome size and structure determine efficiency of postinternalization steps and gene transfer of capsid-modified adenovirus vectors in a cell-type-specific manner. *J Virol* **78**, 10009-10022, doi:10.1128/JVI.78.18.10009-10022.2004 (2004).
88 Miyazawa, N., Crystal, R. G. & Leopold, P. L. Adenovirus serotype 7 retention in a late endosomal compartment prior to cytosol escape is modulated by fiber protein. *J Virol* **75**, 1387-1400, doi:10.1128/JVI.75.3.1387-1400.2001 (2001).
89 Crimeen-Irwin, B. *et al.* Ligand binding determines whether CD46 is internalized by clathrin-coated pits or macropinocytosis. *The Journal of biological chemistry* **278**, 46927-46937, doi:10.1074/jbc.M308261200 (2003).
90 Fay, N. & Pante, N. Nuclear entry of DNA viruses. *Front Microbiol* **6**, 467, doi:10.3389/fmicb.2015.00467 (2015).
91 Egan, C., Bayley, S. T. & Branton, P. E. Binding of the Rb1 protein to E1A products is required for adenovirus transformation. *Oncogene* **4**, 383-388 (1989).
92 Frisch, S. M. & Mymryk, J. S. Adenovirus-5 E1A: paradox and paradigm. *Nat Rev Mol Cell Biol* **3**, 441-452, doi:10.1038/nrm827 (2002).
93 Hoeben, R. C. & Uil, T. G. Adenovirus DNA replication. *Cold Spring Harbor perspectives in biology* **5**, a013003, doi:10.1101/cshperspect.a013003 (2013).
94 Webster, A., Leith, I. R., Nicholson, J., Hounsell, J. & Hay, R. T. Role of preterminal protein processing in adenovirus replication. *J Virol* **71**, 6381-6389 (1997).
95 Lawrence, F. J., McStay, B. & Matthews, D. A. Nucleolar protein upstream binding factor is sequestered into adenovirus DNA replication centres during infection without affecting RNA polymerase I location or ablating rRNA synthesis. *J Cell Sci* **119**, 2621-2631, doi:10.1242/jcs.02982 (2006).
96 Mangel, W. F. & San Martin, C. Structure, function and dynamics in adenovirus maturation. *Viruses* **6**, 4536-4570, doi:10.3390/v6114536 (2014).
97 Ostapchuk, P. & Hearing, P. Minimal cis-acting elements required for adenovirus genome packaging. *J Virol* **77**, 5127-5135 (2003).
98 Ahi, Y. S. & Mittal, S. K. Components of Adenovirus Genome Packaging. *Front Microbiol* **7**, 1503, doi:10.3389/fmicb.2016.01503 (2016).
99 Berget, S. M., Moore, C. & Sharp, P. A. Spliced segments at the 5' terminus of adenovirus 2 late mRNA. *Proceedings of the National Academy of Sciences of the United States of America* **74**, 3171-3175 (1977).
100 Franqueville, L. *et al.* Protein crystals in Adenovirus type 5-infected cells: requirements for intranuclear crystallogenesis, structural and functional analysis. *PLoS One* **3**, e2894, doi:10.1371/journal.pone.0002894 (2008).
101 Rosa-Calatrava, M. *et al.* Adenovirus protein IX sequesters host-cell promyelocytic leukaemia protein and contributes to efficient viral proliferation. *EMBO Rep* **4**, 969-975, doi:10.1038/sj.embor.embor943 (2003).
102 Hall, K., Blair Zajdel, M. E. & Blair, G. E. Unity and diversity in the human adenoviruses: exploiting alternative entry pathways for gene therapy. *Biochem J* **431**, 321-336, doi:10.1042/BJ20100766 (2010).
103 Tollefson, A. E. *et al.* The adenovirus death protein (E3-11.6K) is required at very late stages of infection for efficient cell lysis and release of adenovirus from infected cells. *J Virol* **70**, 2296-2306 (1996).
104 Hendrickx, R. *et al.* Innate immunity to adenovirus. *Hum Gene Ther* **25**, 265-284, doi:10.1089/hum.2014.001 (2014).

105 Zaiss, A. K., Machado, H. B. & Herschman, H. R. The influence of innate and pre-existing immunity on adenovirus therapy. *J Cell Biochem* **108**, 778-790, doi:10.1002/jcb.22328 (2009).
106 Seregin, S. S. & Amalfitano, A. Overcoming pre-existing adenovirus immunity by genetic engineering of adenovirus-based vectors. *Expert Opin Biol Ther* **9**, 1521-1531, doi:10.1517/14712590903307388 (2009).
107 Lichtenstein, D. L., Toth, K., Doronin, K., Tollefson, A. E. & Wold, W. S. Functions and mechanisms of action of the adenovirus E3 proteins. *Int Rev Immunol* **23**, 75-111 (2004).
108 Baltimore, D. Expression of animal virus genomes. *Bacteriol Rev* **35**, 235-241 (1971).
109 Futreal, P. A. *et al.* A census of human cancer genes. *Nat Rev Cancer* **4**, 177-183, doi:10.1038/nrc1299 (2004).
110 Seymour, L. W. & Fisher, K. D. Oncolytic viruses: finally delivering. *Br J Cancer* **114**, 357-361, doi:10.1038/bjc.2015.481 (2016).
111 Sun, X., Burns, J. B., Howell, J. M. & Fujinami, R. S. Suppression of antigen-specific T cell proliferation by measles virus infection: role of a soluble factor in suppression. *Virology* **246**, 24-33, doi:10.1006/viro.1998.9186 (1998).
112 Kelly, E. & Russell, S. J. History of oncolytic viruses: genesis to genetic engineering. *Mol Ther* **15**, 651-659, doi:10.1038/sj.mt.6300108 (2007).
113 Bluming, A. Z. & Ziegler, J. L. Regression of Burkitt's lymphoma in association with measles infection. *Lancet* **2**, 105-106 (1971).
114 Huebner, R. J., Rowe, W. P., Schatten, W. E., Smith, R. R. & Thomas, L. B. Studies on the use of viruses in the treatment of carcinoma of the cervix. *Cancer* **9**, 1211-1218 (1956).
115 Russell, S. J., Peng, K.-W. W. & Bell, J. C. Oncolytic virotherapy. *Nature biotechnology* **30**, 658-670, doi:10.1038/nbt.2287 (2012).
116 Andtbacka, R. H. *et al.* Talimogene Laherparepvec Improves Durable Response Rate in Patients With Advanced Melanoma. *J Clin Oncol* **33**, 2780-2788, doi:10.1200/JCO.2014.58.3377 (2015).
117 Senzer, N. N. *et al.* Phase II clinical trial of a granulocyte-macrophage colony-stimulating factor-encoding, second-generation oncolytic herpesvirus in patients with unresectable metastatic melanoma. *J Clin Oncol* **27**, 5763-5771, doi:10.1200/JCO.2009.24.3675 (2009).
118 Andtbacka, R. H. I. *et al.* 3336 Phase II CALM extension study: Enhanced immune-cell infiltration within the tumour micro-environment of patients with advanced melanoma following intralesional delivery of Coxsackievirus A21. *European Journal of Cancer* **51**, S677, doi:http://dx.doi.org/10.1016/S0959-8049(16)31854-8 (2015).
119 Curti, B. D. *et al.* Activity of a novel immunotherapy combination of intralesional Coxsackievirus A21 and systemic ipilimumab in advanced melanoma patients previously treated with anti-PD1 blockade therapy. *Journal of Clinical Oncology* **35**, 3014-3014, doi:10.1200/JCO.2017.35.15_suppl.3014 (2017).
120 Andtbacka, R. H. I. *et al.* Phase II calm extension study: Coxsackievirus A21 delivered intratumorally to patients with advanced melanoma induces immune-cell infiltration in the tumor microenvironment. *Journal for Immunotherapy of Cancer* **3**, P343-P343, doi:10.1186/2051-1426-3-S2-P343 (2015).
121 Dorig, R. E., Marcil, A., Chopra, A. & Richardson, C. D. The human CD46 molecule is a receptor for measles virus (Edmonston strain). *Cell* **75**, 295-305 (1993).
122 Nakai, R. *et al.* Overexpression of Necl-5 correlates with unfavorable prognosis in patients with lung adenocarcinoma. *Cancer Sci* **101**, 1326-1330, doi:10.1111/j.1349-7006.2010.01530.x (2010).
123 Skelding, K. A., Barry, R. D. & Shafren, D. R. Systemic targeting of metastatic human breast tumor xenografts by Coxsackievirus A21. *Breast Cancer Res Treat* **113**, 21-30, doi:10.1007/s10549-008-9899-2 (2009).
124 Burke, M. J. Oncolytic Seneca Valley Virus: past perspectives and future directions. *Oncolytic Virother* **5**, 81-89, doi:10.2147/OV.S96915ov-5-081 [pii] (2016).

125 Stojdl, D. F. *et al.* Exploiting tumor-specific defects in the interferon pathway with a previously unknown oncolytic virus. *Nat Med* **6**, 821-825, doi:10.1038/77558 (2000).
126 Fiola, C. *et al.* Tumor selective replication of Newcastle disease virus: association with defects of tumor cells in antiviral defence. *Int J Cancer* **119**, 328-338, doi:10.1002/ijc.21821 (2006).
127 Coffey, M. C., Strong, J. E., Forsyth, P. A. & Lee, P. W. Reovirus therapy of tumors with activated Ras pathway. *Science* **282**, 1332-1334 (1998).
128 Farassati, F., Yang, A. D. & Lee, P. W. Oncogenes in Ras signalling pathway dictate host-cell permissiveness to herpes simplex virus 1. *Nat Cell Biol* **3**, 745-750, doi:10.1038/35087061 (2001).
129 Wang, G. *et al.* Infection of human cancer cells with myxoma virus requires Akt activation via interaction with a viral ankyrin-repeat host range factor. *Proceedings of the National Academy of Sciences of the United States of America* **103**, 4640-4645, doi:10.1073/pnas.0509341103 (2006).
130 Altomare, D. A. & Testa, J. R. Perturbations of the AKT signaling pathway in human cancer. *Oncogene* **24**, 7455-7464, doi:10.1038/sj.onc.1209085 (2005).
131 Bischoff, J. R. *et al.* An adenovirus mutant that replicates selectively in p53-deficient human tumor cells. *Science* **274**, 373-376 (1996).
132 Petitjean, A. *et al.* Impact of mutant p53 functional properties on TP53 mutation patterns and tumor phenotype: lessons from recent developments in the IARC TP53 database. *Hum Mutat* **28**, 622-629, doi:10.1002/humu.20495 (2007).
133 Heise, C. *et al.* ONYX-015, an E1B gene-attenuated adenovirus, causes tumor-specific cytolysis and antitumoral efficacy that can be augmented by standard chemotherapeutic agents. *Nat Med* **3**, 639-645 (1997).
134 Rothmann, T., Hengstermann, A., Whitaker, N. J., Scheffner, M. & zur Hausen, H. Replication of ONYX-015, a potential anticancer adenovirus, is independent of p53 status in tumor cells. *J Virol* **72**, 9470-9478 (1998).
135 O'Shea, C. C. *et al.* Late viral RNA export, rather than p53 inactivation, determines ONYX-015 tumor selectivity. *Cancer Cell* **6**, 611-623, doi:10.1016/j.ccr.2004.11.012 (2004).
136 Ganly, I. *et al.* A phase I study of Onyx-015, an E1B attenuated adenovirus, administered intratumorally to patients with recurrent head and neck cancer. *Clin Cancer Res* **6**, 798-806 (2000).
137 Jing, X., Cerveny, M., Yang, K. & He, B. Replication of herpes simplex virus 1 depends on the gamma 134.5 functions that facilitate virus response to interferon and egress in the different stages of productive infection. *J Virol* **78**, 7653-7666, doi:10.1128/JVI.78.14.7653-7666.2004 (2004).
138 Raafat, N. *et al.* Preventing vaccinia virus class-I epitopes presentation by HSV-ICP47 enhances the immunogenicity of a TAP-independent cancer vaccine epitope. *Int J Cancer* **131**, E659-669, doi:10.1002/ijc.27362 (2012).
139 Ko, D., Hawkins, L. & Yu, D. C. Development of transcriptionally regulated oncolytic adenoviruses. *Oncogene* **24**, 7763-7774, doi:10.1038/sj.onc.1209048 (2005).
140 DeWeese, T. L. *et al.* A phase I trial of CV706, a replication-competent, PSA selective oncolytic adenovirus, for the treatment of locally recurrent prostate cancer following radiation therapy. *Cancer Res* **61**, 7464-7472 (2001).
141 Rodriguez, R. *et al.* Prostate attenuated replication competent adenovirus (ARCA) CN706: a selective cytotoxic for prostate-specific antigen-positive prostate cancer cells. *Cancer Res* **57**, 2559-2563 (1997).
142 Small, E. J. *et al.* A phase I trial of intravenous CG7870, a replication-selective, prostate-specific antigen-targeted oncolytic adenovirus, for the treatment of hormone-refractory, metastatic prostate cancer. *Mol Ther* **14**, 107-117, doi:10.1016/j.ymthe.2006.02.011 (2006).

143 Ramesh, N. *et al.* CG0070, a conditionally replicating granulocyte macrophage colony-stimulating factor--armed oncolytic adenovirus for the treatment of bladder cancer. *Clin Cancer Res* **12**, 305-313, doi:10.1158/1078-0432.CCR-05-1059 (2006).
144 Chen, C. H. & Chen, R. J. Prevalence of telomerase activity in human cancer. *J Formos Med Assoc* **110**, 275-289, doi:10.1016/S0929-6646(11)60043-0 (2011).
145 Duarte, S., Carle, G., Faneca, H., de Lima, M. C. & Pierrefite-Carle, V. Suicide gene therapy in cancer: where do we stand now? *Cancer Lett* **324**, 160-170, doi:10.1016/j.canlet.2012.05.023 (2012).
146 Lichty, B. D., Breitbach, C. J., Stojdl, D. F. & Bell, J. C. Going viral with cancer immunotherapy. *Nat Rev Cancer* **14**, 559-567, doi:10.1038/nrc3770 (2014).
147 Liu, B. L. *et al.* ICP34.5 deleted herpes simplex virus with enhanced oncolytic, immune stimulating, and anti-tumour properties. *Gene therapy* **10**, 292-303, doi:10.1038/sj.gt.3301885 (2003).
148 Russell, S. J. & Peng, K. W. Oncolytic Virotherapy: A Contest between Apples and Oranges. *Mol Ther* **25**, 1107-1116, doi:10.1016/j.ymthe.2017.03.026 (2017).
149 Yan, W. *et al.* Developing novel oncolytic adenoviruses through bioselection. *J Virol* **77**, 2640-2650 (2003).
150 Kaufman, H. L., Kohlhapp, F. J. & Zloza, A. Oncolytic viruses: a new class of immunotherapy drugs. *Nat Rev Drug Discov* **14**, 642-662, doi:10.1038/nrd4663 (2015).
151 Kirn, D. Clinical research results with dl1520 (Onyx-015), a replication-selective adenovirus for the treatment of cancer: what have we learned? *Gene therapy* **8**, 89-98, doi:10.1038/sj.gt.3301377 (2001).
152 Nemunaitis, J. *et al.* Phase II trial of intratumoral administration of ONYX-015, a replication-selective adenovirus, in patients with refractory head and neck cancer. *J Clin Oncol* **19**, 289-298, doi:10.1200/JCO.2001.19.2.289 (2001).
153 Nemunaitis, J. *et al.* Selective replication and oncolysis in p53 mutant tumors with ONYX-015, an E1B-55kD gene-deleted adenovirus, in patients with advanced head and neck cancer: a phase II trial. *Cancer Res* **60**, 6359-6366 (2000).
154 Khuri, F. R. *et al.* a controlled trial of intratumoral ONYX-015, a selectively-replicating adenovirus, in combination with cisplatin and 5-fluorouracil in patients with recurrent head and neck cancer. *Nat Med* **6**, 879-885, doi:10.1038/78638 (2000).
155 Marshall, E. Gene therapy death prompts review of adenovirus vector. *Science* **286**, 2244-2245 (1999).
156 Xia, Z. J. *et al.* [Phase III randomized clinical trial of intratumoral injection of E1B gene-deleted adenovirus (H101) combined with cisplatin-based chemotherapy in treating squamous cell cancer of head and neck or esophagus]. *Ai Zheng* **23**, 1666-1670 (2004).
157 Sheridan, C. Amgen announces oncolytic virus shrinks tumors. *Nat Biotechnol* **31**, 471-472, doi:10.1038/nbt0613-471 (2013).
158 Wollmann, G., Ozduman, K. & van den Pol, A. N. Oncolytic virus therapy for glioblastoma multiforme: concepts and candidates. *Cancer J* **18**, 69-81, doi:10.1097/PPO.0b013e31824671c9 (2012).
159 Breitbach, C. J. *et al.* Intravenous delivery of a multi-mechanistic cancer-targeted oncolytic poxvirus in humans. *Nature* **477**, 99-102, doi:10.1038/nature10358 (2011).
160 Alemany, R. Oncolytic Adenoviruses in Cancer Treatment. *Biomedicines* **2**, 36-49, doi:10.3390/biomedicines2010036 (2014).
161 Duffy, M. R., Parker, A. L., Bradshaw, A. C. & Baker, A. H. Manipulation of adenovirus interactions with host factors for gene therapy applications. *Nanomedicine (Lond)* **7**, 271-288, doi:10.2217/nnm.11.186 (2012).
162 Vogels, R. *et al.* Replication-deficient human adenovirus type 35 vectors for gene transfer and vaccination: efficient human cell infection and bypass of preexisting adenovirus immunity. *J Virol* **77**, 8263-8271 (2003).

163 Carlisle, R. C. *et al.* Human erythrocytes bind and inactivate type 5 adenovirus by presenting Coxsackie virus-adenovirus receptor and complement receptor 1. *Blood* **113**, 1909-1918, doi:10.1182/blood-2008-09-178459 (2009).
164 Guedan, S. *et al.* Hyaluronidase expression by an oncolytic adenovirus enhances its intratumoral spread and suppresses tumor growth. *Mol Ther* **18**, 1275-1283, doi:10.1038/mt.2010.79 (2010).
165 Tedcastle, A., Illingworth, S., Brown, A., Seymour, L. W. & Fisher, K. D. Actin-resistant DNAse I Expression From Oncolytic Adenovirus Enadenotucirev Enhances Its Intratumoral Spread and Reduces Tumor Growth. *Mol Ther* **24**, 796-804, doi:10.1038/mt.2015.233 (2016).
166 Wadell, Y.-F. M. J. S. K. L. G. Comparative analysis of the genome organization of human adenovirus 11, a member of the human adenovirus species B, and the commonly used human adenovirus 5 vector, a member of species C. *Journal of General Virology* **84**, 2061-2071, doi:10.1099/vir.0.19178-0 (2003).
167 Stone, D., Furthmann, A., Sandig, V. & Lieber, A. The complete nucleotide sequence, genome organization, and origin of human adenovirus type 11. *Virology* **309**, 152-165, doi:10.1016/S0042-6822(02)00085-5 (2003).
168 Mei, Y. F., Skog, J., Lindman, K. & Wadell, G. Comparative analysis of the genome organization of human adenovirus 11, a member of the human adenovirus species B, and the commonly used human adenovirus 5 vector, a member of species C. *J Gen Virol* **84**, 2061-2071, doi:10.1099/vir.0.19178-0 (2003).
169 Hawkins, L. K. & Hermiston, T. W. Gene delivery from the E3 region of replicating human adenovirus: evaluation of the ADP region. *Gene therapy* **8**, 1132-1141, doi:10.1038/sj.gt.3301508 (2001).
170 Flomenberg, P. R., Chen, M. & Horwitz, M. S. Sequence and genetic organization of adenovirus type 35 early region 3. *J Virol* **62**, 4431-4437 (1988).
171 Mei, Y. F. & Wadell, G. The nucleotide sequence of adenovirus type 11 early 3 region: comparison of genome type Ad11p and Ad11a. *Virology* **191**, 125-133 (1992).
172 Williams, J. L. *et al.* Lymphoid specific gene expression of the adenovirus early region 3 promoter is mediated by NF-kappa B binding motifs. *The EMBO journal* **9**, 4435-4442 (1990).
173 Tigges, M. A. & Raskas, H. J. Splice junctions in adenovirus 2 early region 4 mRNAs: multiple splice sites produce 18 to 24 RNAs. *J Virol* **50**, 106-117 (1984).
174 Muller, U., Kleinberger, T. & Shenk, T. Adenovirus E4orf4 protein reduces phosphorylation of c-Fos and E1A proteins while simultaneously reducing the level of AP-1. *J Virol* **66**, 5867-5878 (1992).
175 Medghalchi, S., Padmanabhan, R. & Ketner, G. Early region 4 modulates adenovirus DNA replication by two genetically separable mechanisms. *Virology* **236**, 8-17, doi:10.1006/viro.1997.8737 (1997).
176 Bridge, E., Medghalchi, S., Ubol, S., Leesong, M. & Ketner, G. Adenovirus early region 4 and viral DNA synthesis. *Virology* **193**, 794-801, doi:10.1006/viro.1993.1188 (1993).
177 O'Shea, C. *et al.* Adenoviral proteins mimic nutrient/growth signals to activate the mTOR pathway for viral replication. *The EMBO journal* **24**, 1211-1221, doi:10.1038/sj.emboj.7600597 (2005).
178 O'Shea, C. C., Choi, S., McCormick, F. & Stokoe, D. Adenovirus overrides cellular checkpoints for protein translation. *Cell Cycle* **4**, 883-888, doi:10.4161/cc.4.7.1791 (2005).
179 Miron, M. J., Gallouzi, I. E., Lavoie, J. N. & Branton, P. E. Nuclear localization of the adenovirus E4orf4 protein is mediated through an arginine-rich motif and correlates with cell death. *Oncogene* **23**, 7458-7468, doi:10.1038/sj.onc.1207919 (2004).
180 Kanopka, A. *et al.* Regulation of adenovirus alternative RNA splicing by dephosphorylation of SR proteins. *Nature* **393**, 185-187, doi:10.1038/30277 (1998).

181 Querido, E. *et al.* Degradation of p53 by adenovirus E4orf6 and E1B55K proteins occurs via a novel mechanism involving a Cullin-containing complex. *Genes Dev* **15**, 3104-3117, doi:10.1101/gad.926401 (2001).
182 Moyne, G., Pichard, E. & Bernhard, W. Localization of simian adenovirus 7 (SA 7) transcription and replication in lytic infection. An ultracytochemical and autoradiographical study. *J Gen Virol* **40**, 77-92, doi:10.1099/0022-1317-40-1-77 (1978).
183 Martinez-Palomo, A. & Granboulan, N. Electron microscopy of adenovirus 12 replication. II. High-resolution autoradiography of infected KB cells labeled with tritiated thymidine. *J Virol* **1**, 1010-1018 (1967).
184 Martinez-Palomo, A. Ultrastructural study of the replication of human adenovirus type 12 in cultured cells. *Pathol Microbiol (Basel)* **31**, 147-164 (1968).
185 Ornelles, D. A. & Shenk, T. Localization of the adenovirus early region 1B 55-kilodalton protein during lytic infection: association with nuclear viral inclusions requires the early region 4 34-kilodalton protein. *J Virol* **65**, 424-429 (1991).
186 Goodrum, F. D. & Ornelles, D. A. Roles for the E4 orf6, orf3, and E1B 55-kilodalton proteins in cell cycle-independent adenovirus replication. *J Virol* **73**, 7474-7488 (1999).
187 Dyer, A. *et al.* Oncolytic Group B Adenovirus Enadenotucirev Mediates Non-apoptotic Cell Death with Membrane Disruption and Release of Inflammatory Mediators. *Mol Ther Oncolytics* **4**, 18-30, doi:10.1016/j.omto.2016.11.003 (2017).
188 Cotten, M. *et al.* Psoralen treatment of adenovirus particles eliminates virus replication and transcription while maintaining the endosomolytic activity of the virus capsid. *Virology* **205**, 254-261, doi:10.1006/viro.1994.1641 (1994).
189 Tung, J. *et al.* Modern flow cytometry: a practical approach. *Clinics in laboratory medicine* **27**, 453, doi:10.1016/j.cll.2007.05.001 (2007).
190 Fields, B. N., Knipe, D. M. & Howley, P. M. (Wolters Kluwer Health/Lippincott Williams & Wilkins,, Philadelphia, 2007).
191 Wold, W. S. & Gooding, L. R. Region E3 of adenovirus: a cassette of genes involved in host immunosurveillance and virus-cell interactions. *Virology* **184**, 1-8 (1991).
192 Rauschhuber, C., Mueck-Haeusl, M., Zhang, W., Nettelbeck, D. M. & Ehrhardt, A. RNAi suppressor P19 can be broadly exploited for enhanced adenovirus replication and microRNA knockdown experiments. *Sci Rep* **3**, 1363, doi:10.1038/srep01363 (2013).
193 Marino, N. *et al.* Development of a versatile oncolytic virus platform for local intra-tumoural expression of therapeutic transgenes. *PLoS One* **12**, e0177810, doi:10.1371/journal.pone.0177810 (2017).
194 Guinn, B. A., Braidwood, L., Parker, A., Peng, K. W. & Seymour, L. 8th international conference on oncolytic virus therapeutics. *Hum Gene Ther* **25**, 1062-1084, doi:10.1089/hum.2014.118 (2014).
195 Wechman, S. L., Rao, X. M., McMasters, K. M. & Zhou, H. S. Adenovirus with DNA Packaging Gene Mutations Increased Virus Release. *Viruses* **8**, doi:10.3390/v8120333 (2016).
196 Kleinberger, T. Mechanisms of cancer cell killing by the adenovirus E4orf4 protein. *Viruses* **7**, 2334-2357, doi:10.3390/v7052334 (2015).
197 Condezo, G. N. & San Martin, C. Localization of adenovirus morphogenesis players, together with visualization of assembly intermediates and failed products, favor a model where assembly and packaging occur concurrently at the periphery of the replication center. *PLoS Pathog* **13**, e1006320, doi:10.1371/journal.ppat.1006320 (2017).
198 Lethbridge, K. J., Scott, G. E. & Leppard, K. N. Nuclear matrix localization and SUMO-1 modification of adenovirus type 5 E1b 55K protein are controlled by E4 Orf6 protein. *J Gen Virol* **84**, 259-268, doi:10.1099/vir.0.18820-0 (2003).
199 Flint, S. J. & Gonzalez, R. A. Regulation of mRNA production by the adenoviral E1B 55-kDa and E4 Orf6 proteins. *Curr Top Microbiol Immunol* **272**, 287-330 (2003).

200 AbouEl Hassan, M. A., Braam, S. R. & Kruyt, F. A. Paclitaxel and vincristine potentiate adenoviral oncolysis that is associated with cell cycle and apoptosis modulation, whereas they differentially affect the viral life cycle in non-small-cell lung cancer cells. *Cancer Gene Ther* **13**, 1105-1114, doi:10.1038/sj.cgt.7700984 (2006).
201 Cheng, P. H. *et al.* Combination of autophagy inducer rapamycin and oncolytic adenovirus improves antitumor effect in cancer cells. *Virol J* **10**, 293, doi:10.1186/1743-422X-10-293 (2013).
202 Shepelev, M. V., Korobko, E. V., Vinogradova, T. V., Kopantsev, E. P. & Korobko, I. V. LY294002 enhances expression of proteins encoded by recombinant replication-defective adenoviruses via mTOR- and non-mTOR-dependent mechanisms. *Mol Pharm* **10**, 931-939, doi:10.1021/mp3003122 (2013).
203 Ingemarsdotter, C. K. *et al.* Low-dose paclitaxel synergizes with oncolytic adenoviruses via mitotic slippage and apoptosis in ovarian cancer. *Oncogene* **29**, 6051-6063, doi:10.1038/onc.2010.335 (2010).
204 Huang, J. T. & Schneider, R. J. Adenovirus inhibition of cellular protein synthesis involves inactivation of cap-binding protein. *Cell* **65**, 271-280 (1991).
205 Xi, Q., Cuesta, R. & Schneider, R. J. Regulation of translation by ribosome shunting through phosphotyrosine-dependent coupling of adenovirus protein 100k to viral mRNAs. *J Virol* **79**, 5676-5683, doi:10.1128/JVI.79.9.5676-5683.2005 (2005).
206 Yueh, A. & Schneider, R. J. Translation by ribosome shunting on adenovirus and hsp70 mRNAs facilitated by complementarity to 18S rRNA. *Genes Dev* **14**, 414-421 (2000).
207 Sonenberg, N. & Gingras, A. C. The mRNA 5' cap-binding protein eIF4E and control of cell growth. *Curr Opin Cell Biol* **10**, 268-275 (1998).
208 Thomson, A. W., Turnquist, H. R. & Raimondi, G. Immunoregulatory functions of mTOR inhibition. *Nat Rev Immunol* **9**, 324-337, doi:10.1038/nri2546 (2009).
209 Webster, A., Leith, I. R. & Hay, R. T. Domain organization of the adenovirus preterminal protein. *J Virol* **71**, 539-547 (1997).
210 Cravens, P. D. & Lipsky, P. E. Dendritic cells, chemokine receptors and autoimmune inflammatory diseases. *Immunol Cell Biol* **80**, 497-505, doi:10.1046/j.1440-1711.2002.01118.x (2002).
211 Kaiko, G. E., Horvat, J. C., Beagley, K. W. & Hansbro, P. M. Immunological decision-making: how does the immune system decide to mount a helper T-cell response? *Immunology* **123**, 326-338, doi:10.1111/j.1365-2567.2007.02719.x (2008).
212 Austyn, J. M. Antigen-presenting cells. Experimental and clinical studies of dendritic cells. *American journal of respiratory and critical care medicine* **162**, S146-150, doi:10.1164/ajrccm.162.supplement_3.15tac1a (2000).
213 Olszanecki, R., Gebska, A. & Korbut, R. Production of prostacyclin and prostaglandin E2 in resting and IL-1beta-stimulated A549, HUVEC and hybrid EA.HY 926 cells. *J Physiol Pharmacol* **57**, 649-660 (2006).
214 Cai, Z. *et al.* Monocyte chemotactic protein 1 promotes lung cancer-induced bone resorptive lesions in vivo. *Neoplasia* **11**, 228-236 (2009).
215 Yoon, J. *et al.* The immune modulation of Clara cell-10 in human peripheral monocytes and dendritic cells. *International journal of molecular medicine* **26**, 415-423, doi:10.3892/ijmm_00000481 (2010).
216 Muller-Quernheim, U. C., Potthast, L., Muller-Quernheim, J. & Zissel, G. Tumor-cell co-culture induced alternative activation of macrophages is modulated by interferons in vitro. *J Interferon Cytokine Res* **32**, 169-177, doi:10.1089/jir.2011.0020 (2012).
217 Relja, B. *et al.* Decreased Inflammatory Responses of Human Lung Epithelial Cells after Ethanol Exposure Are Mimicked by Ethyl Pyruvate. *Mediators of Inflammation* **2014**, 1-13, doi:10.1155/2014/781519 (2014).

218 Jogler, C. *et al.* Replication properties of human adenovirus in vivo and in cultures of primary cells from different animal species. *J Virol* **80**, 3549-3558, doi:10.1128/JVI.80.7.3549-3558.2006 (2006).
219 Anderson, A. E. *et al.* LPS activation is required for migratory activity and antigen presentation by tolerogenic dendritic cells. *Journal of Leukocyte Biology* **85**, 243-250, doi:10.1189/jlb.0608374 (2009).
220 Frick, J.-S., Grünebach, F. & Autenrieth, I. B. Immunomodulation by semi-mature dendritic cells: A novel role of Toll-like receptors and interleukin-6. *International Journal of Medical Microbiology* **300**, 19-24, doi:10.1016/j.ijmm.2009.08.010 (2010).
221 Spranger, S., Dai, D., Horton, B. & Gajewski, T. F. Tumor-Residing Batf3 Dendritic Cells Are Required for Effector T Cell Trafficking and Adoptive T Cell Therapy. *Cancer Cell* **31**, 711-723 e714, doi:10.1016/j.ccell.2017.04.003 (2017).
222 Luo, X. *et al.* Intratumoral expression of MIP-1beta induces antitumor responses in a pre-established tumor model through chemoattracting T cells and NK cells. *Cell Mol Immunol* **1**, 199-204 (2004).
223 Crittenden, M. *et al.* Expression of inflammatory chemokines combined with local tumor destruction enhances tumor regression and long-term immunity. *Cancer Res* **63**, 5505-5512 (2003).
224 Zibert, A. *et al.* CCL3/MIP-1alpha is a potent immunostimulator when coexpressed with interleukin-2 or granulocyte-macrophage colony-stimulating factor in a leukemia/lymphoma vaccine. *Hum Gene Ther* **15**, 21-34, doi:10.1089/10430340460732436 (2004).
225 Gough, M. *et al.* Gene therapy to manipulate effector T cell trafficking to tumors for immunotherapy. *J Immunol* **174**, 5766-5773 (2005).
226 Mukaida, N., Sasaki, S. & Baba, T. Chemokines in cancer development and progression and their potential as targeting molecules for cancer treatment. *Mediators Inflamm* **2014**, 170381, doi:10.1155/2014/170381 (2014).
227 Liu, M., Guo, S. & Stiles, J. K. The emerging role of CXCL10 in cancer (Review). *Oncol Lett* **2**, 583-589, doi:10.3892/ol.2011.300 (2011).
228 Lore, K. *et al.* Myeloid and plasmacytoid dendritic cells are susceptible to recombinant adenovirus vectors and stimulate polyfunctional memory T cell responses. *J Immunol* **179**, 1721-1729 (2007).
229 Spary, L. K. *et al.* Tumor stroma-derived factors skew monocyte to dendritic cell differentiation toward a suppressive CD14+PD-L1+phenotype in prostate cancer. *OncoImmunology* **3**, doi:10.4161/21624011.2014.955331 (2014).
230 Ciplys, E. *et al.* High-level secretion of native recombinant human calreticulin in yeast. *Microb Cell Fact* **14**, 165, doi:10.1186/s12934-015-0356-8 (2015).
231 Zetterstrom, C. K. *et al.* High mobility group box chromosomal protein 1 (HMGB1) is an antibacterial factor produced by the human adenoid. *Pediatr Res* **52**, 148-154, doi:10.1203/00006450-200208000-00004 (2002).
232 Wu, X., Yano, M., Washida, H. & Kido, H. The second metal-binding site of 70 kDa heat-shock protein is essential for ADP binding, ATP hydrolysis and ATP synthesis. *Biochem J* **378**, 793-799, doi:10.1042/BJ20031680 (2004).
233 Jakeman, P. G. *et al.* Improved in vitro human tumor models for cancer gene therapy. *Hum Gene Ther* **26**, 249-256, doi:10.1089/hum.2015.028 (2015).
234 Jakeman, P. G., Hills, T. E., Fisher, K. D. & Seymour, L. W. Macrophages and their interactions with oncolytic viruses. *Curr Opin Pharmacol* **24**, 23-29, doi:10.1016/j.coph.2015.06.007 (2015).
235 Vachon, V. K. & Conn, G. L. Adenovirus VA RNA: An essential pro-viral non-coding RNA. *Virus Res* **212**, 39-52, doi:10.1016/j.virusres.2015.06.018 (2016).

236 Shao, R. *et al.* E1A sensitizes cells to tumor necrosis factor-induced apoptosis through inhibition of IkappaB kinases and nuclear factor kappaB activities. *The Journal of biological chemistry* **274**, 21495-21498 (1999).
237 Jennings-Gee, J. E. *et al.* Coordinate inhibition of cytokine-mediated induction of ferritin H, manganese superoxide dismutase, and interleukin-6 by the adenovirus E1A oncogene. *The Journal of biological chemistry* **281**, 16428-16435, doi:10.1074/jbc.M600038200 (2006).
238 Cook, J. L., Walker, T. A., Worthen, G. S. & Radke, J. R. Role of the E1A Rb-binding domain in repression of the NF-kappa B-dependent defense against tumor necrosis factor-alpha. *Proceedings of the National Academy of Sciences of the United States of America* **99**, 9966-9971, doi:10.1073/pnas.162082999 (2002).
239 Thomas, P. G. & Mathews, M. B. DNA replication and the early to late transition in adenovirus infection. *Cell* **22**, 523-533, doi:10.1016/0092-8674(80)90362-1 (1980).
240 Minamitani, T., Iwakiri, D. & Takada, K. Adenovirus virus-associated RNAs induce type I interferon expression through a RIG-I-mediated pathway. *J Virol* **85**, 4035-4040, doi:10.1128/JVI.02160-10 (2011).
241 Weber, M. *et al.* Incoming RNA virus nucleocapsids containing a 5'-triphosphorylated genome activate RIG-I and antiviral signaling. *Cell Host Microbe* **13**, 336-346, doi:10.1016/j.chom.2013.01.012 (2013).
242 Higginbotham, J. N., Seth, P., Blaese, R. M. & Ramsey, W. J. The release of inflammatory cytokines from human peripheral blood mononuclear cells in vitro following exposure to adenovirus variants and capsid. *Hum Gene Ther* **13**, 129-141, doi:10.1089/10430340152712683 (2002).
243 Thaci, B., Ulasov, I. V., Wainwright, D. A. & Lesniak, M. S. The challenge for gene therapy: innate immune response to adenoviruses. *Oncotarget* **2**, 113-121, doi:10.18632/oncotarget.231 (2011).
244 Mei, Y.-F., Skog, J., Lindman, K. & Wadell, G. Comparative analysis of the genome organization of human adenovirus 11, a member of the human adenovirus species B, and the commonly used human adenovirus 5 vector, a member of species C. *Journal of General Virology* **84**, 2061-2071, doi:10.1099/vir.0.19178-0 (2003).
245 Seya, T., Hirano, A., Matsumoto, M., Nomura, M. & Ueda, S. Human membrane cofactor protein (MCP, CD46): multiple isoforms and functions. *The international journal of biochemistry & cell biology* **31**, 1255-1260 (1999).
246 Wang, G., Liszewski, M. K., Chan, A. C. & Atkinson, J. P. Membrane cofactor protein (MCP; CD46): isoform-specific tyrosine phosphorylation. *Journal of immunology (Baltimore, Md. : 1950)* **164**, 1839-1846 (2000).
247 Hawkins, E. D. & Oliaro, J. CD46 signaling in T cells: linking pathogens with polarity. *FEBS letters* **584**, 4838-4844, doi:10.1016/j.febslet.2010.09.003 (2010).
248 Astier, A., Trescol-Biémont, M. C., Azocar, O., Lamouille, B. & Rabourdin-Combe, C. Cutting edge: CD46, a new costimulatory molecule for T cells, that induces p120CBL and LAT phosphorylation. *Journal of immunology (Baltimore, Md. : 1950)* **164**, 6091-6095 (2000).
249 Pache, L., Venkataraman, S., Nemerow, G. R. & Reddy, V. S. Conservation of fiber structure and CD46 usage by subgroup B2 adenoviruses. *Virology* **375**, 573-579, doi:10.1016/j.virol.2008.02.013 (2008).
250 Wang, H. *et al.* Identification of CD46 Binding Sites within the Adenovirus Serotype 35 Fiber Knob. *Journal of Virology* **81**, 12785-12792, doi:10.1128/jvi.01732-07 (2007).
251 Fleischli, C. *et al.* The distal short consensus repeats 1 and 2 of the membrane cofactor protein CD46 and their distance from the cell membrane determine productive entry of species B adenovirus serotype 35. *J Virol* **79**, 10013-10022, doi:10.1128/JVI.79.15.10013-10022.2005 (2005).

252 Krieg, A. M. *et al.* Sequence motifs in adenoviral DNA block immune activation by stimulatory CpG motifs. *Proceedings of the National Academy of Sciences of the United States of America* **95**, 12631-12636 (1998).
253 Hoelzer, K., Shackelton, L. A. & Parrish, C. R. Presence and role of cytosine methylation in DNA viruses of animals. *Nucleic Acids Res* **36**, 2825-2837, doi:10.1093/nar/gkn121 (2008).
254 Deryckere, F. & Burgert, H. G. Tumor necrosis factor alpha induces the adenovirus early 3 promoter by activation of NF-kappaB. *The Journal of biological chemistry* **271**, 30249-30255 (1996).
255 Morelli, A. E. *et al.* Recombinant Adenovirus Induces Maturation of Dendritic Cells via an NF-κB-Dependent Pathway. *Journal of Virology* **74**, 9617-9628, doi:10.1128/JVI.74.20.9617-9628.2000 (2000).
256 Oeckinghaus, A. & Ghosh, S. The NF- B Family of Transcription Factors and Its Regulation. *Cold Spring Harbor perspectives in biology* **1**, doi:10.1101/cshperspect.a000034 (2009).
257 Garrod, D. & Chidgey, M. Desmosome structure, composition and function. *Biochim Biophys Acta* **1778**, 572-587, doi:10.1016/j.bbamem.2007.07.014 (2008).
258 Philipson, L. & Pettersson, R. F. The coxsackie-adenovirus receptor--a new receptor in the immunoglobulin family involved in cell adhesion. *Curr Top Microbiol Immunol* **273**, 87-111 (2004).
259 Adams, W. C. *et al.* Adenovirus serotype 5 infects human dendritic cells via a coxsackievirus–adenovirus receptor-independent receptor pathway mediated by lactoferrin and DC-SIGN. *Journal of General Virology* **90**, 1600-1610, doi:10.1099/vir.0.008342-0 (2009).
260 Lee, S. W. *et al.* CD46 is phosphorylated at tyrosine 354 upon infection of epithelial cells by Neisseria gonorrhoeae. *The Journal of Cell Biology* **156**, 951-957, doi:10.1083/jcb.200109005 (2002).
261 Zhu, J., Huang, X. & Yang, Y. Innate immune response to adenoviral vectors is mediated by both Toll-like receptor-dependent and -independent pathways. *Journal of virology* **81**, 3170-3180, doi:10.1128/JVI.02192-06 (2007).
262 Lam, E., Stein, S. & Falck-Pedersen, E. Adenovirus Detection by the cGAS/STING/TBK1 DNA Sensing Cascade. *Journal of Virology* **88**, 974-981, doi:10.1128/JVI.02702-13 (2014).
263 Machitani, M. *et al.* Adenovirus Vector-Derived VA-RNA-Mediated Innate Immune Responses. *Pharmaceutics* **3**, 338-353, doi:10.3390/pharmaceutics3030338 (2011).
264 Mahr, J. A., Boss, J. M. & Gooding, L. R. The adenovirus e3 promoter is sensitive to activation signals in human T cells. *J Virol* **77**, 1112-1119 (2003).
265 Machitani, M. *et al.* NF-kappaB promotes leaky expression of adenovirus genes in a replication-incompetent adenovirus vector. *Sci Rep* **6**, 19922, doi:10.1038/srep19922 (2016).
266 Carmody, R. J., Maguschak, K. & Chen, Y. H. A novel mechanism of nuclear factor-kappaB regulation by adenoviral protein 14.7K. *Immunology* **117**, 188-195, doi:10.1111/j.1365-2567.2005.02277.x (2006).
267 Hiscott, J., Kwon, H. & Genin, P. Hostile takeovers: viral appropriation of the NF-kappaB pathway. *J Clin Invest* **107**, 143-151, doi:10.1172/JCI11918 (2001).
268 Kropp, K. A., Angulo, A. & Ghazal, P. Viral Enhancer Mimicry of Host Innate-Immune Promoters. *PLoS Pathogens* **10**, doi:10.1371/journal.ppat.1003804 (2014).
269 Felix, N. J. & Allen, P. M. Specificity of T-cell alloreactivity. *Nature reviews. Immunology* **7**, 942-953, doi:10.1038/nri2200 (2007).
270 Tanaka, H., Demeure, C. E., Rubio, M., Delespesse, G. & Sarfati, M. Human monocyte-derived dendritic cells induce naive T cell differentiation into T helper cell type 2 (Th2) or Th1/Th2 effectors. Role of stimulator/responder ratio. *J Exp Med* **192**, 405-412 (2000).
271 Obar, J. J. *et al.* CD4+ T cell regulation of CD25 expression controls development of short-lived effector CD8+ T cells in primary and secondary responses. *Proceedings of the National Academy of Sciences of the United States of America* **107**, 193-198, doi:10.1073/pnas.0909945107 (2010).

272 Anantharaman, A. *et al.* Programmed death-ligand 1 (PD-L1) characterization of circulating tumor cells (CTCs) in muscle invasive and metastatic bladder cancer patients. *BMC Cancer* **16**, 744, doi:10.1186/s12885-016-2758-3 (2016).
273 Adams, W. C. *et al.* Adenovirus type-35 vectors block human CD4+ T-cell activation via CD46 ligation. *Proceedings of the National Academy of Sciences* **108**, 7499-7504, doi:10.1073/pnas.1017146108 (2011).
274 Mackay, C. R. Dual personality of memory T cells. *Nature* **401**, 659-660, doi:10.1038/44309 (1999).
275 Kishimoto, H. & Sprent, J. Strong TCR ligation without costimulation causes rapid onset of Fas-dependent apoptosis of naive murine CD4+ T cells. *J Immunol* **163**, 1817-1826 (1999).
276 Kanhere, A. *et al.* T-bet and GATA3 orchestrate Th1 and Th2 differentiation through lineage-specific targeting of distal regulatory elements. *Nat Commun* **3**, 1268, doi:10.1038/ncomms2260 (2012).
277 Ahmed, R. & Gray, D. Immunological memory and protective immunity: understanding their relation. *Science* **272**, 54-60 (1996).
278 Midgley, R. S. *et al.* HLA-A11-restricted epitope polymorphism among Epstein-Barr virus strains in the highly HLA-A11-positive Chinese population: incidence and immunogenicity of variant epitope sequences. *J Virol* **77**, 11507-11516 (2003).
279 Hay, J., Carter, D., Lieber, A. & Astier, A. L. Recombinant Ad35 adenoviral proteins as potent modulators of human T cell activation. *Immunology*, doi:10.1111/imm.12391 (2014).
280 Minami, K. *et al.* Negative feedback regulation of T helper type 1 (Th1)/Th2 cytokine balance via dendritic cell and natural killer T cell interactions. *Blood* **106**, 1685-1693, doi:10.1182/blood-2004-12-4738 (2005).
281 Parker, B. S., Rautela, J. & Hertzog, P. J. Antitumour actions of interferons: implications for cancer therapy. *Nat Rev Cancer* **16**, 131-144, doi:10.1038/nrc.2016.14 (2016).
282 Wei, S. *et al.* Plasmacytoid dendritic cells induce CD8+ regulatory T cells in human ovarian carcinoma. *Cancer Res* **65**, 5020-5026, doi:10.1158/0008-5472.CAN-04-4043 (2005).
283 Marchi, L. H., Paschoalin, T., Travassos, L. R. & Rodrigues, E. G. Gene therapy with interleukin-10 receptor and interleukin-12 induces a protective interferon-gamma-dependent response against B16F10-Nex2 melanoma. *Cancer Gene Ther* **18**, 110-122, doi:10.1038/cgt.2010.58 (2011).
284 Buchbinder, E. I. & Desai, A. CTLA-4 and PD-1 Pathways: Similarities, Differences, and Implications of Their Inhibition. *Am J Clin Oncol* **39**, 98-106, doi:10.1097/COC.0000000000000239 (2016).
285 Barchet, W. *et al.* Complement-induced regulatory T cells suppress T-cell responses but allow for dendritic-cell maturation. *Blood* **107**, 1497-1504, doi:10.1182/blood-2005-07-2951 (2006).
286 Sallusto, F. & Lanzavecchia, A. Efficient presentation of soluble antigen by cultured human dendritic cells is maintained by granulocyte/macrophage colony-stimulating factor plus interleukin 4 and downregulated by tumor necrosis factor alpha. *The Journal of Experimental Medicine* **179**, 1109-1118, doi:10.1084/jem.179.4.1109 (1994).
287 Truxova, I. *et al.* Day 3 Poly (I:C)-activated dendritic cells generated in CellGro for use in cancer immunotherapy trials are fully comparable to standard Day 5 DCs. *Immunology letters* **160**, 39-49, doi:10.1016/j.imlet.2014.03.010 (2014).
288 Chapuis, F. *et al.* Differentiation of human dendritic cells from monocytes in vitro. *European Journal of Immunology* **27**, 431-441, doi:10.1002/eji.1830270213 (1997).
289 Koch, F. *et al.* High level IL-12 production by murine dendritic cells: upregulation via MHC class II and CD40 molecules and downregulation by IL-4 and IL-10. *J Exp Med* **184**, 741-746 (1996).
290 Nair, S., Archer, G. E. & Tedder, T. F. Isolation and generation of human dendritic cells. *Curr Protoc Immunol* **Chapter 7**, Unit7 32, doi:10.1002/0471142735.im0732s99 (2012).
291 Banchereau, J. & Palucka, A. K. Dendritic cells as therapeutic vaccines against cancer. *Nat Rev Immunol* **5**, 296-306, doi:10.1038/nri1592 (2005).

292 Leon, B., Lopez-Bravo, M. & Ardavin, C. Monocyte-derived dendritic cells. *Semin Immunol* **17**, 313-318, doi:10.1016/j.smim.2005.05.013 (2005).
293 Zhou, L. *et al.* Impact of human granulocyte and monocyte isolation procedures on functional studies. *Clin Vaccine Immunol* **19**, 1065-1074, doi:10.1128/CVI.05715-11 (2012).
294 Alderson, M. R. *et al.* CD40 expression by human monocytes: regulation by cytokines and activation of monocytes by the ligand for CD40. *J Exp Med* **178**, 669-674 (1993).
295 Bodmer, W. F. The HLA system: structure and function. *J Clin Pathol* **40**, 948-958 (1987).
296 Khanna, R. Tumour surveillance: missing peptides and MHC molecules. *Immunol Cell Biol* **76**, 20-26, doi:10.1046/j.1440-1711.1998.00717.x (1998).
297 Harris, N. L. & Ronchese, F. The role of B7 costimulation in T-cell immunity. *Immunol Cell Biol* **77**, 304-311, doi:10.1046/j.1440-1711.1999.00835.x (1999).
298 Kogo, H., Shimizu, M., Negishi, Y., Uchida, E. & Takahashi, H. Suppression of murine tumour growth through CD8+ cytotoxic T lymphocytes via activated DEC-205+ dendritic cells by sequential administration of alpha-galactosylceramide in vivo. *Immunology* **151**, 324-339, doi:10.1111/imm.12733 (2017).
299 Breloer, M. & Fleischer, B. CD83 regulates lymphocyte maturation, activation and homeostasis. *Trends Immunol* **29**, 186-194, doi:10.1016/j.it.2008.01.009 (2008).
300 Nociari, M., Ocheretina, O., Schoggins, J. W. & Falck-Pedersen, E. Sensing Infection by Adenovirus: Toll-Like Receptor-Independent Viral DNA Recognition Signals Activation of the Interferon Regulatory Factor 3 Master Regulator. *Journal of Virology* **81**, 4145-4157, doi:10.1128/JVI.02685-06 (2007).

9 Appendix

9.1 Part A

Transmission electron microscopy pictures of EnAd-infected A549 showed free formed virus particles (FVP) distributed across the cellular nucleus without any other apparent nuclear structure. Ad11p- and Ad5-infected A549 cells displayed a more structured nucleus, where free formed virus particles were relatively in low numbers, some clusters of particle assembly (VPAC, also known as epitaxy[100]) were locally distinguishable, as well as chromatin (Cro.) was seen at the periphery of the nucleus. In particular, large crystal inclusions (Cry.), possibly of virus protein, were also observed in Ad5-infected cell nucleus (Figure 9.1).

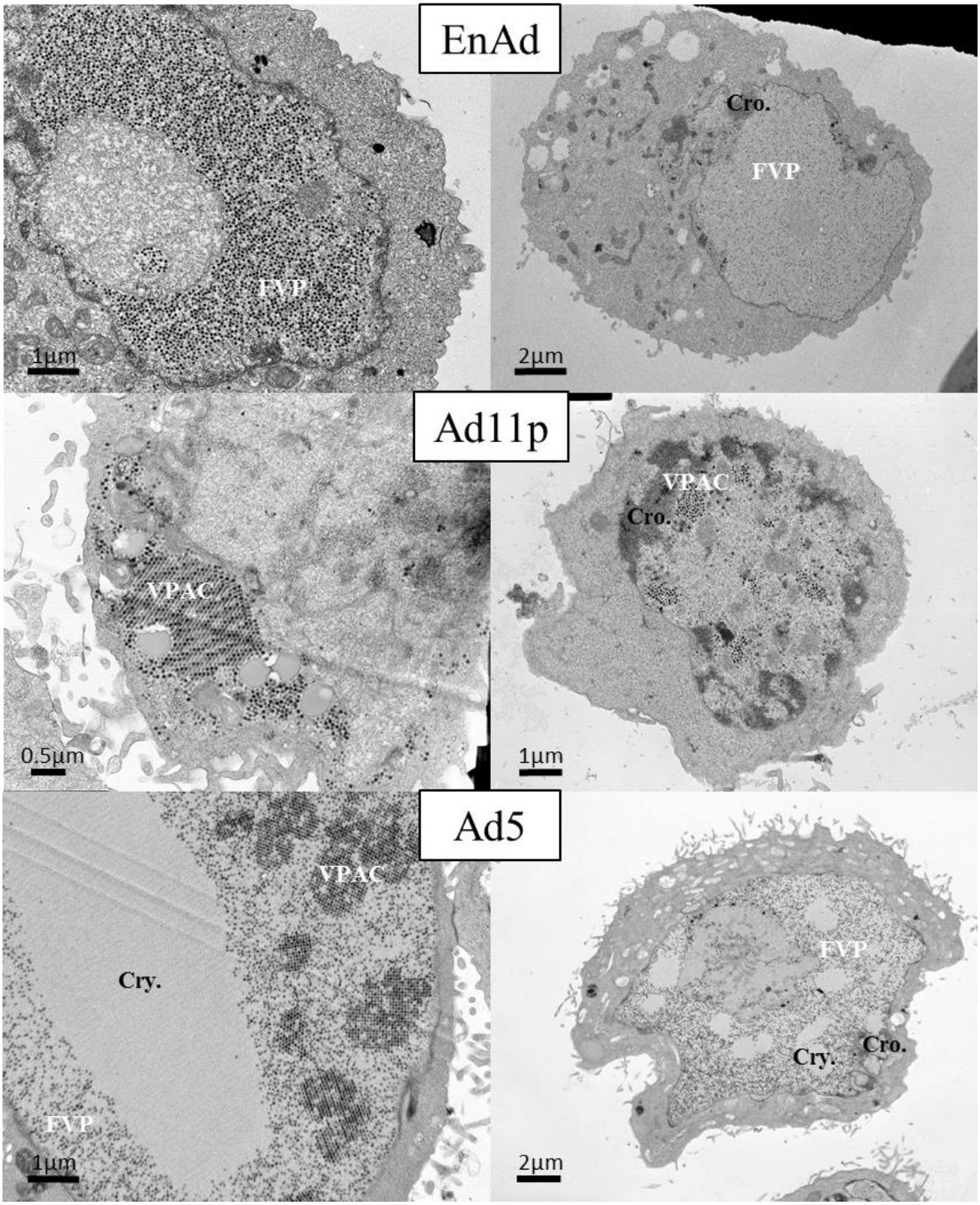


Figure 9.1 Representative transmission electron microscopy pictures of EnAd-, Ad11p- and Ad5-infected A549 cells. Pictures were kindly provided by Leonard Seymour, generated accordingly with previous publication[187]. Cro.=Chromatin, Cry.= crystal inclusion of virus protein, FVP= formed virus particles and VPAC= virus particles assembling cluster, were identified accordingly with previous publications[100,101]. Scale bars show 0.5-2 µm.

9.2 Part B

A key challenge when setting out to address the virus adjuvant effect of EnAd on tumour-infiltrating DCs (Chapter 4, 5 and 6), was to develop a model system in which to investigate the interactions between the virus, tumour cells and DCs. Syngeneic animal tumour models are not permissive to human adenovirus infection due to their species-specificity[218], and while xenografted human tumours in immunodeficient mice are permissive, there is no adaptive immune surveillance from the immunocompromised murine host. Studies with oncolytic adenoviruses in animals have therefore largely focused on investigating non-immune mechanisms of action in immune-compromised animals bearing human xenograft tumours. Monocytes cultured for 7 days in GM-CSF and IL-4 media, can fully differentiate into immature DC[286], and although iDC have tolerogenic properties[287], many stimuli can promote pro-inflammatory functions[220]. Monocytes cultured in RPMI medium supplemented with GMC-SF/IL4, differentiate into early monocyte-derived immature DC after 2 days[288]. The rationale was then to establish an *ex vivo* human immature dendritic cell culture system, as cells had a limited antigen presenting and costimulatory molecules expression suggesting poor T cell priming abilities, phenotype shared with TIDCs[51,52].

9.2.1 PBMC isolation and monocyte selection method

DC can be directly obtained from blood[289], although only in small quantities[290]. Alternatively, large numbers of immature DC can be produced by differentiation *ex vivo* from human monocytes isolated from peripheral blood mononuclear cell (PBMCs) and used in multiple applications[291]. To achieve this, isolated monocytes are generally cultured for 7 days with the cytokines, granulocyte macrophage colony-stimulating factor (GM-CSF) and interleukin (IL)-4, to generate immature (i)DC[292]. However, a diverse methodology exists for monocyte

isolation from PBMC, with multiple levels of cell purity[292]. In this section, two monocyte isolation methods were compared to select the one most suitable to generate larger quantities of high purity iDCs.

PBMCs from leukocyte cones – a by-product generated during leuko-reduction process for blood transfusions – and whole blood (both purchased from the NHS Blood and Transplant services and equivalent to one unit of blood) were isolated by Ficoll gradients to identify the method yielding more monocytes. Leukocyte cones yielded higher total live PBMCs and considerably more cells of interest than whole blood (Figure 9.2 A). Also, leukocyte cones significantly reduced the time required for PBMC isolation as only one fifth the volume had to be overlaid on Ficoll gradients, compared to whole blood. This allowed cells from multiple donors to be processed at the same time.

Initial studies showed that around 15% of PBMCs were monocytes after Ficoll isolation (Figure 9.2 B). Monocytes are often isolated from PBMCs by plastic adherence, however colleagues from this lab had previously shown that this approach gave relatively low monocyte purity. Therefore, an alternative approach was used based on magnetic-activated cell sorting (MACS), to minimise contamination with other cell types[293]. MACS was performed using a commercially available CD14+ isolation kit recommended for positive selection of monocytes (see Materials and Methods). The monocyte preparation obtained after this process across all fresh donors was always over 95% viable (Figure 9.2 C). The isolated monocytes were seeded in endotoxin-free DC differentiation medium, namely RPMI medium supplemented with 10% serum and human recombinant IL-4 and GM-CSF.

A

	Whole Blood	Leukocyte cone
Format		
Total live cells	4e8	8e8
Total live CD14+ cells	1.89e6	1.09e7

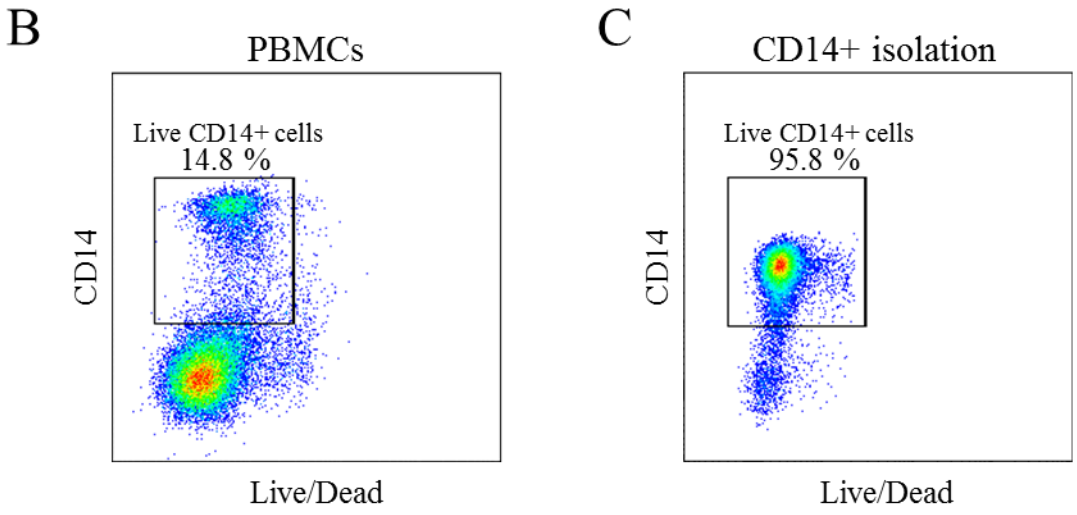


Figure 9.2 Comparison of two PBMCs isolation methods and typical monocyte enrichment. PBMCs from whole blood and leukocyte cone – equivalent to whole blood unit – were isolated by Ficoll gradient (see Material and Method). (A) Total live cells determined by trypan blue staining and total live monocytes calculated by flow cytometry staining are shown on freshly isolated PBMCs. (B) Freshly isolated PBMCs and (C) MACS-isolated CD14+ cells (see Materials and Methods) were stained with vital dye and CD14-FITC monoclonal antibody for flow cytometry analysis. Data from individual donors, but representative of n>2.

9.2.2 Immunophenotyping human monocytes during their differentiation into DCs by flow cytometry

Cell surface expression of various DC maturation markers, costimulatory molecules, and receptors for antigens were monitored by flow cytometry on monocytes and monocyte-derived DC. Accordingly, antibodies against CD40, HLA-DR, HLA-ABC, CD86, and CD83 were used to stain freshly isolated monocytes and monocyte-derived DC cultured for 3, 5 and 7 days in DC differentiation medium.

CD40, is a DC maturation marker that can also be used to distinguish monocyte-derived DC from undifferentiated monocytes[294]. CD40 was not detectable on freshly isolated CD14+ cells, however cells generally (>80%) stained positive for this marker, and at later timepoints nearly all cells (>90%) were CD40+ (Figure 9.3 A and F). This suggests that monocytes had differentiated into iDC from as early as 3 days in differentiation cultures.

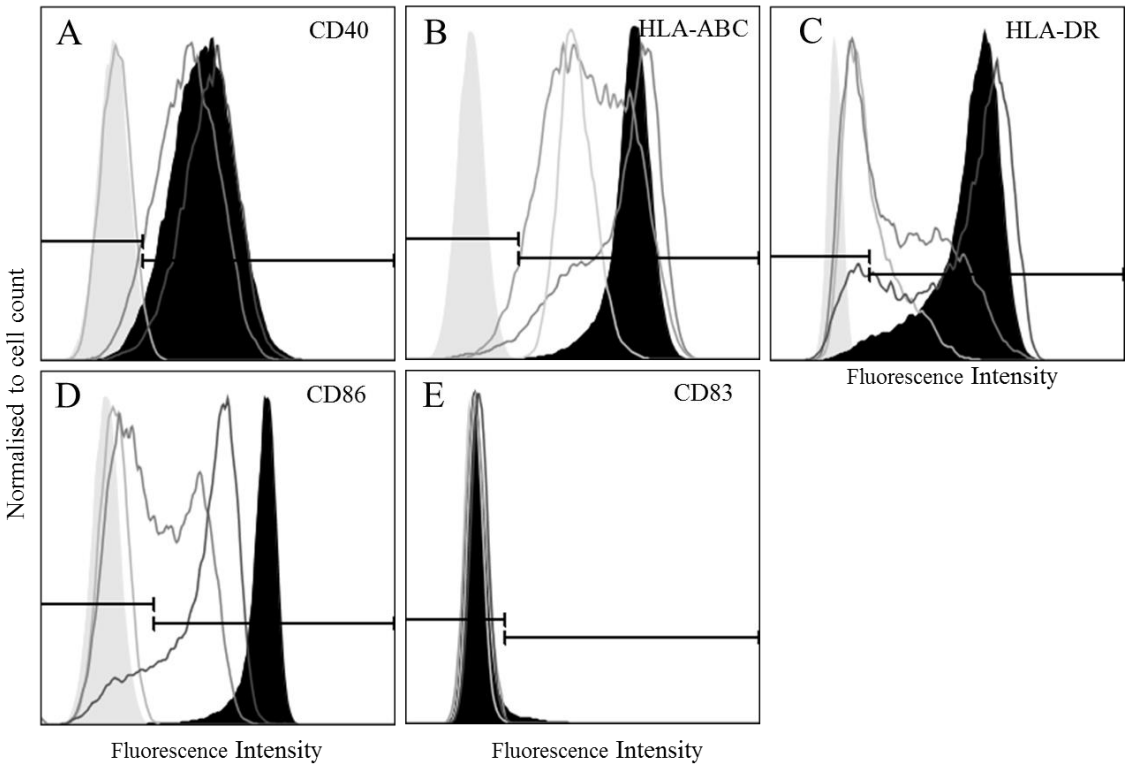
Both HLA-DR (Class II) and HLA-ABC (Class I) are the human antigen presenting molecules of the major histocompatibility complex (MHC), essential for activating antigen-specific T cells[295]. The down regulation of both these molecules on tumour and immune cells has been associated with tumour immune escape[49,296]. By day 3, HLA-ABC, which is broadly expressed by all cell types as part of the immune surveillance of virus and tumour antigens, was expressed already on monocytes and through the later differentiation process. Day 3 cell populations were scattered between dim to strong HLA-ABC expression (fluorescence intensity), with the expression levels gradually increasing over time (Figure 9.3 B and F). The expression of HLA-DR, on the other hand, is generally restricted to innate immune cells and mediates extracellular antigen presentation to initiate adaptive immunity. Freshly isolated monocytes were either weakly positive (37.5%) or negative (62,5%) for HLA-DR. After differentiation (day 3), cells started to up-regulate the HLA-DR marker, shifting the population towards HLA-DR+, and after 7 days in differentiation medium all cells were positive (Figure 9.3 C and F).

CD86 (or B7.2) is a positive costimulatory molecule necessary for T cell priming[297]. Several reports show low costimulatory molecule expression on peripheral and tumour-infiltrating DC[44,52,298], probably contributing to a T cell tolerization mechanism. Here it was shown that freshly isolated monocytes were CD86 negative. On day 3, nearly half the population (49%) of cells had increased the marker to dim expression, representing, whilst the remainder were CD86 negative. This dual negative/positive population was seen again at day 5 cells, with 84% of cells showing detectable CD86. By day 7 iDC, CD86 marker was fully up-regulated on all cells to high expression (Figure 9.3 D and F). The expression of this marker was variable from donor to donor, for instance DCs from some donors remained mainly CD86 negative on day 5, but generally positive by day 7.

The role of CD83 on DC is not well understood yet, but its expression is correlated with fully matured DC phenotype, usually being induced by cytokines or danger stimulus[299]. Interestingly CD83 expression appeared to be missing both in the fresh monocyte and at the multiple time points during differentiation (Figure 9.3 E and F), suggesting that full maturity of the DC had not been achieved.

The increased expression of CD40 on cells cultured for 3 days in differentiation medium suggested that cells were committed to differentiate into DCs, as previously suggested[288,300]. However, day 3 DCs were likely to be immature (CD83-), with low or absent expression of HLA-DR and CD86, compared to DCs in later differentiation stages. Interestingly, day 3 and day 5 immature DCs appeared to share the TIDC feature of limited or absent antigen presenting and costimulatory molecules. Therefore, DC from these two timepoints were considered as models for studying the adjuvant effect of EnAd virus particles on tumour-infiltrating DCs. However, day 5 DCs after 48hrs they showed inherently high levels of expression of antigen presenting and costimulatory markers, leaving no window to assess the virus effect on these markers. Consequently, it was judged that the underdeveloped antigen-presenting abilities for

monocytes at day 3 schedule (d3iDC) provided the most representative model from a cancer immunology perspective, considering the previously reported immature phenotype of TIDC[52].



F

Marker	Day 0 (%)	Day 3 (%)	Day 5 (%)	Day 7 (%)
CD40+	0.3	81.9	95.4	92.1
HLA-DR+	37.5	59.3	85.4	99.5
HLA-ABC+	99.6	95.2	96.7	99.9
CD86+	0.3	49.0	83.9	97.1
CD83+	0.2	0.3	1.4	2.2

Figure 9.3 Immunophenotyping of monocytes and monocyte-derived DCs by flow cytometry. CD14+ cells MACS-sorted from PBMCs isolated from a leukocyte cone, were cultured in GMC-SF/IL-4 RPMI medium –replaced every 2-3 days. At day 0 (clearest grey line), 3 (middle grey line), 5 (dark grey line) and 7 (solid black) cells were stained with vital dye and monoclonal antibodies against (A) CD40 (B) HLA-DR, (C) HLA-ABC, (D) CD86 and (E) CD83, or corresponding isotype (solid grey). Cells were acquired by flow cytometry with unchanged settings over time and gated on live monocyte/DC. (A-E) The data from multiple timepoints are overlaid, normalised to cell count and presented in individual markers histograms. (F) Isotype controls were used to define +populations for each marker. Data generated from one donor, representative of n≥2 donors.

9.2.3 Assessment of soluble factors produced by d3iDC cells stimulated with LPS

DC derived from human monocytes in differentiation medium over 7 days, are commonly matured with lipopolysaccharide (LPS), a TLR4 agonist. During this process, cells secret specific inflammatory cytokines such as TNF-alpha (TNF-a), IL-6 and IL1-beta (IL1-b), and large quantities of polarising cytokines such as IL-12, and IL-10 to a certain extent[219,220]. Accordingly, d3iDC were stimulated with LPS and after 48hrs (accordingly with timeline in Figure 4.1) supernatants were assessed for more than 30 soluble factors (Table 4.1) using the Proteome profiler (see Material and Methods).

LPS induced on d3iDC the expression of cytokines IL-4, IL-6, IL-8 and TNF-a consistently across all donors. Whereas IL-5 was variably expressed across donors, and IL-10 appeared to be slightly expressed in one donor. Finally, IL-1b and IL-12 cytokines were not induced on d3iDC by LPS (Figure 9.4).

Although pro-inflammatory cytokines TNF-a and IL-6 were induced in matured d3iDC, LPS failed to promote the expression of the characteristic IL-12 and IL1-b cytokines, and other cytokines, notably IL-4 but also IL-5 or IL-10, which supress anti-cancer cellular immune responses, were induced[211].

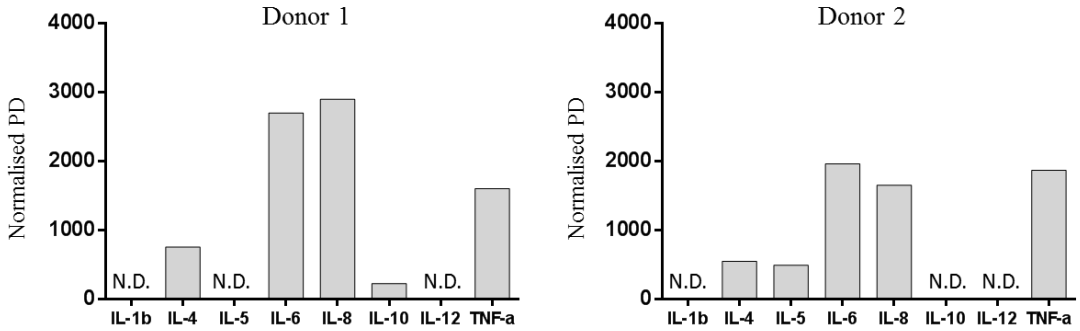


Figure 9.4 Assessment of soluble cytokines and chemokines induced by LPS on day 3 DC. Accordingly with Figure 4.1 A, supernatants from d3iDC treated with 100 ng/ml LPS or untreated, were evaluated with the Proteome Profiler Human Cytokine Array Kit (R&Dsystems, see Material and Methods). The pixel density (PD) of each cytokine from LPS-treated samples were normalised against untreated samples. Two different donors run in independent experiments are shown.

Summarising, monocytes cultured for 7 days in GM-CSF and IL-4 media, can fully differentiate into immature DC[286], and although iDC have tolerogenic properties[287], many stimuli can promote pro-inflammatory functions[220]. Monocytes cultured in RPMI medium supplemented with GMC-SF/IL-4, differentiate into early monocyte-derived immature DC after 2 days[288]. Day 3 monocyte-derived immature DC expressed limited antigen presenting molecules and costimulatory molecules, phenotype shared with TIDCs[51,52], and had a 48hrs window in which this phenotype was maintained. It is believed that the low expression of this molecules on TIDCs results on a poor ability to prime T cell responses, leading to T cell anergy and suppression[40,43-45]. The priming ability of TIDCs are often evaluated by assessing the T cell activation and proliferation in a functional allogeneic mixed leukocyte reaction assay[51,219]. In fact, the d3iDC model was not functional to induce either on T cells (see Chapter 6). In addition, day 3 skewed DC stimulated with LPS failed to produce IL-12 and IL1-beta consistently across all donors. Both cytokines are generally seen on pro-inflammatory day 7 monocyte-derived DC stimulated with LPS[219,220]. Also, this simple method rapidly produced large amounts of cells in a consistent manner across several donors. Altogether, this new approach was used to produce TIDC-like cells to evaluate the main hypothesis of this thesis.